



**André da
Silva Reis**

**Encurvadura por esforço transversal em
vigas metálicas compostas de alma cheia
expostas ao fogo**

**Shear buckling in steel plate girders
exposed to fire**



**André da
Silva Reis**

**Encurvadura por esforço transversal em
vigas metálicas compostas de alma cheia
expostas ao fogo**

Dissertação apresentada à Universidade de Aveiro para cumprimento dos requisitos necessários à obtenção do grau de Doutor em Engenharia Civil, realizada sob a orientação científica do Doutor Nuno Filipe Ferreira Soares Borges Lopes, Professor Auxiliar do Departamento de Engenharia Civil da Universidade de Aveiro e coorientação científica do Doutor Paulo Jorge de Melo Matias Faria de Vila Real, Professor Catedrático do Departamento de Engenharia Civil da Universidade de Aveiro.



**André da
Silva Reis**

**Shear buckling in steel plate girders
exposed to fire**

Thesis submitted to the University of Aveiro to fulfil the necessary requirements for the degree of Doctor of Philosophy in Civil Engineering, made under the scientific supervision of Doctor Nuno Filipe Ferreira Soares Borges Lopes, Assistant Professor at the Civil Engineering Department of University of Aveiro and scientific co-supervision of Doctor Paulo Jorge de Melo Matias Faria de Vila Real, Professor at the Civil Engineering Department of University of Aveiro.

o júri

presidente

Prof. Doutor João Manuel da Costa e Araújo Pereira Coutinho
professor catedrático da Universidade de Aveiro

Prof. Doutor Luís Alberto Proença Simões da Silva
professor catedrático da Faculdade de Ciências e Tecnologia, Universidade de Coimbra

Prof. Doutora Esther Real Saladrigas
professora associada da Universidade Politécnica da Catalunha, Barcelona

Prof. Doutor Paulo Alexandre Gonçalves Piloto
professor coordenador da Esc. Sup. de Tecnologia e de Gestão, Instituto Politécnico de Bragança

Prof. Doutor Nuno Filipe Ferreira Soares Borges Lopes
professor auxiliar da Universidade de Aveiro

Doutor Carlos André Soares Couto
consultor Lindab S.A.

the jury

chairman

Prof. Doctor João Manuel da Costa e Araújo Pereira Coutinho
professor at the University of Aveiro

Prof. Doctor Luís Alberto Proença Simões da Silva
professor at the Faculty of Sciences and Technology, University of Coimbra

Prof. Doctor Esther Real Saladrigas
associated professor at the Polytechnic University of Catalunya, Barcelona

Prof. Doctor Paulo Alexandre Gonçalves Piloto
coordinating professor at the Polytechnic Institute of Bragança

Prof. Doctor Nuno Filipe Ferreira Soares Borges Lopes
assistant professor at the University of Aveiro

Doctor Carlos André Soares Couto
consultant Lindab S.A.

agradecimentos

O desenvolvimento desta dissertação não seria possível sem a excelente orientação do Professor Nuno Lopes, a quem estou muito grato por todo o conhecimento transmitido e por todas as experiências partilhadas nos últimos anos.

Ao meu coorientador Professor Paulo Vila Real, sempre direto e frontal, pelos conselhos e pelas valiosas sugestões fornecidas durante a preparação desta tese de doutoramento.

Estou igualmente grato à Professora Esther Real, pela calorosa receção e supervisão proporcionadas durante o período de investigação na Universidade Politécnica da Catalunha, Espanha.

Ao Governo Português através da Fundação para a Ciência e a Tecnologia (FCT) e ao Fundo Social Europeu através do Programa Operacional Capital Humano (POCH) pelo apoio financeiro dado sob a forma de bolsa de doutoramento.

Muito obrigado



acknowledgements

The development of this thesis would not be possible without the excellent supervision of Professor Nuno Lopes, to whom I am very grateful for all the transmitted knowledge and all the shared experiences over the last years.

To my co-supervisor, Professor Paulo Vila Real, always straight and frontal, for the advices and the valuable suggestions provided during the preparation of this doctoral thesis.

I am also grateful to Professor Esther Real for the warm welcome and supervision provided during my research period at the Polytechnic University of Catalunya, Spain.

To the Portuguese Government through the Foundation for Science and Technology (FCT) and to the European Social Fund through the Human Capital Operating Programme (POCH) for the financial support given in the form of a doctoral scholarship.

Thank you all



palavras-chave

Encurvadura por esforço transversal, fogo, modelação numérica, Eurocódigo 3.

resumo

A presente tese resulta de um trabalho de investigação, cujo propósito se centrou no aumento de conhecimento do comportamento de vigas metálicas compostas de alma cheia sujeitas a encurvadura por esforço transversal em situação de incêndio.

O principal objetivo desta tese consiste em suprir a ausência de regras para o dimensionamento de elementos estruturais metálicos sujeitos a encurvadura por esforço transversal a temperaturas elevadas.

Com essa finalidade, foi desenvolvido um modelo numérico no programa de elementos finitos SAFIR para a simulação do comportamento deste tipo de vigas quando sujeitas a temperaturas elevadas. Estas análises numéricas enquadram-se na metodologia habitualmente designada por GMNIA – geometrically and materially non-linear imperfect analysis. Após a validação do modelo numérico com ensaios experimentais da literatura, foi também avaliada a influência das imperfeições geométricas e das tensões residuais na capacidade resistente das vigas, tanto à temperatura normal como a temperaturas elevadas.

O Eurocódigo 3 estabelece que a resistência à encurvadura por esforço transversal de vigas em I resulta da soma de duas componentes, a resistência da alma e a contribuição dos banzos. Começou-se por avaliar a contribuição dos banzos e verificou-se que os resultados obtidos com as expressões do Eurocódigo 3 poderiam ser melhorados. Assim, foi proposta a aplicação de um fator corretivo de forma a melhorar as previsões do Eurocódigo 3 para a contribuição dos banzos para a resistência à encurvadura por esforço transversal.

A principal parcela da resistência à encurvadura por esforço transversal é dada pela alma. As expressões do Eurocódigo 3 para a determinação da resistência da alma à encurvadura por esforço transversal foram avaliadas. Esta análise demonstrou que a alguns dos resultados não estão do lado da segurança e que a precisão das expressões de dimensionamento do Eurocódigo 3 poderia ser melhorada. Portanto, foram propostas alterações a estas expressões usadas para o dimensionamento à temperatura normal. Para além disso, foram propostas novas expressões para o dimensionamento deste tipo de elementos em caso de exposição ao fogo.

A expressão do Eurocódigo 3 usada para a verificação da segurança de elementos estruturais metálicos sujeitos à interação entre esforço transversal e momento fletor foi também avaliada, verificando-se que a aplicação das propostas para modificação das expressões usadas para a determinação da resistência à encurvadura por esforço transversal origina melhorias nos resultados desta expressão, principalmente a temperaturas elevadas.

Por fim, apresenta-se uma análise da influência de diferentes parâmetros na capacidade resistente de vigas compostas de alma cheia sujeitas a encurvadura por esforço transversal, tais como a espessura da alma, a altura da alma, a espessura dos banzos e a tensão de cedência do aço.

keywords

Shear buckling, fire, numerical modelling, Eurocode 3.

abstract

This thesis is a research work aiming the increasing of knowledge of the behaviour of steel plate girders subjected to shear buckling in fire situation.

The main objective of this thesis is to overcome the lack of rules for the design of steel structural elements subjected to shear buckling at high temperatures.

For this purpose, a numerical model was developed in the finite element software SAFIR to simulate the behaviour of steel plate girders under shear loading at elevated temperatures. These numerical analyses fall into the methodology commonly referred as GMNIA – geometrically non-linear materially imperfect analysis. After validation of the numerical model with experimental tests from the literature, the influence of the geometric imperfections and residual stresses on the bearing capacity of the girders, at both normal and elevated temperatures, was evaluated.

Eurocode 3 states that the shear buckling resistance of steel I girders is given by the sum of two components, the web resistance and the contribution from the flanges. Firstly it was assessed the contribution from flanges and it was found that the results obtained with the Eurocode 3 expressions could be improved. Thus, it was proposed the application of a corrective factor in order to improve the predictions of Eurocode 3 for the contribution from the flanges to the shear buckling resistance.

The main part of the shear buckling resistance comes from the web. The expressions of Eurocode 3 for determining the web resistance to shear buckling were evaluated. This analysis demonstrated that some of the results are not on the safe side and the accuracy of these expressions could be improved. So, changes to the expressions applied for the design at normal temperature were proposed. Furthermore, new expressions for fire design of such structural elements were also proposed.

The expression of Eurocode 3 used for the safety calculation of steel structural elements under interaction between shear and bending was also evaluated. It was verified that the application of the proposals for modification of the expressions used to determine the shear buckling resistance introduces improvements on the results provided by this expression, mainly at elevated temperatures.

Finally, an analysis of the influence of different parameters on the ultimate shear strength of steel plate girders subjected to shear buckling, such as the web thickness, the web depth, the flange thickness and the steel yield strength, is presented.

Contents

List of figures	xix
List of tables	xxvii
Notation	xxxii
Chapter 1 Introduction	3
1.1 Background of the problem	3
1.2 Motivation and objectives	7
1.3 Document outline	8
Chapter 2 Literature review	13
2.1 Behaviour of plate girders under shear	13
2.2 Tension field models	16
2.3 Current state of research	22
Chapter 3 Eurocode design rules	29
3.1 General considerations	29
3.2 Shear resistance	29
3.2.1 Resistance from the web to shear buckling	30
3.2.2 Contribution from the flanges	34
3.2.3 Verification	36
3.3 Interaction between shear and bending	37
3.4 Stiffeners	38
3.4.1 Transverse stiffeners	41
3.4.1.1 Rigid end posts	43

3.4.1.2	Non-rigid end posts	44
3.4.1.3	Intermediate transverse stiffeners	45
3.4.2	Longitudinal stiffeners	46
3.5	Design at elevated temperatures	46
Chapter 4 Numerical modelling		51
4.1	Model description	51
4.1.1	FEM model	51
4.1.2	Material model	53
4.1.3	Initial imperfections	56
4.1.3.1	Geometric imperfections	56
4.1.3.2	Residual stresses	57
4.2	Validation of the numerical model	58
4.2.1	Review of experimental tests	58
4.2.1.1	Normal temperature	58
4.2.1.2	Elevated temperatures	61
4.2.2	Comparisons between numerical and experimental results	63
4.2.2.1	Normal temperature	63
4.2.2.2	Elevated temperatures	66
4.3	Influence of the initial imperfections	68
4.3.1	Geometric imperfections	68
4.3.1.1	Normal temperature	68
4.3.1.2	Elevated temperatures	69
4.3.2	Residual stresses	70
4.3.2.1	Normal temperature	70
4.3.2.2	Elevated temperatures	71
4.4	Conclusions	72
Chapter 5 Basis for the parametric study		75
5.1	Characteristics of the analysed plate girders	75

5.2	Methodology for analysis of results	80
5.3	Sequence of analysis of the results	82
Chapter 6 Contribution from the flanges to the shear resistance		87
6.1	General considerations	87
6.2	Evaluation of the EC3 expression to predict the distance between plastic hinges	88
6.3	Proposal of a corrective coefficient for the EC3 expression to predict the distance between plastic hinges	90
6.4	Influence of the corrective coefficient on design shear resistance	91
6.4.1	Normal temperature	91
6.4.2	Elevated temperatures	95
6.5	Conclusions	99
Chapter 7 Shear buckling resistance		103
7.1	Failure mechanism	103
7.2	Evaluation of the EC3 expressions to predict the web resistance to shear buckling	108
7.3	Proposal of new design expressions	119
7.4	Statistical analysis	124
7.5	Conclusions	142
Chapter 8 Shear-bending interaction		145
8.1	Failure modes	145
8.2	Evaluation of the EC3 expression to check the interaction between shear and bending	147
8.3	Statistical analysis	149

8.4	Conclusions	152
Chapter 9 Influence of different parameters on the ultimate shear strength of steel plate girders		155
9.1	Shear strength in function of cross-section properties	155
9.1.1.	Normal temperature	155
9.1.2.	Elevated temperatures	162
9.2	Reduction of strength caused by the elevated temperatures	167
9.3	End posts	168
9.3.1	Increase of strength given by the rigid end posts	168
9.3.2	Influence of the configuration of the rigid end post	172
9.4	Conclusions	178
Chapter 10 Final considerations		183
10.1	Conclusions	183
10.2	Future developments	185
Bibliographic references		191

List of figures

Figure 1.1 – Common uses of steel plate girders	4
Figure 1.2 – Key elements of a steel plate girder	4
Figure 1.3 – Shear buckling in a steel plate girder after fire (Franssen & Vila Real, 2010)	5
Figure 2.1 – Stresses in a plate girder (Vila Real, 2010)	13
Figure 2.2 – Post-critical response of slender webs (Beg et al., 2010)	14
Figure 2.3 – Different steps of the behaviour of a plate girder under shear loading	15
Figure 2.4 – Analogy between Pratt truss and a plate girder subjected to shear buckling	16
Figure 2.5 – First tension field theoretical models	17
Figure 2.6 – State of stress in a plate girder subjected to shear with transverse stiffeners at the ends only according to the Rotated Stress Field Method (Johansson et al., 2007)	20
Figure 2.7 – Rotated Stress Field Method vs. experimental tests (Höglund, 1997)	21
Figure 3.1 – Reduction curves for the web contribution to shear buckling	31
Figure 3.2 – End supports	31
Figure 3.3 – Notation used to obtain the web slenderness parameter and the shear buckling coefficient of a stiffened plate girder	33
Figure 3.4 – Effective cross-section of stiffeners	33
Figure 3.5 – Anchorage of the tension field in the flanges	35
Figure 3.6 – Calculation algorithm	36
Figure 3.7 – Shear-bending interaction diagram for profiles with Class 1 or 2	37
Figure 3.8 – Shear-bending interaction diagram for profiles with Class 3 or 4	38

Figure 3.9 – Common applications of transverse and longitudinal stiffeners (Beg et al., 2010)	39
Figure 3.10 – Typical cross-sections of stiffeners (Beg et al., 2010)	40
Figure 3.11 – Effective cross-section of stiffeners (Beg et al., 2010)	40
Figure 3.12 – Scheme for rigid transverse stiffeners (Beg et al., 2010; Johansson et al., 2007)	42
Figure 3.13 – General loading conditions affecting the transverse stiffeners (Johansson et al., 2007)	43
Figure 3.14 – Rigid end post details	43
Figure 3.15 – Non-rigid end post details	44
Figure 3.16 – Development of axial force in the intermediate transverse stiffener	45
Figure 3.17 – Reduction factors for the steel stress-strain relationship at elevated temperatures	47
Figure 3.18 – Schematic representation of the application of the reduction factors to the design expressions at normal temperature	48
Figure 4.1 – Mesh refinement sensitivity analysis	52
Figure 4.2 – Numerical model	52
Figure 4.3 – Steel stress-strain relationship at elevated temperatures	54
Figure 4.4 – Stress-strain relationship of steel at elevated temperatures	55
Figure 4.5 – Example of a buckling mode	57
Figure 4.6 – Pattern of residual stresses typical of welded I-sections (C – compression; T – tension)	57
Figure 4.7 – Incorporation of the residual stresses into the numerical model (blue – compression; red – tension)	58

Figure 4.8 – Geometry of the plate girders tested by Lee and Yoo	59
Figure 4.9 – Geometry of the plate girders tested at the University of Minho	60
Figure 4.10 – Geometry of the plate girders tested at the Nanyang Technological University	62
Figure 4.11 – Numerical and experimental (Lee & Yoo, 1999) out of plane web buckling in the non-rigid end post of PG2	64
Figure 4.12 – Numerical and experimental (Lee & Yoo, 1999) deformed shape after test of PG4	64
Figure 4.13 – Numerical and experimental (Lee & Yoo, 1999) deformed shape after test of PG7	64
Figure 4.14 – Numerical and experimental (Gomes et al., 2000) deformed shape after test of PG13	65
Figure 4.15 – Experimental and numerical ultimate resistance of all the analysed steel plate girders at normal temperature	66
Figure 4.16 – Numerical and experimental deformed shape after test of PG16	67
Figure 4.17 – Numerical and experimental deformed shape after test of PG21	68
Figure 4.18 – Experimental and numerical ultimate resistance of all the analysed steel plate girders at elevated temperatures	68
Figure 5.1 – Geometric configuration of the plate girders analysed in groups I and II	76
Figure 5.2 – Cross-section notation of the analysed plate girders	78
Figure 5.3 – Geometric configuration of the plate girders with rigid end posts analysed in groups III and IV	79
Figure 5.4 – Zones definition on the shear-bending interaction diagram	81
Figure 6.1 – Schematic representation of plate girders (group I) considered in this Chapter	87

Figure 6.2 – Scheme of the methodology adopted for the analysis of results	88
Figure 6.3 – Illustration of the distance c	89
Figure 6.4 – Ratio c/a for the analysed plate girders	89
Figure 6.5 – Proposal of a β coefficient to improve the EC3 expression to determine the distance c at both normal and elevated temperatures	91
Figure 6.6 – Ultimate shear strength of the group I plate girders at normal temperature	92
Figure 6.7 – Web resistance to shear buckling of group I plate girders at normal temperature	95
Figure 6.8 – Ultimate shear strength of the group I plate girders at 500°C	96
Figure 6.9 – Web resistance to shear buckling of group I plate girders at 500°C	98
Figure 7.1 – Tension field development at normal temperature (blue – compression; red – tension)	104
Figure 7.2 – Failure mechanism at normal temperature	104
Figure 7.3 – Evolution of principal stresses distribution until failure in a steel plate girder tested at normal temperature (blue – compression; red – tension)	105
Figure 7.4 – Color scale of the out-of-plane web displacements in a steel plate girder tested at normal temperature	106
Figure 7.5 – Tension field development at 500°C (blue – compression; red – tension)	107
Figure 7.6 – Failure mechanism at 500°C	107
Figure 7.7 – Utilisation ratio at normal temperature of all the analysed plate girders	109
Figure 7.8 – Utilisation ratio at elevated temperatures of all the analysed plate girders	109
Figure 7.9 – Improvements on the EC3 predictions given by the application of the corrective coefficient for the contribution from the flanges to the shear buckling resistance at normal temperature	111

Figure 7.10 – Web contribution to shear buckling at normal temperature	112
Figure 7.11 – Improvements on the EC3 predictions given by the application of the corrective coefficient for the contribution from the flanges to the shear buckling resistance at elevated temperatures	113
Figure 7.12 – Web contribution to shear buckling at elevated temperatures	114
Figure 7.13 – Ultimate shear strength at 20°C in function of the web slenderness for the group II plate girders with $h_w=1000$ mm	115
Figure 7.14 – Ultimate shear strength at 500°C in function of the web slenderness for the group II plate girders with $h_w=1000$ mm	116
Figure 7.15 – Ultimate shear strength at 20°C in function of the ratio between the flanges and web thicknesses for the group II plate girders with $h_w=1000$ mm	117
Figure 7.16 – Ultimate shear strength at 500°C in function of the ratio between the flanges and web thicknesses for the group II plate girders with $h_w=1000$ mm	118
Figure 7.17 – New proposal for the web contribution to shear buckling at normal temperature	121
Figure 7.18 – New proposal for the web contribution to shear buckling at elevated temperatures	122
Figure 7.19 – Improvements on the EC3 predictions given by the application of the proposals for normal temperature	123
Figure 7.20 – Improvements on the EC3 predictions given by the application of the proposals for elevated temperatures	123
Figure 7.21 – Statistical analysis of the zone 1 results at normal temperature	127
Figure 7.22 – Statistical analysis of the zone 2 results at normal temperature	128
Figure 7.23 – Statistical analysis of the zone 3 results at normal temperature	129
Figure 7.24 – Statistical analysis of the zone 1 results at elevated temperatures	130

Figure 7.25 – Statistical analysis of the zone 2 results at elevated temperatures	131
Figure 7.26 – Statistical analysis of the zone 3 results at elevated temperatures	132
Figure 7.27 – Utilisation ratio in function of the web slenderness parameter for the plate girders with non-rigid end posts analysed at normal temperature	136
Figure 7.28 – Web contribution to shear buckling of the group II plate girders in function of the plate girders aspect ratio	137
Figure 7.29 – Utilisation ratio in function of the web slenderness at elevated temperatures	138
Figure 7.30 – Web contribution to shear buckling of the group II plate girders in function of the ratio between the flanges and web thicknesses	139
Figure 7.31 – Average utilisation ratio and standard deviation in function of the steel grade	140
Figure 7.32 – Utilisation ratio in function of the temperature	141
Figure 8.1 – Example of the failure modes observed for PG 1000x10+300x20_S235 at 500°C	146
Figure 8.2 – Different failure modes observed for PG 600x4+200x7_S460 at 500°C	147
Figure 8.3 – Improvements for the zone 2 girders	148
Figure 9.1 – Increase of strength at 20°C given by the increase of the web thickness for the girders with non-rigid end posts	157
Figure 9.2 – Increase of strength at 20°C given by the increase of the web thickness for the girders with rigid end posts	158
Figure 9.3 – Increase of strength at 20°C given by the increase of the web depth for the girders with $t_w=5$ mm	159
Figure 9.4 – Increase of strength at 20°C given by the increase of the flanges thickness for the girders with $h_w=1000$ mm	160

Figure 9.5 – Increase of strength at 20°C given by the increase of the steel yield strength for the girders with non-rigid end posts	161
Figure 9.6 – Increase of strength at 20°C given by the increase of the steel yield strength for the girders with rigid end posts	162
Figure 9.7 – Increase of strength at 500°C given by the increase of the web thickness for the girders with $h_w=1200$ mm	164
Figure 9.8 – Increase of strength at 500°C given by the increase of the web depth for the girders with $t_w=5$ mm	164
Figure 9.9 – Increase of strength at 500°C given by the increase of the flanges thickness for the girders with $h_w=1000$ mm	165
Figure 9.10 – Increase of strength at 500°C given by the increase of the steel yield strength for the girders with non-rigid end posts	166
Figure 9.11 – Increase of strength at 500°C given by the increase of the steel yield strength for the girders with rigid end posts	167
Figure 9.12 – Strength reduction caused by the temperature increase	168
Figure 9.13 – Difference between rigid and non-rigid end posts on the web contribution to shear buckling of the group II plate girders in function of the aspect ratio at 20°C and 500°C	169
Figure 9.14 – Average increase of strength given by the rigid end posts	171
Figure 9.15 – Influence of different geometrical ratios on the increase of strength given by the rigid end posts	171
Figure 9.16 – Rigid end post configurations analysed in this section (example for $a/h_w=1.0$)	172
Figure 9.17 – Influence of the distance between the transverse stiffeners which form the rigid end post for the girders with $t_s = 20$ mm	176

Figure 9.18 – Influence of the thickness of the external transverse stiffener of the rigid end post for the girders with $e = 200$ mm

177

List of tables

Table 2.1 – Tension field theories in steel plate girders (Galambos, 1988)	19
Table 3.1 – Reduction factor for the web contribution to shear buckling (χ_w)	31
Table 3.2 – Reduction factors for steel stress-strain relationship at elevated temperatures	47
Table 4.1 – Boundary conditions (Δ – displacement, θ – rotation; 0 – free, 1 – fixed)	52
Table 4.2 – Expressions to define the steel stress-strain relationship at elevated temperatures	54
Table 4.3 – Dimensions of the plate girders tested at normal temperature	60
Table 4.4 – Material properties of the plate girders tested at normal temperature	61
Table 4.5 – Dimensions of the plate girders tested at elevated temperatures	62
Table 4.6 – Material properties of the plate girders tested at elevated temperatures	63
Table 4.7 – Comparison between the numerical and experimental results of the steel plate girders tested by Lee and Yoo	63
Table 4.8 – Comparison between the numerical and experimental results of the steel plate girders tested at the University of Minho	65
Table 4.9 – Comparison between the numerical and experimental results of the steel plate girders tested at the Nanyang Technological University	67
Table 4.10 – Geometric imperfections sensitivity analysis at normal temperature	69
Table 4.11 – Geometric imperfections sensitivity analysis at elevated temperatures	70
Table 4.12 – Residual stresses sensitivity analysis at normal temperature	71
Table 4.13 – Residual stresses sensitivity analysis at elevated temperatures	72
Table 5.1 – Details of the plate girders analysed in group I	76
Table 5.2 – Details of the plate girders analysed in group II	76

Table 5.3 – Details of the plate girders analysed in group III	78
Table 5.4 – Details of the plate girders analysed in group IV	78
Table 5.5 – Material properties considered in the parametric study	79
Table 5.6 – Number of numerical simulations performed in this parametric study	80
Table 5.7 – Ratio of shear force to bending moment according to the zone of the shear-bending interaction diagram	81
Table 6.1 – Web resistance to shear buckling numerically obtained ($\chi_{w,SAFIR}$) at 20°C	94
Table 7.1 – Proposal for the reduction factor for the web contribution to shear buckling resistance (χ_w) at normal temperature	119
Table 7.2 – Proposal for the reduction factor for the web contribution to shear buckling resistance ($\chi_{w,\theta}$) at elevated temperatures	120
Table 7.3 – Statistical analysis at normal temperature	124
Table 7.4 – Statistical analysis at elevated temperatures	124
Table 7.5 – Detailed statistical analysis of the zone 1 plate girders tested at normal temperature	134
Table 7.6 – Detailed statistical analysis of the zone 1 plate girders subjected to elevated temperatures	135
Table 8.1 – Detailed statistical analysis of the zone 2 plate girders tested at normal temperature	150
Table 8.2 – Detailed statistical analysis of the zone 2 plate girders subjected to elevated temperatures	151
Table 9.1 – Influence of the rigid end post configuration on the ultimate shear strength of steel plate girders at normal temperature	174
Table 9.2 – Influence of the rigid end post configuration on the ultimate shear strength of steel plate girders at 500°C	175

Table 9.3 – Influence of the rigid end post configuration on the safety nature of the EC3 predictions at normal temperature

178

Notation

The symbols have not been all placed, because some of them are described throughout the document.

Roman upper case letters

A	area of the cross-section	[mm ²]
E	Young's modulus	[MPa]
$E_{a,\theta}$	slope of the linear elastic range	[MPa]
I	moment of inertia about the neutral axis	[mm ⁴]
I_{st}	moment of inertia of a stiffener	[mm ⁴]
L	girder length	[mm]
M_{Ed}	design bending moment	[N · mm]
$M_{f,Rd}$	moment of resistance of the cross-section consisting of the effective area of the flanges only	[N · mm]
$M_{pl,Rd}$	design plastic resistance of the cross-section consisting of the effective area of the flanges and the fully effective web irrespective of its section class	[N · mm]
M_{SAFIR}	bending moment numerically obtained	[N · mm]
P	ultimate load	[kN]
$V_{b,Rd}$	design resistance for shear	[N]
$V_{bf,Rd}$	contribution from the flanges to the design resistance for shear	[N]
$V_{bw,Rd}$	contribution from the web to the design resistance for shear	[N]
V_{cr}	elastic critical buckling load	[N]
V_{Ed}	design shear force including shear from torque	[N]
V_{SAFIR}	shear resistance numerically obtained	[kN]

Roman lower case letters

a	plate length between transverse stiffeners	[mm]
b	plate width	[mm]
b_f	flange width	[mm]
b_{ls}	longitudinal stiffener width	[mm]
c	distance between plastic hinges	[mm]
$f_{p,\theta}$	proportional limit	[MPa]
f_y	yield strength	[MPa]
f_{yf}	flange yield strength	[MPa]
f_{yw}	web yield strength	[MPa]
$f_{y,\theta}$	effective yield strength	[MPa]
h_w	clear web depth between flanges	[mm]
$h_{w,i}$	clear web depth between flanges of sub panels i	[mm]
k_τ	shear buckling coefficient	[-]
$k_{\tau,i}$	shear buckling coefficient of sub panels i	[-]
$k_{E,\theta}$	reduction factor for Young's modulus	[-]
$k_{y,\theta}$	reduction factor for effective yield strength	[-]
$k_{0.2p,\theta}$	reduction factor for Class 4 cross-sections	[-]
t	plate thickness	[mm]
t_f	flange thickness	[mm]
t_{ls}	thickness of the longitudinal stiffener	[mm]
t_s	thickness of the transverse stiffener	[mm]
t_w	web thickness	[mm]
ν	Poisson's coefficient	[-]

Greek lower case letters

α	aspect ratio $\alpha = a/h_w$	[–]
β	corrective coefficient for the EC3 prediction of c	[–]
γ_{M0}	partial safety factor	[–]
γ_{M1}	partial safety factor	[–]
$\varepsilon_{p,\theta}$	strain at the proportional limit	[–]
$\varepsilon_{t,\theta}$	limit strain for yield strength	[–]
$\varepsilon_{u,\theta}$	ultimate strain	[–]
$\varepsilon_{y,\theta}$	yield strain	[–]
η	coefficient depending on the steel grade	[–]
θ	inclination of the tension field	[°]
$\bar{\lambda}_w$	web slenderness parameter	[–]
$\bar{\lambda}_{w,\theta}$	web slenderness parameter at elevated temperatures	[–]
σ_1	principal tensile stresses	[MPa]
σ_2	principal compressive stresses	[MPa]
σ_E	Euler's critical stress $\sigma_E = \frac{\pi^2 E}{12(1-\nu^2)} \left(\frac{t_w}{h_w}\right)^2$	[MPa]
σ_h	horizontal component of the tension field	[MPa]
τ_{cr}	elastic critical buckling stress of a plate under pure shear	[MPa]
χ_f	factor for the flange contribution to shear buckling resistance	[–]
χ_w	reduction factor from the web contribution to shear buckling resistance	[–]
$\chi_{w,\theta}$	reduction factor from the web contribution to shear buckling resistance at elevated temperatures	[–]
$\chi_{w,SAFIR}$	reduction factor for the contribution of the web to shear buckling resistance numerically obtained	[–]

Abbreviations

AISC	American Institute of Steel Construction
CEN	European Committee for Standardization
EC3	Eurocode 3
ECCS	European Convention for Structural Steelwork
GMNIA	Geometrically and Materially Non-linear Imperfect Analysis
IPQ	Portuguese Quality Institute

Chapter 1

Introduction

Chapter 1 Introduction

- 1.1 Background of the problem
- 1.2 Motivation and objectives
- 1.3 Document outline

Chapter 1 Introduction

1.1 Background of the problem

Steel plate girders are widely used as structural members in the construction industry due to their capacity to support heavy loads over long spans. A plate girder is basically an I-beam assembled from steel plates which are welded to each other. The common uses include bridges, medium and long span floors in buildings and crane girders in industrial structures (see Figure 1.1).

Nowadays, finding the best cost-effective solution is a must in engineering. In steel construction, to overcome this challenge requires a compromise between weight-cost and strength which results in the use of slender cross-sections, as those typical from steel plate girders. Generally, they are used to carry loads which cannot be economically supported by hot-rolled beams. Standard hot-rolled cross-sections may be adequate for many of the usual structures, but in situations where the load is heavier and the span is also large, its application is usually uneconomical.

The slender cross-sections of steel plate girders are usually composed by an assembly of plates which are commonly stated as web (internal element) and flanges (outstand elements). The web becomes deep and thin to reduce weight, making it susceptible to buckling when submitted to compressive stresses, thus affecting the ultimate bearing capacity of the plate girder. Therefore, it is common to design plate girders with transverse stiffeners and in some cases with longitudinal stiffeners (see Figure 1.2), in order to increase the buckling strength of the web plates. A good web design comprises finding the best combination of plate thickness and distance between transverse stiffeners that leads to an economic solution regarding material and fabrication costs.

Moving on to some more technical details, it is important knowing that steel plate girders are normally subjected to various loading conditions, as for example bending, shear or patch loading. Each one of its components are designed to support a specific load, the flanges must resist compressive/tensile forces resulting from the bending stress distribution, while the slender webs should be able to withstand heavy shear loads as well as concentrated compressive loads due to patch loads. The web together with stiffeners must be capable to handle the tension field actions that result from shear buckling.



a) Illinois bridge (MDT, 2011)



b) Building (SC, 2012)

Figure 1.1 – Common uses of steel plate girders

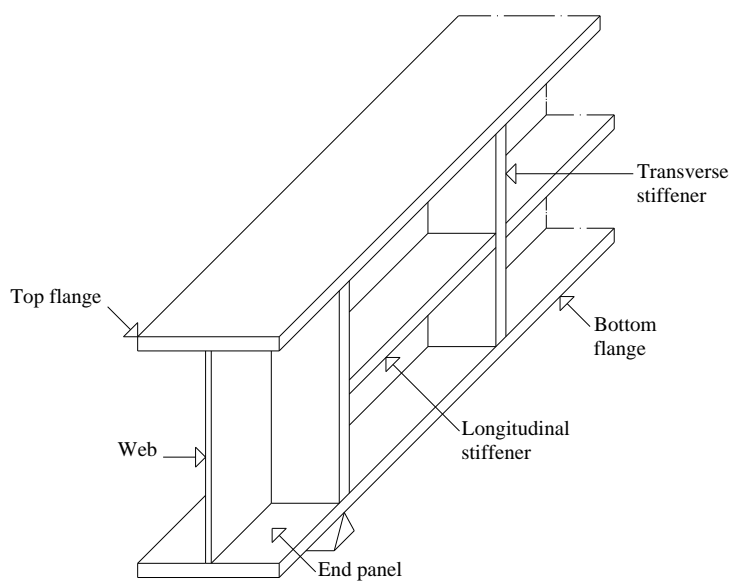


Figure 1.2 – Key elements of a steel plate girder

Fire is one of the most serious environmental hazards to which a steel structure can be subjected during its lifetime. This accidental action may cause a severe impact on steel structures, resulting in significant economic and public losses. Historical events suggest that fires are a significant hazard to steel bridges, with some of them causing the bridges to collapse (see Figure 1.3). A research conducted by the New York Department of Transportation (NYDOT) found that 53 of the total recorded bridge failures up to 2011 are caused by fires and only 18 are caused by earthquakes (Garlock et al., 2011).

People safe evacuation during a fire requires structural integrity. Steel plate girders are often placed in key points of buildings due to their capacity to support heavy loads over long spans, which highlights their importance and relevance for life safety. The exposure to elevated temperatures decreases substantially the stiffness and strength of steel structural elements and may even change their behaviour when compared to design at normal temperature (Kodur et al., 2013).

Kodur and Naser (2014) found that shear capacity can decrease faster than bending capacity meaning the shear limiting state may be a dominant failure mode in steel plate girders subjected to fire. However, the results of this thesis showed an opposite trend. Furthermore, strong differences in the slenderness of the cross-sections, as it is the case for plate girders with thin webs and massive flanges, may increase the effect of the elevated temperatures developed during a fire (Scandella et al., 2014).



Figure 1.3 – Shear buckling in a steel plate girder after fire (Franssen & Vila Real, 2010)

Over the past decades, the European Commission developed a set of harmonized procedures for the design of construction works, aiming the elimination of technical obstacles to trade in the Member States of the European Community. These design procedures were established and published by the European Committee for Standardization (CEN) that led to the development of the Structural Eurocodes. The Eurocodes are divided in ten parts (numbered from 0 to 9) addressing different topics: basis of structural design; actions necessary for the design of structures; specific rules and recommendations for structures made of different materials (concrete, steel, composite, timber, masonry and aluminium); earthquake resistance; geotechnical design.

The Structural Eurocodes were developed with the objective of providing safe, economical and, as much as possible, simple procedures for the design of structures. Regarding fire design, simplified procedures given by those codes of practice are extremely important for civil engineers who do not always have access to applications dealing with advanced calculation methods.

Eurocode 3 (EC3) is the one devoted to the design of steel structures (Simões da Silva et al., 2010). It is composed by twelve parts (numbered from 1 to 12). The first provides general rules for the design of steel structures (CEN, 2010a) and the remaining concern to particular characteristics of steel structures. There are two parts of EC3 with high relevance for this work. Part 1-5 of EC3 “Plated structural elements”, also named as EN 1993-1-5 (CEN, 2006b), gives procedures for the design of plated structural elements at room temperature. Design rules for steel plate girders affected by shear buckling at normal temperature may be found in this part of EC3.

Concerning fire resistance, Part 1-2 of EC3 “General rules – Structural fire design”, also named as EN 1993-1-2 (CEN, 2010b), gives prescriptions for the design of steel structural elements subjected to elevated temperatures. However, Part 1-2 of EC3 does not establish a procedure for checking the shear buckling resistance at elevated temperatures. One way to perform fire design is to use the shear design rules at normal temperature provided by Part 1-5 of EC3, adapted to fire design by the direct application of the reduction factors for stress-strain relationship of carbon steel at elevated temperatures from Part 1-2 of EC3.

1.2 Motivation and objectives

Local buckling phenomena are very important for the design of steel structural elements with thin-walled cross-sections, as it is the case of steel plate girders. Therefore, these have been a common topic of several investigations over the past decades and the design of steel plate girders is well understood at normal temperature.

Fire is a more common hazard than one would first think. However, local buckling in structural elements subjected to fire has not been receiving the same attention and only limited research has been conducted to predict the ultimate shear strength at elevated temperatures.

Unfortunately, this hazard to steel structures is aggravated by the lack of fire design guidelines in the European Standards. This problem, together with the fact that elevated temperatures can cause a substantial reduction in the ultimate shear strength of steel plate girders, reinforces the interest of this thesis, which allowed evaluating if the procedures adopted in Part 1-5 of EC3 for the verification of shear buckling resistance at normal temperature are suitable for the same verification in case of fire, using the reduction factors for the steel stress-strain relationship at elevated temperatures.

Due to the limited size of furnaces and the high cost of the fire resistance experimental tests, several studies about fire resistance of steel structures have been performed in recent years based on numerical simulations. However, it is necessary to duly validate numerical models before performing parametric studies and calibrated numerical models are still lacking.

The main objective of this thesis is to develop more comprehensive, safe and economic guidance on the design of steel plate girders subjected to shear buckling, especially when subjected to fire. The overall objective was achieved through the following particular objectives:

- to develop numerical models duly calibrated with experimental tests found in the literature;
- to perform a solid parametric numerical study in order to generate results on commonly used plate girders in buildings;
- to evaluate the accuracy of the expressions implemented in the European Standards for the design of steel plate girders at normal temperature;

- to evaluate the application of the design expressions for normal temperature to fire design;
- to propose, if necessary, new expressions for design of steel plate girders subjected to shear buckling at elevated temperatures;
- to ensure that the proposed expressions are in a format that is readily disseminated and used in the European Union by incorporating them into European Standards;

This thesis is directly relevant for the construction industry where the use of steel plate girders is usual. The research presented here will allow filling the lack of guidance in the European Standards for the fire design of this type of structural elements. The proposed design rules are crucial to produce safe and cost-effective structures, being relevant to the life safety and society. Moreover, this thesis does not only result in shear design rules but also deliver a calibrated numerical model which may be relevant for future works of the research community.

1.3 Document outline

The achievement of the objectives described above is directly related to the realization of several studies performed during the development of this research. This section summarizes the main tasks carried out throughout this research work and how they are organized in the contents of the thesis.

This thesis is organized in 10 Chapters. In Chapter 1 is done a brief introduction about the problem under investigation. The motivation and the main objectives are also presented here, as well as the structure of the document.

The state of the art is presented in Chapter 2. The literature presented in this chapter is the result of a deep bibliographic search for scientific papers and publications dealing with the occurrence of shear buckling in steel plate girders. After a brief description of the behaviour of plate girders under shear loading, a summary of the theoretical models historically developed to predict the shear resistance of steel plate girders is presented. Finally, a compilation of the most relevant research developed over the last years is presented.

In Chapter 3 the prescribed design rules for both normal temperature and fire design, according to Part 1-5 and Part 1-2 of EC3 (CEN, 2006b, 2010b), are presented. First, the EC3 design procedure is presented, to predict the shear resistance of steel plate girders affected by shear buckling at normal temperature. Then, the procedure to evaluate the interaction between shear and bending is described. Furthermore, the design rules for stiffeners are also presented in this chapter. Finally, the methodology used to evaluate the shear resistance of steel plate girders exposed to fire is presented, since no guidance is given in Part 1-2 of EC3 for the shear buckling evaluation in fire situation.

Chapter 4 mainly deals with the numerical modelling with SAFIR (Franssen, 2005, 2011) based on the finite element method. This chapter comprises the presentation of the numerical model, including boundary conditions and loading, as well as the material model at both normal and elevated temperatures. The initial imperfections incorporated into the numerical model are also described in this chapter. Furthermore, the validation of the numerical model with experimental tests collected from the literature is presented. The chapter concludes with the presentation of sensitivity analyses about the influence of the geometric imperfections and residual stresses on the numerical modelling of steel plate girders subjected to shear buckling.

In Chapter 5 are described the bases for the parametric study presented in the following chapters. The geometric and material properties of the plate girders analysed at both normal and elevated temperatures are presented, as well as the methodology of analysis of results based on the shear-bending interaction diagram.

Chapters 6 to 8 are dedicated to the analysis and discussion of the numerical results, resulting from the parametric study considering the girders presented in Chapter 5. The analysis of the contribution from the flanges to the shear buckling resistance is presented in Chapter 6. The EC3 expression to predict the additional resistance given by the flanges is evaluated and the application of a corrective coefficient to the expression used for calculating the distance where the plastic hinges form in the flanges is proposed.

In Chapter 7 a similar analysis is presented for the resistance from the web to shear buckling. The failure mechanism is described and new reduction factors for the web

contribution to shear buckling resistance are proposed for both normal and elevated temperatures. Furthermore, a detailed statistical analysis of the results is performed.

In Chapter 8 the evaluation of the interaction between shear and bending is presented. The failure modes of the girders are also presented in this chapter, in function of the dominant effort which causes the collapse. Furthermore, a statistical analysis from the results of the girders which fail due to the interaction between shear and bending is presented.

Chapter 9 is dedicated to the study of the influence of different parameters on the ultimate shear strength of steel plate girders. The increase of strength given by the increase of the cross-section properties is presented here, as well as the reduction of strength caused by the elevated temperatures. In addition, the influence of the configuration of the end posts on the ultimate bearing capacity of steel plate girders is also presented.

Finally, general and specific conclusions reached throughout the thesis are presented in Chapter 10, together with suggestions for future research on the behaviour of steel plate girders subjected to shear buckling in fire situation.

Chapter 2

Literature review

Chapter 2 Literature review

- 2.1 Behaviour of plate girders under shear
- 2.2 Tension field models
- 2.3 Current state of research

Chapter 2 Literature review

2.1 Behaviour of plate girders under shear

A literature review of relevant research on shear resistance of steel plate girders is presented in this Chapter. Plate girders are formed by isolated plates that can be supported in their ends and subjected to forces in its plane due to shear and bending. The behaviour of the girder is defined by the behaviour of these individual plates. The stresses caused by shear forces and bending moments in a plate girder are represented in Figure 2.1. The flanges are subjected to uniform normal stresses and the web is subjected to non-uniform normal stresses and tangential or shear stresses (Vila Real, 2010).

Thick stocky webs reach their ultimate shear strength by material yielding, while thin slender webs may be susceptible to the occurrence of out-of-plane shear buckling. However, limiting a web under shear stresses to its elastic buckling capacity τ_{cr} may be excessively conservative due to the additional post-critical strength reserve characteristic of plated elements (see Figure 2.2). The additional post-critical strength depends on the web slenderness, with larger gains obtained by plates where the material yield stress is significantly higher than the elastic critical buckling stress. Plate girders may be provided with transverse or longitudinal stiffeners to limit lateral deflections and thus increase the local buckling resistance.

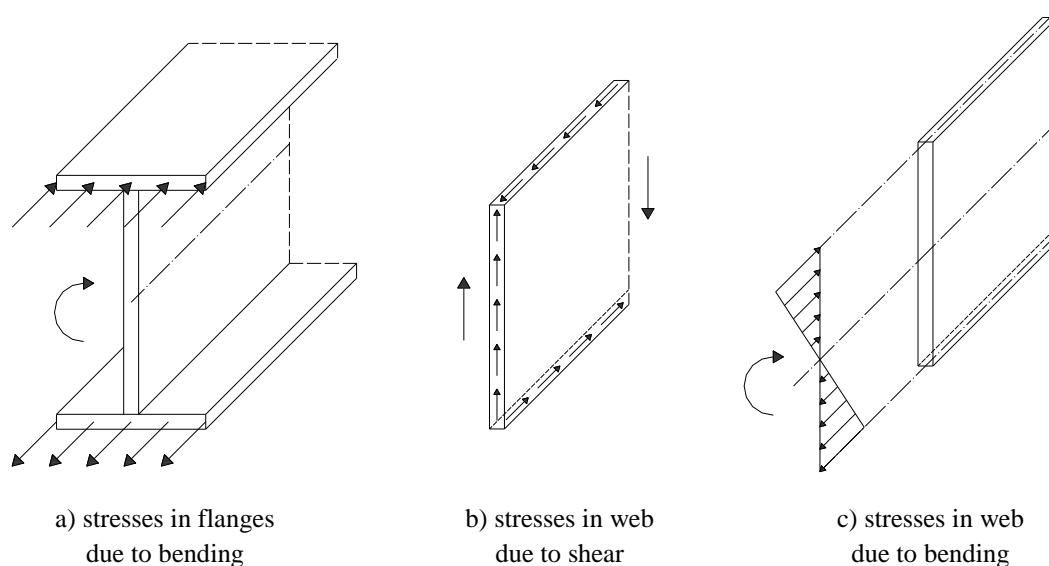


Figure 2.1 – Stresses in a plate girder (Vila Real, 2010)

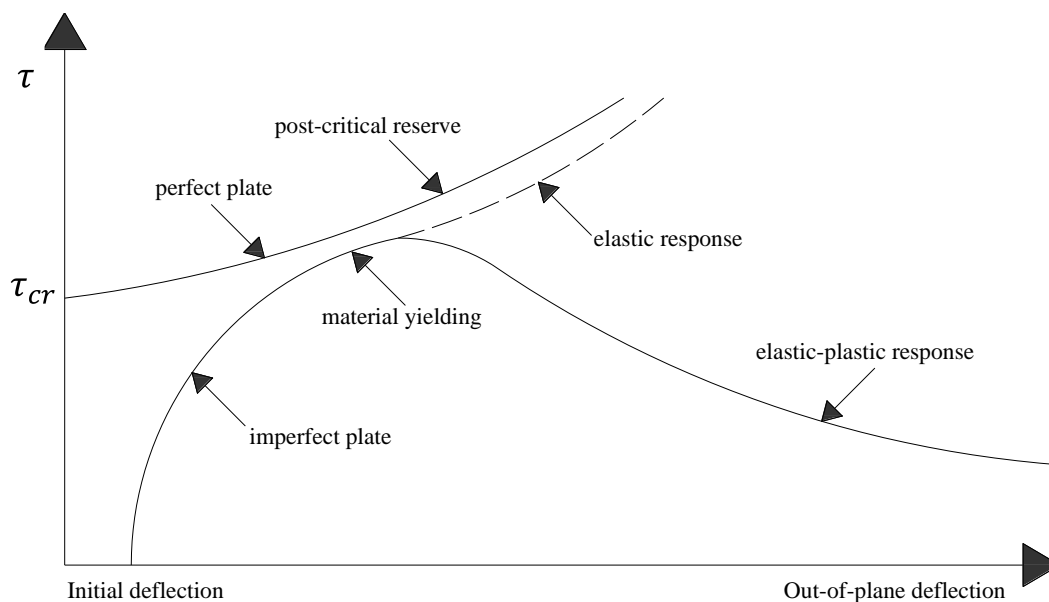


Figure 2.2 – Post-critical response of slender webs (Beg et al., 2010)

So the response of a web plate when subjected to shear can be divided in two different phases: before and after buckling. Before buckling, it is installed a combination of tensile and compressive stresses with equal magnitude (see Figure 2.3a). The principal compressive stress is the main responsible by the buckling of the web plate. After buckling, the buckled area of the web plate has no more compression capacity and a new load carrying mechanism develops, whereby the additional force is supported by the development of a tensile membrane stress field, the so-called “tension field” (see Figure 2.3b). But, it is only possible if the plate girder has capacity to anchor the tensile stresses. Some authors consider that when the capacity of tension field is reached, the flanges contribute to shear buckling resistance of the plate girder (see Figure 2.3c).

The tension field in a girder with stiffeners is anchored by the flanges and the stiffeners. But, even plate girders without transverse stiffeners are capable to achieve an ultimate shear strength that is much higher than the shear buckling resistance of the web. It is also important to note that the flanges clearly bend inwards under the action of the tension field and its dimension and inclination is highly affected by the rigidity of the flanges (Porter et al., 1975). The tensile stress grows with the increasing of the applied loading until the tensile stress combined with the buckling stress reaches the steel yield stress. The final collapse occurs when the web has yielded and plastic hinges have formed in the flanges.

As represented in Figure 2.3, most of the theories about the ultimate strength of plates subjected to shear buckling include three components (Eq. (2.1)):

- the elastic critical buckling load (V_{cr});
- the load corresponding to tension field (V_t);
- and, in some cases, the load corresponding to frame action (V_f):

$$V_{ult} = V_{cr} + V_t + V_f \quad (2.1)$$

The critical load is the first component of shear resistance capacity and it is obtained using the linear theory of buckling as follows

$$V_{cr} = h_w t_w \tau_{cr} \quad (2.2)$$

The elastic critical buckling stress τ_{cr} can be obtained assuming buckling as an instability phenomenon by bifurcation of equilibrium, based in the following assumptions:

- Plate is perfectly plane;
- Deflections due to buckling are moderate;
- Plate is requested by loads applied at its middle plane;
- Material with perfectly linear elastic behavior.

Thus, the elastic critical buckling stress of a plate without imperfections can be taken as

$$\tau_{cr} = k_\tau \sigma_E \quad (2.3)$$

where σ_E is the Euler's critical stress and it may be obtained by Eq. (2.4); the shear buckling coefficient k_τ is defined by Eqs. (3.7) to (3.9).

$$\sigma_E = \frac{\pi^2 E}{12(1-\nu^2)} \left(\frac{t_w}{h_w} \right)^2 \quad (2.4)$$

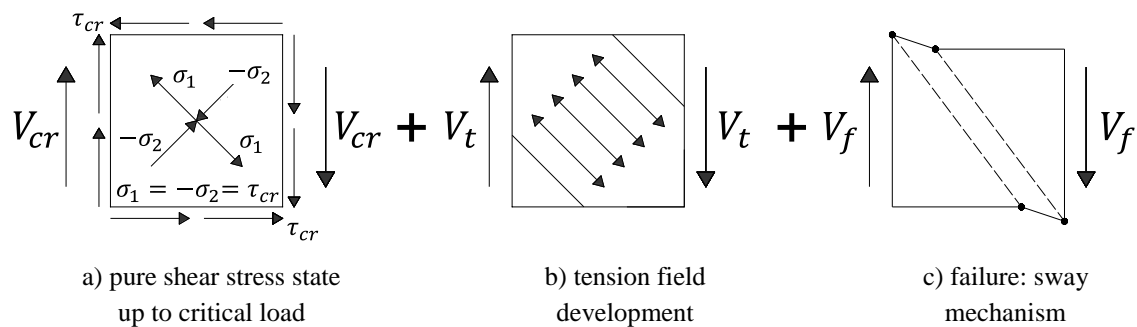


Figure 2.3 – Different steps of the behaviour of a plate girder under shear loading

2.2 Tension field models

Design shear resistance of steel plate girders is very important, since it is widely used in construction. Significant experimental and analytical research has been performed over the past century and several tension field models have been developed. Basically, and as it was described before, the tension field is a membrane stress field that makes the ultimate shear strength of the girder higher than its shear buckling resistance.

After buckling, the behaviour of a plate girder is similar to the behaviour of Pratt truss (see Figure 2.4). Diagonals support the tensile stresses and the posts resist to compressive stresses. In this analogy, each panel of a plate girder, limited by transverse stiffeners, acts as a module of Pratt truss. The web acts as a tensioned member, while transverse stiffeners act as compressed members to support the vertical component of tensile stresses that were developed on the web. Thus, it is assumed that transverse stiffeners are not loaded before the buckling occurrence and after buckling they are compressed (as the posts of Pratt truss). The horizontal component of tensile stresses is supported by the flanges of the adjacent panel.

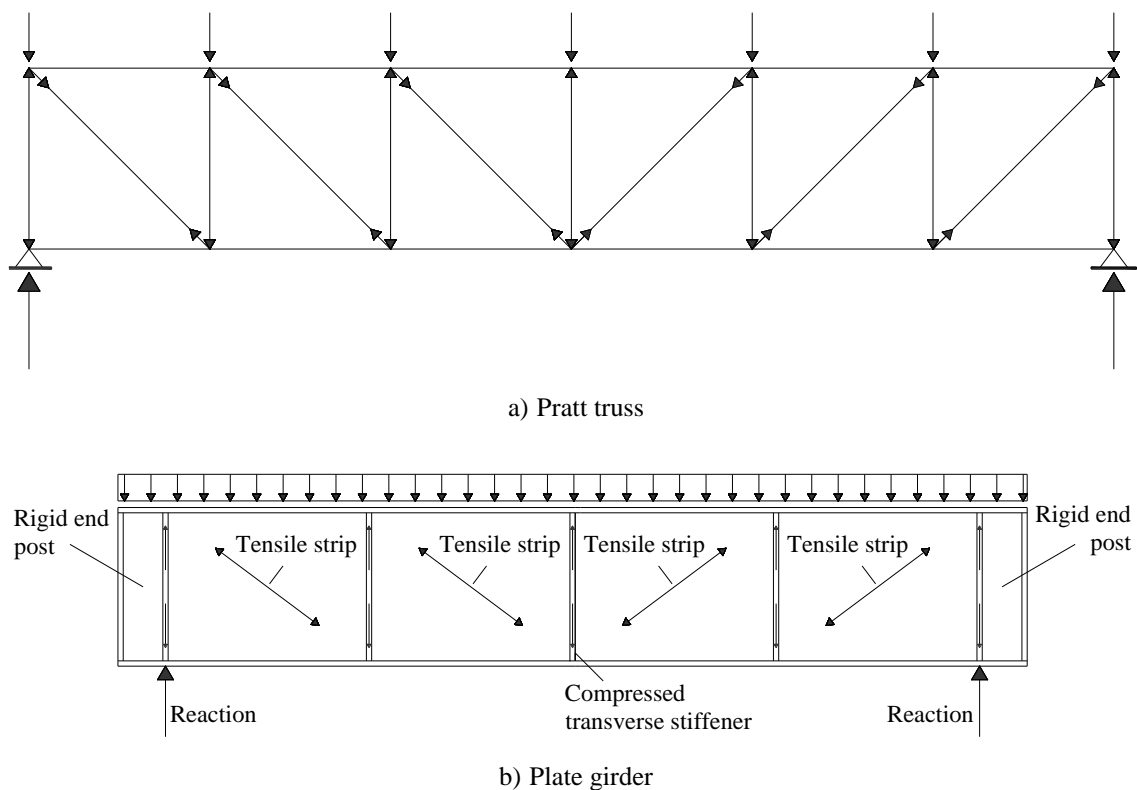


Figure 2.4 – Analogy between Pratt truss and a plate girder subjected to shear buckling

Historically, the tension field contribution to the ultimate shear strength of thin plates was recognized for the first time by Wilson (1886). Two decades later, investigations of post-critical behaviour conducted by Foppl (1907) and von Karman (1910) showed that web plates normally possess a huge post-critical reserve, but it was mobilized only at very large deflections (Bazant, 2000). The development of aeronautical science stimulated the study of shear resistance capacity of membrane-type structures, such as aircrafts. The condition to design this type of structures – minimize the self-weight of the structure – led to the utilization of very slender webs, which resulted on the application of the tension field concept (Gervásio, 1998).

According to Basler (1961a,1961b), the mathematical formulation of tension field effect was firstly presented by Rode (1916). The proposal consisted in evaluating the influence of tension field considering a tensile diagonal with a width equal to 50 times the web thickness (see Figure 2.5a). However, this theory was never used for design of plate girders because it was never experimentally tested. Later, Wagner (1931) presented the pure tension field theory (see Figure 2.5b) for girders with infinitely rigid flanges and very thin webs. Wagner developed his formulation based on the assumption that webs work as membranes with a uniform tension field, only supporting tensile forces.

Since then, a lot of investigations were focused on the ultimate shear strength of plate girders considering partial tension fields. Lahde and Wagner (1936) published empirical data based on deflection measures of buckled rectangular plates. Levy et al. (1945, 1946) studied the case of webs with transverse stiffeners forming square panels. Afterwards, several tests were conducted by the National Advisory Committee for Aeronautics (NACA) under coordination of Kuhn (1956). However, these initial studies were made with the aircraft design goal and had little applicability in the problems founded on design of plate girders in structures of buildings and bridges.

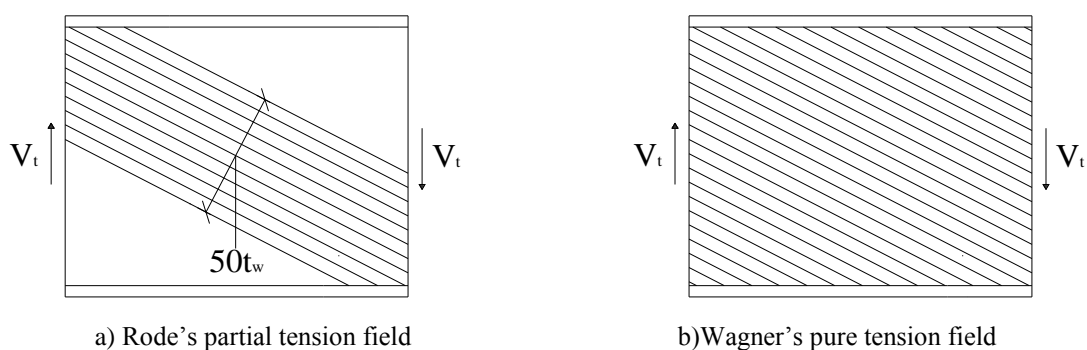


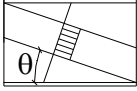
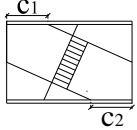
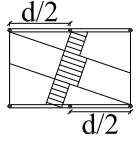
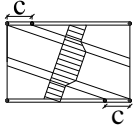
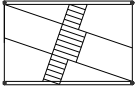
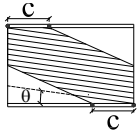
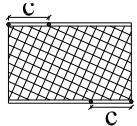
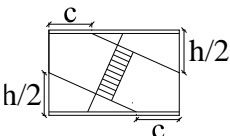
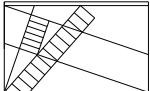
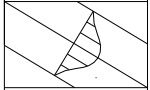
Figure 2.5 – First tension field theoretical models

During sixties and seventies, the consideration of the post-buckling behaviour of plates loaded in shear was extended from aeronautical applications to civil engineering. Investigations on the post-buckling behaviour of web panels conducted by Basler and Thürlimann (1959a, 1959b) led the American Institute of Steel Construction (AISC) to adopt the formulation suggested by them (AISC, 1963). In contrast to the assumption of infinitely rigid flanges made by Wagner, Basler and Thürlimann assumed conservatively that flanges are too flexible and thus not capable to support the lateral loading from tension field. Thus, the tension field would be anchored only in transverse stiffeners. However, soon after the appearance of this model, experimental results shown big differences when compared to the results obtained with the theoretical model. First it was assumed it was because the formulation was excessively simplified, but the true motive was the no consideration of the flanges resistance.

Since 1960, a lot of variations of the post buckling tension field have been developed following the Basler-Thürlimann model. Significant contributions were made by Rockey and Skaloud (1968, 1972) through experiments and analytical models. It was found that the post-buckling behaviour of a plate girder under shear loading was strongly influenced by the flexural rigidity of the flanges and the occurrence of collapse involved the formation of plastic hinges in both flanges. Based on these evidences, they proposed a method to predict the loads for which the webs of I cross-sections fail under shear, the so called Tension Field Method (Rockey et al., 1974). The precision of this model was established by comparisons with results of 58 tests obtained by various sources. These comparisons were summarized by Rockey et al. (1978).

Between these two limit theories, many researchers have provided various tension field models to predict the ultimate shear strength of steel plate girders, incorporating different positions of the plastic hinges if they are involved in the solution, boundary conditions of the web panel assumed for calculation of shear buckling stress and distributions of tension field action. Among these, the most relevant are the theories presented by Takeuchi (1964), Chern and Ostapenko (1969), Fujii (1971), Komatsu (1971), Sharp and Clark (1971), Steinhardt and Schroter (1971), Höglund (1971a, 1971b) and (Herzog, 1974). The main characteristics of these models are summarised in Table 2.1. More detailed information about them may be found in Galambos (1988).

Table 2.1 – Tension field theories in steel plate girders (Galambos, 1988)

Author	Mechanism	Web Buckling Edge Support	Unequal Flanges	Longitudinal Stiffener	Shear and Moment
Basler (1961a,1961b)		$\begin{matrix} & S & \\ S & & S \\ & S & \end{matrix}$	-	Yes, (Cooper, 1965)	Yes
Takeuchi (1964)		$\begin{matrix} & S & \\ S & & S \\ & S & \end{matrix}$	Yes	No	No
Fujii (1971)		$\begin{matrix} & F & \\ S & & S \\ & F & \end{matrix}$	Yes	Yes	Yes
Komatsu (1971)		$\begin{matrix} & F & \\ S & & S \\ & F & \end{matrix}$	No	Yes, at mid-depth	No
Chern and Ostapenko (1969)		$\begin{matrix} & F & \\ S & & S \\ & F & \end{matrix}$	Yes	Yes	Yes
Rockey et al. (1974)		$\begin{matrix} & S & \\ S & & S \\ & S & \end{matrix}$	Yes	Yes	Yes
Höglund (1971a, 1971b)		$\begin{matrix} & S & \\ S & & S \\ & S & \end{matrix}$	No	No	Yes
Herzog (1974)		Web buckling component neglected	Yes, in evaluating c	Yes	Yes
Sharp and Clark (1971)		$\begin{matrix} & F/2 & \\ S & & S \\ & F/2 & \end{matrix}$	No	No	No
Steinhardt and Schroter (1971)		$\begin{matrix} & S & \\ S & & S \\ & S & \end{matrix}$	Yes	Yes	Yes

The Rockey's Tension Field Method was adopted in the experimental version of Part 1-1 of EC3 (IPQ, 1998) to calculate the ultimate shear strength of plate girders with transverse stiffeners. In this first version of Part 1-1 of EC3, it was also implemented the Simple Method of Post Critical Strength, a more conservative method that could be used for girders with or without transverse stiffeners. In this method the contribution of the flanges is not taken into account. Presently, these methods are no longer in the European Standards and the Rotated Stress Field Method developed by Höglund (1972) is the basis of the expressions adopted in Part 1-5 of EC3 (CEN, 2006b) for design of steel plate girders subjected to shear buckling.

Rotated Stress Field Method is based on the assumption that the web panel is under a pure shear stress state that occurs preceding buckling. If these shear stresses τ were transformed in principal stresses, they would correspond to principal tensile stresses σ_1 and principal compressive stresses σ_2 with equal magnitude ($\sigma_1 = \sigma_2$) and inclined by 45° relatively to the longitudinal axis of the girder. Once buckling occurs ($\tau = \tau_{cr}$), the web panel has no more compression capacity and it can be assumed that the principal compressive stresses (σ_2) remain equal to the elastic critical buckling stress (τ_{cr}). But, for webs in shear, there is a substantial post-critical reserve. After buckling, the web plate achieves the post-critical stress state, while a shear buckle forms in the direction of the principal tensile stresses (σ_1) and the increase of load is resisted by an increase in the principal tensile stresses (σ_1). As a result, stress values of different magnitude occur ($\sigma_1 > \sigma_2$) which, to keep the equilibrium, leads to a rotation of the stress field. This method is illustrated in Figure 2.6. Detailed information about it may be found in Höglund (1972, 1997).

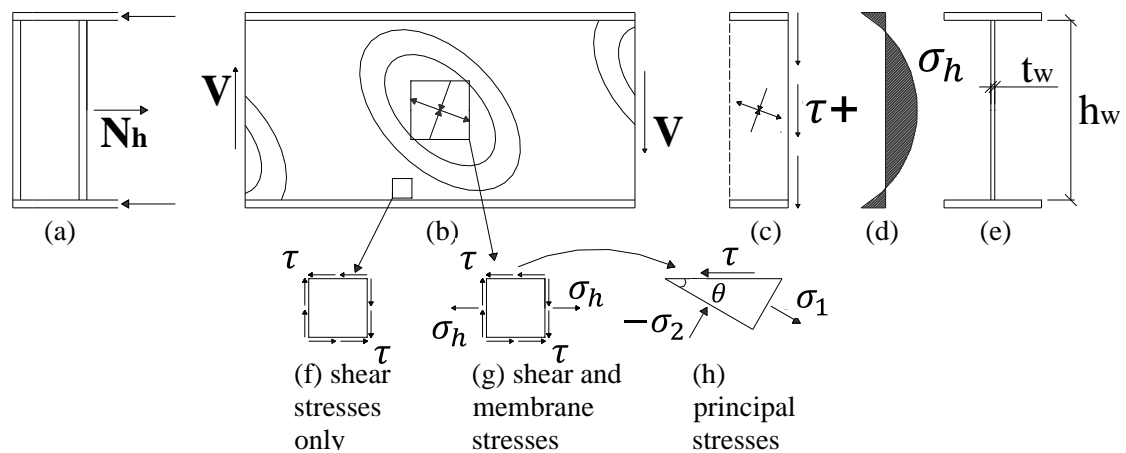


Figure 2.6 – State of stress in a plate girder subjected to shear with transverse stiffeners at the ends only according to the Rotated Stress Field Method (Johansson et al., 2007)

In this model, the horizontal component of the tension field (σ_h) acting across the web depth is resisted by the end panels, which act as beams resting on the girders flanges. These end panels, also called end posts, may be composed by pairs of transverse stiffeners placed in each side of the girder. They may be designed as rigid or non-rigid. Unlike other tension field models which are limited to specific aspect ratios (typically $a/h_w \leq 3$), the Rotated Stress Field Model may be applied for all aspect ratios and can be equally applied for stiffened and unstiffened plate girders. A reduction factor for the web contribution to shear buckling (χ_w) is introduced to allow for initial imperfections observed in experimental tests. The predictions of the Rotated Stress Field Method were compared with experimental tests, as shown in Figure 2.7. A complete description of this method may be found in Höglund (1997).

In the last years, the accuracy of these methods at normal temperature have been extensively analysed by Lee and his research group. The boundary conditions have been conservatively assumed as simply supported when calculating the elastic critical buckling stress, but Lee et al. (1996) stated that the real boundary conditions of the web panel should be considered in the formulations. Moreover, they concluded that the boundary conditions are highly influenced by the presence of the flanges (Lee & Yoo, 1998). Recently, based on numerical investigations, Yoo and Lee (2006) found that compressive stresses may not remain constant over the web panel, but may increase progressively nearness the edges of the web panel where the out-of-plane deflections are smaller. It has also been found that Basler's equation is not applicable to long web panels ($a/h_w \geq 3$) since it underestimates their post-buckling strength (Lee et al., 2008).

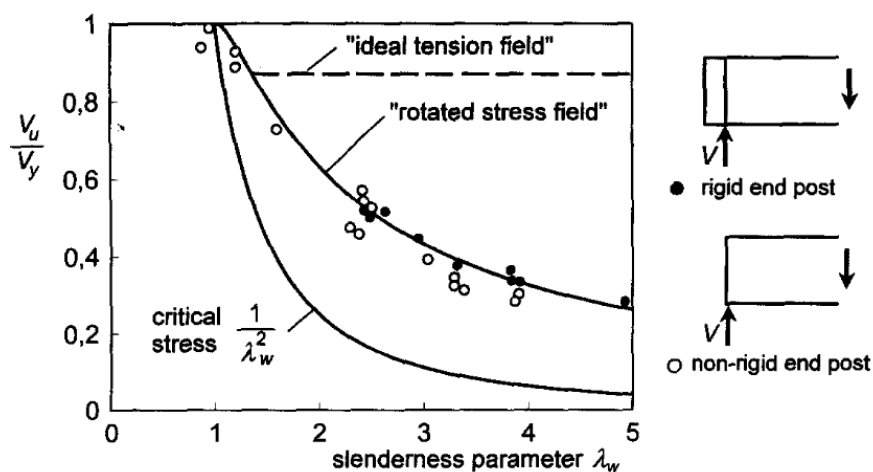


Figure 2.7 – Rotated Stress Field Method vs. experimental tests (Höglund, 1997)

2.3 Current state of research

As already mentioned, the ultimate shear strength of steel plate girders was widely studied at normal temperature. For that reason, researchers have been focusing their investigations over the past decade on different topics within the ultimate shear strength of plate girders, such as: design of stainless steel plate girders; interaction between shear and bending; and fire design of steel plate girders.

Since the procedures for design of carbon steel structures subjected to shear buckling at normal temperature were well established, stainless steel has become the focus of the shear buckling study at normal temperature. Traditionally, the stainless steel design rules have been based on analogies with those adopted for carbon steel, with some adjustments made when necessary to fit with test results. Olsson (2001) provided a method based on the Rotated Stress Field Method with some modifications in the expressions for the calculation of the reduction factor for the web resistance to shear buckling and in the definition of the distance where the plastic hinges appear. This method was included in Part 1-4 of EC3 (CEN, 2006a) for the design of stainless steel plate girders subjected to shear buckling.

Experimental campaigns were carried out at Polytechnic University of Catalunya (UPC) to better understand the response of stainless steel plate girders under shear loading (Real et al., 2007). The comparative analysis of the experimental results with current codes' prescriptions showed that shear design procedures are overly conservative (Estrada et al., 2007a). The experimental tests results were used by the same authors for calibration of numerical models, which were used in an extended numerical analysis carried out concerning the evaluation of the post-buckling strength in stainless steel plate girders (Estrada et al., 2007b). These experimental tests were also used for calibration of a numerical model for stainless steel plate girders subjected to shear buckling at elevated temperatures (Reis et al., 2016b). The numerical results also showed that the prescriptions present in EC3 for the design of stainless steel plate girders are too conservative, which led to the development of a new approach based on the Rotated Stress Field Method and adequately adapted to the particular features of stainless steel (Saliba et al., 2014), which was already accepted for incorporation in Part 1-4 of EC3 (CEN, 2006a).

Recently, the interaction between shear and bending has also become a common topic on the research activities of several authors. Part 1-5 of EC3 (CEN, 2006b) has adopted an expression for the verification of the shear-bending interaction in plate girders, which is based on slightly modified Basler's approach (Basler et al., 1960; Basler, 1961b).

Sinur and Beg (2013b) performed experimental tests to better understanding the behaviour of steel plate girders subjected to combination of shear force and bending moment and to get data for the validation of the numerical model in order to evaluate the reliability of the existing models (Sinur & Beg, 2013a). Longitudinally stiffened and unstiffened webs were considered. It was observed that the resistance strongly depends on the stress distribution in the sub-panels and on the rigidity of the longitudinal stiffeners. Graciano and Ayestarán (2013) concluded that the interaction between shear and bending may cause a significant reduction on the ultimate resistance of steel plate girders. Other authors as Kövesdi et al. (2014a, 2014b) also studied this topic considering longitudinally unstiffened and stiffened plate girders, resulting on the proposal of new design expressions.

Despite the growing interest about the fire performance of steel plate girders affected by shear buckling, only limited experimental tests have been performed at elevated temperatures. Vimonsatit et al. (2007) were the first to perform fire resistance experimental tests in steel plate girders loaded in shear. They tested transversally stiffened plate girders with slender webs in a three-point bending configuration at normal temperature and under three different uniform temperatures: 400°C, 550°C and 700°C. Tension field action and formation of plastic hinges were observed. Elevated temperatures caused a reduction on the ultimate shear strength of approximately 15-31% at 400°C, 52-66% at 550°C and 78-86% at 700°C.

Tan and Qian (2008) conducted similar tests but with addition of axial restrains in order to simulate the thermal restraint effects of adjacent cooler parts of steel-framed structure in fire. It was observed that the ultimate shear strength decreased significantly under a thermal restraint effect, mainly for the plate girders with more slender webs. These experiments are very important since they allow observing the significant degradation of the ultimate bearing capacity caused by exposing a steel plate girder to elevated temperatures such as those which occur during a fire. They are also important in confirming that the failure modes observed at normal temperature are also observed at

elevated temperatures. Moreover, fire resistance experimental tests are crucial for the validation of numerical models used to perform extended parametric studies (Reis et al., 2016a, 2016b). Thus, these fire resistance experimental tests were part of all experimental tests considered for the validation of the numerical model developed within the scope of the study of the shear buckling occurrence in steel plate girders exposed to fire (Reis et al., 2016c, 2016d).

Vimonsatit et al. (2007a) conducted a numerical investigation using a numerical model duly validated with their fire resistance experimental tests. From this investigation a new model to predict the ultimate shear strength of steel plate girders subjected to elevated temperatures has been proposed. This model is based on Rockey's model (Rockey et al., 1974) and considers the material properties in function of the temperature according to Part 1-2 of EC3 (CEN, 2010b). In order to simplify, uniform temperature distribution is assumed within the full web depth.

Numerical investigations conducted by Payá-Zaforteza and Garlock (2012) and Garlock and Glassman (2014) indicated that incorporating strain-hardening in material model had little effect on the ultimate shear strength and longitudinally restricted models deflected substantially less than those that were free. Furthermore, it was possible to observe the development of thermal gradients across the cross-section depth.

A numerical study about thin steel plates loaded in shear at non-uniform elevated temperatures was performed by Scandella et al. (2014) in which it was shown that the non-uniform temperatures can impose additional loading and even change the failure mode. The large differences between the flanges and web thicknesses can lead to a faster heating in the web than flanges, resulting in the development of thermally induced compressive stresses in the web, which will accelerate the local failure. Thus, a steel plate girder with a bending dominant failure at normal temperature may instead exhibit a shear dominant failure at elevated temperatures with non-uniform heating. However, it is important do not forget the difficulty of implementing in the European Standards a simple calculation method that includes non-uniform temperatures.

A new design method for predicting the shear resistance of thin steel plate at non-uniform elevated temperatures has been proposed by Salminen and Heinisuo (2014). The basic idea of the method is to reduce the ultimate shear strength of the plate based on a reference temperature, which is hotter than the average temperature but colder than

the maximum temperature. The authors suggested that non-uniform temperature distributions should be converted into an equivalent uniform temperature, which highlights the importance to use simple design methods giving safe predictions.

Although this Chapter is mainly focused on the behaviour of plate girders under shear loading, it is important to note that in practice plate girders also require bending resistance and the shear-bending interaction should also be taken into account. Furthermore, although it has been tried to refer all the essential studies, others relevant research works may have been unconsciously omitted.

Chapter 3

Eurocode design rules

Chapter 3 Eurocode design rules

- 3.1 General considerations
- 3.2 Shear resistance
 - 3.2.1 Resistance from the web to shear buckling
 - 3.2.2 Contribution from the flanges
 - 3.2.3 Verification
- 3.3 Interaction between shear and bending
- 3.4 Stiffeners
 - 3.4.1 Transverse stiffeners
 - 3.4.1.1 Rigid end posts
 - 3.4.1.2 Non-rigid end posts
 - 3.4.1.3 Intermediate transverse stiffeners
 - 3.4.2 Longitudinal stiffeners
- 3.5 Design at elevated temperatures

Chapter 3 Eurocode design rules

3.1 General considerations

In order to better understand the design formulation proposed in EC3, in first place it is important to understand what a plated structure is: “A *plated structure* is a structure built up from nominally flat plates which are connected together; the plates may be stiffened or unstiffened” (CEN, 2006b).

This section dedicated to the design procedures is divided in several parts dealing with different topics. In the first part it is presented the design rules according to Part 1-5 of EC3 (CEN, 2006b) to determinate the design shear resistance at normal temperatures. The second part is dedicated to the interaction between the shear force and the bending moment. On the third part some considerations about stiffeners are made and finally, it is presented the methodology adopted to predict the ultimate shear strength of steel plate girders under fire, based on Parts 1-2 (CEN, 2010b) and 1-5 of EC3 (CEN, 2006b).

3.2 Shear resistance

As mentioned before, Torsten Höglund developed the so-called Rotated Stress Field Method (Höglund, 1972) which was implemented in Part 1-5 of EC3 (CEN, 2006b) with some modifications (Höglund, 1997). Originally, it was developed for girders with web stiffeners at the supports only, because the other existing methods were very conservative for this case. It has in consideration the resistance from the web to shear buckling and the resistance contribution from the flanges to the same instability phenomenon, which are obtained separately. The web resistance to shear buckling includes a reduction factor to account for different features which influence the bearing capacity of the girders, as for example the initial imperfections. This reduction factor depends on the girder end posts: rigid or non-rigid. Girders with rigid end posts are supposed to reach higher ultimate loads.

According to Part 1-5 of EC3, the shear buckling resistance has to be checked when the following conditions are satisfied:

- For unstiffened webs: $\frac{h_w}{t_w} > 72 \frac{\epsilon}{\eta}$
- For stiffened webs: $\frac{h_w}{t_w} > 31 \frac{\epsilon}{\eta} \sqrt{k_\tau}$

where $\varepsilon = \sqrt{\frac{235}{f_y}} \sqrt{\frac{E}{210000}}$ with f_y and E in [MPa].

In case these limits are exceeded, the girder should be provided with transverse stiffeners at the supports.

The design shear resistance ($V_{b,Rd}$) is taken as a sum of the resistance from the web to shear buckling ($V_{bw,Rd}$) and the flanges contribution ($V_{bf,Rd}$). However, the design shear resistance cannot be higher than the plastic shear resistance of the web alone, as presented in in Eq. (3.1).

$$V_{b,Rd} = V_{bw,Rd} + V_{bf,Rd} \leq h_w t_w \frac{\eta f_{yw}}{\sqrt{3} \gamma_{M1}} \quad (3.1)$$

According to Part 1-5 of EC3, the recommended values for η are as follows

$$\begin{aligned} \eta &= 1.2 \text{ for } f_y \leq 460 \text{ MPa} \\ \eta &= 1.0 \text{ for } f_y > 460 \text{ MPa} \end{aligned} \quad (3.2)$$

It is important to note that the National Annexes of EC3 may give different values for η , depending on the field of application.

3.2.1 Resistance from the web to shear buckling

The contribution from the web to shear buckling resistance may be obtained as follows

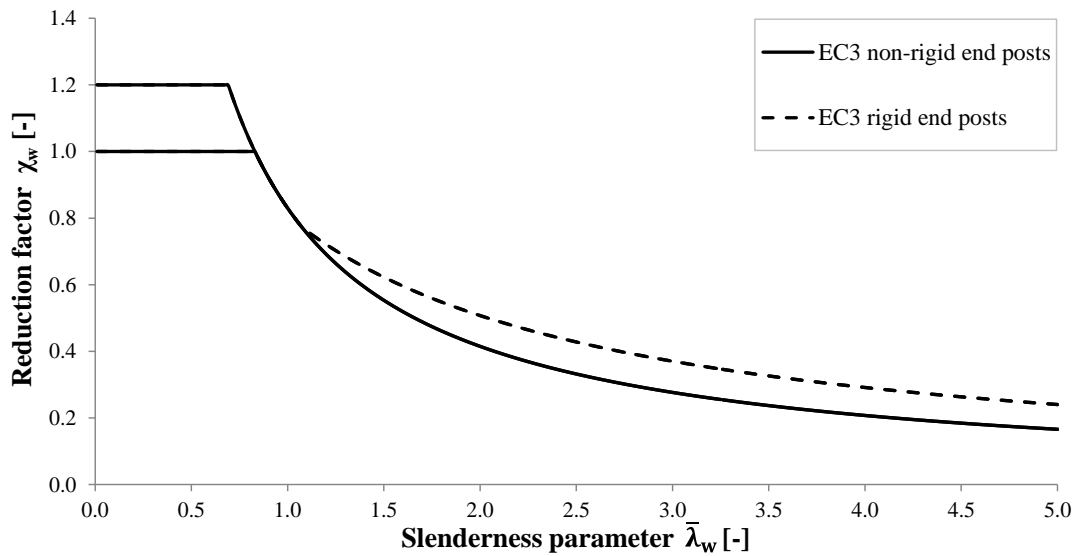
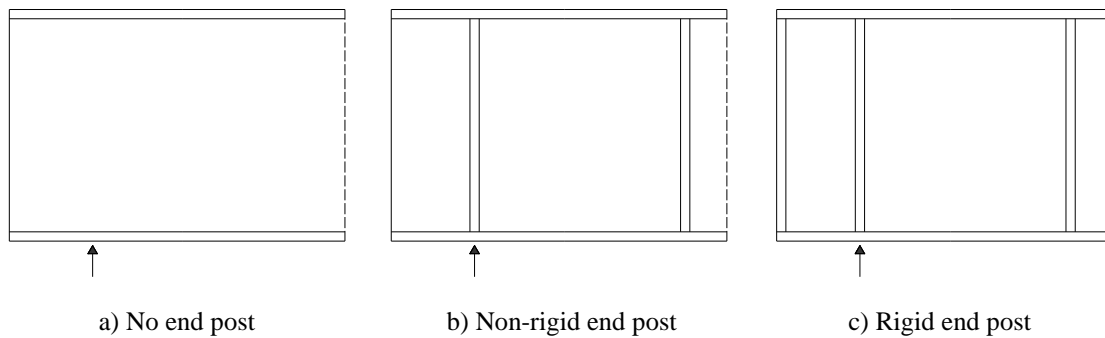
$$V_{bw,Rd} = \chi_w h_w t_w \frac{f_{yw}}{\sqrt{3} \gamma_{M1}} \quad (3.3)$$

The reduction factor for the web contribution to shear buckling resistance is valid for both unstiffened and stiffened webs and may be obtained from Table 3.1. This reduction factor is also plotted in Figure 3.1 in function of the web slenderness parameter, depending on the end supports (see Figure 3.2).

As shown in Figure 3.1, χ_w can take values larger than 1.0 for plate girders with steel yield strength up to 460 MPa due to strain hardening. Tests on stocky beams showed, for this range of steel yield strength, that the ultimate shear strength may reach 70% to 80% of the tensile yield strength, which corresponds approximately to an increase of 20% of the shear yield strength. It may be accepted since it does not lead to excessive deformations (Beg et al., 2010).

Table 3.1 – Reduction factor for the web contribution to shear buckling (χ_w)

	Rigid end post	Non-rigid end post
$\bar{\lambda}_w < 0.83/\eta$	η	η
$0.83/\eta \leq \bar{\lambda}_w < 1.08$	$0.83/\bar{\lambda}_w$	$0.83/\bar{\lambda}_w$
$\bar{\lambda}_w \geq 1.08$	$1.37/(0.7 + \bar{\lambda}_w)$	$0.83/\bar{\lambda}_w$

**Figure 3.1 – Reduction curves for the web contribution to shear buckling****Figure 3.2 – End supports**

As it was said before, the reduction factor for the web contribution to shear buckling can be applied for the verification of both unstiffened and stiffened webs. The web slenderness parameter $\bar{\lambda}_w$ is determined using Eq. (3.4) for unstiffened webs. In case of a stiffened panel, the $\bar{\lambda}_w$ largest value of all sub-panels should be used. To simplify the application of Eq. (3.4) to stiffened panels, $\bar{\lambda}_w$ can be obtained by Eqs. (3.5) and (3.6).

- For unstiffened plate girders:

$$\bar{\lambda}_w = \frac{h_w}{37.4 t_w \varepsilon \sqrt{k_\tau}} \quad (3.4)$$

- For transverse stiffeners at supports only ($k_\tau = 5.34$):

$$\bar{\lambda}_w = \frac{h_w}{86.4 t_w \varepsilon} \quad (3.5)$$

- For transverse stiffeners at supports plus intermediate stiffeners or longitudinal stiffeners or both (see Figure 3.3):

$$\bar{\lambda}_w = \max\left(\frac{h_w}{37.4 t_w \varepsilon \sqrt{k_\tau}}; \frac{h_{w,i}}{37.4 t_w \varepsilon \sqrt{k_{\tau,i}}}\right) \quad (3.6)$$

The Annex A.3 of Part 1-5 of EC3 (CEN, 2006b) explains how to obtain the shear buckling coefficient k_τ . This is a hand calculation process, but buckling charts and advanced software may also be used.

- For panels without longitudinal stiffeners such as sub-panels of stiffened panels or for panels with rigid transverse stiffeners only ($k_{\tau sl} = 0$):

$$\begin{aligned} k_\tau &= 4.00 + 5.34 \left(\frac{h_w}{a}\right)^2 & \text{for } \frac{a}{h_w} < 1.0 \\ k_\tau &= 5.34 + 4.00 \left(\frac{h_w}{a}\right)^2 & \text{for } \frac{a}{h_w} \geq 1.0 \end{aligned} \quad (3.7)$$

- For stiffened panels with one or two longitudinal stiffeners and $\alpha = a / h_w < 3.0$:

$$k_\tau = 4.10 + \frac{6.30 + 0.18 \frac{I_{sl}}{t^3 h_w}}{\alpha^2} + 2.20 \sqrt[3]{\frac{I_{sl}}{t^3 h_w}} \quad (3.8)$$

- For stiffened panels with one or two longitudinal stiffeners and $\alpha = a / h_w \geq 3.0$
or

for stiffened panels with more than two longitudinal stiffeners:

$$\begin{aligned} k_\tau &= 4.00 + 5.34 \left(\frac{h_w}{a}\right)^2 + k_{\tau sl} & \text{for } \frac{a}{h_w} < 1.0 \\ k_\tau &= 5.34 + 4.00 \left(\frac{h_w}{a}\right)^2 + k_{\tau sl} & \text{for } \frac{a}{h_w} \geq 1.0 \end{aligned} \quad (3.9)$$

with

$$k_{\tau sl} = \max \left(9.00 \left(\frac{h_w}{a} \right)^2 \sqrt[4]{\left(\frac{I_{sl}}{t^3 h_w} \right)^3}; \frac{2.10}{t} \sqrt[3]{\frac{I_{sl}}{h_w}} \right) \quad (3.10)$$

The moment of inertia of the longitudinal stiffener I_{sl} is obtained considering an effective plate width of $15\epsilon t$ above and below of the stiffener until the maximum existing geometrical width without overlapping parts, as illustrated in Figure 3.4. It is obtained for perpendicular buckling to the plane of the plate. For stiffened panels with two or more longitudinal stiffeners, I_{sl} is calculated as the sum of all individual stiffeners either if they have an equidistant spacing between them or not. More information about stiffeners is presented later in this Chapter.

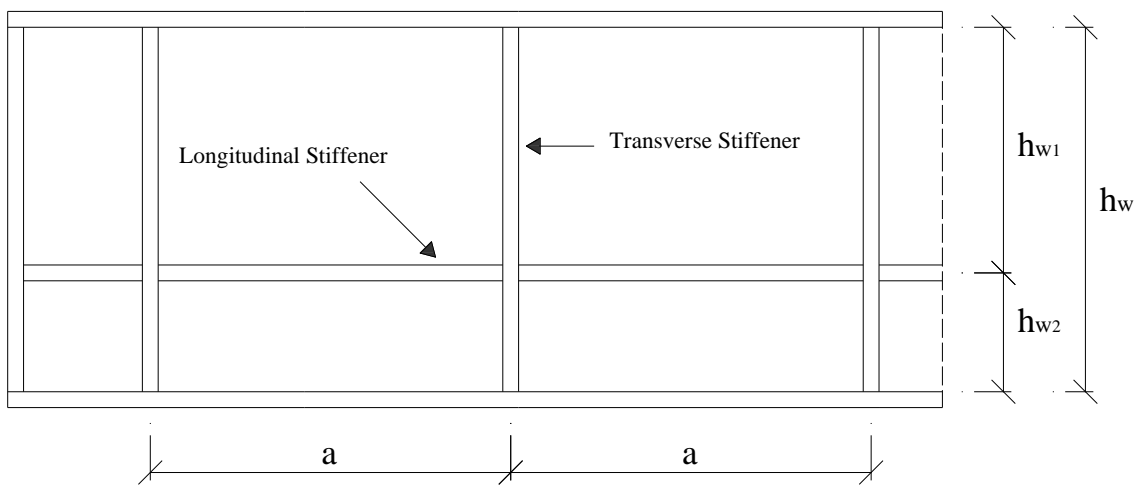


Figure 3.3 – Notation used to obtain the web slenderness parameter and the shear buckling coefficient of a stiffened plate girder

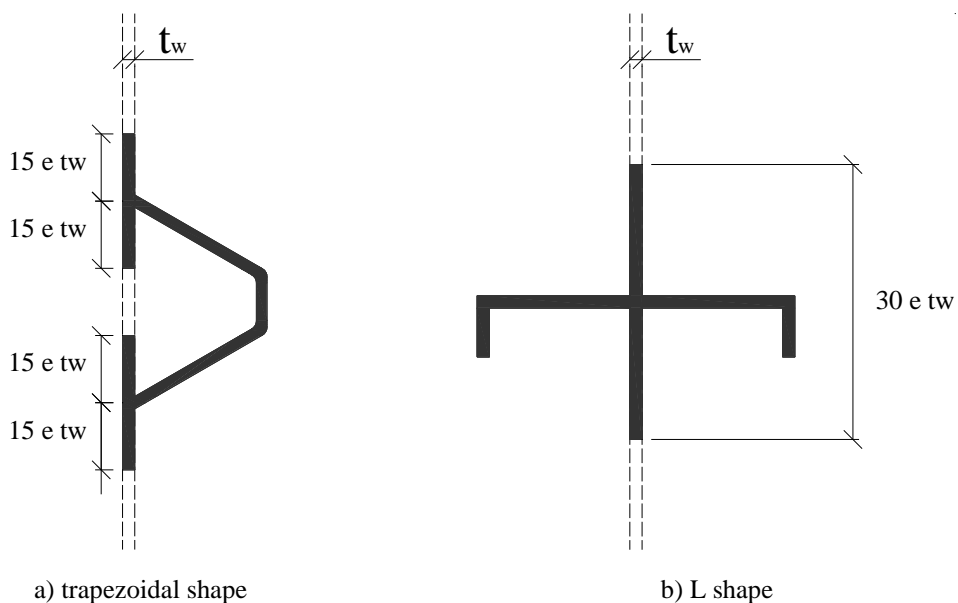


Figure 3.4 – Effective cross-section of stiffeners

During the calculation of the shear buckling coefficient (k_t), a reduction of the moment of inertia of the longitudinal stiffener (I_{sl}) to 1/3 of its actual value is required. Eqs. (3.8) and (3.9) already take this reduction into account. However, some investigations (Kuhlmann et al., 2007; Pavlovčič et al., 2007) have shown that such reduction is only necessary for stiffeners with a small torsional rigidity (e.g. flat bar stiffeners). Concerning longitudinal stiffeners with large torsional rigidity (e.g. trapezoidal shaped stiffeners), the actual value of the moment of inertia may be considered (Beg et al., 2010).

Part 1-5 of EC3 has verification schemes for the case of utilization of intermediate non-rigid transverse stiffeners, but no formulas are given to determinate the shear buckling coefficients for girders provided with this type of stiffeners, with exception of girders provided with non-rigid transverse stiffeners at supports only. One solution to this lack of guidance is to calculate the shear buckling coefficient using adequate software. However, it is important to note that, in modern steel structures, intermediate non-rigid transverse stiffeners are rarely applied in practice, since the increase of strength may be very low. Even intermediate rigid transverse stiffeners are not widely used, because their utilization normally does not compensate the additional cost of welding.

3.2.2 Contribution from the flanges

The flanges contribution to shear buckling resistance is given Eq. (3.11), which assumes the formation of four plastic hinges in the flanges at the distance c (see Figure 3.5).

$$V_{bf,Rd} = \frac{b_f t_f^2}{c} \frac{f_{yf}}{\gamma_{M1}} \left[1 - \left(\frac{M_{Ed}}{M_{f,Rd}} \right)^2 \right] \quad (3.11)$$

where M_{Ed} should be taken as the largest moment within the panel and c is obtained by

$$c = a \left(0.25 + \frac{1.60 b_f t_f^2 f_{yf}}{t_w h_w^2 f_{yw}} \right) \quad (3.12)$$

Eq. (3.1) can be rewritten using Eqs. (3.3) and (3.11) as follows

$$V_{b,Rd} = V_{bw,Rd} + V_{bf,Rd} = (\chi_w + \chi_f) h_w t_w \frac{f_{yw}}{\sqrt{3} \gamma_{M1}} \quad (3.13)$$

where χ_w is obtained from Table 3.1 and χ_f , the reduction factor for the flange contribution to shear buckling resistance, is given by Eq. (3.14).

$$\chi_f = \frac{b_f t_f^2 f_{yf} \sqrt{3}}{c t_w h_w f_{yw}} \left[1 - \left(\frac{M_{Ed}}{M_{f,Rd}} \right)^2 \right] \quad (3.14)$$

Note that the flange width should not exceed $15\epsilon t$ on each side of the web and b_f and t_f are the dimensions of the flange with the least axial resistance.

The contribution from the flanges is reduced if they resist to longitudinal stresses due to normal force N_{Ed} or bending moment M_{Ed} . This reduction is considered in the last term of Eq. (3.11). The resistance moment of the cross-section consisting of the effective area of the flanges only ($M_{f,Rd}$) is obtained according to Eq. (3.15), being reduced when N_{Ed} is acting.

$$M_{f,Rd} = \frac{M_{f,k}}{\gamma_{M0}} \left[1 - \frac{N_{Ed}}{(A_{f1} + A_{f2}) \frac{f_{yf}}{\gamma_{M0}}} \right] \quad (3.15)$$

where

$$M_{f,k} = \min(A_{f,1} f_{yf,1} h_f; A_{f,2} f_{yf,2} h_f);$$

$A_{f,1} = b_{f,1} t_{f,1}$ and $A_{f,2} = b_{f,2} t_{f,2}$ are the cross-sectional areas of flange 1 and 2;

$f_{yf,1}$ and $f_{yf,2}$ are the yield strengths of flange 1 and 2;

h_f is the distance between mid-plane of flanges (see Figure 3.5).

So Eqs. (3.11) and (3.15) considers an interaction between shear force, bending moment and normal force for $M_{Ed} < M_{f,Rd}$. It is important to note that for $M_{Ed} \geq M_{f,Rd}$, $V_{bf,Rd}$ is null and the design shear resistance is given by the web only.

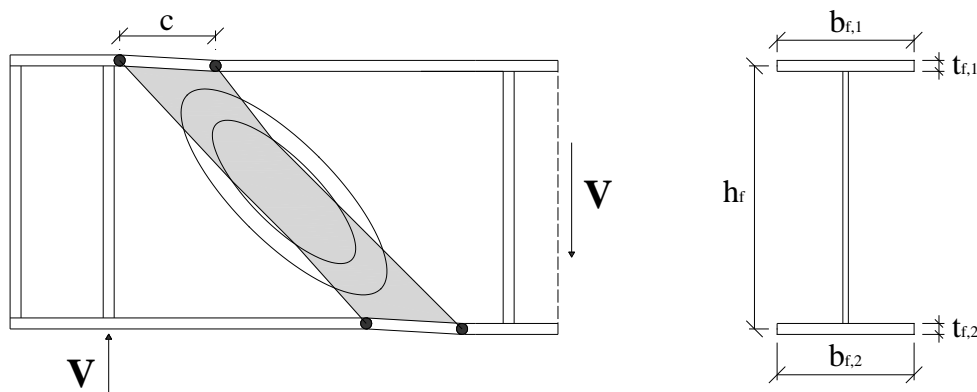


Figure 3.5 – Anchorage of the tension field in the flanges

3.2.3 Verification

The verification of a plate girder under shear loading is done as follows

$$\eta_3 = \frac{V_{Ed}}{V_{b,Rd}} \leq 1.0 \quad (3.16)$$

Figure 3.6 shows the steps needed to check the shear resistance of a steel plate girder.

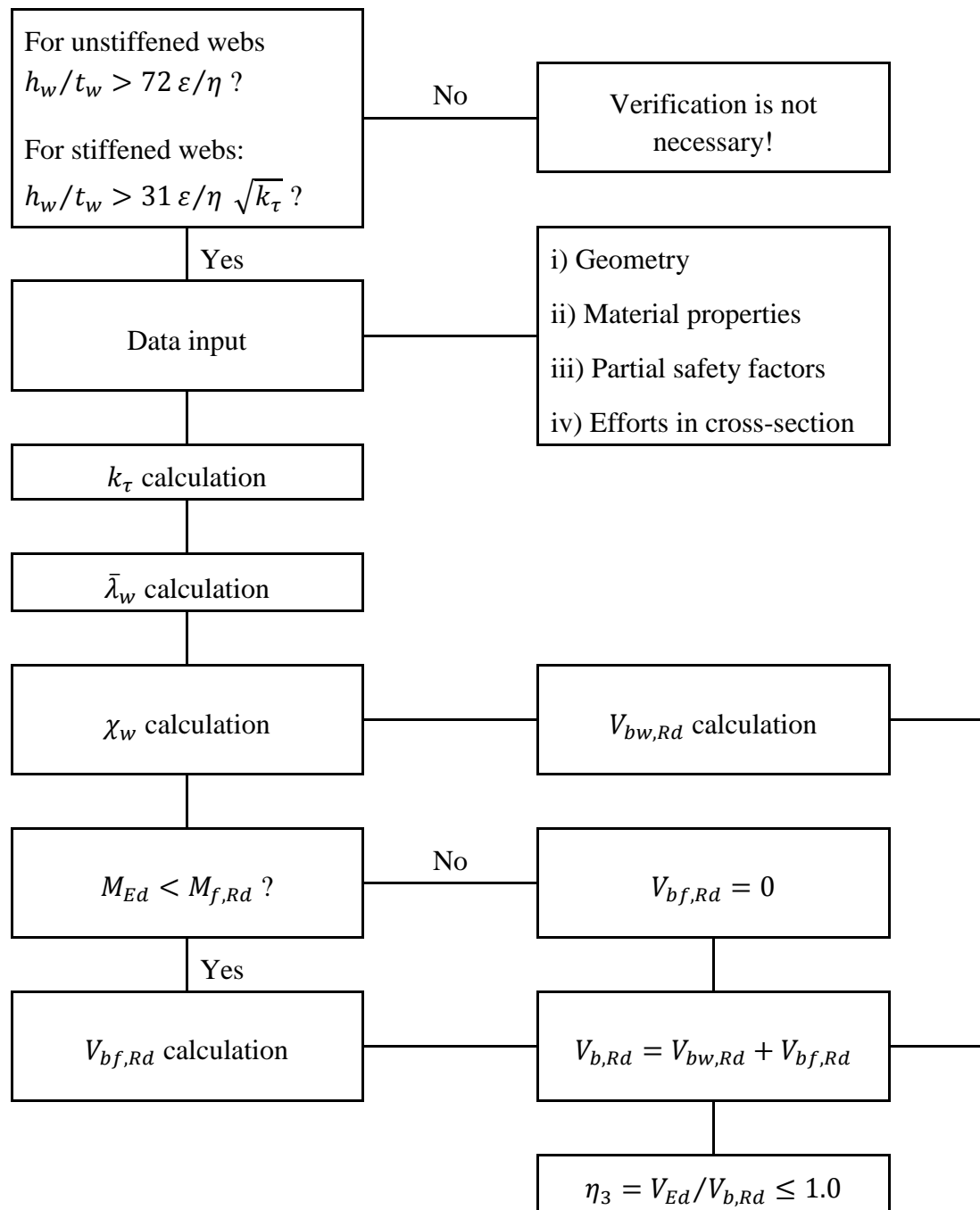


Figure 3.6 – Calculation algorithm

3.3 Interaction between shear and bending

Clause 7 of Part 1-5 of EC3 (CEN, 2006b) states that the shear-bending interaction should be checked and satisfy Eq. (3.17) when the two following criteria are satisfied:

- $V_{Ed} > 0.5V_{bw,Rd}$
- $M_{Ed} \geq M_{f,Rd}$

$$\frac{M_{Ed}}{M_{pl,Rd}} + \left(1 - \frac{M_{f,Rd}}{M_{pl,Rd}}\right) \left(\frac{2V_{Ed}}{V_{bw,Rd}} - 1\right)^2 \leq 1 \quad (3.17)$$

in which $M_{pl,Rd}$ is the design plastic resistance of the cross-section, considering the effective area of the flanges and the fully effective web, irrespective of its section class.

Note that the bending resistance also needs to be checked, according to point 4.6 of Part 1-5 of EC3. Therefore, in the case of sections with Class 1 or 2, the interaction curve given by Eq. (3.17) must be truncated by the vertical line that cuts the horizontal axis in $M_{pl,Rd}$ (see Figure 3.7), the plastic resistance bending moment. Regarding sections with Class 3 or 4, it should be truncated by the vertical line that cuts the horizontal axis in $M_{c,Rd}$ (see Figure 3.8), the elastic resistance bending moment or the effective resistance bending moment, respectively.

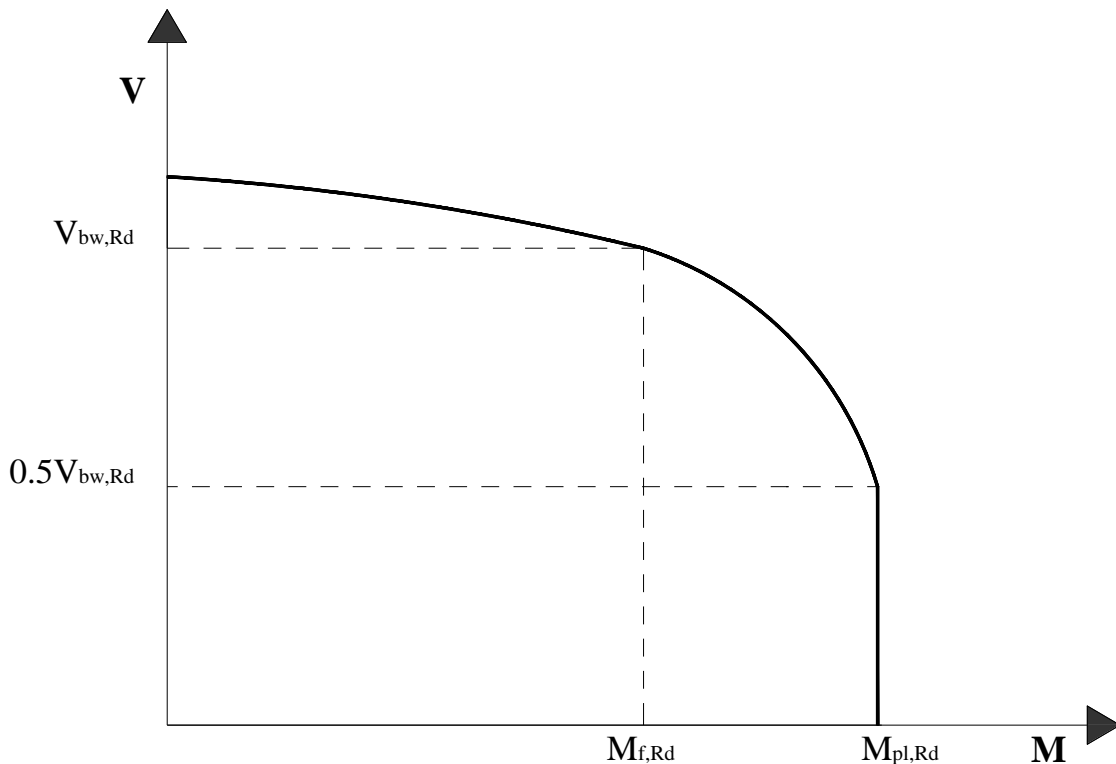


Figure 3.7 – Shear-bending interaction diagram for profiles with Class 1 or 2

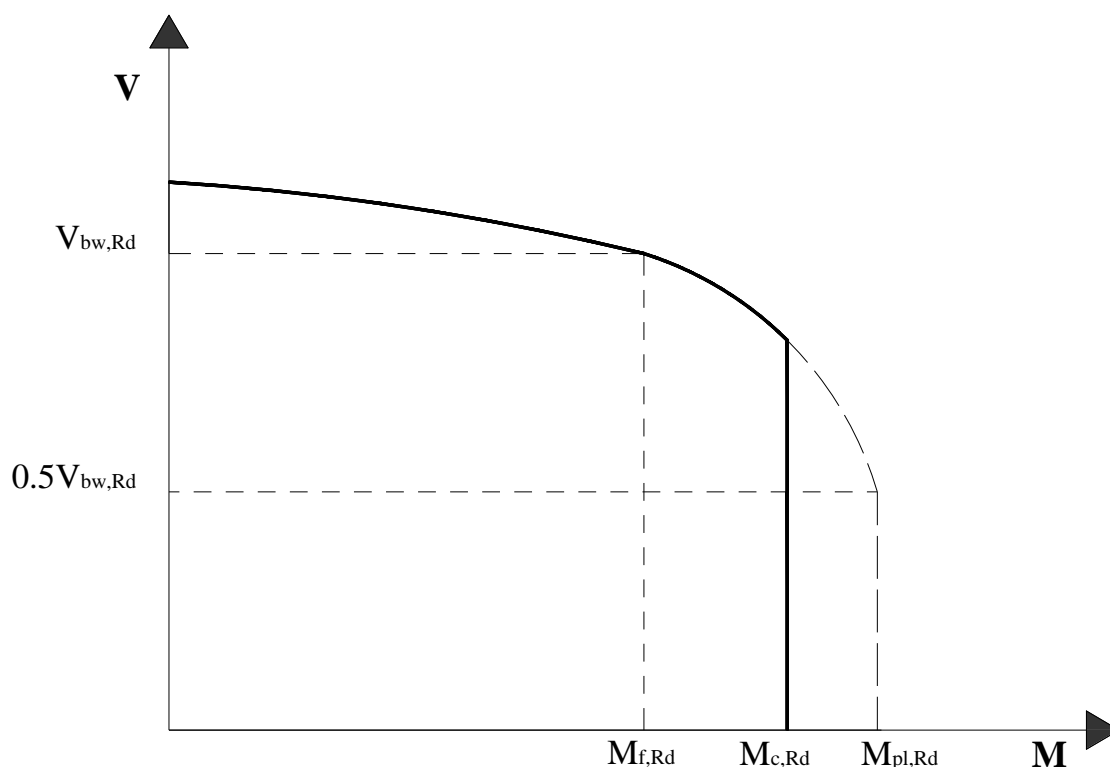


Figure 3.8 – Shear-bending interaction diagram for profiles with Class 3 or 4

It is worth mentioning that $M_{pl,Rd}$ in Figure 3.7 is the full plastic moment of the gross cross-section, but in Figure 3.8 it is the design plastic resistance of the cross-section consisting of the effective area of the flanges and the fully effective web, irrespective of its section class.

3.4 Stiffeners

The webs of plate girders are usually reinforced with transverse and longitudinal stiffeners. Part 1-5 of EC3 (CEN, 2006b) gives, in section 9, design rules for stiffeners in plated structures and other detailing rules that are important for the evaluation of the plate buckling resistance.

Figure 3.9 shows the most common situations where transverse and longitudinal stiffeners are used to increase the resistance of plated structural elements subjected to different types of loading, such as: direct stresses, shear stresses, patch loading, etc. In some cases, the stiffeners design is integrated into the design of the plated elements and, in other cases, separate checks need to be made (Beg et al., 2010). Figure 3.10 shows some typical shapes of stiffeners cross-sections. For individual design, the cross-section of a transverse or longitudinal stiffener may be taken as the gross area of the stiffener

itself (A_s) plus the contributing width of the plate equal to $15\epsilon t$ on each side of the stiffener. This width should not be more than the actual dimension available, avoiding any overlapping of the contributing widths of adjacent stiffeners (see Figure 3.11).

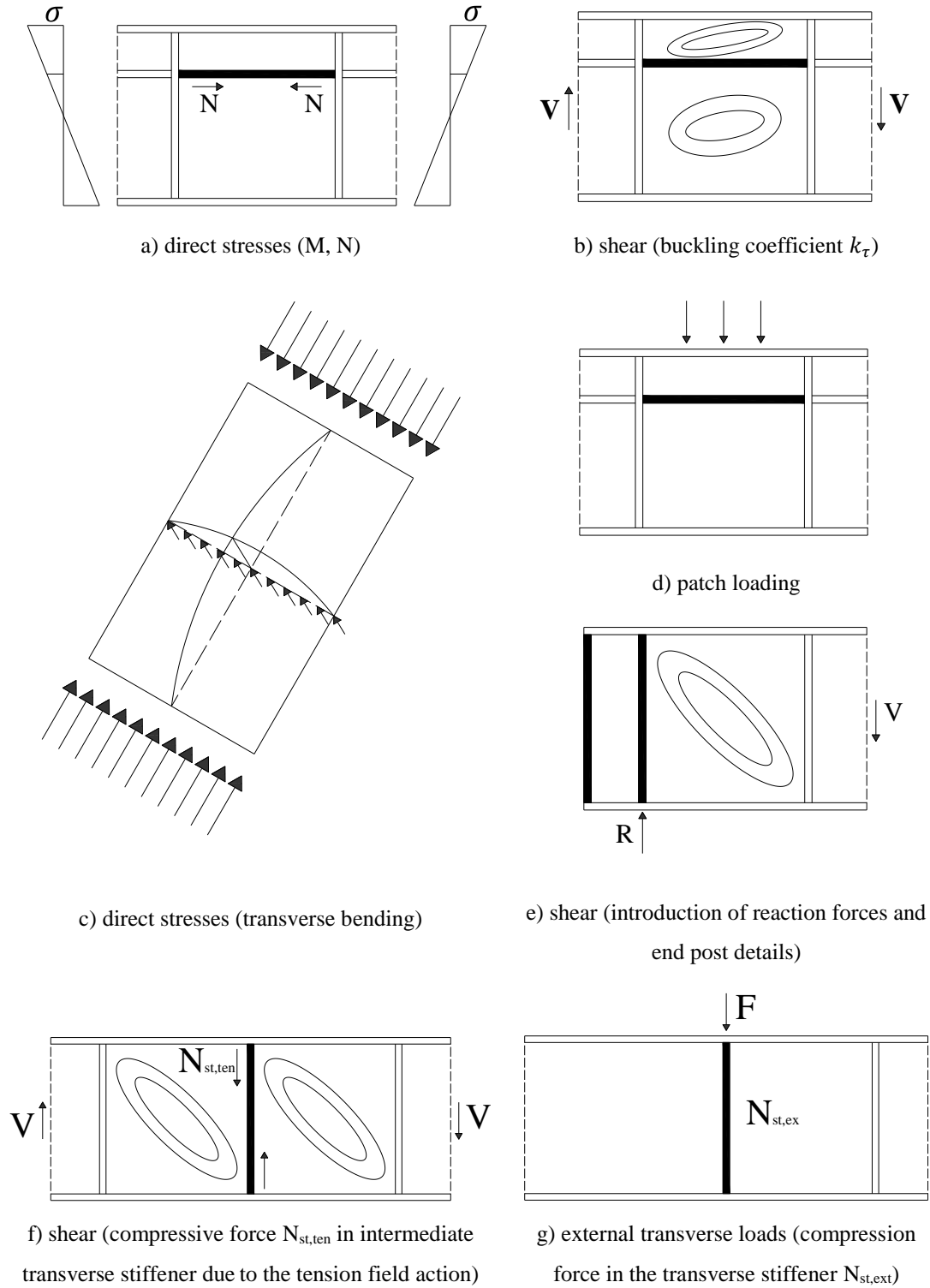


Figure 3.9 – Common applications of transverse and longitudinal stiffeners (Beg et al., 2010)

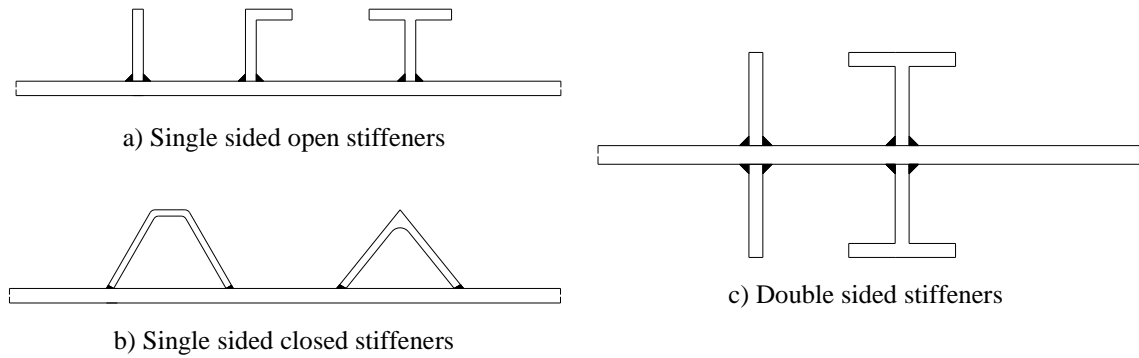


Figure 3.10 – Typical cross-sections of stiffeners (Beg et al., 2010)

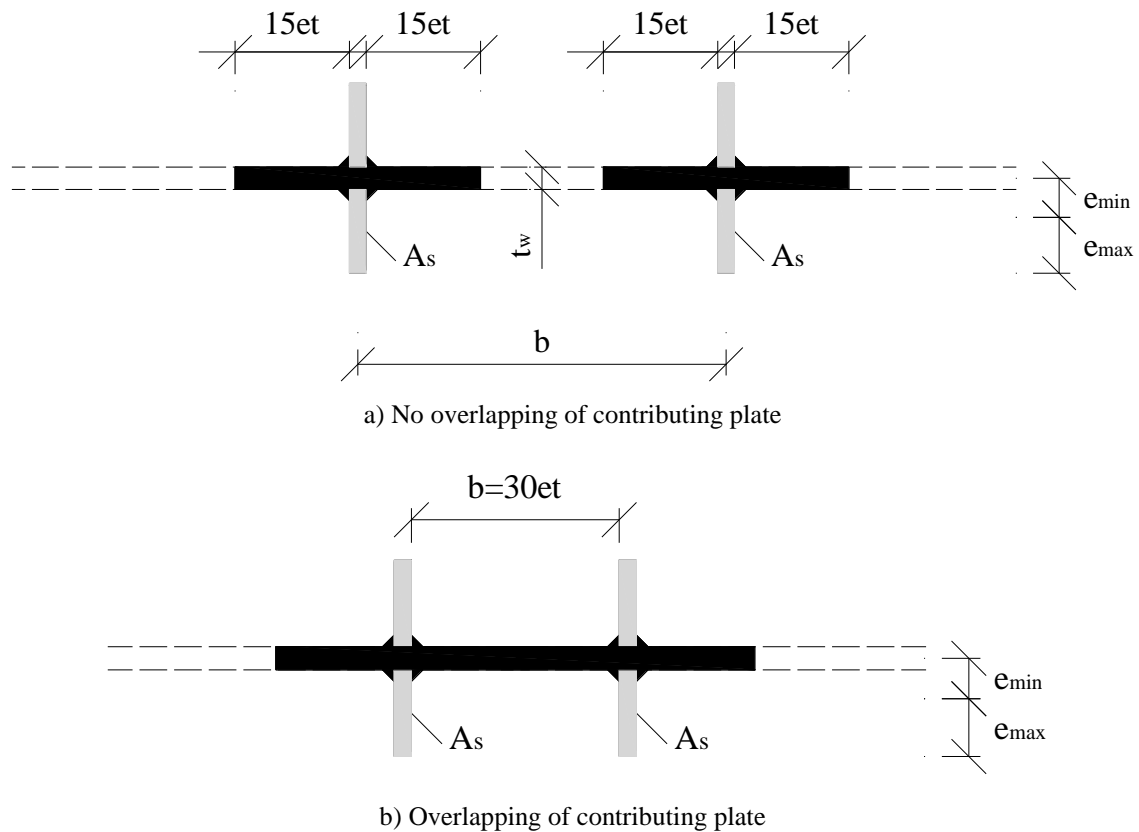


Figure 3.11 – Effective cross-section of stiffeners (Beg et al., 2010)

Normally, transverse stiffeners are flat bars or T profiles. Intermediate transverse stiffeners are usually single-sided, unless they support large concentrated forces, while the stiffeners at supports are always double-sided to avoid eccentricity at the introduction of large reaction forces (Beg et al., 2010). By another hand, longitudinal stiffeners have frequently a closed trapezoidal shape because of its great torsional rigidity, but they can also be open flat bars, T or L shape profiles (see Figure 3.10).

The cross-sections of open stiffeners are always designed as Class 3 cross-sections or lower to ensure adequate stiffness. Generally this rule is also applied to closed stiffeners. However, some new concepts in the design of stiffened plates led to the choice of a smaller number of large trapezoidal stiffeners instead of a large number of smaller stiffeners. In this case, it may happen that the stiffener belongs to a Class 4 cross-section, which must be considered in the design procedure.

3.4.1 Transverse stiffeners

Transverse stiffeners have many functions. The most important is to increase the shear resistance, but they also ensure lateral supports to longitudinal stiffeners and provide support to concentrated transverse forces, being therefore frequently applied at supports and load points to prevent web crippling. They are commonly designed as rigid stiffeners and consequently the panels between two rigid transverse stiffeners can be designed individually without interaction with adjacent panels. In Part 1-5 of EC3 are given prescriptions for the design of rigid transverse stiffeners. However, it does not give detailed information for the design of flexible transverse stiffeners.

Furthermore, transverse stiffeners should be able to support the deviation forces originated from the longitudinal compressive forces of the adjacent panels (N_{Ed}), caused by the inevitable geometrical imperfections. These deviation forces induce out of plane bending (see Figure 3.12). Transverse stiffeners should be designed not only for strength but also for stiffness in order to provide rigid support for the plate. Based on a second order analysis, the following criteria should be satisfied (Beg et al., 2010; Johansson et al., 2007; CEN, 2006b):

- maximum stress in the stiffener at the ultimate limit state should not exceed the yield strength ($\sigma_{max} \leq \frac{f_y}{\gamma_{M1}}$);
- additional lateral deflection w at the ultimate limit state should not exceed $b/300$.

The scheme used for the verification of transverse stiffeners subjected to direct stresses is present in Figure 3.12. The transverse stiffener under checking has a sinusoidal geometric imperfection with amplitude w_0 . Both adjacent stiffeners need to be straight and rigid. The adjacent compressed panels, including longitudinal stiffeners, are considered to be simply supported along the transverse stiffeners.

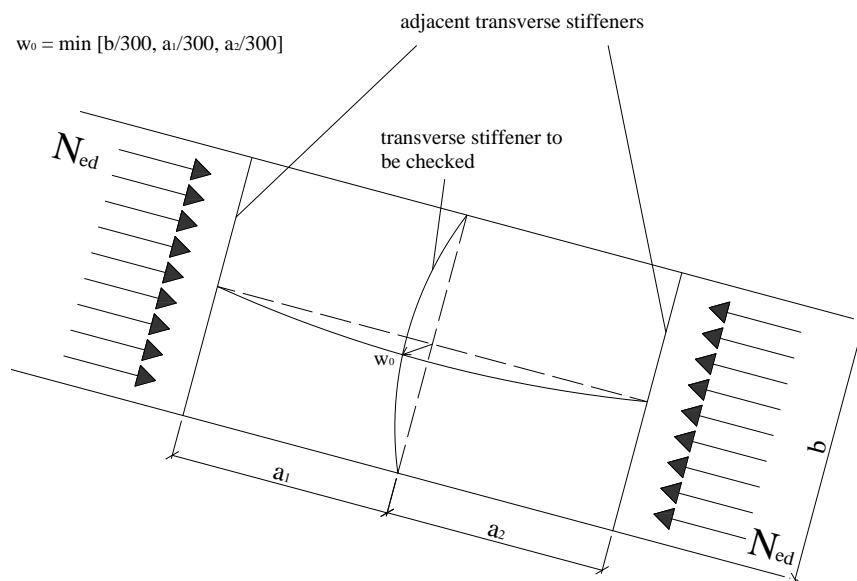


Figure 3.12 – Scheme for rigid transverse stiffeners (Beg et al., 2010; Johansson et al., 2007)

Regarding shear, transverse stiffeners are influenced in two different ways. At the plate buckling, rigid transverse stiffeners should prevent the lateral movements of the plate at the stiffener position. Thus, adjacent transverse stiffeners should have appropriate stiffness. Normally, the verification of stiffeners is made only for intermediate stiffeners, because by definition the stiffeners placed at supports are much stronger. On post-buckling state, tension field action subject transverse stiffeners to additional axial forces and induces additional bending moments at the plate girder end posts due to the anchorage of the tension field. Separate checks for additional axial forces are necessary only at intermediate transverse stiffeners, since at stiffeners above the supports all axial actions are taken into account in the reaction forces considered relevant for their design.

In the most general case (see Figure 3.13), a transverse stiffener may be loaded with:

- a transverse deviation force (q_{dev}), originated from the longitudinal compressive force of the adjacent panels (N_{Ed});
- an external transverse loading (q_{Ed}) in the horizontal direction;
- a compressive force in transverse stiffener ($N_{st,ext}$), coming from the external transverse loads;
- a compressive force ($N_{st,ten}$) in intermediate transverse stiffener due to the tension field action.

More information about design of transverse stiffeners may be found in (Beg et al., 2010; Johansson et al., 2007).

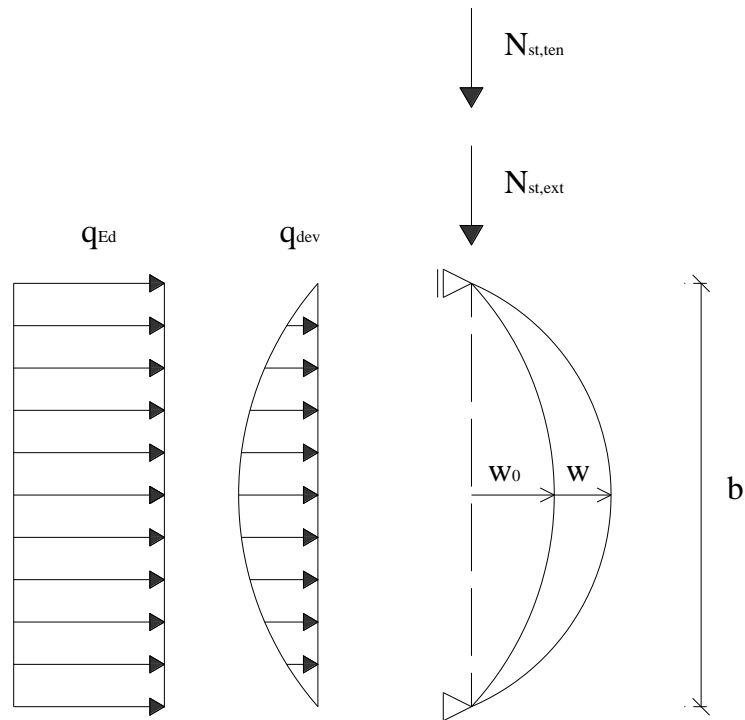


Figure 3.13 – General loading conditions affecting the transverse stiffeners (Johansson et al., 2007)

3.4.1.1 Rigid end posts

Rigid end posts should have the form of a vertical I profile at the end of the girder. Two double-sided stiffeners can be used for this purpose (Beg et al., 2010). Figure 3.14 shows some details of a rigid end post.

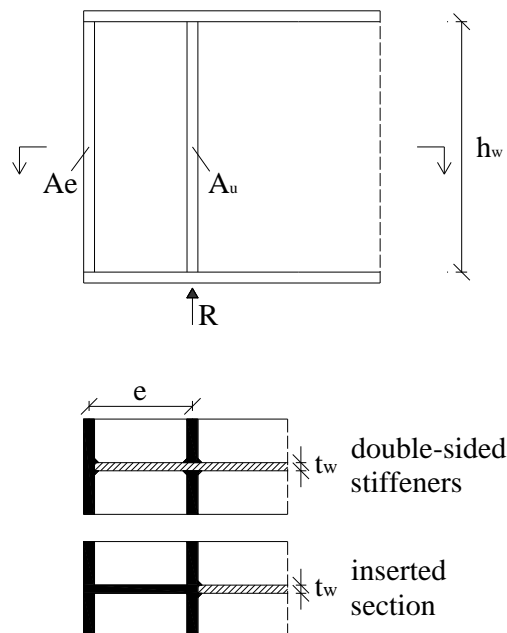


Figure 3.14 – Rigid end post details

The end post is provided of appropriate stiffness and strength if the following conditions are satisfied:

- $e \geq 0.1 h_w$
- $A_e \geq \frac{4 h_w t^2}{e}$

where e is the centre to centre distance between the stiffeners (see Figure 3.14).

The second stiffener of an end post with cross-section A_u should be checked also as a bearing stiffener to carry the reaction force R .

When end posts are made with inserted profiles, the section modulus of such profiles should not be less than $4h_w t^2$, considering bearing around the horizontal axis perpendicular to the web.

3.4.1.2 Non-rigid end posts

When design criteria for rigid end posts are not satisfied, the end post should be considered as non-rigid. A non-rigid end post consists on the application of a transverse stiffener on the reaction point. Generally, a single double-sided stiffener may be used as non-rigid end post. Figure 3.15 shows an example of a typical configuration of a non-rigid end post, where it may act as bearing stiffener for the reaction.

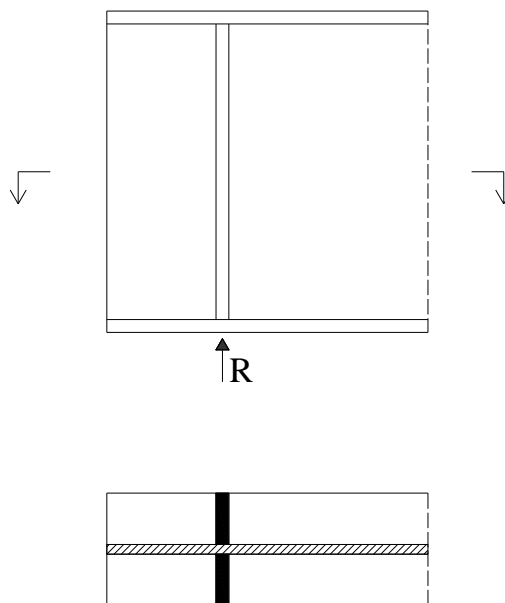


Figure 3.15 – Non-rigid end post details

3.4.1.3 Intermediate transverse stiffeners

An intermediate transverse stiffener is considered rigid for shear buckling of the plate if the following conditions are satisfied:

- $I_{st} \geq \frac{1.5 h_w^3 t^3}{a^2}$ for $\alpha = \frac{a}{h_w} < \sqrt{2}$
- $I_{st} \geq 0.75 h_w t^3$ for $\alpha = \frac{a}{h_w} \geq \sqrt{2}$

where I_{st} is the moment of inertia of an intermediate transverse stiffener with a cross-section according to Figure 3.11, for the parallel axis to the web plate. Normally, the results given by the expressions presented above do not lead to very strong stiffeners.

The tension field action imposes an axial force $N_{st,ten}$ in the intermediate transverse stiffener that may be determined as follows

$$N_{st,ten} = V_{Ed} - \frac{1}{\lambda_w^2} t_w h_w \frac{f_y}{\sqrt{3} \gamma_{M1}} \quad (3.18)$$

At variable shear forces, V_{Ed} is taken at the distance $0.5 h_w$ from the edge of the panel with the largest shear force (see Figure 3.16). Note that the values given by Eq. (3.18) are very conservative (by a factor 2 or more) and overestimates the level of the axial force (Beg et al., 2010). This may be problematic, mainly for single-sided stiffeners where eccentric introduction of the axial force should be taken into account. When Eq. (3.18) gives a negative value, the axial force $N_{st,ten}$ should be considered equal to 0.

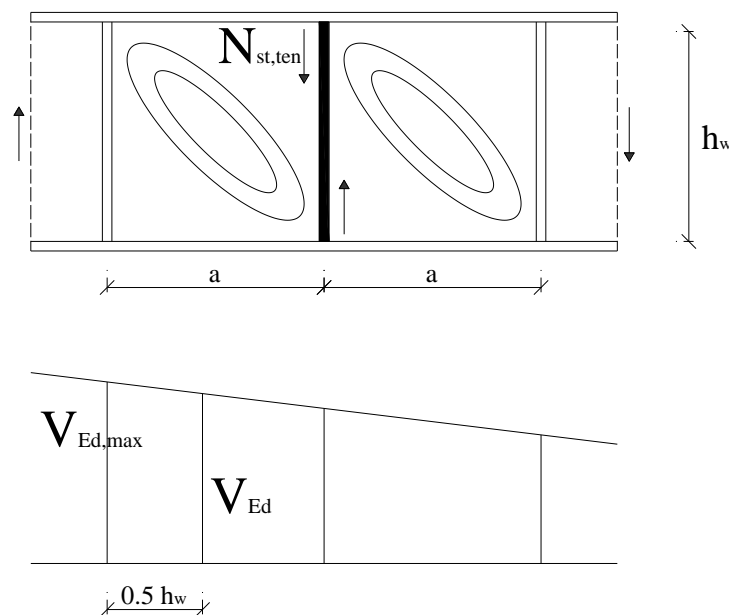


Figure 3.16 – Development of axial force in the intermediate transverse stiffener

3.4.2 Longitudinal stiffeners

Longitudinal stiffeners are used to increase the shear resistance, the resistance to direct stresses or the resistance to patch loading (see Figure 3.9). Typically they are designed to be most effective. Generally this is achieved when an increase in resistance of the stiffener's cross-section does not result in a significant strength enhancement by the stiffened plate. When stiffened plates are loaded in shear, no special design checks are needed for longitudinal stiffeners. Their influence is considered when calculating the shear buckling coefficient k_τ of the stiffened panel (Eqs. (3.8) and (3.9)).

3.5 Design at elevated temperatures

As presented, the ultimate shear strength at normal temperature of steel plate girders is obtained according to Part 1-5 of EC3 (CEN, 2006b). In the European Standards there is one part that is dedicated to structural fire design of steel structures, Part 1-2 (CEN, 2010b). However, no guidance is given in Part 1-2 of EC3 for the shear buckling evaluation in fire situation. Thus, the design prescriptions at normal temperature, adapted to fire situation by the direct application of the reduction factors for the stress-strain relationship of steel at elevated temperatures, are used. The reduction factors used in this procedure are presented in Table 3.2 and plotted in Figure 3.17. The reduction factor to reduce the steel yield strength at elevated temperatures of profiles with Class 4 cross-sections, given in Annex E of Part 1-2 of EC3, is also presented.

When checking the ultimate shear strength in fire situation, $k_{y,\theta}$ is used to consider the reduction of the steel yield strength caused by the elevated temperatures, whereas $k_{E,\theta}$ is applied to reduce the Young's modulus in Eq. (3.19) (Franssen & Vila Real, 2010), for the calculation of the parameter ε_θ necessary for obtaining the web slenderness parameter at elevated temperatures $\bar{\lambda}_{w,\theta}$. Finally, $k_{0.2p,\theta}$ is used for Class 4 cross-sections to consider the reduction of the flanges resistance to the bending moment at elevated temperatures. It is important to note that $k_{p,\theta}$ is only used to build the constitutive law presented in Figure 4.3.

$$\varepsilon_\theta = \sqrt{\frac{235}{f_y k_{y,\theta}}} \sqrt{\frac{E k_{E,\theta}}{210000}} \quad (3.19)$$

with f_y and E in [MPa].

Table 3.2 – Reduction factors for steel stress-strain relationship at elevated temperatures

Steel Temperature θ_a [°C]	Reduction factors at temperature θ_a relative to the value of f_y or E_a at 20°C			
	Reduction factor (relative to f_y) for effective yield strength	Reduction factor (relative to E_a) for the slope of the linear elastic range	Reduction factor (relative to f_y) for the design strength of hot rolled and welded thin walled sections (Class 4)	Reduction factor (relative to f_y) for proportional limit
	$k_{y,\theta} = f_{y,\theta}/f_y$	$k_{E,\theta} = E_{a,\theta}/E_a$	$k_{0.2p,\theta} = f_{y,\theta}/f_y$	$k_{p,\theta} = f_{p,\theta}/f_y$
20	1.0000	1.0000	1.0000	1.0000
100	1.0000	1.0000	1.0000	1.0000
200	1.0000	0.9000	0.8900	0.8070
300	1.0000	0.8000	0.7800	0.6130
400	1.0000	0.7000	0.6500	0.4200
500	0.7800	0.6000	0.5300	0.3600
600	0.4700	0.3100	0.3000	0.1800
700	0.2300	0.1300	0.1200	0.0750
800	0.1100	0.0900	0.0700	0.0500
900	0.0600	0.0675	0.0500	0.0375
1000	0.0400	0.0450	0.0300	0.0250
1100	0.0200	0.0230	0.0200	0.0130
1200	0.0000	0.0000	0.0000	0.0000

NOTE: For intermediate values of steel temperature, linear interpolation may be used.

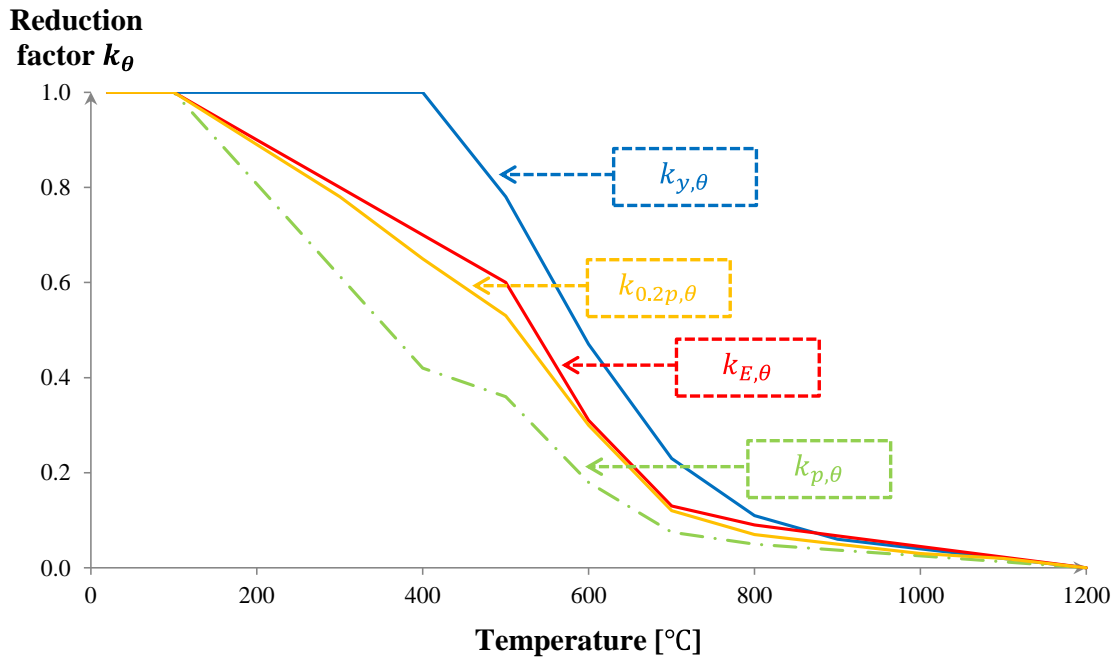
**Figure 3.17 – Reduction factors for the steel stress-strain relationship at elevated temperatures**

Figure 3.18 shows the application of the reduction factors to the design expressions at normal temperature. It is important to note that $M_{f,Rd}$ and $M_{pl,Rd}$ are affected by $k_{0.2p,\theta}$ only if the cross-section is class 4, otherwise they are affected by $k_{y,\theta}$.

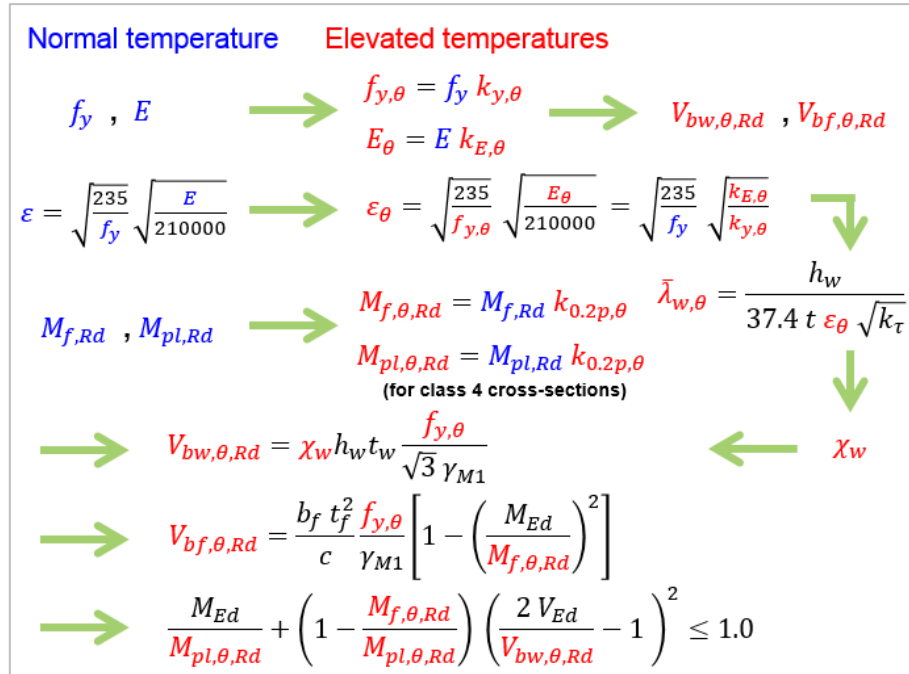


Figure 3.18 – Schematic representation of the application of the reduction factors to the design expressions at normal temperature

Chapter 4

Numerical modelling

Chapter 4 Numerical modelling

- 4.1 Model description
 - 4.1.1 FEM model
 - 4.1.2 Material model
 - 4.1.3 Initial imperfections
 - 4.1.3.1 Geometric imperfections
 - 4.1.3.2 Residual stresses
- 4.2 Validation of the numerical model
 - 4.2.1 Review of experimental tests
 - 4.2.1.1 Normal temperature
 - 4.2.1.2 Elevated temperatures
 - 4.2.2 Comparisons between numerical and experimental results
 - 4.2.2.1 Normal temperature
 - 4.2.2.2 Elevated temperatures
- 4.3 Influence of the initial imperfections
 - 4.3.1 Geometric imperfections
 - 4.3.1.1 Normal temperature
 - 4.3.1.2 Elevated temperatures
 - 4.3.2 Residual stresses
 - 4.3.2.1 Normal temperature
 - 4.3.2.2 Elevated temperatures
- 4.4 Conclusions

Chapter 4 Numerical modelling

4.1 Model description

4.1.1 FEM model

In engineering practice, the resistance of steel plate girders can be determined in different ways, i.e. by means of experimental tests, computer simulations or using available formulae in design codes. Herein, the ultimate shear strength of steel plate girders is calculated by means of non-linear finite element analysis and then the numerical values are compared with the codes predictions in the next Chapters.

The 3-D models for steel plate girders loaded in a three-point bending were developed using the FEM software SAFIR (Franssen, 2005, 2011), a computer software developed at University of Liege for the simulation of the behaviour of structures subjected to fire. The plates of the web, flanges and stiffeners were discretized into several quadrangular shell elements with 4 integration nodes and 6 degrees of freedom (3 translations and 3 rotations). These shell elements adopt the Kirchhoff's theory formulation and have been previously validated by Talamona and Franssen (2005).

A sensitivity analysis was performed in order to find the necessary mesh refinement to obtain reliable results (see Figure 4.1). A mesh refinement with 30 elements in the web, 10 elements in the flanges and 100 divisions per meter of beam length, which amounts to 5000 finite elements per meter of beam length, was considered adequate to accurately represent the beam behaviour, as marked with a circle in Figure 4.1. The integration on the shell element follows a Gauss scheme with 4 nodes on the surface and 4 levels through the thickness.

The boundary conditions are presented in Table 4.1 and illustrated in Figure 4.2. Lateral torsional buckling was prevented through the application of lateral bracings in the upper flange equidistantly at $L/10$ (see Figure 4.2). The loading were applied to the model as forces at mid-span, distributed on the entire web depth in order to avoid numerical problems (see Figure 4.5). The plate girders were always provided with transverse stiffeners at the load points, i.e. at the girder ends and at mid-span.

Table 4.1 – Boundary conditions (Δ – displacement, θ – rotation; 0 – free, 1 – fixed)

Boundary		Δ_x	Δ_y	Δ_z	θ_x	θ_y	θ_z
Left support	Web	0	1	0	0	0	0
	Lower flange	0	0	1	0	0	0
Right support	Web	0	1	0	0	0	0
	Lower flange	1	0	1	0	0	0
Lateral bracings	Upper flange	0	1	0	0	0	0

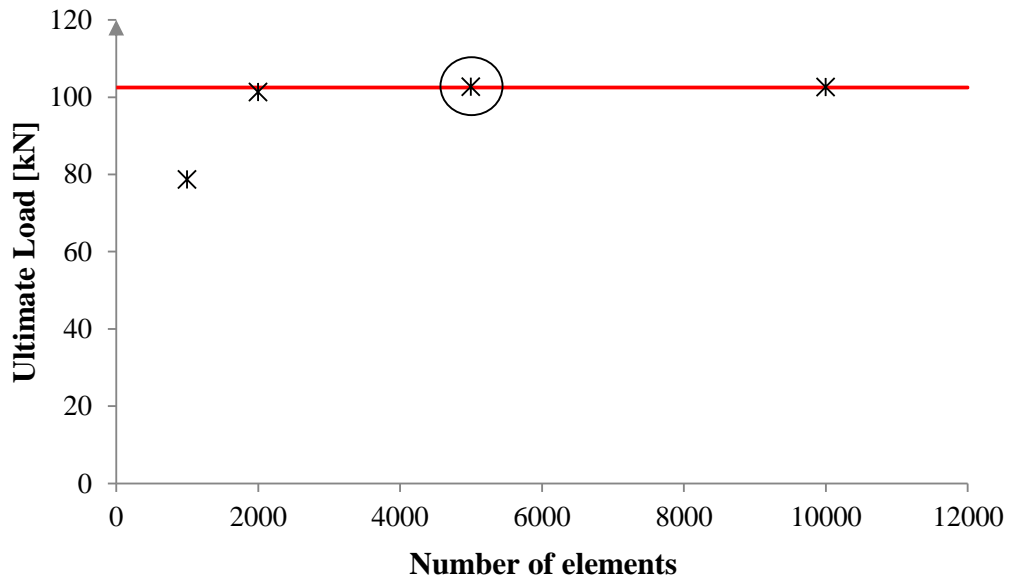


Figure 4.1 – Mesh refinement sensitivity analysis

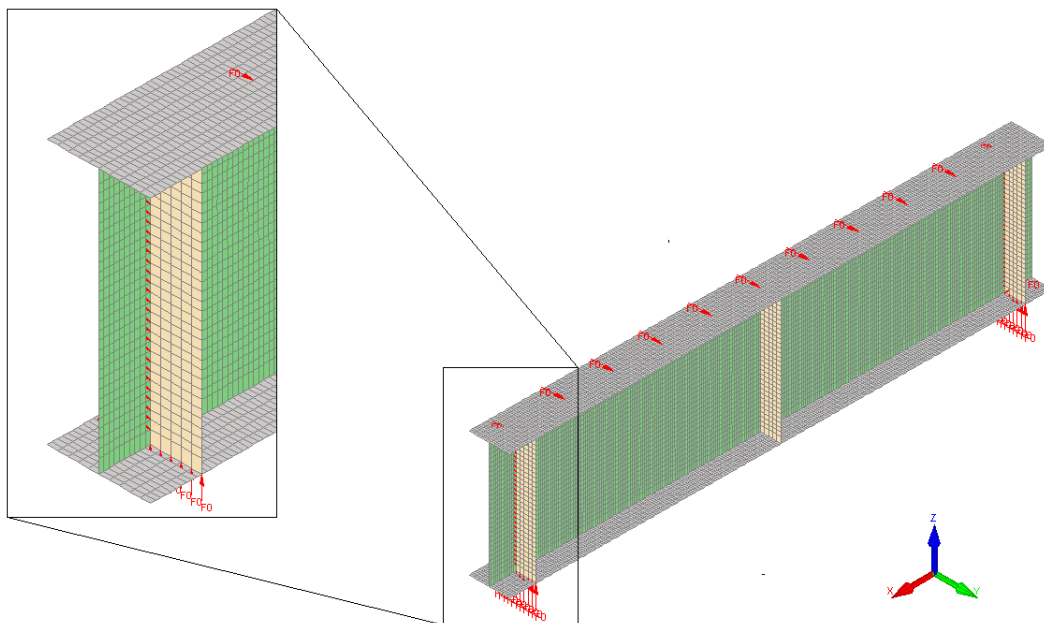


Figure 4.2 – Numerical model

4.1.2 Material model

The bi-linear material model with a yielding plateau was used in the analyses at 20°C, according to Annex C of Part 1-5 of EC3 (CEN, 2006b). For elevated temperatures with heating rates between 2 and 50°C/min, the steel mechanical properties of resistance and deformability may be obtained according to the recommendations presented in Clause 3.2.2 of Part 1-2 of EC3 (CEN, 2010b). The parameters given in Table 4.2 are the parameters involved on the determination of the steel stress-strain relationship at elevated temperatures presented in Figure 4.3, which was the steel material law considered in the numerical modelling. Strain-hardening was not considered in the steel material law at both normal and elevated temperatures.

At elevated temperatures, the shape of the stress-strain curve is modified compared to the shape at room temperature. However, it is important to note that the bi-linear constitutive law with a yielding plateau and without strain-hardening used for normal temperature is compatible with the constitutive law for elevated temperatures, meaning that at 20°C they are the same. At 20°C $f_{p,\theta}$ is equal to f_y resulting in $\varepsilon_{p,\theta} = \varepsilon_{y,\theta}$, which leads to not having the transition phase that follows the equation of an ellipse and having again an elastic-plastic law without strain hardening.

The stress-strain steel curve at elevated temperatures may be divided into four zones:

- the first is a linear zone until the proportional limit. This relation can be described by the Hooke law with the modulus of elasticity $E_{a,\theta}$;
- the second is a transition phase that follows the equation of an ellipse (Rubert & Schaumann, 1985) and stops at the yield strength, considered as the stress at 2 % of total strain. This phase corresponds to the beginning of the yielding;
- the third represents the yield (plastic zone), characterized by values of constant stresses equal to the yield strength;
- the fourth zone relates to a linear decreasing branch, which was introduced to represent the softening of the steel and to achieve finite numerical ductility.

Table 4.2 – Expressions to define the steel stress-strain relationship at elevated temperatures

Strain range	Stress σ	Tangent modulus		
$\varepsilon \leq \varepsilon_{p,\theta}$	$E_{a,\theta}\varepsilon$	$E_{a,\theta}$		
$\varepsilon_{p,\theta} < \varepsilon < \varepsilon_{y,\theta}$	$f_{p,\theta} - c + (b/a) \left[a^2 - (\varepsilon_{y,\theta} - \varepsilon)^2 \right]^{0.5}$	$\frac{b(\varepsilon_{y,\theta} - \varepsilon)}{a \left[a^2 - (\varepsilon_{y,\theta} - \varepsilon)^2 \right]^{0.5}}$		
$\varepsilon_{y,\theta} \leq \varepsilon \leq \varepsilon_{t,\theta}$	$f_{y,\theta}$	0.00		
$\varepsilon_{t,\theta} < \varepsilon < \varepsilon_{u,\theta}$	$f_{y,\theta} \left[1 - (\varepsilon - \varepsilon_{t,\theta}) / (\varepsilon_{u,\theta} - \varepsilon_{t,\theta}) \right]$	-		
$\varepsilon = \varepsilon_{u,\theta}$	0.00	-		
Parameters	$\varepsilon_{p,\theta} = f_{p,\theta} / E_{a,\theta}$	$\varepsilon_{y,\theta} = 0.02$	$\varepsilon_{t,\theta} = 0.15$	$\varepsilon_{u,\theta} = 0.20$
Functions	$a^2 = (\varepsilon_{y,\theta} - \varepsilon_{p,\theta})(\varepsilon_{y,\theta} - \varepsilon_{p,\theta} + c/E_{a,\theta})$ $b^2 = c(\varepsilon_{y,\theta} - \varepsilon_{p,\theta})E_{a,\theta} + c^2$ $c = \frac{(f_{y,\theta} - f_{p,\theta})^2}{(\varepsilon_{y,\theta} - \varepsilon_{p,\theta})E_{a,\theta} - 2(f_{y,\theta} - f_{p,\theta})}$			

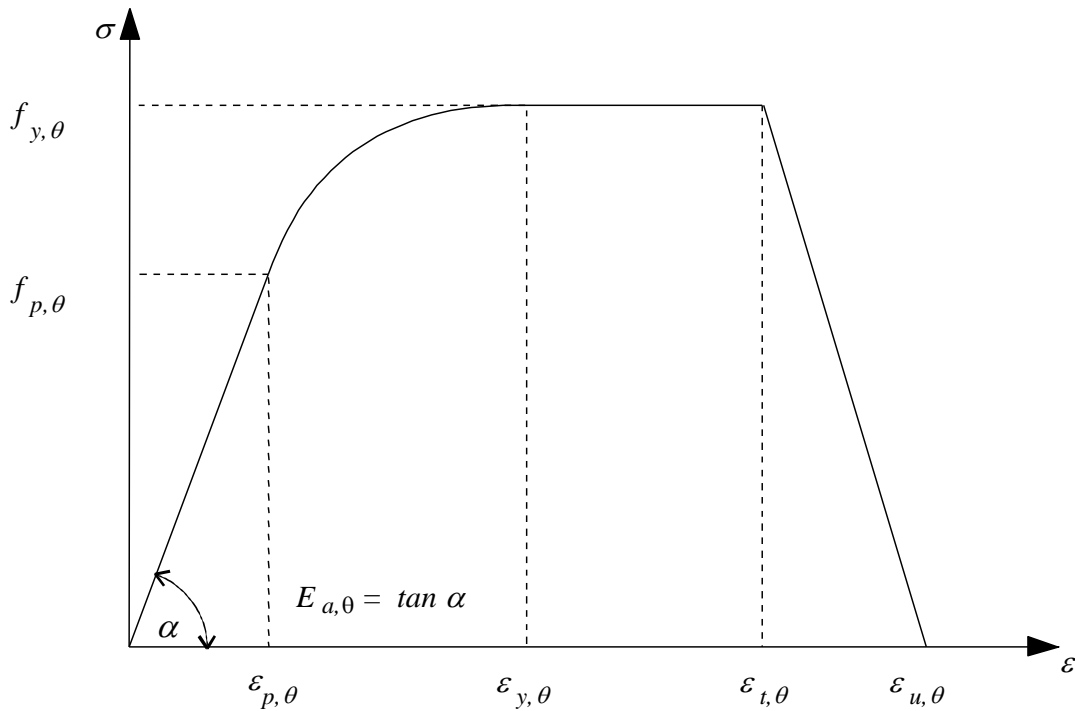


Figure 4.3 –Steel stress-strain relationship at elevated temperatures

The mechanical properties of steel decrease significantly when subjected to fire. Figure 4.4 shows the variation of the steel stress-strain relationship with the temperature, obtained according to the expressions presented in Table 4.2 and reduction factors of Table 3.2. As one can observe, the steel strength decreases as the temperature increases,

for temperatures larger than 400°C. Figure 4.4b shows in more detail the elastic-elliptic-perfectly plastic model of the stress-strain curve at elevated temperatures.

In an accidental limit state as fire, higher strains are acceptable. Therefore, EC3 recommends a yield strength corresponding to 2% total strain instead of the 0.2% proof strength. However, for members with Class 4 cross-sections, EC3 recommends design yield strength based on the 0.2% proof strength.

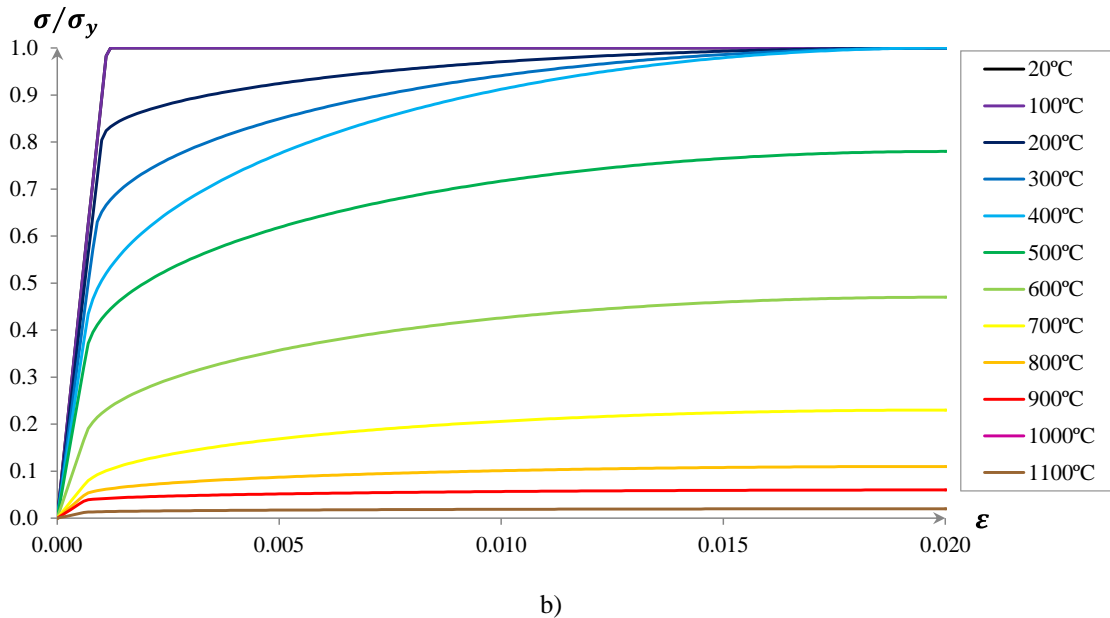
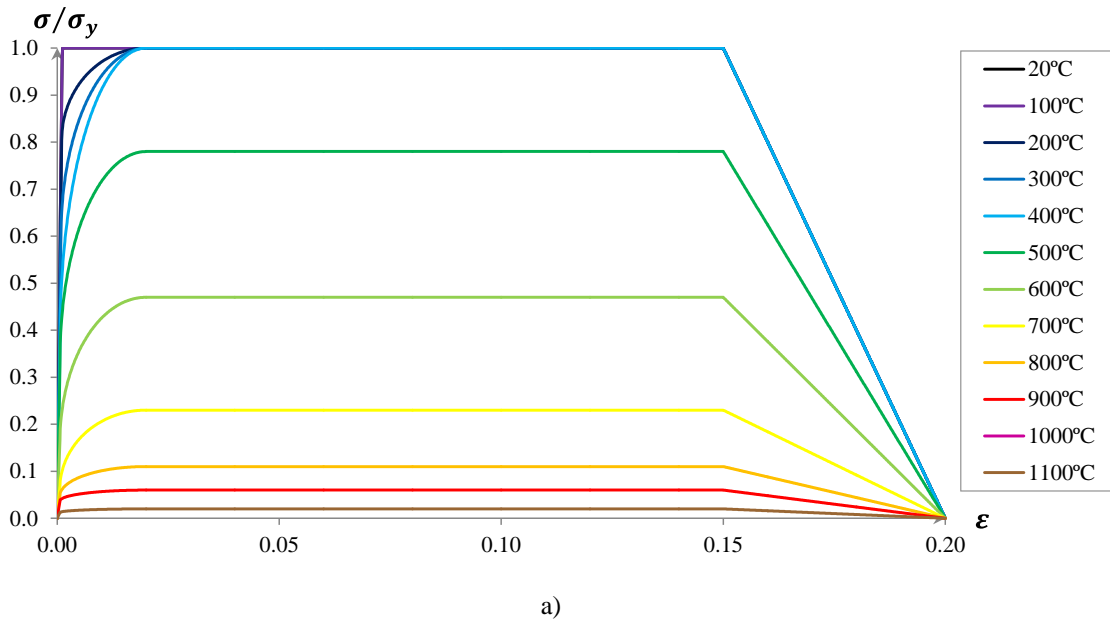


Figure 4.4 – Stress-strain relationship of steel at elevated temperatures

4.1.3 Initial imperfections

4.1.3.1 Geometric imperfections

Steel plate girders are not perfectly straight because of the geometric imperfections resulting from the production and fabrication process, which may cause a significant reduction on the ultimate bearing capacity of steel plate girders and consequently it is imperative to take them into account in the numerical modelling.

In this work, the initial geometric imperfections were incorporated into the numerical model by modifying the nodal coordinates. As the global buckling was restrained by the application of lateral bracings in the upper flange, only local imperfections were considered. The shape for the geometric imperfections was taken as the first eigenmode of a linear buckling analysis. A procedure written in CAST3M (CEA, 2012) was used to obtain the eigenmodes, being the interface between SAFIR and CAST3M assured by RUBY (Couto et al., 2013). Figure 4.5 shows an example of the shape of a first eigenmode resulting from a linear buckling analysis.

Regarding the maximum amplitude considered for the geometric imperfections, two different situations need to be considered. On the one hand, if one is modelling experimental tests, the pattern of the geometric imperfections observed in the experiments should be taken into account. When the geometric imperfections were not measured in the experimental test, a maximum amplitude of the geometric imperfections equal to $t_w/10$ was considered on the simulation of the experimental tests for the validation of the numerical model, as used in different studies of plate buckling at normal temperature (Hancock, 1981; Real et al., 2007) and at elevated temperature (Quiel & Garlock, 2010).

On the other hand, if one is evaluating the accuracy of design expressions adopted in the European Standards, the worst case scenario should be considered. Therefore, the maximum amplitude of the geometric imperfections is generally more severe in numerical studies concerning the evaluation of design expressions, when compared to the one used for modelling of experimental tests. Thus, in the parametric numerical studies performed in this thesis, the maximum amplitude was considered equal to 80% of the essential manufacturing tolerances for welded profiles, obtained from EN 1090-2 (CEN, 2011), as recommended in Part 1-5 of EC3 (CEN, 2006b). Accordingly, the

maximum amplitude considered for the geometric imperfections was $0.8b_f/100$ in the flanges and $0.8h_w/100$ in the web.

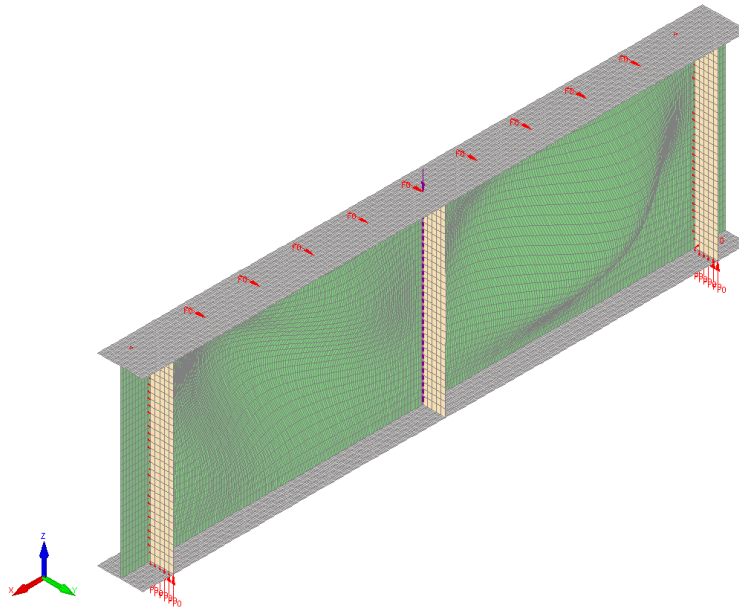


Figure 4.5 – Example of a buckling mode

4.1.3.2 Residual stresses

Despite the effect of the residual stresses on the ultimate shear strength of steel plate girders subjected to elevated temperatures has little influence (Quiel & Garlock, 2010), the residual stresses were introduced into the numerical modelling because they affect the ultimate shear strength at normal temperature (see Figure 4.7). The pattern of residual stresses considered is depicted in Figure 4.6, with the values of the residual stresses according to (ECCS, 1976, 1984).

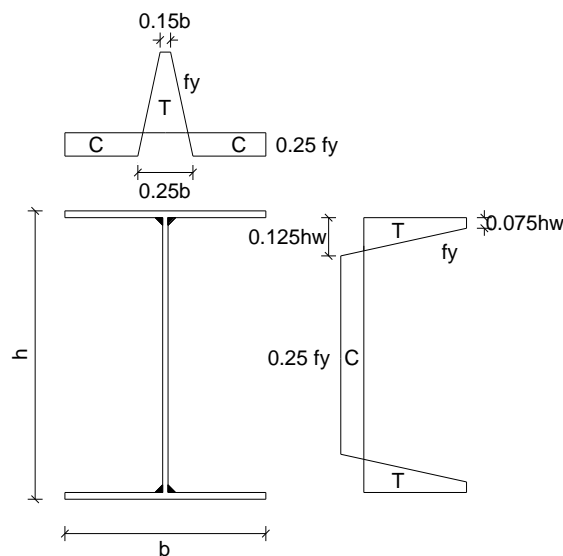


Figure 4.6 – Pattern of residual stresses typical of welded I-sections (C – compression; T – tension)

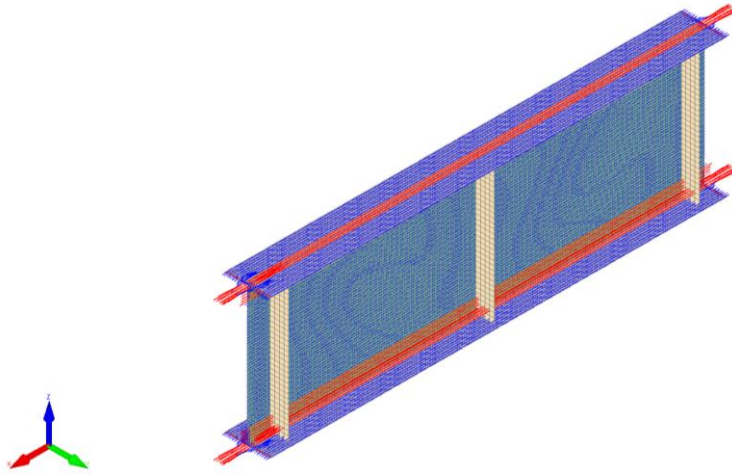


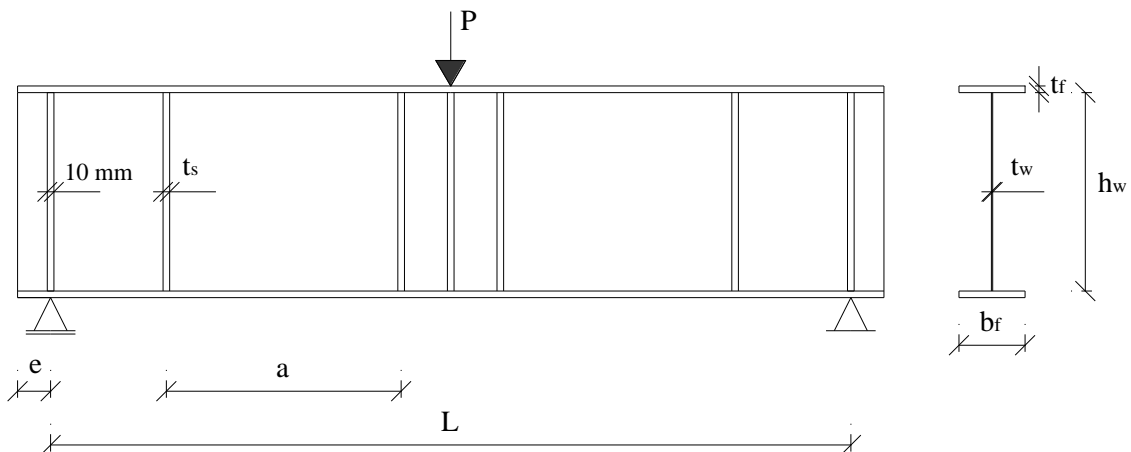
Figure 4.7 – Incorporation of the residual stresses into the numerical model (blue – compression; red – tension)

4.2 Validation of the numerical model

4.2.1 Review of experimental tests

4.2.1.1 Normal temperature

In 1999, an experimental study of steel plate girders with non-rigid end posts was performed by Lee and Yoo (1999). A shear dominant failure mode characterized by the web shear buckling was observed. The girders were simply supported and the loading was applied at mid-span. Figure 4.8 shows the geometry of the tested girders. The girders dimensions and the material properties are presented in Table 4.3 and Table 4.4, respectively. The width of the transverse stiffeners is half of the flanges width and the horizontal dimension of the two small end panels is 300 mm. All transverse stiffeners have 6 mm thickness (t_s) with exception of those placed at the supports forming the non-rigid end post which have 10 mm thickness.



a) girders with 400 mm web depth (PG1 and PG4)

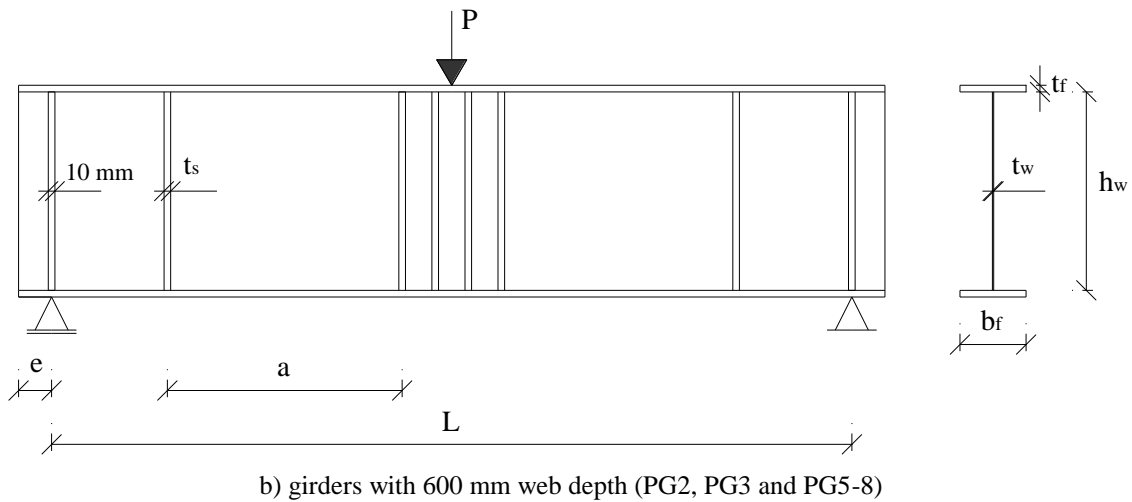
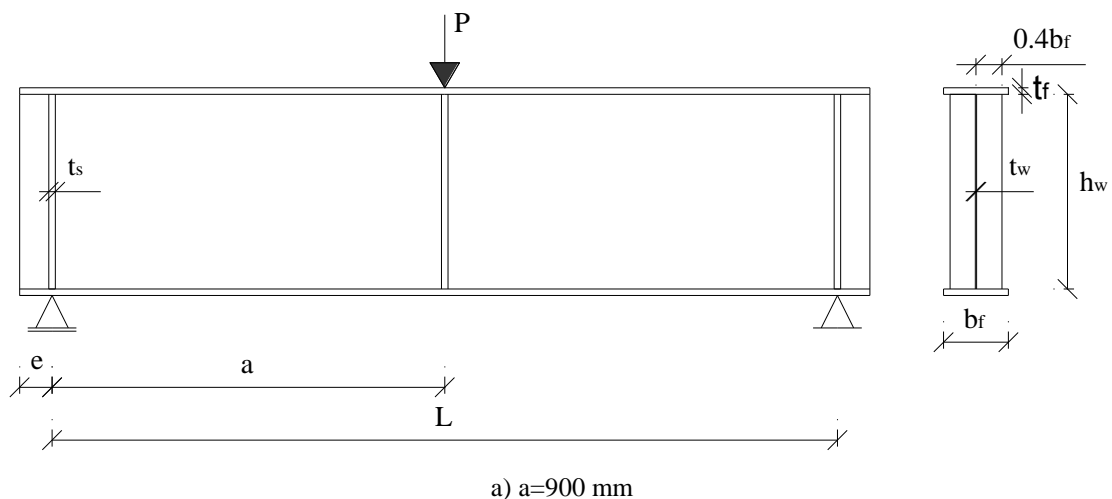


Figure 4.8 – Geometry of the plate girders tested by Lee and Yoo

Other experimental campaign performed at the University of Minho (Gomes et al., 2000) tested a total of six plate girders with non-rigid end posts divided into two series of three girders each. The girders from the first series only had transverse stiffeners, spaced by 300, 600 and 900 mm (see Figure 4.9). In the second series, a longitudinal stiffener was added to each girder tested in the first series. The longitudinal stiffener was placed 60 mm from the bottom surface of the upper flange. Table 4.3 shows the dimensions of the tested girders. The steel mechanical properties are presented in Table 4.4. The steel yield strength and the Young's modulus were obtained from tensile tests, using for this 18 samples from the 6 steel plates, 3 samples for each.



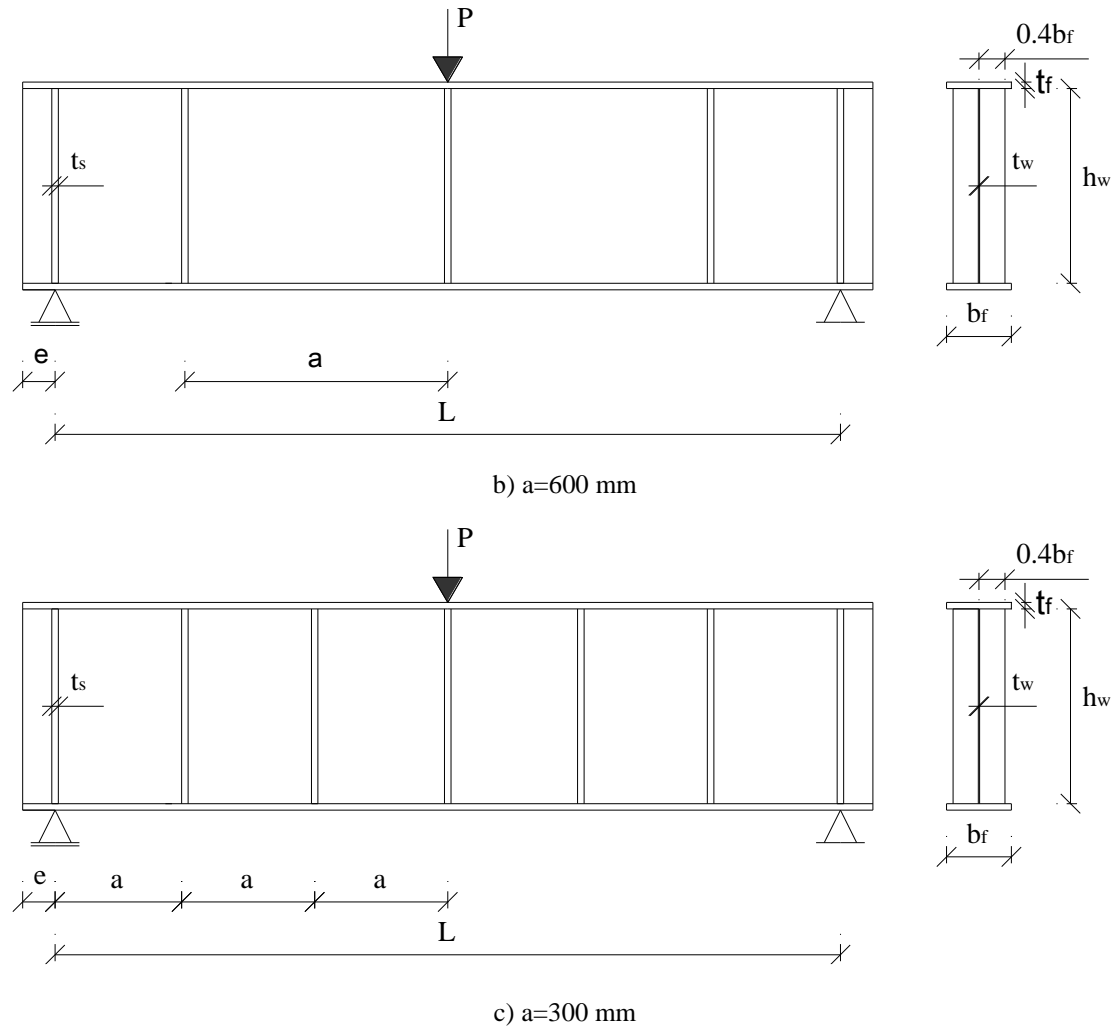


Figure 4.9 – Geometry of the plate girders tested at the University of Minho

Table 4.3 – Dimensions of the plate girders tested at normal temperature

Label	Reference	T [°C]	L [mm]	a [mm]	e [mm]	h_w [mm]	t_w [mm]	b_f [mm]	t_f [mm]	t_s [mm]	t_{ls} [mm]	b_{ls} [mm]	a/h_w [-]
PG1		20	1700	400	80	400	4.0	130	15.0	6.0	-	-	1.00
PG2		20	2100	600	100	600	4.0	200	10.0	6.0	-	-	1.00
PG3		20	2100	600	100	600	4.0	200	15.0	6.0	-	-	1.00
PG4	Lee and Yoo (1999)	20	2100	600	80	400	4.0	130	15.0	6.0	-	-	1.50
PG5		20	2700	900	100	600	4.0	200	10.0	6.0	-	-	1.50
PG6		20	2700	900	100	600	4.0	200	20.0	6.0	-	-	1.50
PG7		20	3300	1200	100	600	4.0	200	10.0	6.0	-	-	2.00
PG8		20	3300	1200	100	600	4.0	200	15.0	6.0	-	-	2.00
PG9		20	1800	900	100	300	2.0	100	5.0	5.0	-	-	3.00
PG10		20	1800	600	100	300	2.0	100	5.0	5.0	-	-	2.00
PG11	Gomes et al. (2000)	20	1800	300	100	300	2.0	100	5.0	5.0	-	-	1.00
PG12		20	1800	900	100	300	2.0	100	5.0	5.0	5.0	50	3.00
PG13		20	1800	600	100	300	2.0	100	5.0	5.0	5.0	50	2.00
PG14		20	1800	300	100	300	2.0	100	5.0	5.0	5.0	50	1.00

Table 4.4 – Material properties of the plate girders tested at normal temperature

Label	Reference	Web		Flanges		Stiffeners	
		f_y [MPa]	E [GPa]	f_y [MPa]	E [GPa]	f_y [MPa]	E [GPa]
PG1	Lee and Yoo (1999)	318.5	210.0	303.8	210.0	318.5	210.0
PG2		318.5	210.0	303.8	210.0	318.5	210.0
PG3		318.5	210.0	303.8	210.0	318.5	210.0
PG4		318.5	210.0	303.8	210.0	318.5	210.0
PG5		318.5	210.0	303.8	210.0	318.5	210.0
PG6		318.5	210.0	303.8	210.0	318.5	210.0
PG7		285.2	210.0	303.8	210.0	285.2	210.0
PG8		285.2	210.0	303.8	210.0	285.2	210.0
PG9	Gomes et al. (2000)	274.0	206.0	274.0	206.0	274.0	206.0
PG10		274.0	206.0	274.0	206.0	274.0	206.0
PG11		274.0	206.0	274.0	206.0	274.0	206.0
PG12		274.0	206.0	274.0	206.0	274.0	206.0
PG13		274.0	206.0	274.0	206.0	274.0	206.0
PG14		274.0	206.0	274.0	206.0	274.0	206.0

4.2.1.2 Elevated temperatures

In 2007, an experimental campaign at normal and elevated temperature was carried out at Nanyang Technological University (Vimonsatit et al., 2007b). This was the first reported experimental work under elevated temperatures in the scope of shear buckling in steel plate girders. A total of 18 plate girders were tested, divided into five series. Beams with stocky hot-rolled cross-sections were tested in the two first series and for this reason they are not studied in this work. Only two series involving 8 plate girders with slender web panels that fail by shear are modelled in this thesis, since some technical problems were registered in one of the experimental series and the results were not good. The girders are simply supported and the loading is applied at the mid-span. They were tested at elevated temperatures in electrical heating furnaces under steady-state conditions. The temperature was applied uniformly until the girder reached the specified temperature and after that the loading was applied until failure. The geometry of the girders is presented in Figure 4.10. The thickness of the flange stiffener is 12 mm and a same thickness for the transverse stiffeners was assumed. The dimensions and the material properties of the girders are presented in Table 4.5 and Table 4.6, respectively.

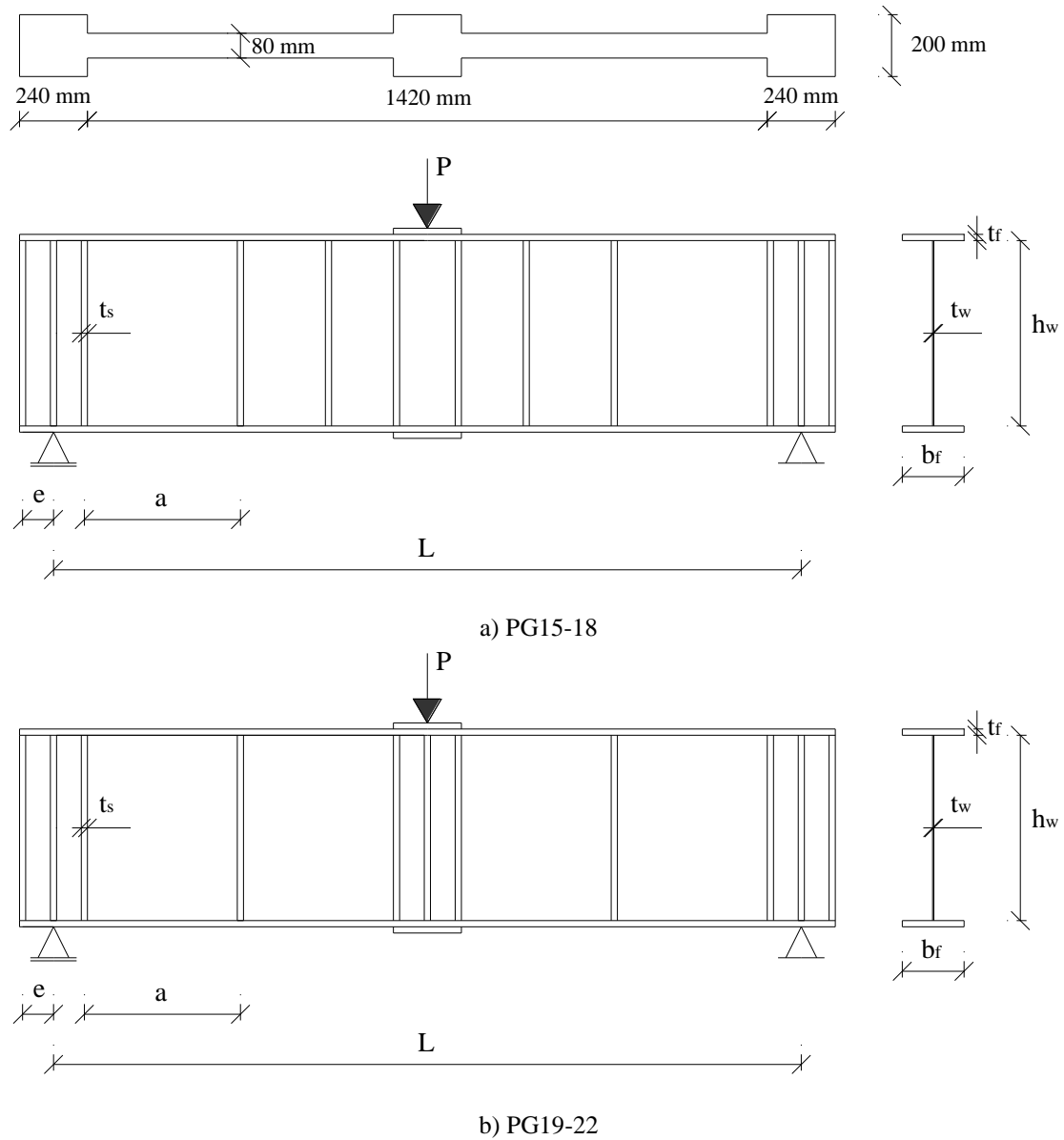


Figure 4.10 – Geometry of the plate girders tested at the Nanyang Technological University

Table 4.5 – Dimensions of the plate girders tested at elevated temperatures

Label	Reference	T [°C]	L [mm]	a [mm]	e [mm]	h _w [mm]	t _w [mm]	b _f [mm]	t _f [mm]	t _s [mm]	t _{is} [mm]	b _{is} [mm]	a/h _w [-]
PG15	Vimonsatit et al. (2007b)	20	1660	305	120	305	2.0	80	6.0	12.0	-	-	1.00
PG16		400	1660	305	120	305	2.0	80	6.0	12.0	-	-	1.00
PG17		565	1660	305	120	305	2.0	80	6.0	12.0	-	-	1.00
PG18		690	1660	305	120	305	2.0	80	6.0	12.0	-	-	1.00
PG19		20	1660	305	120	305	1.5	80	6.0	12.0	-	-	1.00
PG20		400	1660	305	120	305	1.5	80	6.0	12.0	-	-	1.00
PG21		550	1660	305	120	305	1.5	80	6.0	12.0	-	-	1.00
PG22		700	1660	305	120	305	1.5	80	6.0	12.0	-	-	1.00

Table 4.6 – Material properties of the plate girders tested at elevated temperatures

Label	Reference	Web		Flanges		Stiffeners	
		f_y [MPa]	E [GPa]	f_y [MPa]	E [GPa]	f_y [MPa]	E [GPa]
PG15		287.8	200.0	274.5	204.0	274.5	204.0
PG16		287.8	200.0	274.5	204.0	274.5	204.0
PG17		287.8	200.0	274.5	204.0	274.5	204.0
PG18	Vimonsatit	287.8	200.0	274.5	204.0	274.5	204.0
PG19	et al. (2007b)	332.0	200.0	277.0	204.0	277.0	204.0
PG20		332.0	200.0	277.0	204.0	277.0	204.0
PG21		332.0	200.0	277.0	204.0	277.0	204.0
PG22		332.0	200.0	277.0	204.0	277.0	204.0

4.2.2 Comparisons between numerical and experimental results

4.2.2.1 Normal temperature

The steel plate girders tested by Lee and Yoo (1999) were numerically modelled using the SAFIR software. The results are presented in Table 4.7. It is shown that the ultimate load of the analysed plate girders is very well predicted by the numerical model. The average deviation between the numerical and the experimental tests was 1.5%. It was calculated in absolute. As it can be seen in Table 4.7, the maximum conservative deviation was 2.8% and the maximum not conservative deviation was 1.7%.

The out of plane web buckling observed in PG2 is illustrated in Figure 4.11. Figures 4.12 and 4.13 show the web buckling at the end of the test of plate girders with aspect ratio equal to 1.5 and 2.0, respectively. As shown in these figures, the failure modes numerically obtained are quite similar to those observed in the experimental tests, particularly the web shear buckling and the formation of plastic hinges in the flanges.

Table 4.7 – Comparison between the numerical and experimental results of the steel plate girders tested by Lee and Yoo

Label	Ultimate load [kN]		Deviation [%]
	Exp. test (1)	SAFIR (2)	[(2)-(1)]/(1)
PG1	564.9	560.1	-0.8
PG2	664.9	662.6	-0.3
PG3	674.7	680.3	0.8
PG4	537.6	523.0	-2.7
PG5	572.7	582.7	1.7
PG6	625.7	609.2	-2.6
PG7	517.8	517.2	-0.1
PG8	552.9	537.5	-2.8

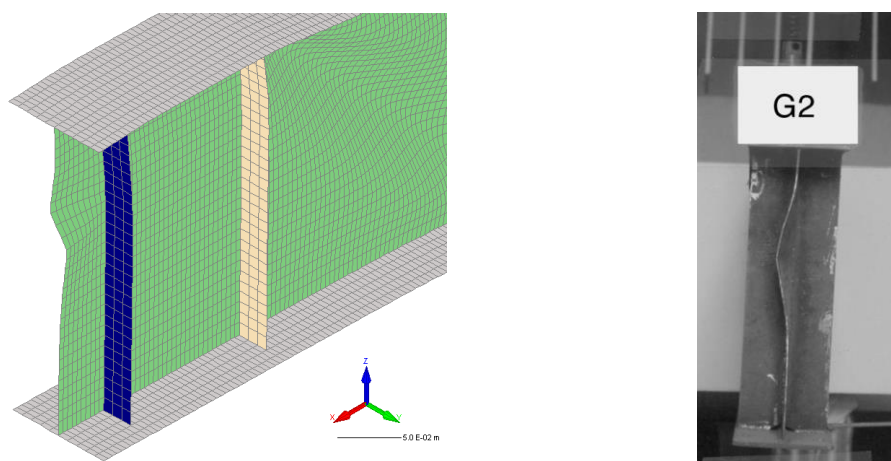


Figure 4.11 – Numerical and experimental (Lee & Yoo, 1999) out of plane web buckling in the non-rigid end post of PG2

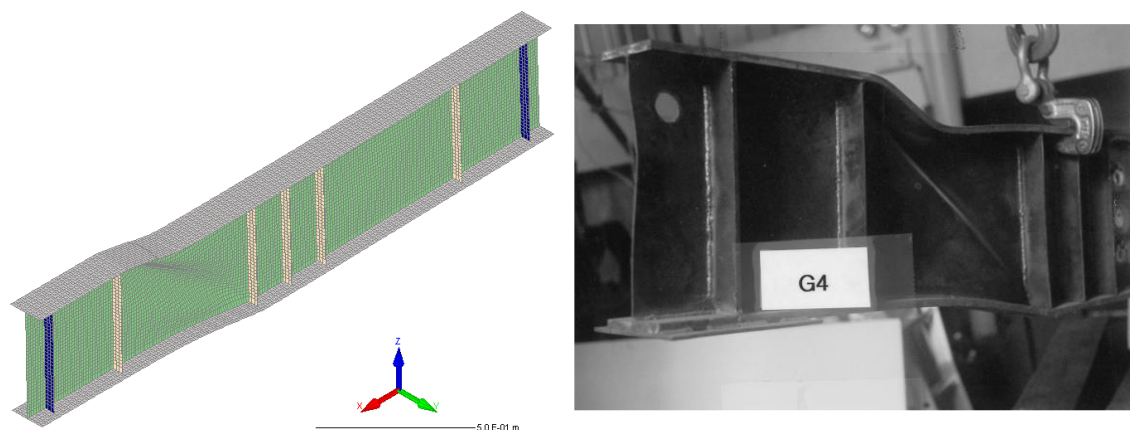


Figure 4.12 – Numerical and experimental (Lee & Yoo, 1999) deformed shape after test of PG4

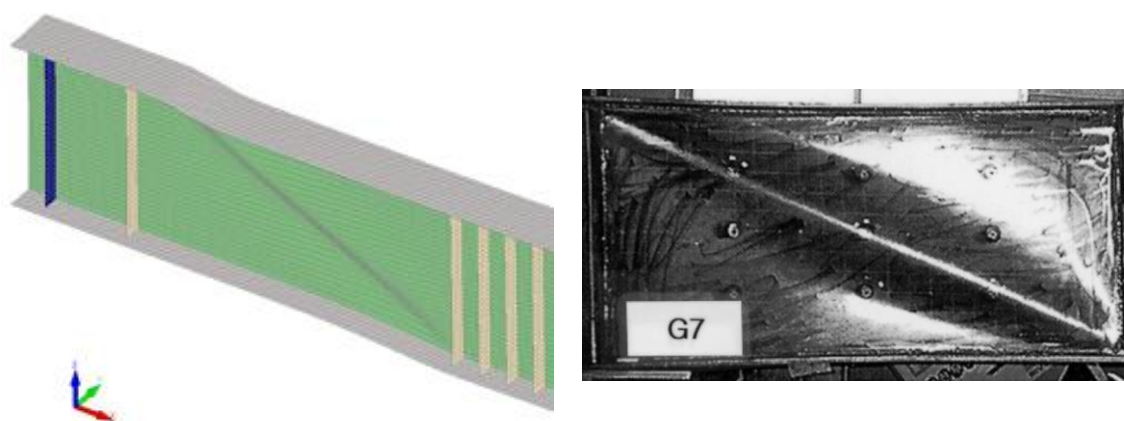


Figure 4.13 – Numerical and experimental (Lee & Yoo, 1999) deformed shape after test of PG7

The experimental tests performed at University of Minho (Gomes et al., 2000) were also numerically modelled in SAFIR. The ultimate loads obtained in the experimental tests are compared with those resulting from the numerical model. The results are presented in Table 4.8. Through the comparison of results it is possible to observe that the numerical model provides a good approximation to the actual behaviour of the tested girders, with an average deviation equal to 4.1%. The average deviation was determined in absolute. Table 4.8 shows a maximum conservative deviation of 9.7% and a maximum not conservative deviation of 4.9%, which is considered acceptable. Figure 4.14 shows the similarity between the failure modes observed after the numerical and experimental tests of PG13, a plate girder provided with a longitudinal stiffener. The shear buckling in the web panel may be observed in both experimental and numerical tests. Moreover, flange buckling may also be observed.

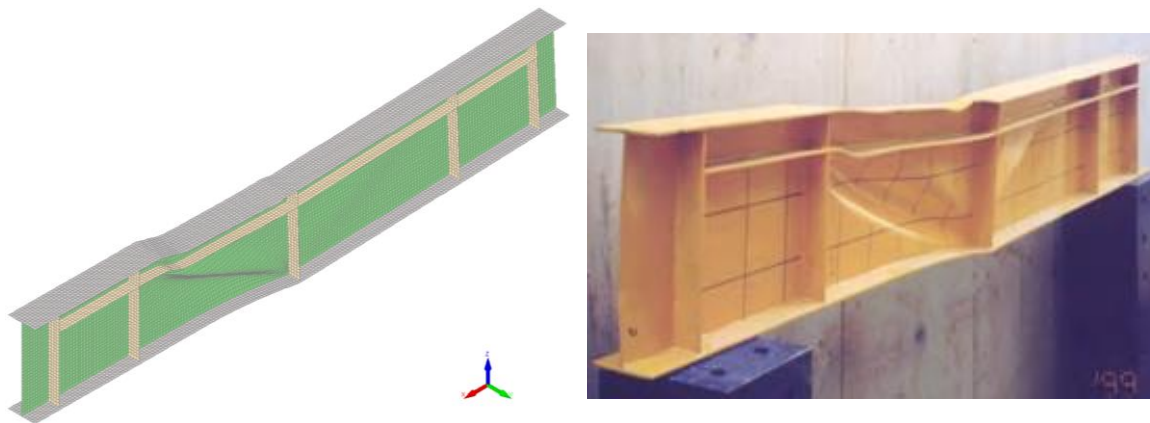


Figure 4.14 – Numerical and experimental (Gomes et al., 2000) deformed shape after test of PG13

Table 4.8 – Comparison between the numerical and experimental results of the steel plate girders tested at the University of Minho

Label	Ultimate load [kN]		Deviation [%] [(2)-(1)]/(1)
	Exp. test (1)	SAFIR (2)	
PG9	110.0	113.0	2.8
PG10	110.0	115.4	4.9
PG11	150.0	143.9	-4.1
PG12	130.0	132.0	1.5
PG13	133.0	135.3	1.7
PG14	172.0	155.4	-9.7

The graphical comparison between the numerical and experimental results of all the analysed plate girders at normal temperature is presented in Figure 4.15. The differences are always lower than 10%, most of the times on the safe side. The differences are larger than 3% in four simulations only (PG10, PG11, PG14, PG19) and just two registered a difference larger than 5% (PG14 and PG19). So, it may be concluded that there is a very good agreement between the numerical and experimental results, in terms of both ultimate loads and deformed shape at failure.

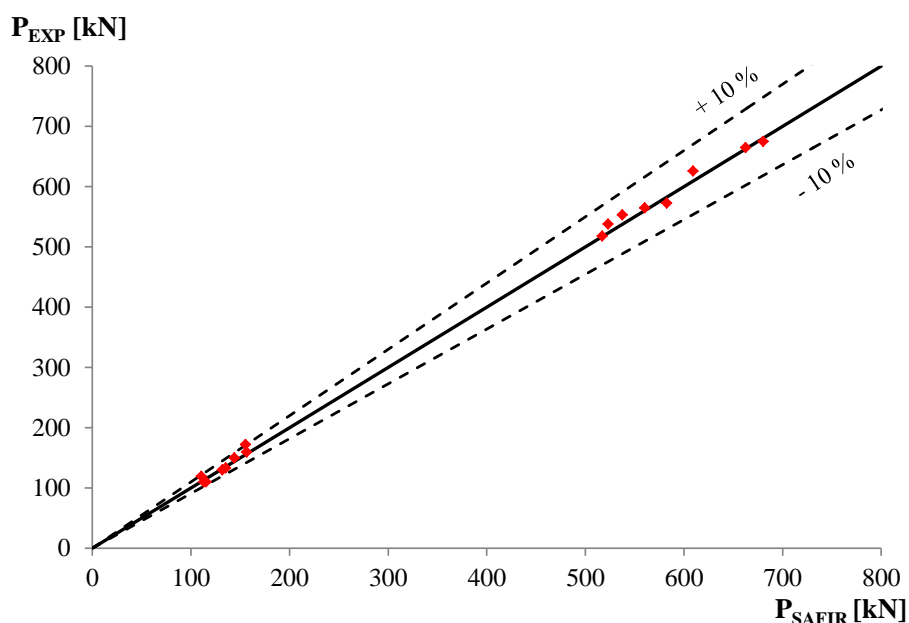


Figure 4.15 – Experimental and numerical ultimate resistance of all the analysed steel plate girders at normal temperature

4.2.2.2 Elevated temperatures

Fire resistance experimental tests were conducted at Nanyang Technological University in Singapore (Vimonsatit et al., 2007b). These tests were also numerically reproduced by Vimonsatit et al. (2007b) using the MARC software (MSC, 2001). The ultimate loads of the overall test results are presented in Table 4.9, as well as a comparison between the numerical and the experimental results. A good agreement between the results of the numerical model developed in SAFIR and the experiments was obtained.

From the results at normal temperature (PG15 and PG19), an average deviation between SAFIR and the experimental tests equal to 4.6% was observed, whereas the results obtained from the authors using MARC software presented a 13.8% average deviation

when compared with the experimental tests. Comparing the results at elevated temperatures (PG16-18 and PG20-22), SAFIR presents an average deviation of 4.2% when compared with the experimental tests, whereas an average deviation equal to 10.4% was observed between MARC and the experiments.

Therefore, it can be said that SAFIR provides results generally on the safe side agreeing well with the experiments. Figure 4.16 and Figure 4.17 show the similarity on the web shear buckling observed in the experimental tests and numerical simulations for two of the analysed plate girders. Finally, the experimental and numerical results obtained at elevated temperatures are plotted in Figure 4.18.

It was shown that the numerical model developed in SAFIR provides a good approximation to the actual behaviour of steel plate girders at both normal and elevated temperatures. Therefore, the numerical model is considered duly validated.

Table 4.9 – Comparison between the numerical and experimental results of the steel plate girders tested at the Nanyang Technological University

Label	T [°C]	Ultimate load [kN]			Deviation [%]	
		Exp. test (1)	MARC (2)	SAFIR (3)	[(2)-(1)]/(1)	[(3)-(1)]/(1)
PG15	20	159.7	176.0	156.6	10.2	-2.0
PG16	400	135.3	132.0	128.8	-2.4	-4.8
PG17	565	68.7	76.8	74.6	11.8	8.6
PG18	690	34.3	32.8	32.1	-4.4	-6.3
PG19	20	119.2	140.0	110.6	17.4	-7.2
PG20	400	92.8	106.8	89.7	15.1	-3.3
PG21	550	57.2	65.0	56.3	13.6	-1.5
PG22	700	20.3	23.4	20.2	15.2	-0.6

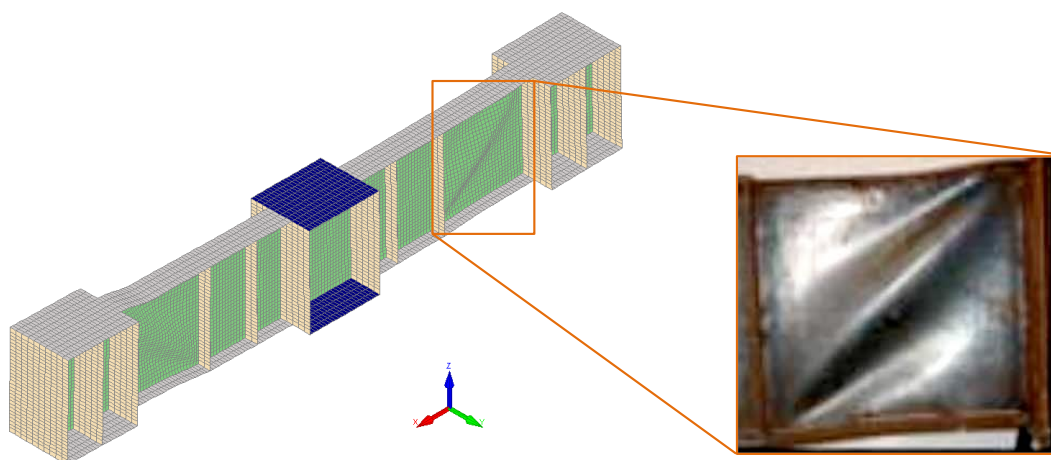


Figure 4.16 – Numerical and experimental deformed shape after test of PG16

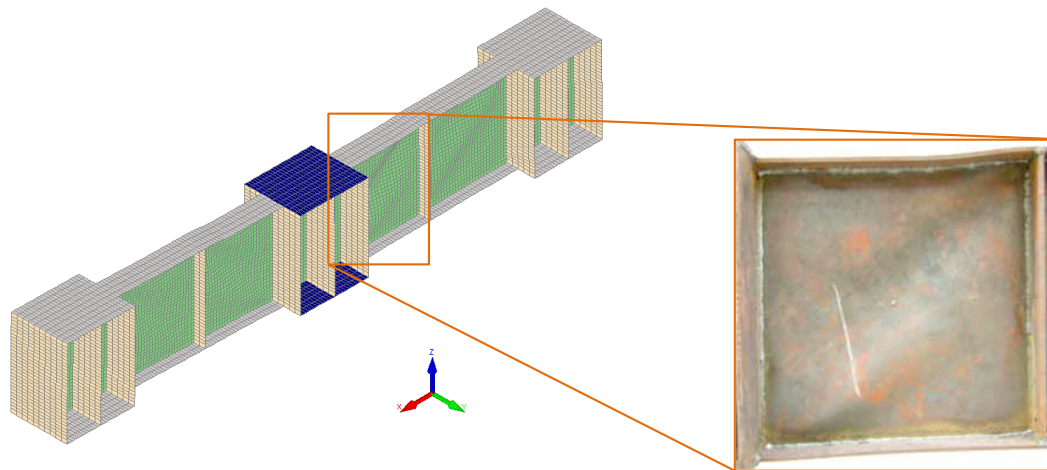


Figure 4.17 – Numerical and experimental deformed shape after test of PG21

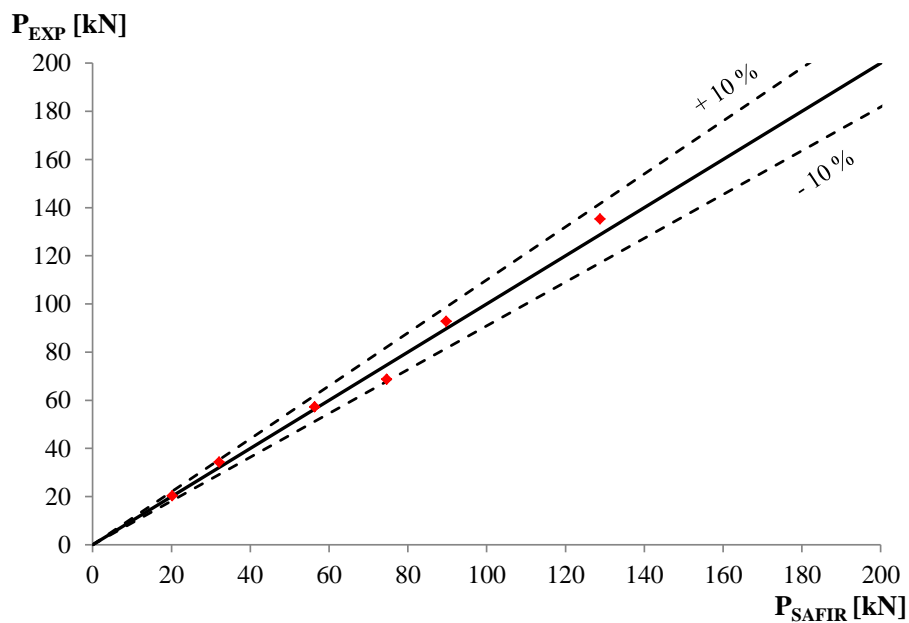


Figure 4.18 – Experimental and numerical ultimate resistance of all the analysed steel plate girders at elevated temperatures

4.3 Influence of the initial imperfections

4.3.1 Geometric imperfections

4.3.1.1 Normal temperature

Based on the configuration of the steel plate girders tested by Lee and Yoo (1999), whose geometry and dimensions were presented in section 4.2.1, a sensitivity analysis about the influence of the maximum amplitude of the geometric imperfections (m.a.g.i.)

on the ultimate shear strength has been performed. Different maximum amplitudes of the geometric imperfections were considered based on the web thickness (t_w , $t_w/2$, $t_w/10$ and $t_w/100$), as well as the maximum amplitude recommended in EC3 ($0.8b_f/100$ in the flanges and $0.8h_w/100$ in the web), as stated in section 4.1.3.1.

The results are presented in Table 4.10 listed from highest to lowest maximum amplitude. As expected, the higher the maximum amplitude is, the more conservative the results are. Comparing numerical and experimental results, the average deviation is 4.6% on safe side when the maximum amplitude recommended in EC3 is used. When the maximum amplitude is taken as 10% of the web thickness the average deviation is 0.9% on the safe side. Finally, considering a maximum amplitude equal to 1% of the web thickness is too soft, being the average deviation 1.2% on the unsafe side, i.e. the ultimate loads numerically obtained are generally higher than those observed in the experimental tests. Furthermore, the consideration of the maximum amplitude recommended in EC3 is too severe for the numerical modelling of experimental tests, being $t_w/10$ an appropriate value to use for that purpose.

Table 4.10 – Geometric imperfections sensitivity analysis at normal temperature

Label	Exp. test a/h_w	Maximum amplitude of the geometric imperfections (m.a.g.i.)											
				t_w		EC3		$t_w/2$		$t_w/10$		$t_w/100$	
		P	P	Dev.	P	Dev.	P	Dev.	P	Dev.	P	Dev.	
		[kN]	[kN]	[%]	[kN]	[%]	[kN]	[%]	[kN]	[%]	[kN]	[%]	
PG1	1.00	564.9	515.7	-8.7	518.0	-8.3	527.3	-6.6	560.1	-0.8	585.5	3.7	
PG2	1.00	664.9	652.9	-1.8	651.8	-2.0	654.7	-1.5	662.6	-0.3	665.2	0.0	
PG3	1.00	674.7	670.0	-0.7	669.2	-0.8	672.1	-0.4	680.3	0.8	682.9	1.2	
PG4	1.50	537.6	468.6	-12.9	475.5	-11.6	489.5	-9.0	523.0	-2.7	558.4	3.9	
PG5	1.50	572.7	564.2	-1.5	561.0	-2.0	574.0	0.2	582.7	1.7	584.7	2.1	
PG6	1.50	625.7	591.1	-5.5	590.9	-5.6	598.8	-4.3	609.2	-2.6	610.7	-2.4	
PG7	2.00	517.8	512.9	-1.0	510.1	-1.5	520.0	0.4	517.2	-0.1	527.4	1.9	
PG8	2.00	552.9	528.9	-4.3	524.8	-5.1	539.1	-2.5	537.5	-2.8	549.2	-0.7	
Average deviation [%]				-4.6	-4.6	-3.0	-0.9	1.2					

4.3.1.2 Elevated temperatures

The influence of the maximum amplitude of the geometric imperfections was also analysed under fire conditions using the same plate girders analysed at normal temperature (see Table 4.11). In this case, the plate girders are subjected to three different uniform temperatures (350°C, 500°C and 600°C) under steady-state conditions, i.e. the temperature is considered constant while the load is increased. Two different

maximum amplitudes were considered: the one used in the modelling of experimental tests and the one recommended in EC3. It was found that considering geometric imperfections causes a significant reduction on the ultimate shear strength and not considering them conducts to unrealistic shear buckling resistances. However, at elevated temperatures the maximum amplitude of the geometric imperfections has no significant influence on the ultimate capacity of the analysed plate girders. The average deviation is equal to 0.6% for all the analysed temperatures.

Table 4.11 – Geometric imperfections sensitivity analysis at elevated temperatures

Label	a/h _w	350°C			500°C			600°C			
		tw/10 P [kN]	EC3 P [kN]	Dev. [%]	tw/10 P [kN]	EC3 P [kN]	Dev. [%]	tw/10 P [kN]	EC3 P [kN]	Dev. [%]	
PG1	1.00	450.0	451.8	0.4	349.1	350.4	0.4	207.1	207.9	0.4	
PG2	1.00	529.5	531.0	0.3	409.4	410.7	0.3	241.2	242.1	0.4	
PG3	1.00	568.9	571.0	0.4	441.2	443.0	0.4	260.9	262.0	0.4	
PG4	1.50	375.2	375.9	0.2	290.3	290.5	0.1	170.9	171.2	0.2	
PG5	1.50	438.5	440.8	0.5	337.8	339.6	0.5	197.5	198.5	0.5	
PG6	1.50	503.4	505.9	0.5	390.1	392.1	0.5	229.7	231.1	0.6	
PG7	2.00	364.0	368.3	1.2	278.8	282.0	1.1	161.5	163.3	1.2	
PG8	2.00	382.5	388.9	1.7	294.7	299.5	1.6	172.1	174.7	1.5	
Average deviation [%]				0.6				0.6			

4.3.2 Residual stresses

4.3.2.1 Normal temperature

The authors of the experimental tests did not measure the residual stresses and therefore, they were not considered in the validation of the numerical model. However, in this section their influence on the ultimate shear strength of steel plate girders is evaluated. For taking the residual stresses into account, SAFIR transform them into residual strains and add them to the other strains in the first calculation (Franssen, 1993; Lopes et al., 2010). The pattern of residual stresses considered was the one presented in Figure 4.6. One may observe that the influence of the residual stresses on the ultimate shear strength of steel plate girders is high, with the ultimate loads of the analysed girders on average 8.6% lower when a maximum amplitude of the geometric imperfections equal to $t_w/10$ is used. When a higher maximum amplitude of the geometric imperfections is considered, like the one recommended in EC3, the reduction on the ultimate loads is not so high, being on average 5.3%.

Table 4.12 – Residual stresses sensitivity analysis at normal temperature

Label	With imperfections only		With imperfections plus residual stresses			
	m.a.g.i.= $t_w/10$	m.a.g.i.=EC3	m.a.g.i.= $t_w/10$		m.a.g.i.=EC3	
	P [kN]	P [kN]	P [kN]	Deviation [%]	P [kN]	Deviation [%]
PG1	560.1	518.0	505.2	-9.8	499.4	-3.6
PG2	662.6	651.8	624.1	-5.8	626.3	-3.9
PG3	680.3	669.2	646.7	-4.9	647.3	-3.3
PG4	523.0	475.5	465.1	-11.1	443.0	-6.8
PG5	582.7	561.0	523.6	-10.1	525.9	-6.2
PG6	609.2	590.9	571.6	-6.2	572.6	-3.1
PG7	517.2	510.1	463.8	-10.3	469.1	-8.0
PG8	537.5	524.8	479.1	-10.9	487.5	-7.1
Average deviation [%]				-8.6		-5.3

4.3.2.2 Elevated temperatures

As performed in the sensitivity analysis of the geometric imperfections, herein the plate girders were also subjected to a uniform temperature equal to 500°C under steady-state conditions. Table 4.13 shows the influence of the residual stresses on the ultimate shear strength of steel plate girders subjected to elevated temperatures. It is shown that there is no substantial reduction on the ultimate loads of the analysed plate girders and, consequently, one can conclude that the residual stresses do not need to be taken into account on the numerical analysis of steel plate girders subjected to elevated temperatures.

The results showed that residual stresses are not so important for the ultimate shear strength of steel plate girders exposed to fire. Tide (1998) and Quiel and Garlock (2010) affirm that a relaxation of initial residual stresses is likely to occur when a steel member is exposed to fire due to an increase in steel temperature. However, it is important bearing in mind that the evolution of the residual stresses when a profile is exposed to fire is not very well known and their influence may not be always considered appropriately in the numerical calculation (Franssen, 1993).

Table 4.13 – Residual stresses sensitivity analysis at elevated temperatures

Label	With imperfections only		With imperfections plus residual stresses			
	m.a.g.i.= $t_w/10$	m.a.g.i.=EC3	m.a.g.i.= $t_w/10$		m.a.g.i.=EC3	
	P [kN]	P [kN]	P [kN]	Deviation [%]	P [kN]	Deviation [%]
PG1	349.1	350.4	348.8	-0.1	350.2	-0.1
PG2	409.4	410.7	409.0	-0.1	409.9	-0.2
PG3	441.2	443.0	440.0	-0.3	441.7	-0.3
PG4	290.3	290.5	289.7	-0.2	290.0	-0.2
PG5	337.8	339.6	337.2	-0.2	338.7	-0.3
PG6	390.1	392.1	389.3	-0.2	390.8	-0.3
PG7	278.8	282.0	276.9	-0.7	280.4	-0.6
PG8	294.7	299.5	292.5	-0.7	297.5	-0.7
Average deviation [%]				-0.3	-0.3	

4.4 Conclusions

Based on the work presented in Chapter 4, the following general conclusions are drawn:

- The numerical model developed in SAFIR is able to accurately reproduce the behaviour of steel plate girders under shear loading at both normal and elevated temperatures;
- Do not have into account the geometric imperfections conduct to unrealistic shear buckling resistances;
- The maximum amplitude of the geometric imperfections has significant influence on the ultimate shear strength of steel plate girders analysed at normal temperature. However, it is not relevant in fire situation;
- The higher the maximum amplitude is, the more conservative the results are;
- The application of the maximum amplitude recommended in EC3 is too severe for the numerical modelling of experimental tests. An appropriate value to use for that purpose is $t_w/10$;
- Residual stresses cause a considerable reduction of bearing capacity of steel plate girders affected by shear buckling at normal temperature. However, they have no substantial influence at elevated temperatures.

Chapter 5

Basis for the parametric study

Chapter 5 Basis for the parametric study

- 5.1 Characteristics of the analysed plate girders
- 5.2 Methodology for analysis of results
- 5.3 Sequence of analysis of the results

Chapter 5 Basis for the parametric study

5.1 Characteristics of the analysed plate girders

The main objective of the parametric study is to evaluate the accuracy of the design expressions implemented in EC3 to predict the ultimate shear strength of steel plate girders affected by shear buckling, which includes the web resistance to shear buckling, the flanges contribution and the interaction between shear and bending. With this purpose, four groups of simply supported steel plate girders have been analysed. Steel plate girders with rigid and non-rigid end posts have been considered, while steel plate girders with no end posts were not considered because they are affected by web crippling, which is out of the scope of this thesis.

The first group was designed to assess the accuracy of the expressions used to obtain the contribution from the flanges to the shear buckling resistance. Simply supported 2-panels plate girders were considered (see Figure 5.1). The girders were provided with double-sided transverse stiffeners at load points (supports and mid-span). The web thickness was fixed ($t_w=4$ mm) and the flanges thickness was ranged between 12 and 20 mm. For the web depth, values between 800 and 1600 mm were considered. The girder length was chosen to achieve the desired aspect ratios (a/h_w), which varied from 0.5 up to 3.0. Thus, the girder length, which is twice the transverse stiffeners spacing, ranged between 0.8 and 9.6 m. Table 5.1 shows the geometrical dimensions considered for the girders analysed in group I, which are illustrated in Figure 5.2a.

The properties of the second group of plate girders were quite similar to group I. Figure 5.1a shows the geometry of the plate girders with non-rigid end posts, whereas the geometry of the plate girders with rigid end posts is presented in Figure 5.1b. The differences between group I and II are related to the web and flanges thicknesses. With this group of girders it was intended to analyse the shear buckling resistance. For that purpose, the plate girders were provided with strong flanges ($t_f=20$ mm) in order to have a shear dominant failure in almost all of the girders. The web thickness was ranged between 4 and 10 mm, as presented in Table 5.2. For an easier understanding, Figure 5.2b shows the cross-section of the girders belonging to group II.

Regarding material properties, the steel grade S235 was considered for groups I and II and the Young's modulus at normal temperature was considered equal to 210 GPa.

Table 5.1 – Details of the plate girders analysed in group I

h_w [mm]	t_w [mm]	b_f [mm]	t_f [mm]	t_s [mm]	a/h_w [-]
800, 1000, 1200, 1400 and 1600	4.0	300	12.0, 14.0, 16.0, 18.0 and 20.0	20.0	0.5, 1.0, 1.5, 2.0 and 3.0

Table 5.2 – Details of the plate girders analysed in group II

h_w [mm]	t_w [mm]	b_f [mm]	t_f [mm]	t_s [mm]	a/h_w [-]
800, 1000, 1200, 1400 and 1600	4.0, 5.0, 6.0, 7.0, 8.0, 9.0 and 10.0	300	20.0	20.0	0.5, 1.0, 1.5, 2.0 and 3.0

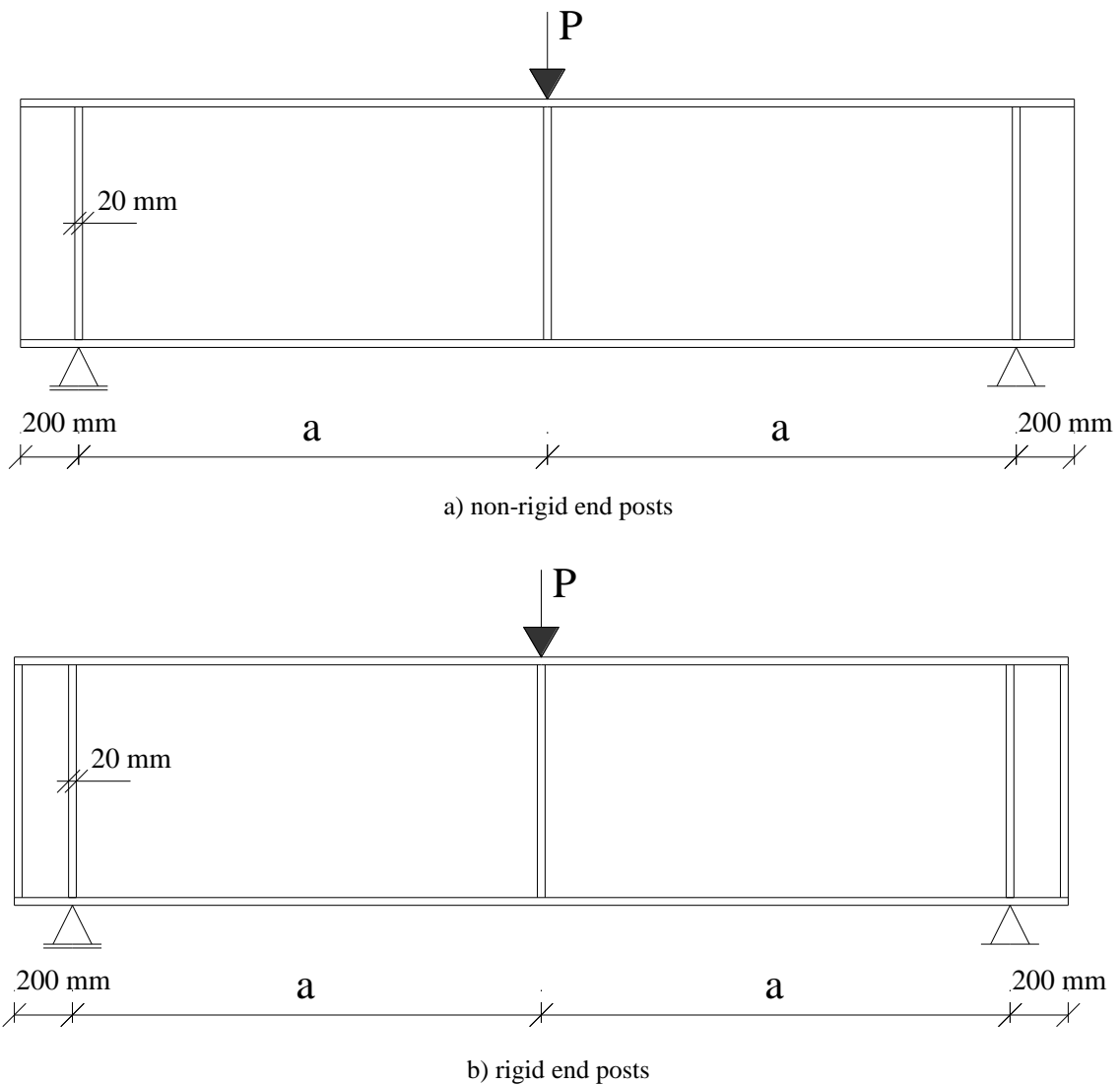
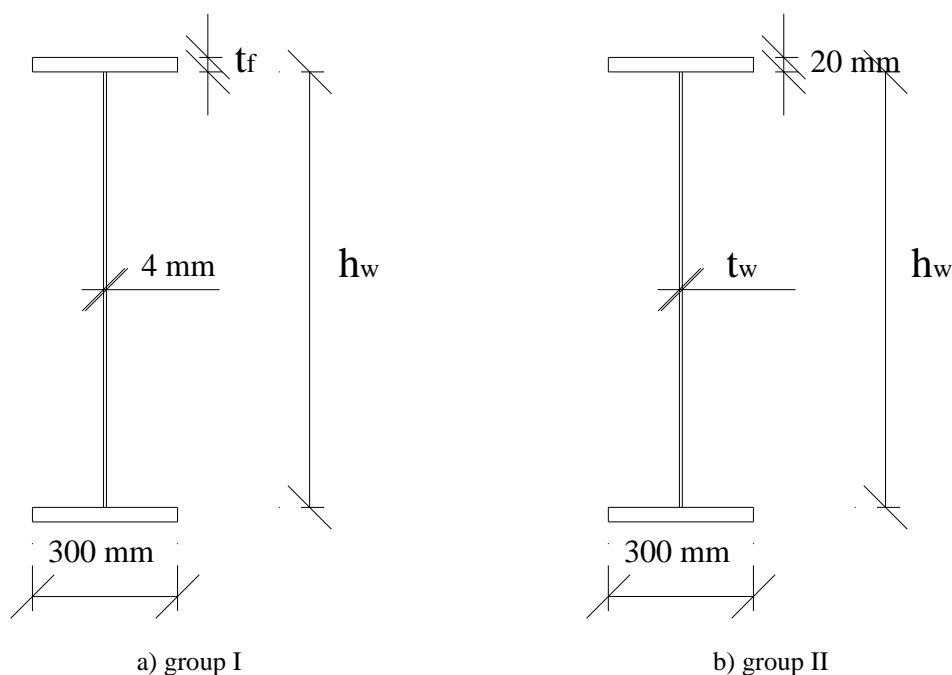


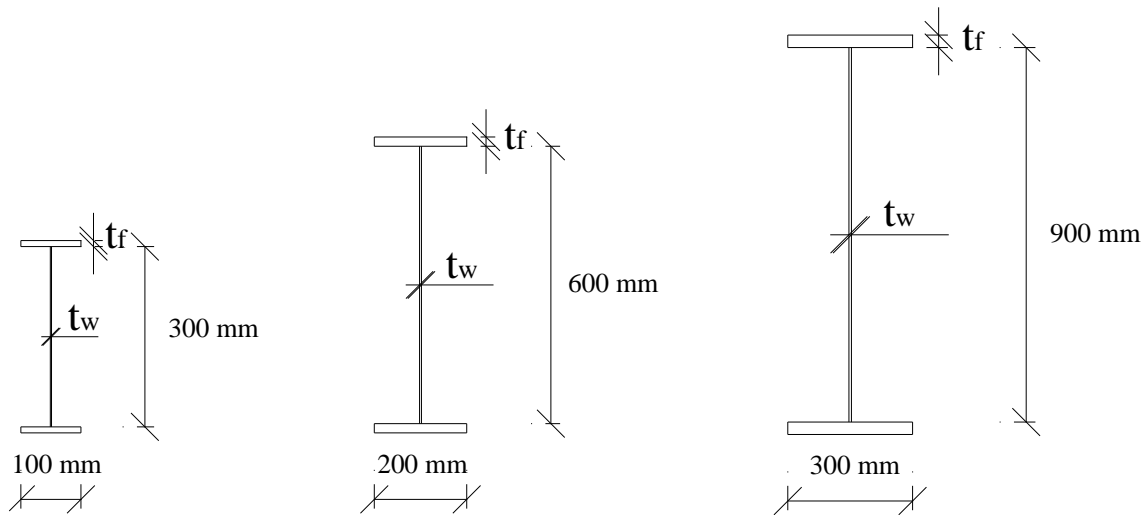
Figure 5.1 – Geometric configuration of the plate girders analysed in groups I and II

In the third group of this parametric study, it was intended to study 4-panels and 6-panels plate girders in addition to the 2-panels plate girders analysed in the two first groups. Simply supported plate girders with rigid and non-rigid end posts were considered. The rigid end post was formed by two stiffeners placed at the end supports spaced by 100 mm. The thickness of these end stiffeners is the same as the intermediate transverse stiffeners. Figure 5.3 shows the geometric configuration of the girders with rigid end posts. The geometric configuration of the girders with non-rigid end posts is the same presented in Figure 5.3, if removed the two end stiffeners (one in each side of the girder). The girder length was 1.8 m and different distances between transverse stiffeners were considered (300, 450, 600 and 900 mm), as presented in Figure 5.3.

Nine different cross-sections were analysed, as presented in Table 5.3. Three web depths (300, 600 and 900 mm), as well as three flange widths (100, 200 and 300 mm) were considered, as illustrated in Figure 5.2c. This way, a wide range of plate girders aspect ratios were analysed, ranging from 0.3 up to 3.0. Finally, different steel grades were considered (S235, S275, S355 and S460).

The fourth and last group of plate girders analysed in this parametric study was based on the plate girders tested in group III. Herein, the main objective was the assessment of the interaction between shear and bending. With this purpose, the thickness of the flanges was reduced to allow more girders exhibiting a combined shear plus bending failure. The dimensions of the girders are presented in Table 5.4.





c) groups III and IV

Figure 5.2 – Cross-section notation of the analysed plate girders

Table 5.3 – Details of the plate girders analysed in group III

h_w [mm]	t_w [mm]	b_f [mm]	t_f [mm]	t_s [mm]	a [mm]
300	1.5	100	5.0	5.0	
300	2.0	100	10.0	5.0	
300	2.5	100	10.0	5.0	
600	3.0	200	10.0	10.0	300, 450,
600	3.5	200	12.0	10.0	600 and
600	4.0	200	12.0	10.0	900
900	4.0	300	12.0	15.0	
900	4.5	300	15.0	15.0	
900	5.0	300	15.0	15.0	

Table 5.4 – Details of the plate girders analysed in group IV

h_w [mm]	t_w [mm]	b_f [mm]	t_f [mm]	t_s [mm]	a [mm]
300	1.5	100	4.0	5.0	
300	2.0	100	5.0	5.0	
300	2.5	100	7.0	5.0	
600	3.0	200	5.0	10.0	300, 450,
600	3.5	200	6.0	10.0	600 and
600	4.0	200	7.0	10.0	900
900	4.0	300	6.0	15.0	
900	4.5	300	7.0	15.0	
900	5.0	300	8.0	15.0	

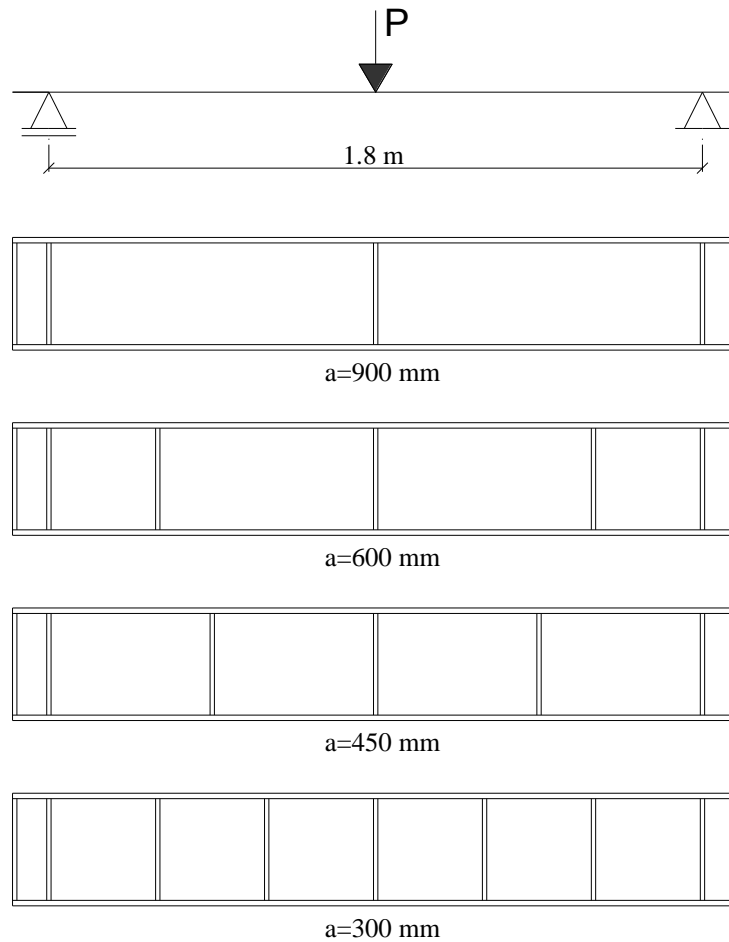


Figure 5.3 – Geometric configuration of the plate girders with rigid end posts analysed in groups III and IV

The steel properties at normal temperature considered in the parametric study performed in this thesis are presented in Table 5.5. At elevated temperatures, they were reduced applying the reduction factors presented in Table 3.2.

Table 5.5 – Material properties considered in the parametric study

	Group			
	I	II	III	IV
Steel yield strength (f_y) [MPa]	235	235	235, 275, 355 and 460	235, 275, 355 and 460
Young's modulus (E) [GPa]	210	210	210	210

The numerical simulations of the plate girders described above were made using the methodology usually designated by GMNIA (geometrically and materially non-linear imperfect analysis). Geometric imperfections and residual stresses were taken into account at both normal and elevated temperatures, as detailed in section 4.1.3.

For the simulations at elevated temperatures a uniform temperature distribution in the cross-section was used, so that the comparison between the numerical results and the EC3 simple design expressions could be possible. The temperatures chosen were 350, 500, 600 °C, in order to cover the majority of practical situations. These temperatures were applied under steady-state conditions, i.e. the temperature is considered constant while the load is increased until failure.

The number of numerical simulations executed in this parametric study for each group of plate girders is presented in Table 5.6. As one can see, 1176 numerical simulations were conducted at normal temperature, while 3528 numerical simulations were performed at elevated temperatures, amounting to 4704 numerical simulations. Each simulation took an average time of 30 minutes on a computer with an Intel® Core™ i5-3570K 3.4 GHz CPU.

Table 5.6 – Number of numerical simulations performed in this parametric study

Group	20°C	350°C	500°C	600°C
I	250	250	250	250
II	350	350	350	350
III	288	288	288	288
IV	288	288	288	288

5.2 Methodology for analysis of results

This thesis focuses on the assessment of the design expressions implemented Part 1-5 of EC3 (CEN, 2006b) to predict the ultimate shear strength of steel plate girders affected by shear buckling. With this purpose, three different zones were considered in the V-M interaction diagram for the analysis and comparison of the numerical results with the EC3 expressions, as illustrated in Figure 5.4. Hence, plate girders exhibiting a shear dominant failure belong to zone 1, while plate girders revealing a bending dominant failure belong to zone 3. Finally, plate girders with a combined shear plus bending failure belong to zone 2. The ratio of shear force to bending moment for each zone of the shear-bending interaction diagram is given in Table 5.7.

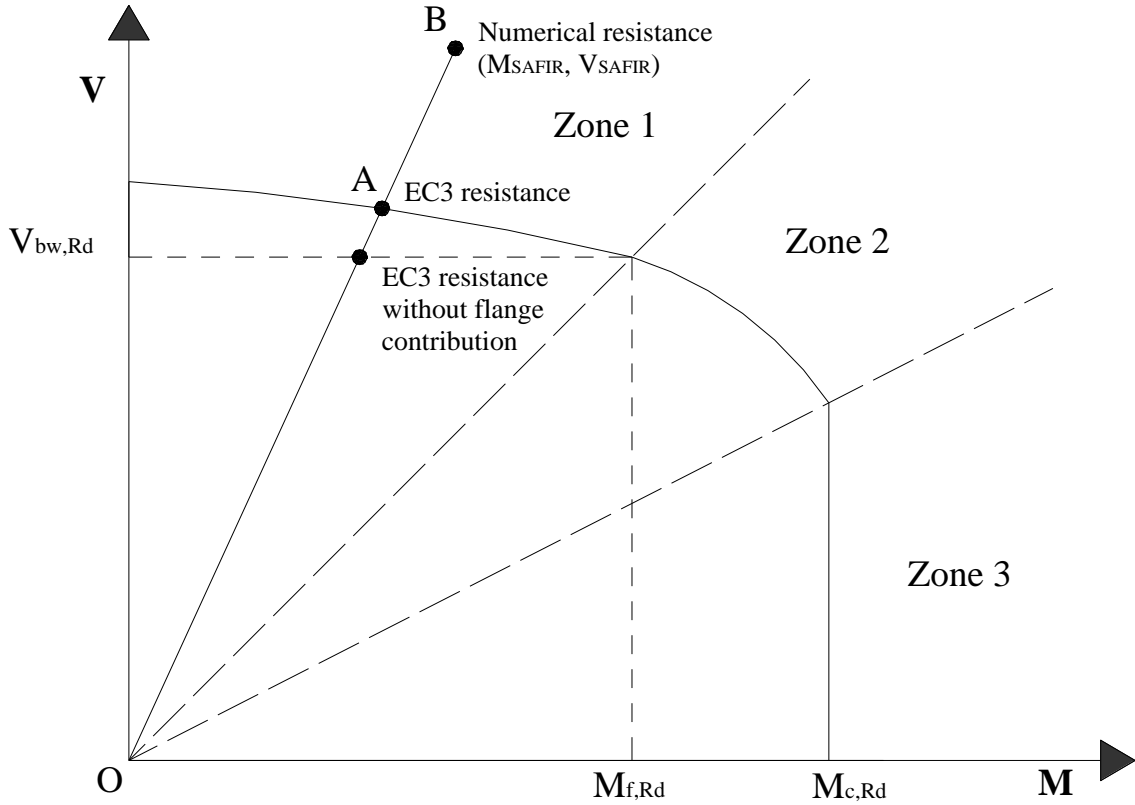


Figure 5.4 – Zones definition on the shear-bending interaction diagram

Table 5.7 – Ratio of shear force to bending moment according to the zone of the shear-bending interaction diagram

Zone	Expression
1	$\frac{V_{SAFIR}}{M_{SAFIR}} > \frac{V_{bw,Rd}}{M_{f,Rd}}$
2	$\frac{V_{SAFIR}}{M_{SAFIR}} \leq \frac{V_{bw,Rd}}{M_{f,Rd}}$ $\frac{V_{SAFIR}}{M_{SAFIR}} \geq 0.5 \frac{V_{bw,Rd}}{M_{c,Rd}} \left(\sqrt{\frac{(1-M_{c,Rd}/M_{pl,Rd})(1-M_{f,Rd}/M_{pl,Rd})}{(1-M_{c,Rd}/M_{pl,Rd})}} + 1 \right)$
3	$\frac{V_{SAFIR}}{M_{SAFIR}} < 0.5 \frac{V_{bw,Rd}}{M_{c,Rd}} \left(\sqrt{\frac{(1-M_{c,Rd}/M_{pl,Rd})(1-M_{f,Rd}/M_{pl,Rd})}{(1-M_{c,Rd}/M_{pl,Rd})}} + 1 \right)$

Since the precise shape of the shear-bending interaction diagram varies with both shear resistance ($V_{bw,Rd}$ and $V_{bf,Rd}$) and bending resistance ($M_{f,Rd}$ and $M_{pl,Rd}$), and since these design parameters are different for each plate girder, a single shear-bending interaction diagram must be drawn for each plate girder. For evaluating the design rules adopted in EC3, a proportional loading is assumed, i.e. the ratio of shear force to bending moment remains constant. The numerical results collected from zone 1 are used to assess the shear buckling resistance predictions from EC3 given by Eq. (3.1), while the numerical results collected from zone 2 are used to evaluate the shear-bending interaction design expression (Eq. (3.17)). The ratio by which each numerical data point

exceeded or fell short of its respective shear-bending interaction diagram was designated utilisation ratio U (in Figure 5.4, $U = \overline{OB}/\overline{OA}$). A value of U larger than 1.0 means a safe result and the numerical data point is positioned outside the interaction diagram. This methodology follows the one established by Saliba et al. (2014). It is important having in mind that the length of the zone 2 curve is smaller in the case of sections with Class 3 or 4, since the curve should be truncated by the vertical line that cuts the horizontal axis in $M_{c,Rd}$, as explained in section 3.3.

Furthermore, in the EC3 design curve for the reduction of the web resistance when subjected to shear buckling, $\eta = 1.0$ was used instead of the EC3 recommended value $\eta = 1.2$, since the applied material model does not take into account the increase of 20% of the shear yield strength due to strain hardening (Beg et al., 2010).

5.3 Sequence of analysis of the results

The analysis of the results obtained in the parametric study follows a logic sequence. As a starting point, the values of the distance c , which defines the position of the plastic hinges, obtained by both numerical results from SAFIR and analytical expression from EC3 (Eq. (3.12)) were compared in Chapter 6 considering the group I of plate girders. Results derived from this comparison demonstrated that the accuracy given by the EC3 analytical expression to calculate the position of the plastic hinges in steel plate girders should be improved. Thus, the application of a β corrective coefficient to the analytical expression to determine the distance c was proposed.

Having improved the ability of this design expression, the consequent analytical formula to obtain the flange contribution to shear buckling resistance (Eq. (3.11)) has been assessed, considering different values for c : the one obtained using the unchanged EC3 expression and the one obtained applying the β coefficient. The accuracy of Eq. (3.12) increases significantly when the β corrective coefficient is applied.

Afterwards, in Chapter 7 the ultimate shear strength given by the numerical model was compared to the one predicted by EC3 through Eq. (3.1). After analysing the ultimate shear strength as a whole, the web contribution in the full resistance of a plate girder was evaluated. For comparison with EC3 analytical expressions, the contribution from the web numerically obtained ($\chi_{w,SAFIR}$) is calculated by Eq. (5.1) subtracting the

flange contribution (χ_f), obtained using Eq. (3.14), from the ultimate shear strength directly predicted by the numerical model. The flange contribution (χ_f) to be subtracted in Eq. (3.14) is calculated considering β proposed in Chapter 6.

$$\chi_{w,SAFIR} = \frac{V_{SAFIR}}{\frac{f_{yw}}{\sqrt{3}} h_w t_w} - \chi_f \quad (5.1)$$

Finally, the interaction between shear and bending is analysed in Chapter 8, where the accuracy of the expression adopted in EC3 (Eq. (3.17)) is evaluated.

Chapter 6

*Contribution from the flanges to the shear
resistance*

Chapter 6 Contribution from the flanges to the shear resistance

- 6.1 General considerations
- 6.2 Evaluation of the EC3 expression to predict the distance between plastic hinges
- 6.3 Proposal of a corrective coefficient for the EC3 expression to predict the distance between plastic hinges
- 6.4 Influence of the corrective coefficient on design shear resistance
 - 6.4.1 Normal temperature
 - 6.4.2 Elevated temperatures
- 6.5 Conclusions

Chapter 6 Contribution from the flanges to the shear resistance

6.1 General considerations

The main goal of this Chapter is to evaluate the accuracy of the design expressions to predict the contribution from the flanges to the shear buckling resistance. However, the EC3 predictions cannot be directly compared with numerical results, since it is not possible to numerically obtain the contribution from the flanges alone. The ultimate resistance given by the numerical model is the full resistance including the web resistance and the contribution from the flanges.

Hence, the methodology used to assess the flanges contribution to shear buckling resistance was based on the analysis of sets of five girders, maintaining the web properties and ranging the thickness of the flanges from 12 to 20 mm (see Figure 6.1). Thus, the increase of strength numerically obtained, caused by an increase of 2 mm on the flanges thickness, could be compared with the increase of strength given by the EC3 predictions. It allowed evaluating the accuracy of the EC3 predictions for the flanges contribution to shear buckling resistance.

In this Chapter the plate girders from group I were analysed. The characteristics of this group of girders were presented in Chapter 5. For the analysis of the numerical results, the procedure presented in Figure 6.2 was followed.

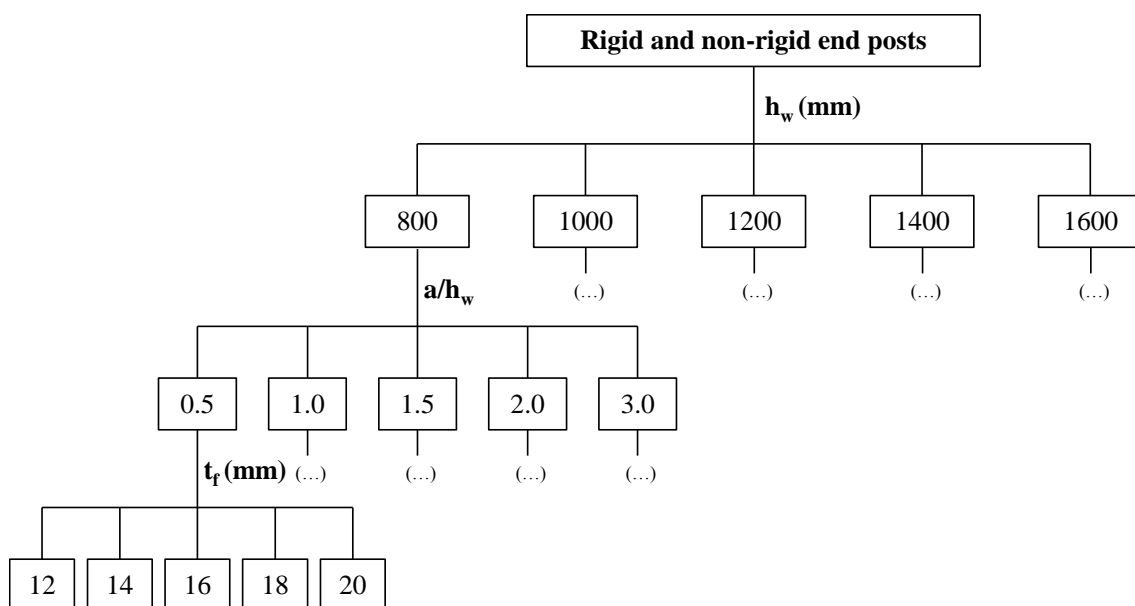


Figure 6.1 – Schematic representation of plate girders (group I) considered in this Chapter

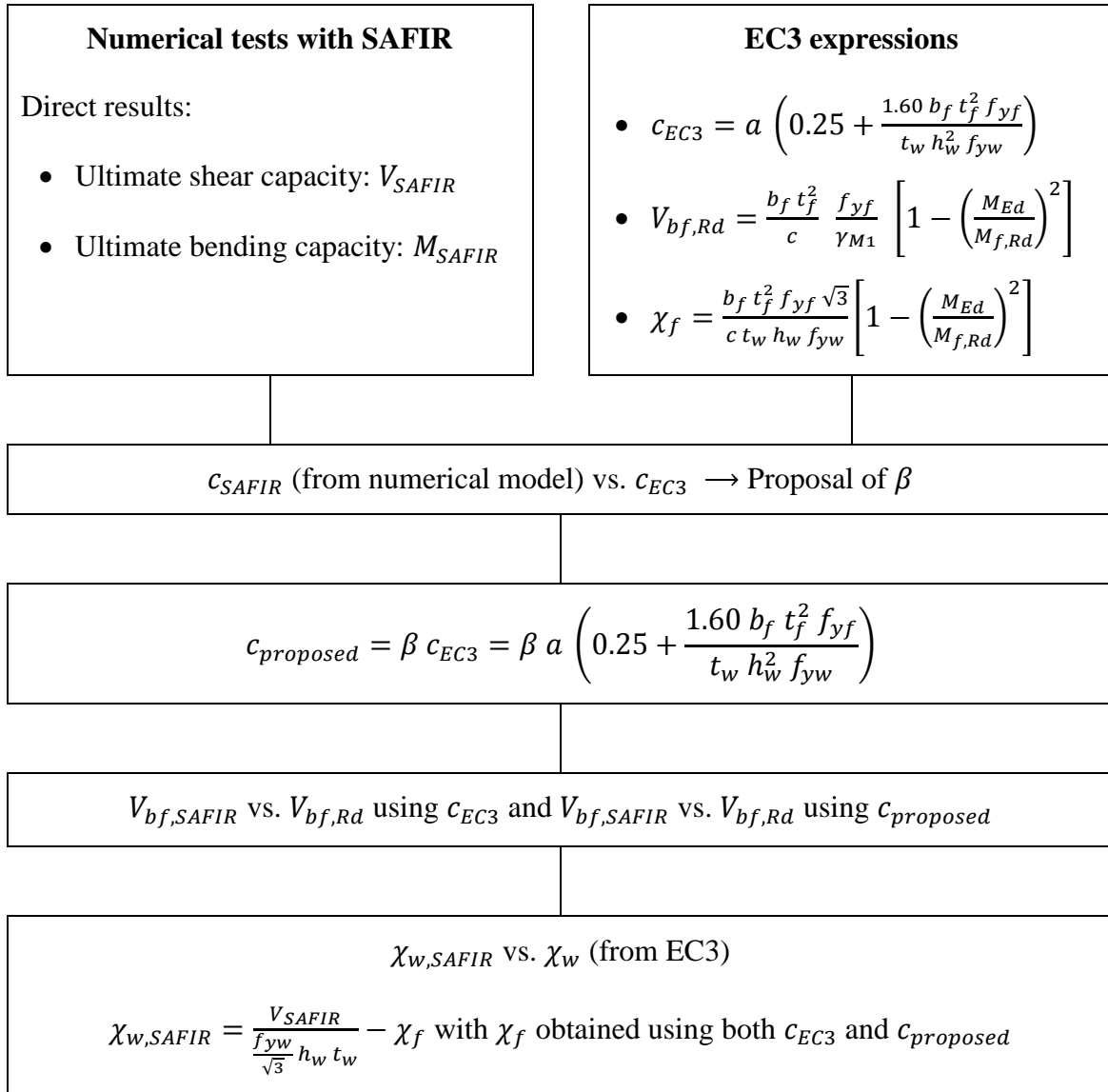


Figure 6.2 – Scheme of the methodology adopted for the analysis of results

6.2 Evaluation of the EC3 expression to predict the distance between plastic hinges

As one can observe in Eq. (3.11), the contribution from the flanges to the shear buckling resistance of a steel plate girder depends on the dimensions of the flanges, the steel yield strength, the design bending moment considering the effective area of the flanges, the largest moment within the panel and the distance c , which is the distance between plastic hinges that forms in flanges (see Figure 6.3).

According to Johansson et al. (2007), the values of c given by the EC3 expression (Eq. (3.12)) are usually smaller than the values observed in the tests, being justified with the fact that in reality there is always an additional support from the web and the plastic

mechanism in the flanges cannot develop freely. Therefore, the web and flanges contributions to shear buckling resistance cannot be completely separated. Tests conducted by Rockey and Skaloud (1969) and Skaloud (1971) showed that the values of c varies between 0.16 and 0.75 times the length of the panel (a). Figure 6.4 shows the ratio c/a for the analysed plate girders. Indeed, the values of c numerically obtained varies between 0.08 and 0.80, limits quite closer to those observed by Rockey and Skaloud (1969) and Skaloud (1971), which are represented by the dashed lines in Figure 6.4. However, this is not observed for the values of c predicted by the EC3 expression, where the ratio c/a ranges between 0.26 and 0.33. Hence, with the numerical analysis of the distance c , it is clear the need to improve the accuracy of the expression adopted in EC3 for prediction of the distance between plastic hinges.

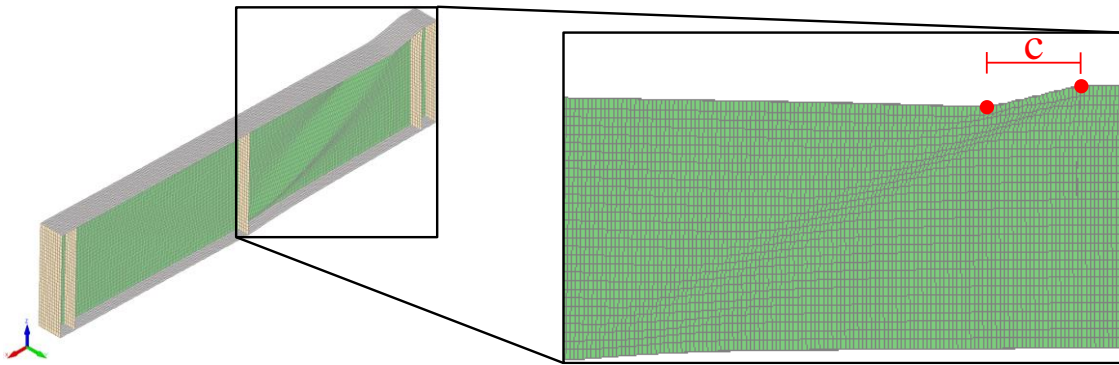


Figure 6.3 – Illustration of the distance c

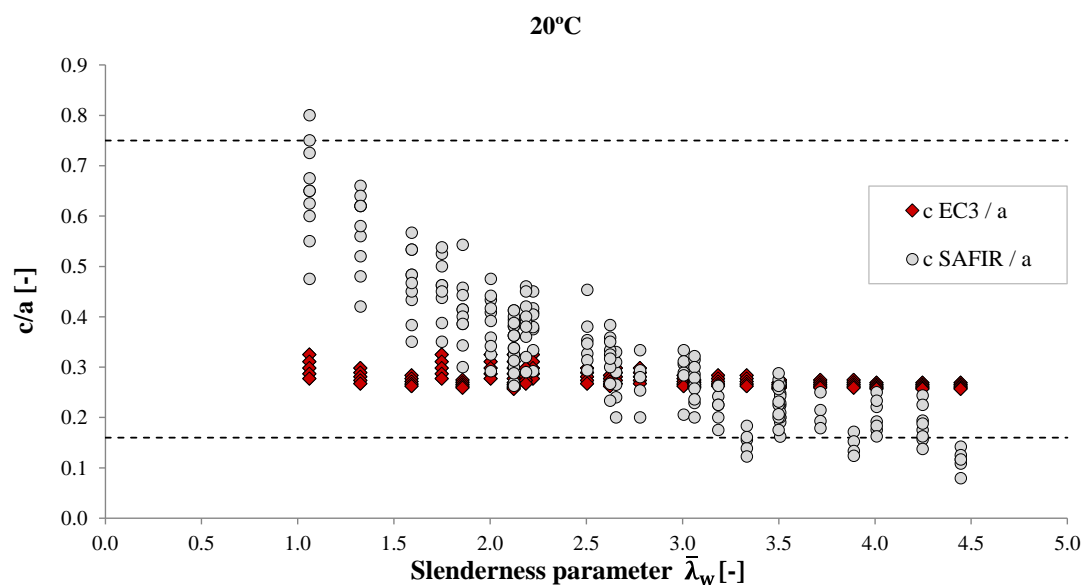


Figure 6.4 – Ratio c/a for the analysed plate girders

6.3 Proposal of a corrective coefficient for the EC3 expression to predict the distance between plastic hinges

Figure 6.4 has showed that the value of the distance c predicted by EC3 through Eq. (3.12) is smaller than the one numerically obtained for plate girders with $\bar{\lambda}_w < 3$. Thus, it was demonstrated that Eq. (3.11) adopted in EC3 overestimates the contribution from the flanges to shear buckling resistance for $\bar{\lambda}_w < 3$. Consequently, it is proposed an improvement on the expression implemented in EC3 to predict the distance c . The new c , called by $c_{proposed}$, is obtained applying a β corrective coefficient to the original expression, as presented in Eq. (6.1). This β coefficient depends on the web slenderness parameter and it is defined by Eq. (6.2) at normal temperature. For simplification, it is only proposed the introduction of a β coefficient, not developing the respective expression to determine c .

EC3 says nothing about the determination of the distance c at elevated temperatures and it was observed that the values of c obtained in the numerical analyses at elevated temperatures were different of those obtained at normal temperature. Therefore, a different β coefficient, called by β_θ , was proposed to improve the results given by Eq. (3.12) at elevated temperatures. β_θ is defined by Eq. (6.3).

The ratio between the values of c obtained from both numerical model and EC3 expression is presented in function of the slenderness parameter of the web in Figure 6.5a for normal temperature and in Figure 6.5b for elevated temperatures. The bold black line represents the proposed coefficient. As one can see, the application of this coefficient to the distance c predicted by EC3 fits better the values of the numerically obtained c . Moreover, β was considered equal to 1.0 for the plate girders with a web slenderness parameter at normal temperature ($\bar{\lambda}_w$) larger than 3.0. At elevated temperatures, $\beta_\theta = 1.0$ for $\bar{\lambda}_{w,\theta} \geq 3.5$. This was because for those plate girders the distance c predicted by EC3 is generally conservative, i.e. higher than the distance c numerically observed.

$$c_{proposed} = \beta c = \beta a \left(0.25 + \frac{1.60 b_f t_f^2 f_{yf}}{t_w h_w^2 f_{yw}} \right) \quad (6.1)$$

with β obtain as follows

$$\beta = -0.60\bar{\lambda}_w + 2.80 \text{ but } \beta \geq 1 \quad \text{for normal temperature} \quad (6.2)$$

$$\beta_{\theta} = -0.70\bar{\lambda}_{w,\theta} + 3.45 \text{ but } \beta_{\theta} \geq 1 \quad \text{for elevated temperatures} \quad (6.3)$$

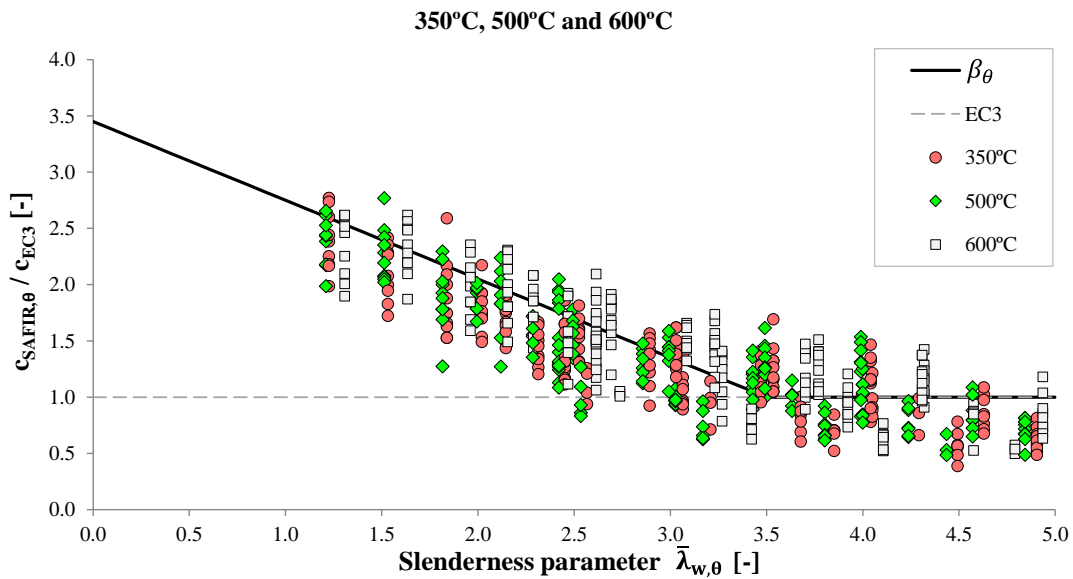
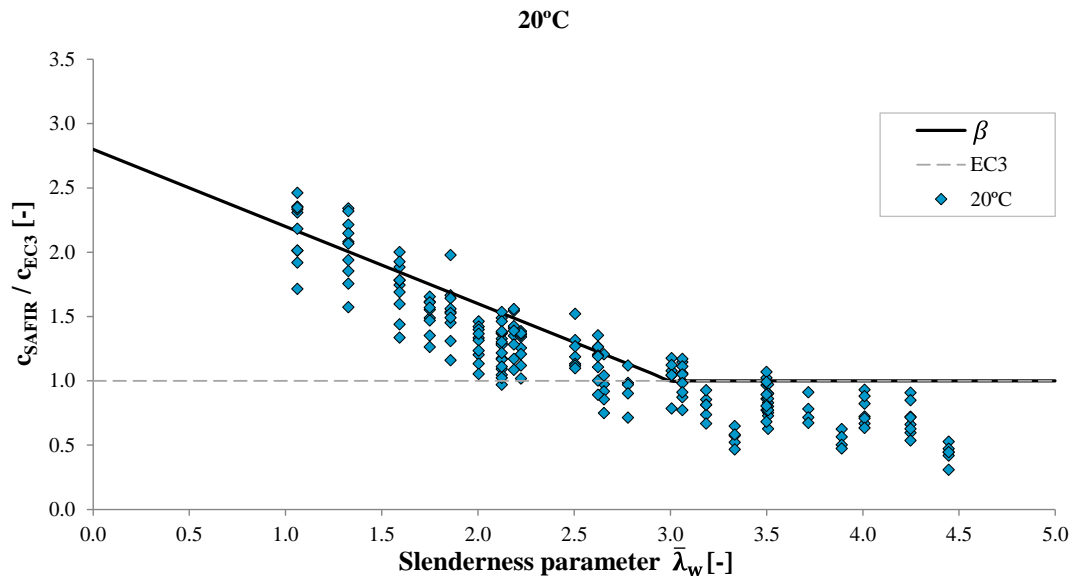


Figure 6.5 – Proposal of a β coefficient to improve the EC3 expression to determine the distance c at both normal and elevated temperatures

6.4 Influence of the corrective coefficient on design shear resistance

6.4.1 Normal temperature

The ultimate shear strength predicted by EC3 ($V_{b,Rd}$) using the expressions presented in Chapter 3 is compared to the ultimate shear capacity given by the numerical model

(V_{SAFIR}), as presented in Figure 6.6. On the calculation of the flanges contribution to shear buckling resistance it was considered the $c_{proposed}$ (given by Eq. (6.1)) and the original value adopted in EC3 (Eq. (3.12)). As one can see, the use of the value of c proposed in this thesis causes a significant improvement on the EC3 predictions for both plate girders with non-rigid end posts and plate girders with rigid end posts, providing safer results for plate girders with web slenderness values lower than 2.5.

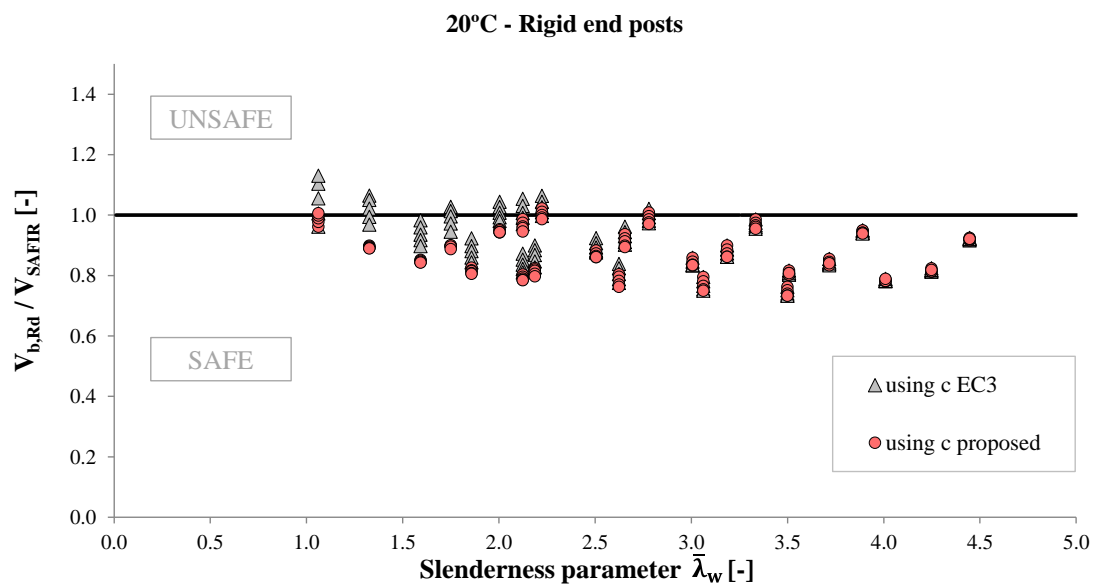
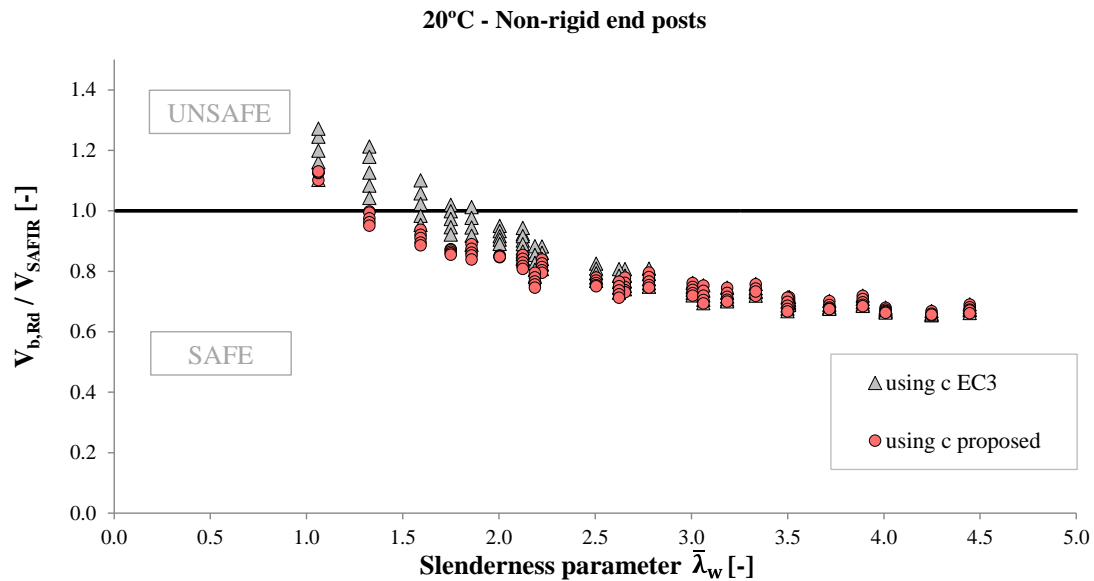


Figure 6.6 – Ultimate shear strength of the group I plate girders at normal temperature

The resistance from the web to shear buckling predicted by EC3 was also compared with the one numerically obtained through the Eq. (5.1), as explained previously. The web contribution was calculated subtracting the flange contribution to the ultimate shear capacity given by the numerical model, considering both the original expression to determine the distance c and the modified expression by the application of the β corrective coefficient.

So, if the contribution from the flanges given by Eq. (3.11) was correct, all girders of each group of five would have different values of χ_f but similar values of $\chi_{w,SAFIR}$. However, big variations on $\chi_{w,SAFIR}$ were observed when the original EC3 expression to determine the distance c is applied, showing that the EC3 expression to predict the contribution from the flanges to the shear buckling resistance is not giving accurate results. The results used in the analysis of the web resistance to shear buckling at normal temperature are presented in Table 6.1. The average $\chi_{w,SAFIR}$ for each group of five girders with the same web slenderness parameter is listed in Table 6.1, as well as the standard deviation and the maximum and minimum values. In order to facilitate the analysis, both average and standard deviation are also plotted in Figure 6.7.

As one can see, the standard deviation obtained using the distance c given by EC3 is too high, mainly for plate girders with web slenderness parameter lower than 2.0. It demonstrates that the EC3 expression to predict the flanges contribution was not providing consistent results and it needed to be improved. Figure 6.7 shows that the introduction of a new c , called by $c_{proposed}$, allowed to reduce significantly the standard deviation of the results.

Looking carefully, it is possible to observe that the results from Figure 6.6 are reflected in Figure 6.7, i.e. the same tendency on safe and unsafe results is observed when analysing the full resistance of the girders (Figure 6.6) or the web resistance only (Figure 6.7). It means that the expression to predict the flanges contribution is providing more accurate results when the factor $c_{proposed}$ is used. This has significant importance since it allows evaluating the EC3 expression to predict resistance from the web to shear buckling making sure that the flange contribution is subtracted in the correct proportions to the full capacity of the girder provided by the numerical model.

Table 6.1 – Web resistance to shear buckling numerically obtained ($\chi_{w,SAFIR}$) at 20°C

h _w [mm]	End Posts	a/h _w	$\bar{\lambda}_w$	using c EC3				using c proposed			
				Av.	St. dev.	Max	Min	Av.	St. dev.	Max	Min
800	NR	0.5	1.062	0.622	0.042	0.690	0.572	0.680	0.006	0.690	0.671
		1.0	1.750	0.493	0.022	0.524	0.461	0.564	0.001	0.564	0.562
		1.5	2.004	0.460	0.010	0.473	0.445	0.500	0.003	0.502	0.495
		2.0	2.124	0.455	0.014	0.473	0.433	0.480	0.006	0.486	0.472
		3.0	2.223	0.451	0.012	0.467	0.433	0.464	0.007	0.472	0.454
	R	0.5	1.062	0.737	0.056	0.822	0.668	0.795	0.016	0.822	0.776
		1.0	1.750	0.565	0.021	0.597	0.538	0.635	0.003	0.639	0.632
		1.5	2.004	0.500	0.014	0.518	0.479	0.539	0.002	0.541	0.536
		2.0	2.124	0.479	0.016	0.502	0.455	0.504	0.007	0.514	0.493
		3.0	2.223	0.455	0.012	0.470	0.437	0.468	0.006	0.475	0.458
1000	NR	0.5	1.327	0.527	0.050	0.595	0.457	0.643	0.013	0.661	0.627
		1.0	2.187	0.479	0.018	0.503	0.452	0.516	0.006	0.523	0.506
		1.5	2.506	0.435	0.007	0.443	0.424	0.451	0.001	0.452	0.448
		2.0	2.655	0.421	0.009	0.431	0.406	0.429	0.006	0.435	0.419
		3.0	2.779	0.392	0.008	0.402	0.380	0.396	0.006	0.403	0.386
	R	0.5	1.327	0.657	0.032	0.703	0.615	0.770	0.001	0.771	0.768
		1.0	2.187	0.565	0.014	0.586	0.546	0.601	0.003	0.605	0.598
		1.5	2.506	0.485	0.008	0.493	0.471	0.500	0.003	0.503	0.495
		2.0	2.655	0.443	0.010	0.455	0.428	0.451	0.007	0.459	0.441
		3.0	2.779	0.396	0.007	0.405	0.385	0.399	0.006	0.406	0.390
1200	NR	0.5	1.593	0.505	0.036	0.552	0.451	0.582	0.011	0.595	0.565
		1.0	2.625	0.437	0.010	0.450	0.421	0.451	0.005	0.458	0.443
		1.5	3.007	0.391	0.002	0.394	0.387	0.391	0.002	0.394	0.387
		2.0	3.186	0.376	0.004	0.379	0.368	0.376	0.004	0.379	0.368
		3.0	3.335	0.345	0.004	0.351	0.339	0.345	0.004	0.351	0.339
	R	0.5	1.593	0.647	0.023	0.677	0.612	0.722	0.003	0.725	0.718
		1.0	2.625	0.529	0.011	0.543	0.514	0.543	0.006	0.550	0.536
		1.5	3.007	0.448	0.003	0.451	0.443	0.448	0.003	0.451	0.443
		2.0	3.186	0.407	0.005	0.412	0.398	0.407	0.005	0.412	0.398
		3.0	3.335	0.351	0.004	0.356	0.345	0.351	0.004	0.356	0.345
1400	NR	0.5	1.858	0.478	0.025	0.513	0.440	0.529	0.008	0.541	0.516
		1.0	3.062	0.398	0.005	0.405	0.390	0.398	0.005	0.405	0.390
		1.5	3.508	0.354	0.001	0.355	0.353	0.354	0.001	0.355	0.353
		2.0	3.717	0.338	0.002	0.340	0.336	0.338	0.002	0.340	0.336
		3.0	3.891	0.310	0.003	0.313	0.306	0.310	0.003	0.313	0.306
	R	0.5	1.858	0.624	0.018	0.648	0.596	0.674	0.002	0.676	0.671
		1.0	3.062	0.490	0.006	0.496	0.481	0.490	0.006	0.496	0.481
		1.5	3.508	0.412	0.002	0.414	0.407	0.412	0.002	0.414	0.407
		2.0	3.717	0.373	0.002	0.375	0.370	0.373	0.002	0.375	0.370
		3.0	3.891	0.317	0.001	0.318	0.315	0.317	0.001	0.318	0.315
1600	NR	0.5	2.124	0.450	0.018	0.474	0.424	0.484	0.006	0.492	0.474
		1.0	3.500	0.365	0.002	0.368	0.362	0.365	0.002	0.368	0.362
		1.5	4.009	0.323	0.002	0.326	0.320	0.323	0.002	0.326	0.320
		2.0	4.248	0.307	0.003	0.309	0.302	0.307	0.003	0.309	0.302
		3.0	4.447	0.281	0.002	0.283	0.279	0.281	0.002	0.283	0.279
	R	0.5	2.124	0.596	0.012	0.611	0.578	0.629	0.001	0.630	0.627
		1.0	3.500	0.453	0.003	0.456	0.449	0.453	0.003	0.456	0.449
		1.5	4.009	0.379	0.004	0.382	0.372	0.379	0.004	0.382	0.372
		2.0	4.248	0.343	0.002	0.345	0.340	0.343	0.002	0.345	0.340
		3.0	4.447	0.290	0.001	0.292	0.289	0.290	0.001	0.292	0.289

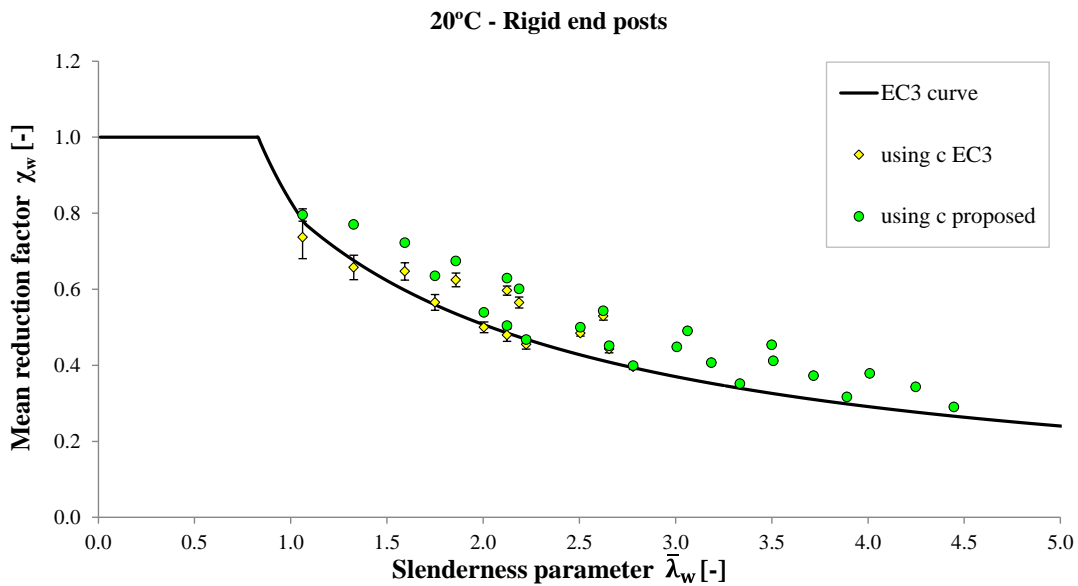
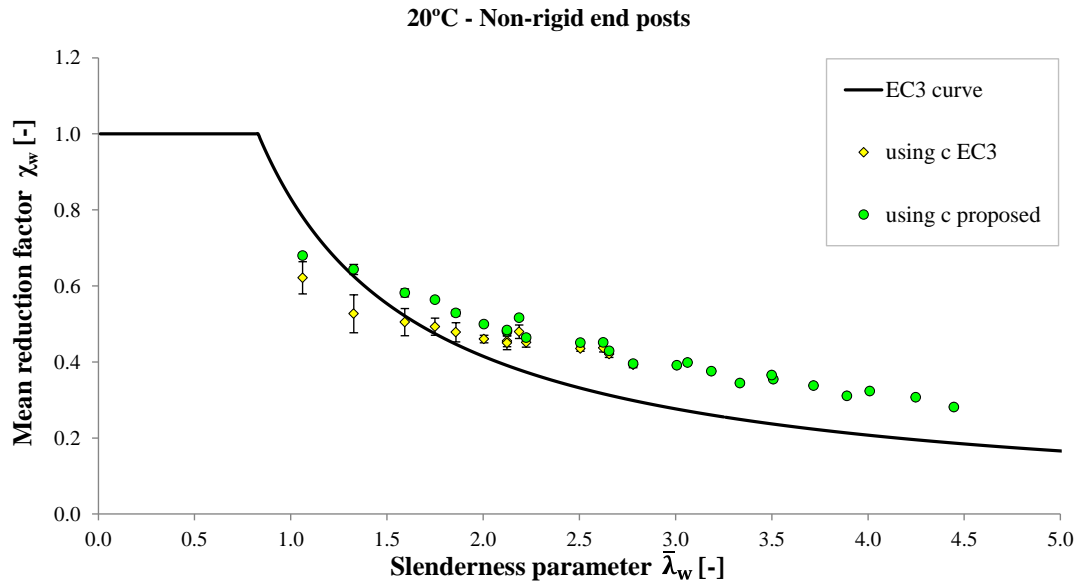
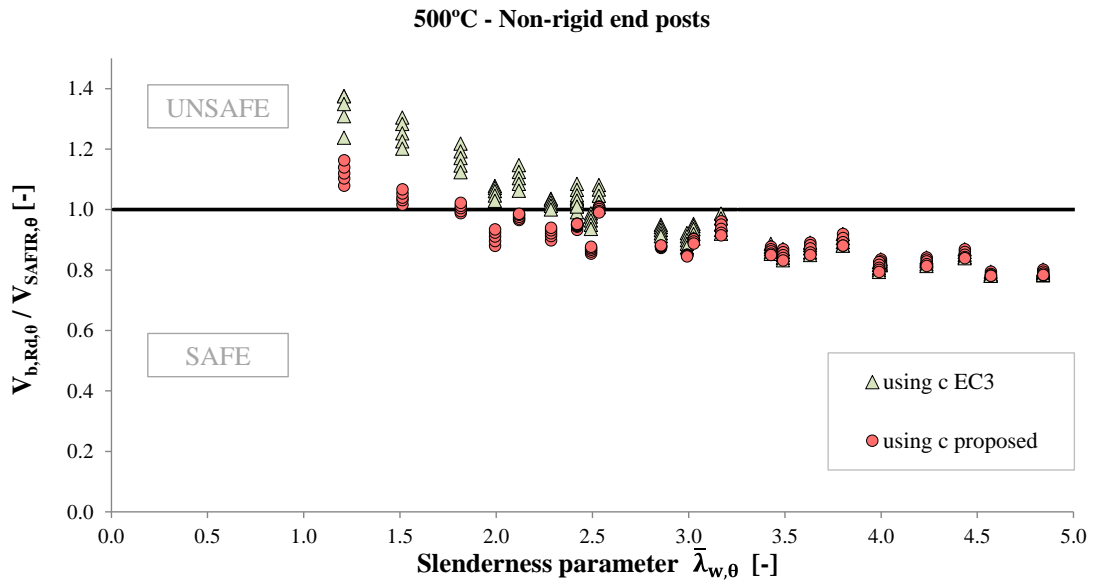


Figure 6.7 – Web resistance to shear buckling of group I plate girders at normal temperature

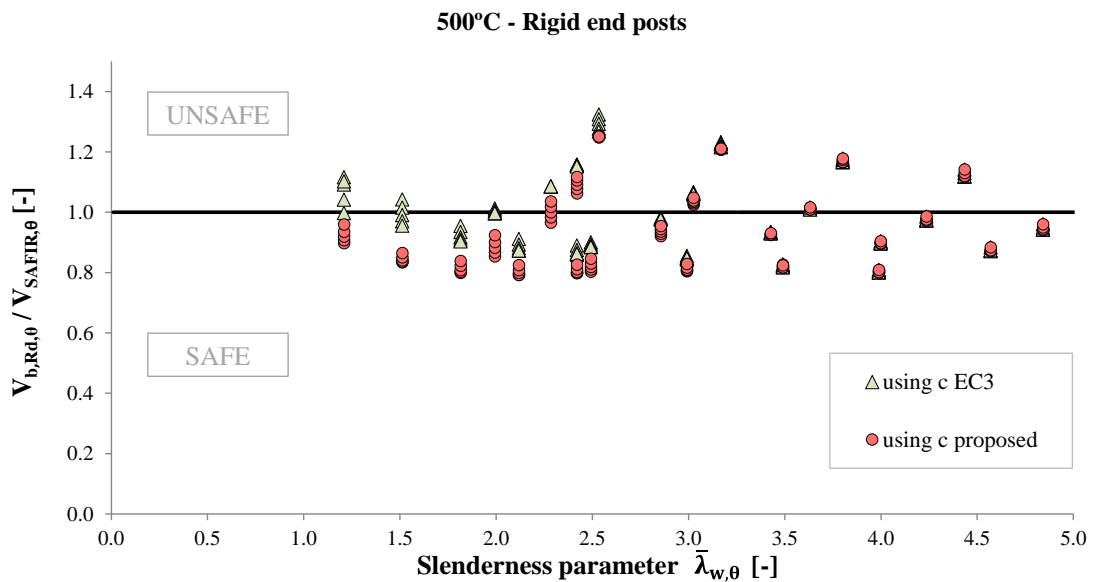
6.4.2 Elevated temperatures

Then, the impact of the application of the β_θ coefficient was evaluated. The ultimate shear strength numerically obtained using SAFIR was compared to the EC3 predictions (see Figure 6.8), considering the unchanged c expression and the c proposed applying β_θ to that expression.

The plate girders were subjected to 350°C, 500°C and 600°C, but since the results are quite similar only the results of the plate girders tested at 500°C are presented here. As one can see, there is a clear improvement on the EC3 predictions when the value of c proposed is used. However, there are still some results which are not on the safe side.



a)



b)

Figure 6.8 – Ultimate shear strength of the group I plate girders at 500°C

Using the methodology presented in Chapter 5, in the web resistance given by the numerical model ($\chi_{w,SAFIR}$) is compared to the one predicted by the EC3 expressions adapted to fire situation by the application of the reduction factors of the steel mechanical properties at elevated temperatures. Similar tables to Table 6.1 have been built for 350°C, 500°C and 600°C. The results for 500°C are presented in Figure 6.9.

As explained before, $\chi_{w,SAFIR}$ should be the same for all girders with same web properties. However, Figure 6.9 shows that the standard deviation of $\chi_{w,SAFIR}$ is high when the distance c predicted by EC3 is considered, mainly for plate girders with web slenderness parameter at elevated temperatures lower than 2.5. It is showed that expression should be improved. For that purpose, a corrective coefficient (β_θ) was proposed and its consideration causes an improvement on the EC3 predictions for the contribution from the flanges to shear buckling resistance. As one can see in Figure 6.9, the standard deviation when β_θ is considered (green points) is lower when compared to the values obtained using the original EC3 expression. It demonstrates that Eq. (3.11) gives more accurate predictions when β_θ is considered.

Moreover, it was observed an increase on $\chi_{w,SAFIR}$ when the proposed distance c is considered. It is because the EC3 predictions overestimate the contribution from the flanges to shear buckling (χ_f), which influences the web resistance numerically obtained using Eq. (5.1). When β_θ is applied, the distance c is higher, so the contribution from the flanges predicted by EC3 is lower. Consequently, a lower χ_f is subtracted in Eq. (5.1) conducting to a higher $\chi_{w,SAFIR}$.

Figure 6.9 also indicates that the EC3 design curve for the web contribution to shear buckling is not fitting the numerical results and must be improved. With this in mind, new expressions to predict the web resistance to shear buckling at elevated temperatures are proposed in Chapter 7 taken into account all the steel plate girders analysed in the parametric numerical study.

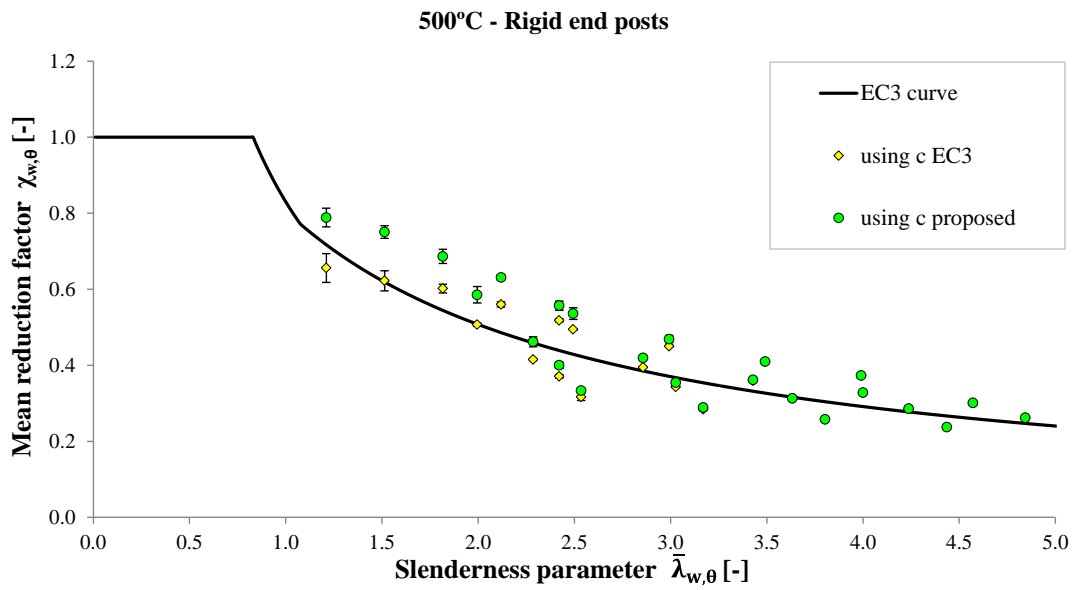
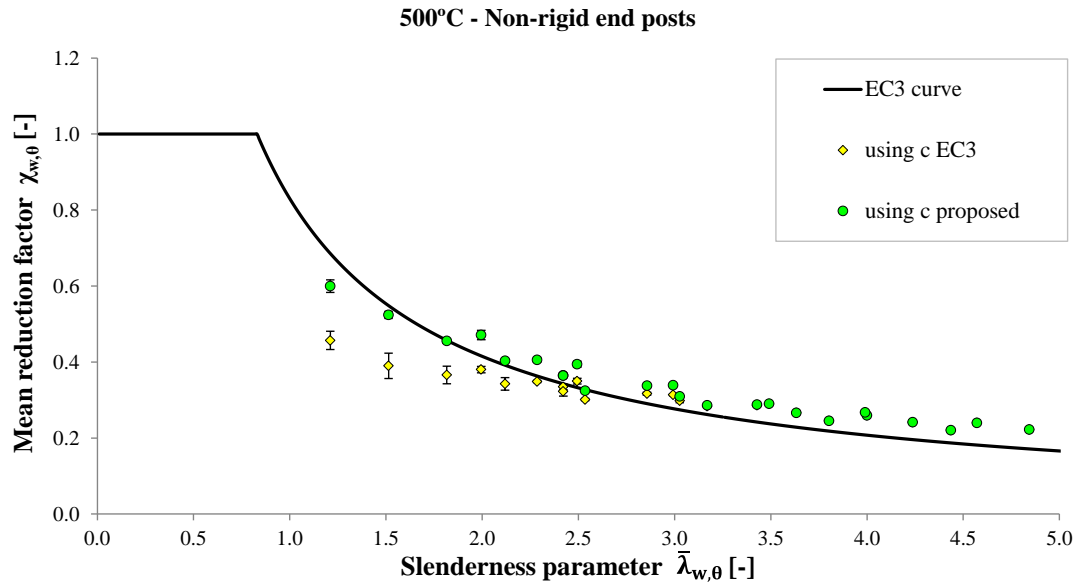


Figure 6.9 – Web resistance to shear buckling of group I plate girders at 500°C

6.5 Conclusions

Based on the work presented in Chapter 6, the following general conclusions are drawn:

- The expression implemented in EC3 to predict the flanges contribution to shear buckling resistance is not providing safe results;
- A corrective coefficient to improve the accuracy of the expression adopted in EC3 to predict the distance between the plastic hinges that forms in the flanges is proposed;
- The EC3 design procedure provides safer and more accurate results when this corrective coefficient is considered.

Chapter 7

Shear buckling resistance

Chapter 7 Shear buckling resistance

- 7.1 Failure mechanism
- 7.2 Evaluation of the EC3 expressions to predict the web resistance to shear buckling
- 7.3 Proposal of new design expressions
- 7.4 Statistical analysis
- 7.5 Conclusions

Chapter 7 Shear buckling resistance

7.1 Failure mechanism

The resistance of steel plate girders affected by shear buckling is currently based on post-critical design methods. Many different models have been developed to illustrate the post buckling behaviour and predict the ultimate shear strength of these structural elements, as presented in Chapter 2.

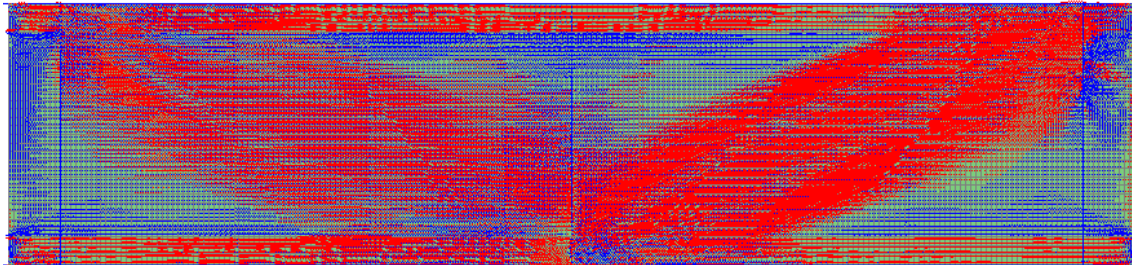
There has been a constant controversy among researchers in an attempt to adequately explain the physical post-buckling behaviour of web panels. In fact, the interaction between the non-linear shear stress and normal stress that develops from the beginning of the shear buckling state until the ultimate strength state is quite complex. The fact that more than ten theories have been developed to explain this phenomenon makes clear the complexity of the tension field action. This may probably be the largest number of failure theories dedicated to a single topic in structural mechanics.

The Rotated Stress Field Method was implemented in EC3 (CEN, 2006b) for the design of plated structural elements subjected to shear buckling and so it has been taken as the basis of this thesis. As described before, it assumes a pure shear stress state in the web panel preceding buckling and the development of a tension field after buckling. The collapse mechanism is characterized by the formation of plastic hinges in the flanges.

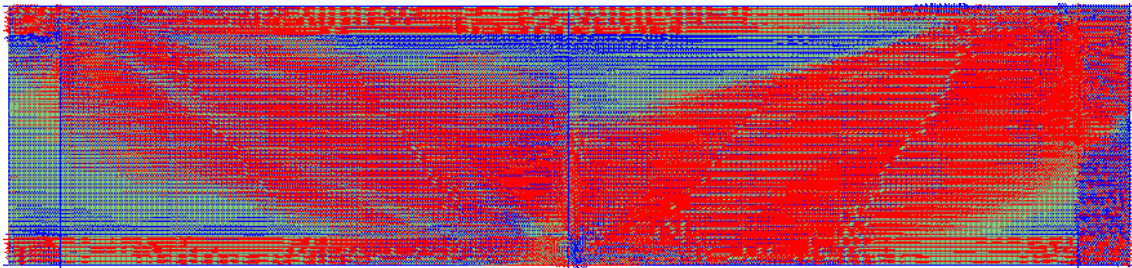
During the analysis of results of the parametric numerical study, the failure mechanism assumed by the Rotated Stress Field Method has been frequently observed in the plate girders with a shear dominant failure. Consequently, it is described here using, as an example, the 2-panel plate girder with the following characteristics: $h_w=1000$ mm; $t_w=4$ mm; $b_f=300$ mm; $t_f=20$ mm; $t_s=20$ mm; $a/h_w=2.0$; $L=4000$ mm; S235.

Figure 7.1 illustrates the principal stresses distribution developed at the moment of collapse for both rigid and non-rigid end posts. The tension field development can be clearly seen. Moreover, it is possible to observe that in the plate girder with non-rigid end posts this tension field is anchored almost exclusively on the flanges. On the other hand, in the plate girder with rigid end posts the anchorage of the tension field is shared between the flanges and the end post. Nevertheless, the tension field amplitude is higher in the girder with rigid end posts when compared to the girder with non-rigid end posts.

Figure 7.2 shows the mechanism of collapse involving the formation of plastic hinges in the flanges. As one can see, the formation of plastic hinges is visible in both plate girders irrespective of the type of end supports. However, it is more pronounced in the girder with rigid end posts.

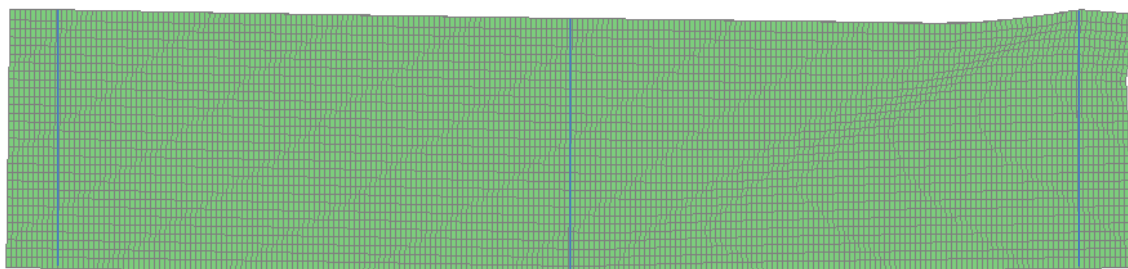


a) non-rigid end posts

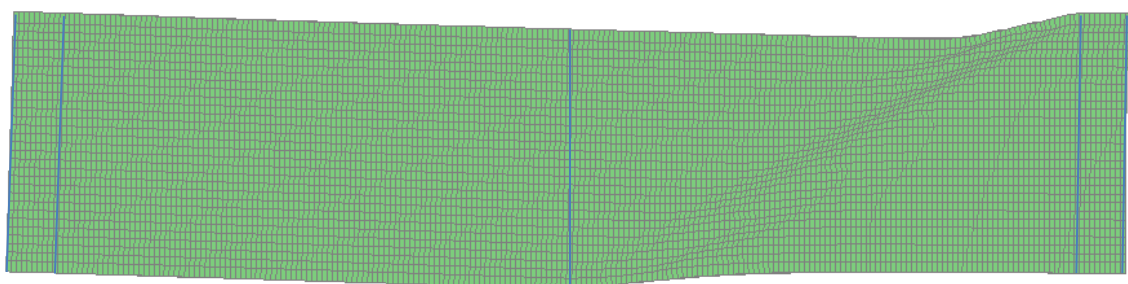


b) rigid end posts

Figure 7.1 – Tension field development at normal temperature (blue – compression; red – tension)



a) non-rigid end posts



b) rigid end posts

Figure 7.2 – Failure mechanism at normal temperature

The evolution of the distribution of principal stresses after buckling until the moment of collapse is presented in Figure 7.3 for the plate girder with rigid end posts above mentioned. As one can see, after buckling the principal tensile stresses start increasing symmetrically since the two panels have the same dimensions. At the moment of collapse, plastic hinges forms in the flanges while the out-of-plane web buckling increases substantially in the panel where the failure mechanism occurs, as may be seen in Figure 7.4c.

The maximum web out-of-plane displacement registered at the beginning of the numerical simulation is 3.8 mm, as shown in Figure 7.4a. The initial web out-of-plane displacements are due the initial geometric imperfections. Afterwards, the maximum web out-of-plane displacement increases progressively up to 16.4 mm in the post-buckling stage (see Figure 7.4a). Finally, when collapse occurs, the right web panel buckle considerably (see Figure 7.4c) with the out-of-plane displacement suddenly increases up to 91.5 mm.

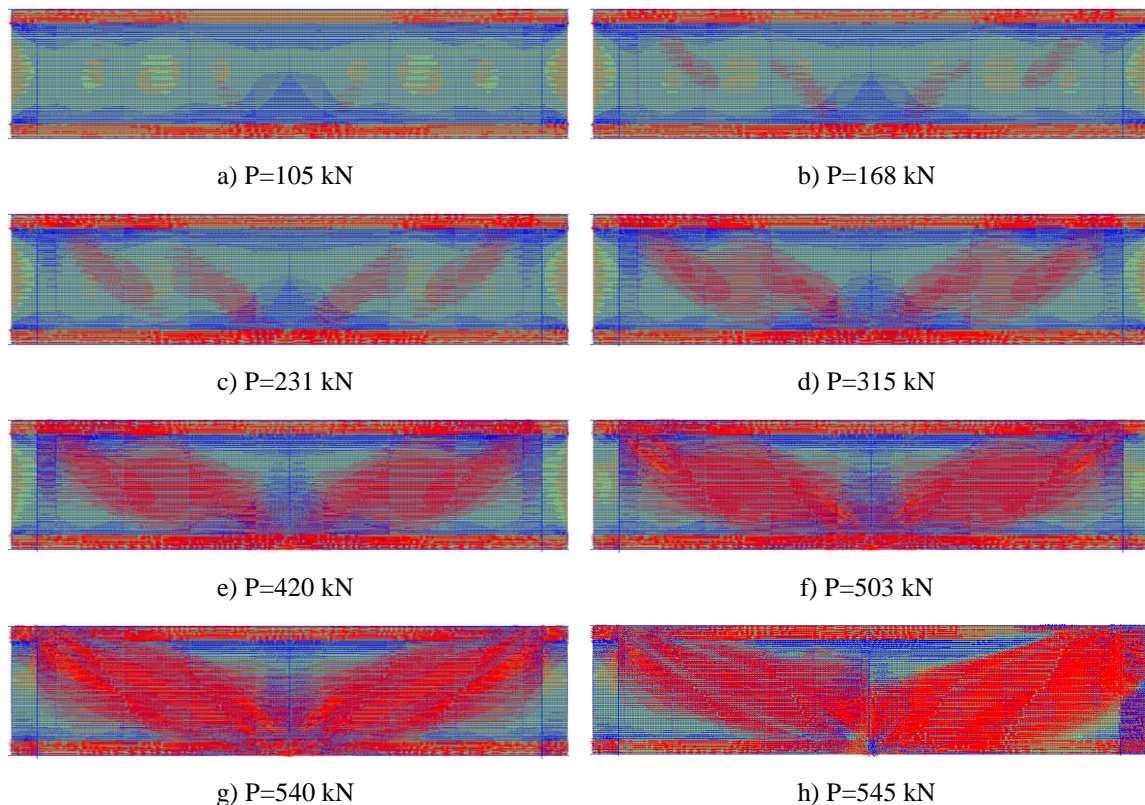


Figure 7.3 – Evolution of principal stresses distribution until failure in a steel plate girder tested at normal temperature (blue – compression; red – tension)

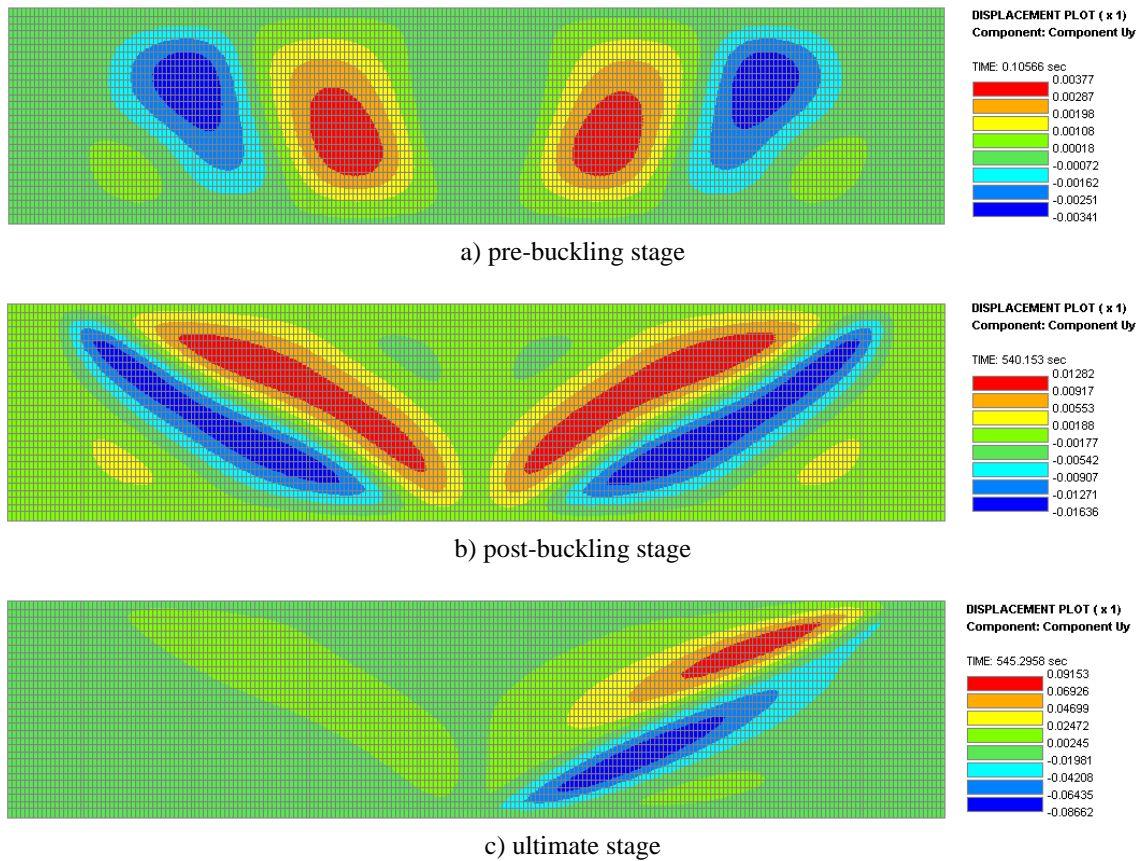
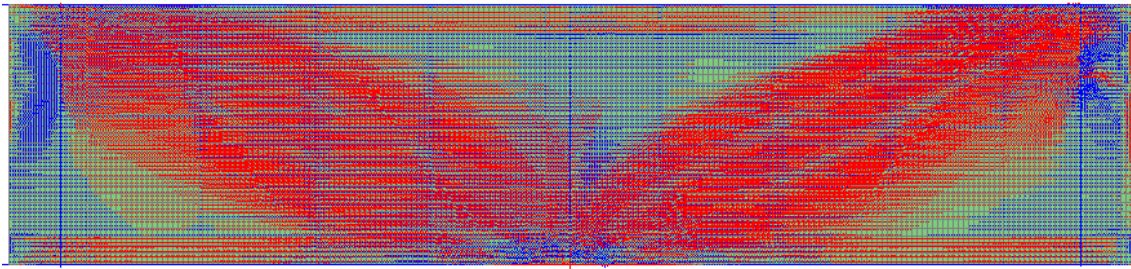


Figure 7.4 – Color scale of the out-of-plane web displacements in a steel plate girder tested at normal temperature

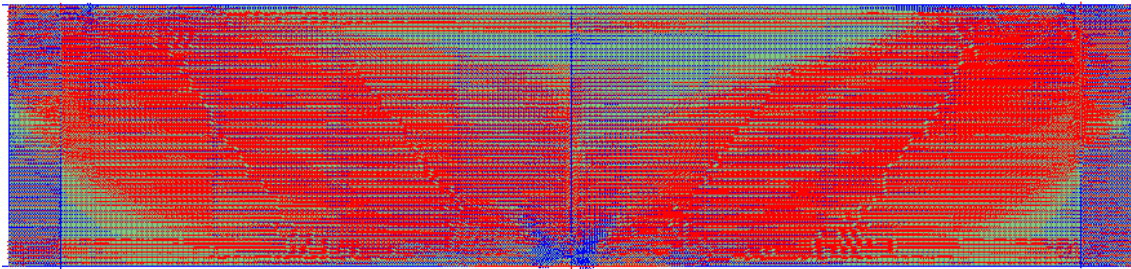
The failure mechanism at elevated temperatures of the analysed plate girders affected by shear buckling is quite similar to the one observed at 20°C, involving the development of the tension field in the web and the formation of plastic hinges in the flanges. To exemplify, it is presented here for the girders analysed above subjected to 500°C.

Figure 7.5 demonstrates the tension field development at the moment of collapse for both rigid and non-rigid end posts. As it happened at normal temperature, the tension field is anchored almost exclusively on the flanges for the girder with non-rigid end posts. In the girder with rigid end posts, these rigid end posts contribute to the anchorage of the tension field. In this plate girder the tension field covers almost the entire web panel.

Figure 7.6 shows the appearance of plastic hinges in the flanges at the moment of collapse in both plate girders. In contrast to what was observed at normal temperature, the differences between the girders with non-rigid and rigid end posts on the web buckle and on the distance between the plastic hinges in the flanges are not so pronounced.

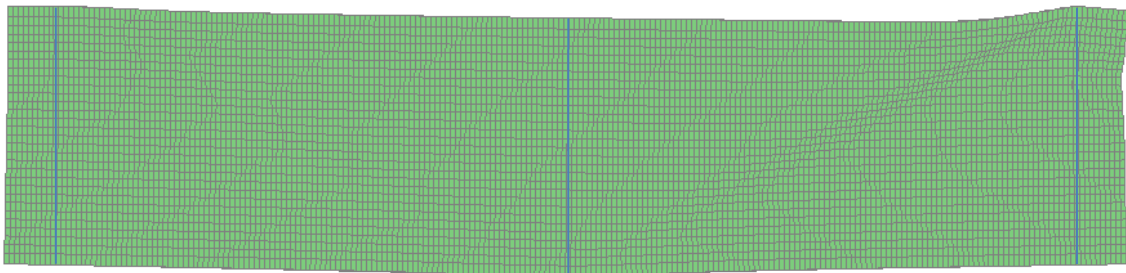


a) non-rigid end posts

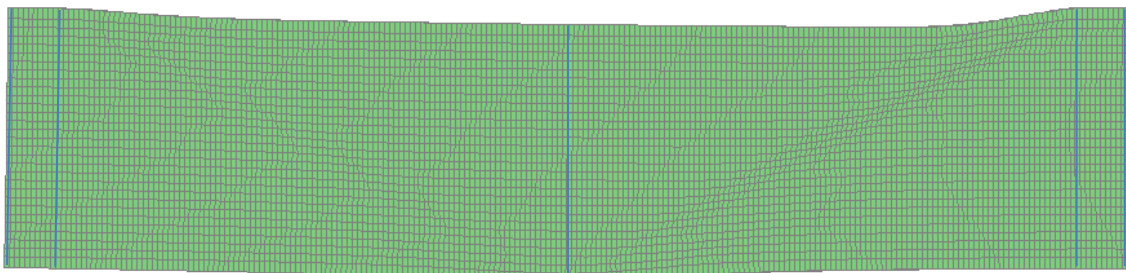


b) rigid end posts

Figure 7.5 – Tension field development at 500°C (blue – compression; red – tension)



a) non-rigid end posts



b) rigid end posts

Figure 7.6 – Failure mechanism at 500°C

7.2 Evaluation of the EC3 expressions to predict the web resistance to shear buckling

This section is dedicated to the assessment of the design expressions implemented in Part 1-5 of EC3 to predict the ultimate shear strength of steel plate girders subjected to shear buckling at normal temperature and the adoption of these expressions for fire design through the application of the reduction factors of the steel mechanical properties at elevated temperatures.

The comparison of all numerical results with those given by the analytical expressions from EC3 is presented in Figure 7.7 for the girders tested at normal temperature and in Figure 7.8 for the girders tested at elevated temperatures. The results are divided into three different zones in function of the type of failure, as explained in section 5.2.

Concerning the results obtained at normal temperature, Figure 7.7 demonstrates that EC3 is providing safe predictions for almost all the girders belonging to zones 2 and 3. However, for the girders exhibiting a shear dominant failure (zone 1), the ultimate shear strength predicted by EC3 is not on the safe side for a considerable part of the analysed girders, particularly for those with the smaller values of slenderness parameter. On the other, for the girders with the higher values of slenderness parameter, the EC3 predictions are frequently too conservative.

As regards the girders tested at elevated temperatures, the analytical results are on the safe side for almost all of the girders exhibiting a bending dominant failure (zone 3). However, the EC3 expressions, adapted to fire design by the application of the reduction factors (see section 3.5), are proving unsafe predictions for a large portion of the girders where shear has an important role on the failure (zones 1 and 2).

It makes clear the need to improve the EC3 expressions, for both normal and fire design, in order to provide safe predictions for all steel plate girders irrespective of their web slenderness parameter.

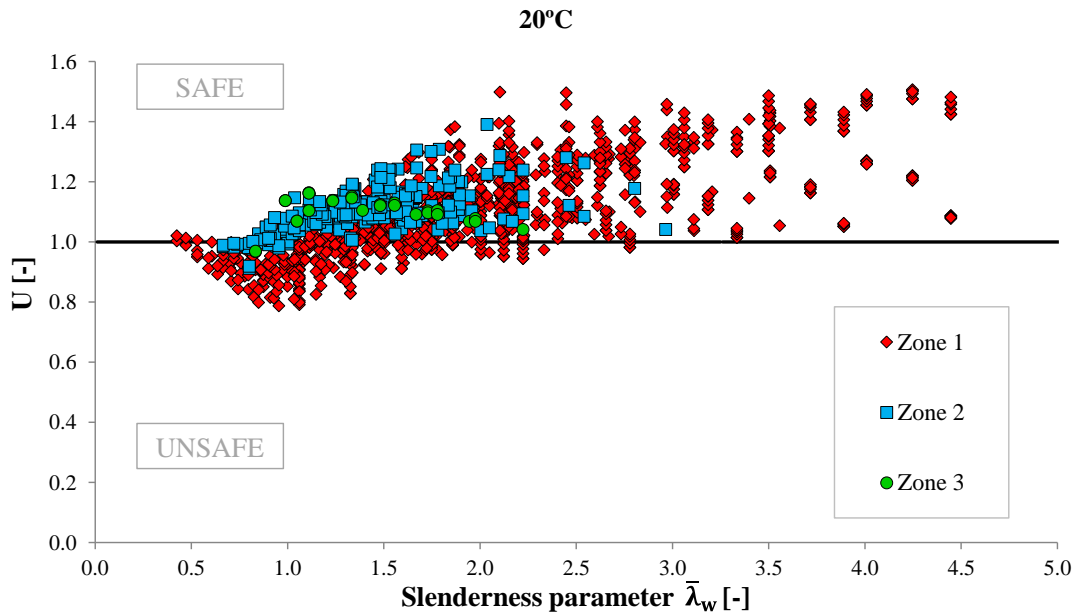


Figure 7.7 – Utilisation ratio at normal temperature of all the analysed plate girders

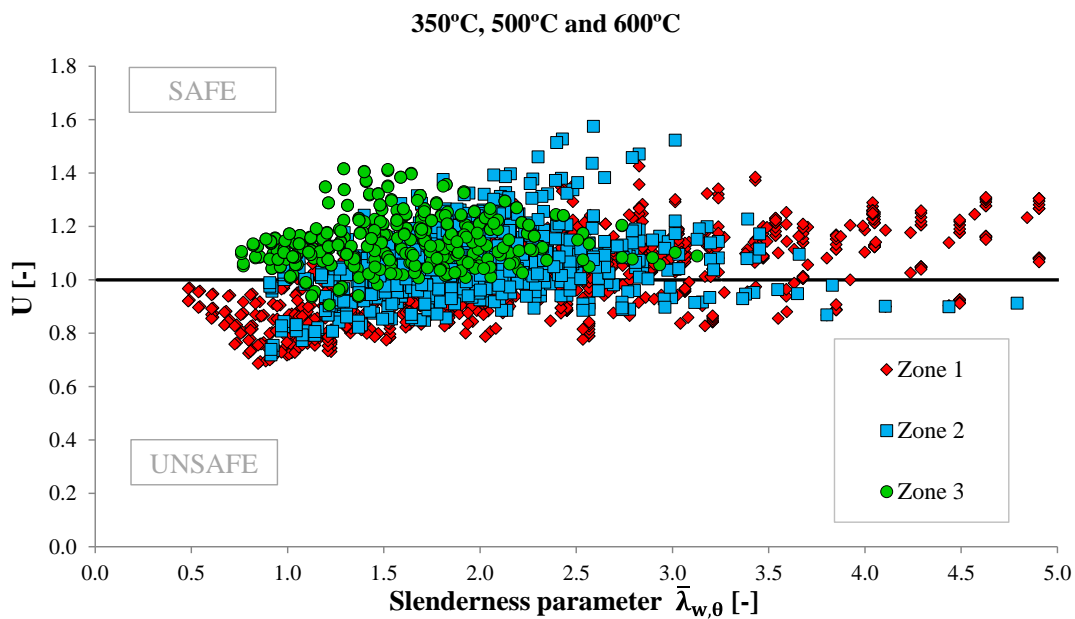


Figure 7.8 – Utilisation ratio at elevated temperatures of all the analysed plate girders

As mentioned before, the ultimate shear strength is given by the web resistance to shear buckling plus the flanges contribution. Actually, it was previously observed in Chapter 6 that the expression implemented in EC3 for the flanges contribution to shear buckling resistance was not giving accurate results, being proposed a corrective coefficient (β), which is detailed in section 6.3 of this document.

Figure 7.9 demonstrates the improvements resulting from the application of this coefficient at normal temperature, mainly for the plate girders with web slenderness parameter between 1.0 and 2.5. However, for the plate girders with web slenderness parameter lower than 1.3, unsafe results are still there. Thus, it is necessary to evaluate design expressions for the resistance from the web to shear buckling.

Figure 7.10 illustrates the comparison between the numerical results and the EC3 design curve for all plate girders exhibiting a shear dominant failure (zone 1). It is also possible to observe the improvements caused by the application of the corrective coefficient β . It is important to have in mind that, for comparison with EC3 design curve, the contribution from the web numerically obtained was calculated by Eq. (5.1) subtracting the flange contribution (χ_f) from the ultimate shear strength directly predicted by the numerical model. Additionally, it is important to note that the EC3 design curve is plotted in Figure 7.10 using the values from Table 3.1, depending on the end posts.

When analysing the effect of the corrective coefficient for the contribution from the flanges to shear buckling, Figure 7.10 shows that its application causes an improvement on the EC3 predictions, for both rigid and non-rigid end posts. On the one hand, the dispersion of results is considerably lower. On the other hand, EC3 predictions are safer when this coefficient is applied, since the original EC3 expression overestimates the flanges contribution to shear buckling, as it was observed in Chapter 6.

Regarding the results of the girders with non-rigid end posts, Figure 7.10a shows that the EC3 design curve does not fit the numerical results. For the girders with web slenderness parameter lower than 1.30, EC3 overestimates the resistance from the web to shear buckling. Furthermore, for the girders with high values of web slenderness parameter, EC3 underestimates the web resistance. It evidences the need to adjust the EC3 design curve and a proposal will be made in the next section of this document.

Concerning plate girders with rigid end posts, Figure 7.10b demonstrates a better agreement between the numerical results and the EC3 design curve. However, it still needs to be improved for girders with low values of web slenderness parameter. Modifications to the current EC3 design curve will also be proposed.

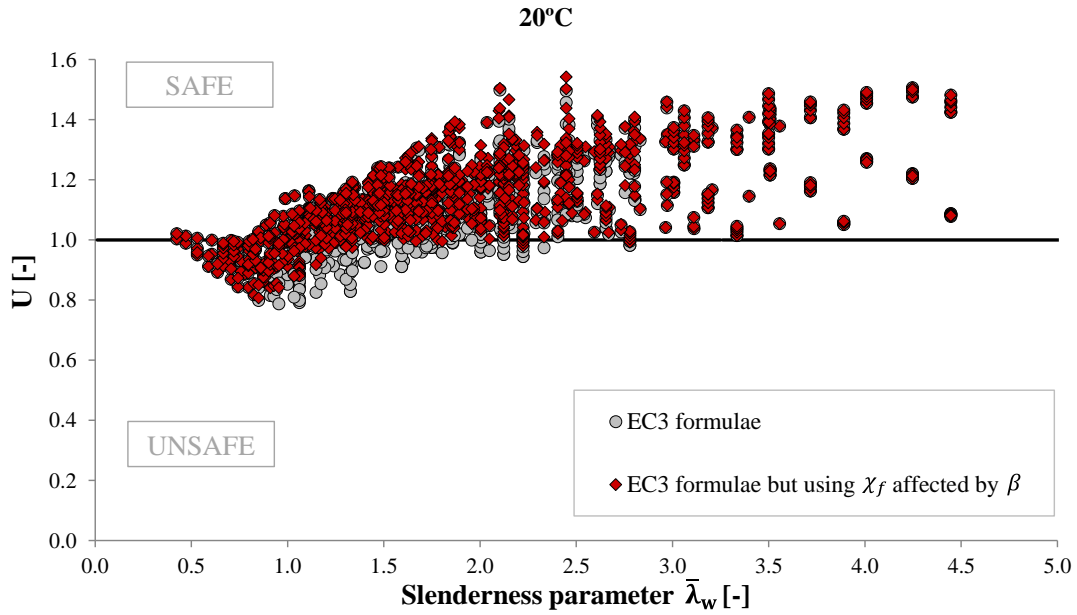
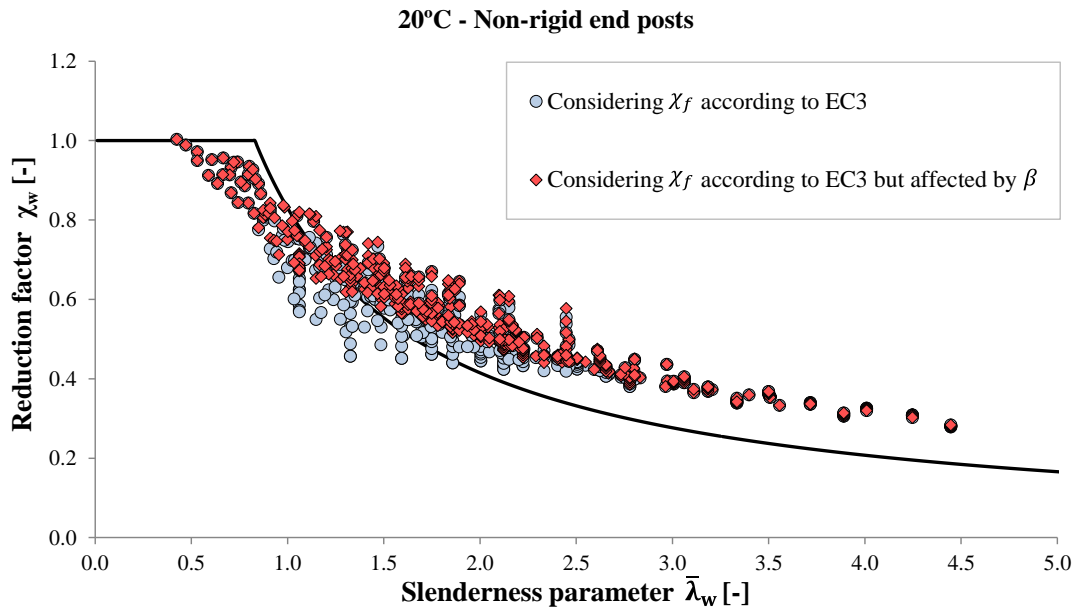


Figure 7.9 – Improvements on the EC3 predictions given by the application of the corrective coefficient for the contribution from the flanges to the shear buckling resistance at normal temperature



a)

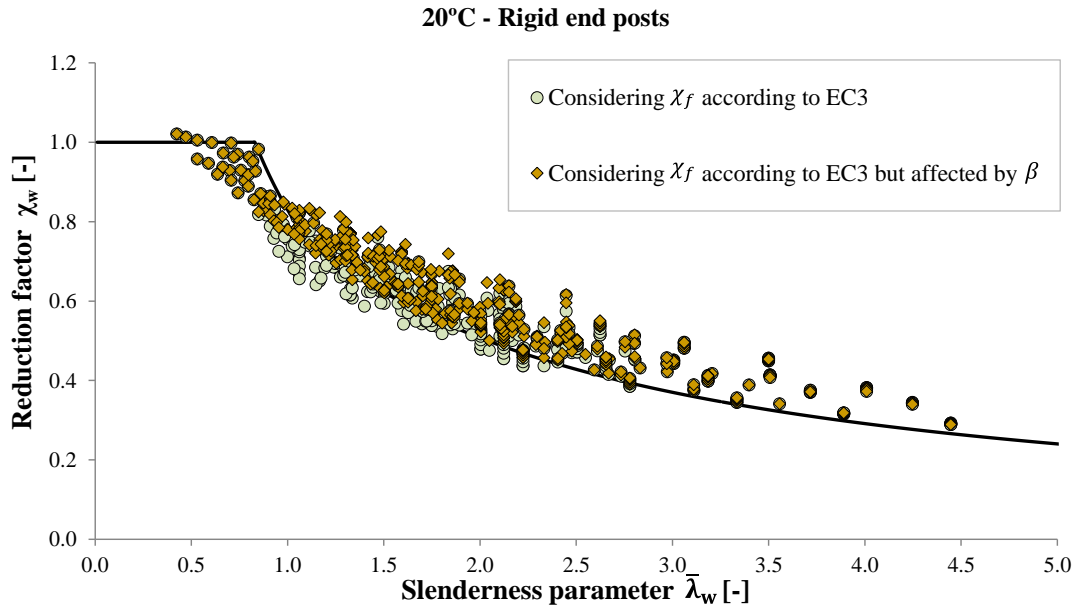


Figure 7.10 – Web contribution to shear buckling at normal temperature

A similar analysis to the one performed at normal temperature was conducted for the plate girders subjected to elevated temperatures. As it has been made for normal temperature, a corrective coefficient (β_θ) was proposed to improve the accuracy of the EC3 expression used to predict the contribution from the flanges to shear buckling. Figure 7.11 shows the improvements obtained just by the application of β_θ to the expression to determine the distance c on the calculation of the contribution from the flanges to shear buckling resistance. However, it is visible that the application of β_θ is not enough because there are still a lot of unsafe results. Consequently, it is important to evaluate the accuracy of the EC3 expressions used to determine the web resistance to shear buckling.

The shear buckling resistance of the web predicted by EC3 is compared with the numerical resistance in Figure 7.12. Figure 7.12a presents this comparison for the girders with non-rigid end posts. As one can see, despite the improvements given by the introduction of β_θ , the EC3 design curve should be improved for fire design, mainly for the girders with web slenderness parameter lower than 2.7. The same behaviour may be observed for the girders with rigid end posts. Figure 7.12b shows that the lowest the web slenderness parameter in fire situation is, the highest the unsafe portion of the numerical results is.

Hence, it is evident that the EC3 design curves, used to predict the web resistance to shear buckling of steel plate girders with rigid and non-rigid end posts, should be improved for fire design. Modifications to these curves are proposed in the next section of this thesis.

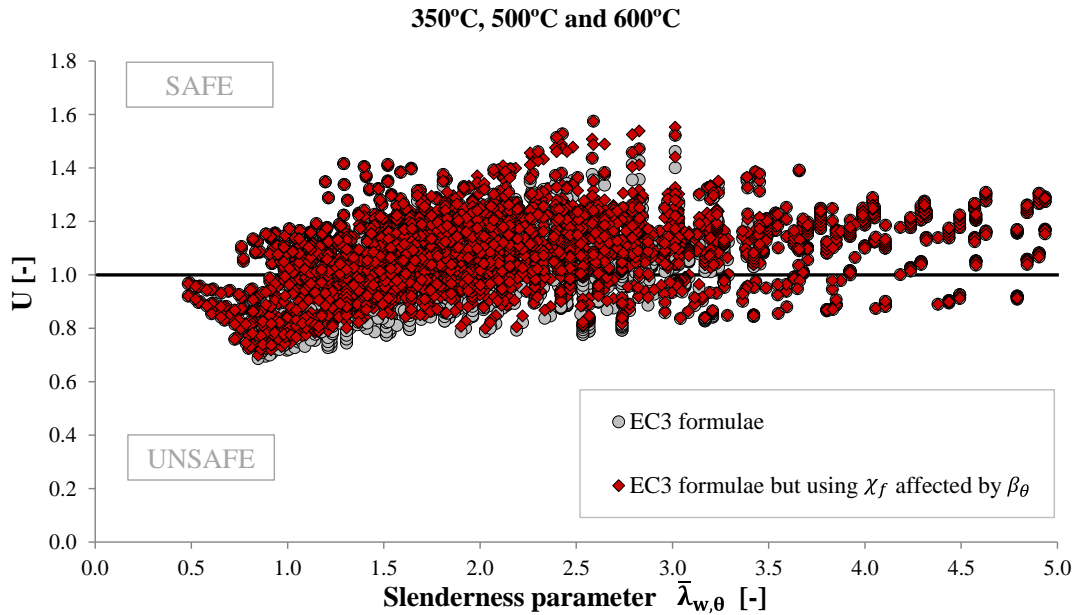
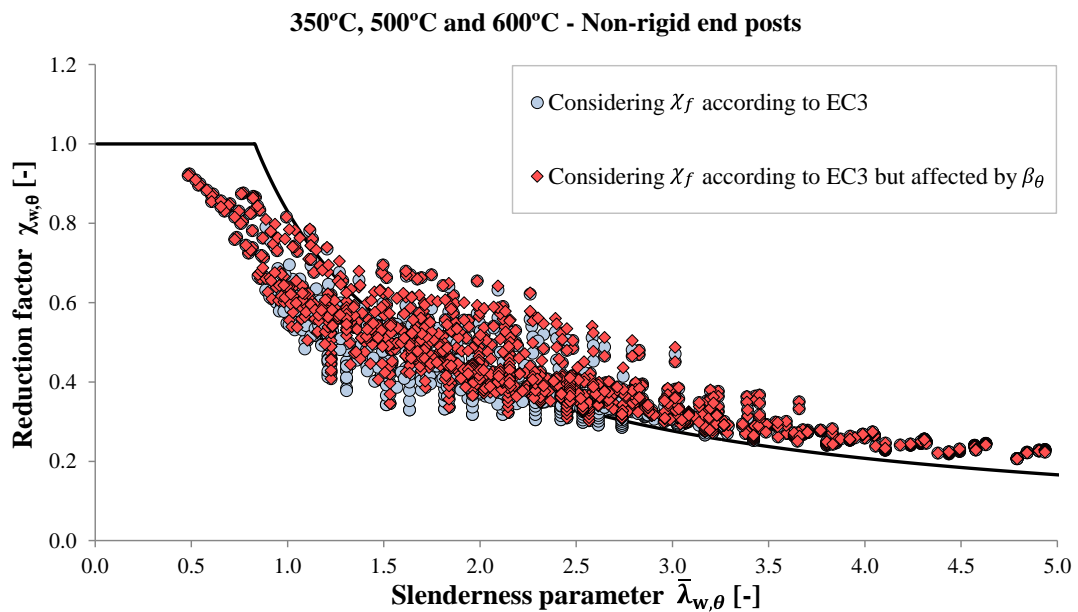


Figure 7.11 – Improvements on the EC3 predictions given by the application of the corrective coefficient for the contribution from the flanges to the shear buckling resistance at elevated temperatures



a)

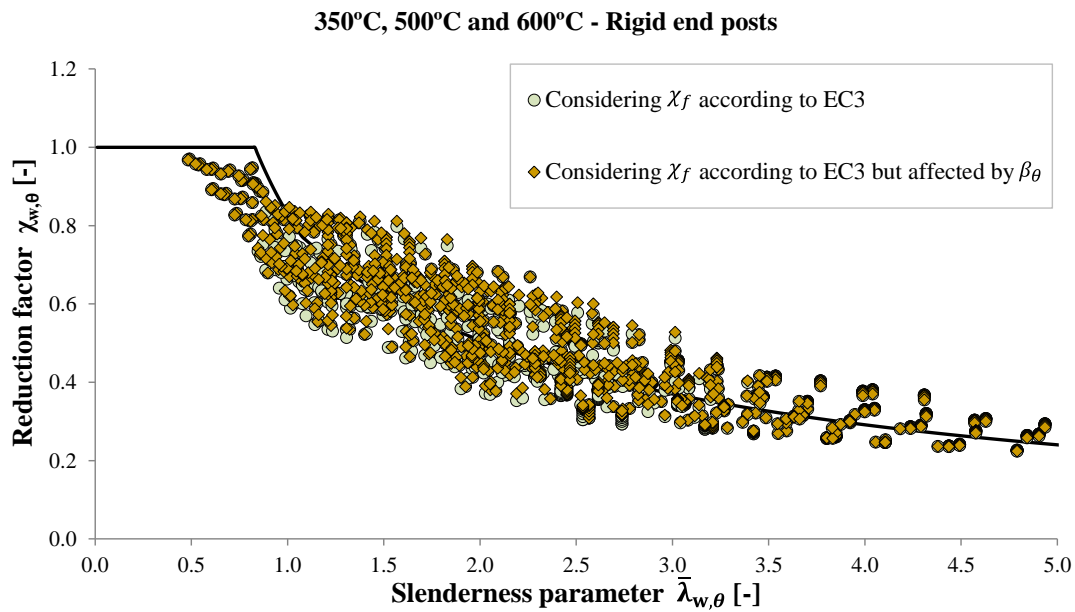


Figure 7.12 – Web contribution to shear buckling at elevated temperatures

In order to understand the variation of the EC3 predictions with different parameters, such as the web slenderness (h_w/t_w), the aspect ratio (a/h_w) and the ratio between the flanges and web thicknesses (t_f/t_w), the results of the plate girders belonging to group II were carefully analysed looking for patterns on the EC3 predictions.

Regarding the web slenderness, it was observed that, generally, the lowest the web slenderness is, the higher the unsafe nature of the EC3 predictions is. As an example, the results of the girders with $h_w=1000$ mm are presented in Figure 7.13 and Figure 7.14, for 20°C and 500°C, respectively. In the charts below, “NREP” means non-rigid end posts, while “REP” means rigid end posts. Trend lines were used for SAFIR results in order to facilitate the comparison with EC3 results.

With respect to the nature of the EC3 predictions in terms of the aspect ratio of the girders, it was observed that the most unsafe predictions are clearly those for girders with $a/h_w=0.5$, at both normal and elevated temperatures.

Figure 7.15 demonstrates that the safe nature of the EC3 predictions at 20°C varies with the ratio t_f/t_w . The highest the ratio t_f/t_w is, the highest the safe nature of EC3 predictions is. At elevated temperatures it is even more evident, as shown in Figure 7.16.

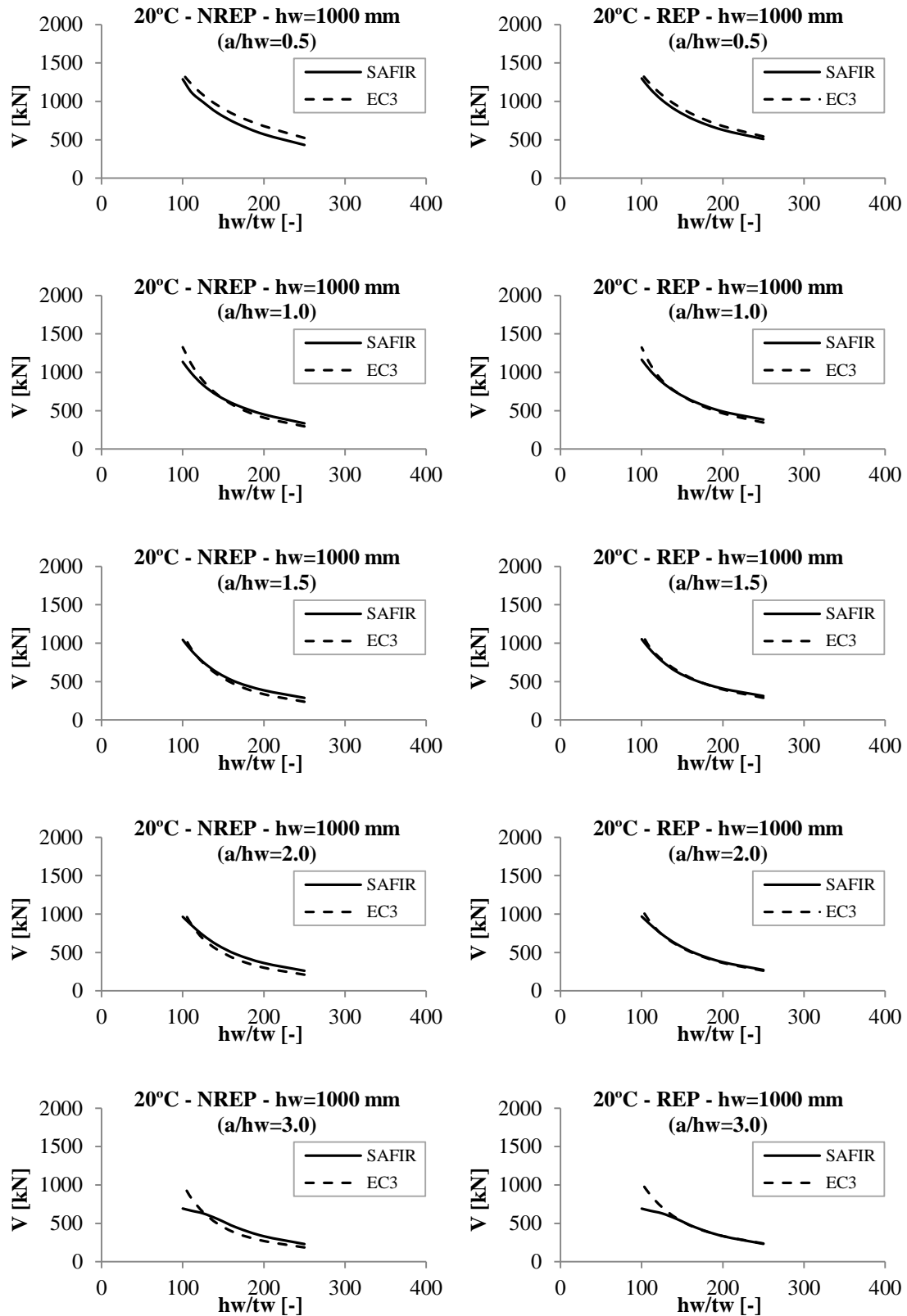


Figure 7.13 – Ultimate shear strength at 20°C in function of the web slenderness for the group II plate girders with $h_w = 1000$ mm

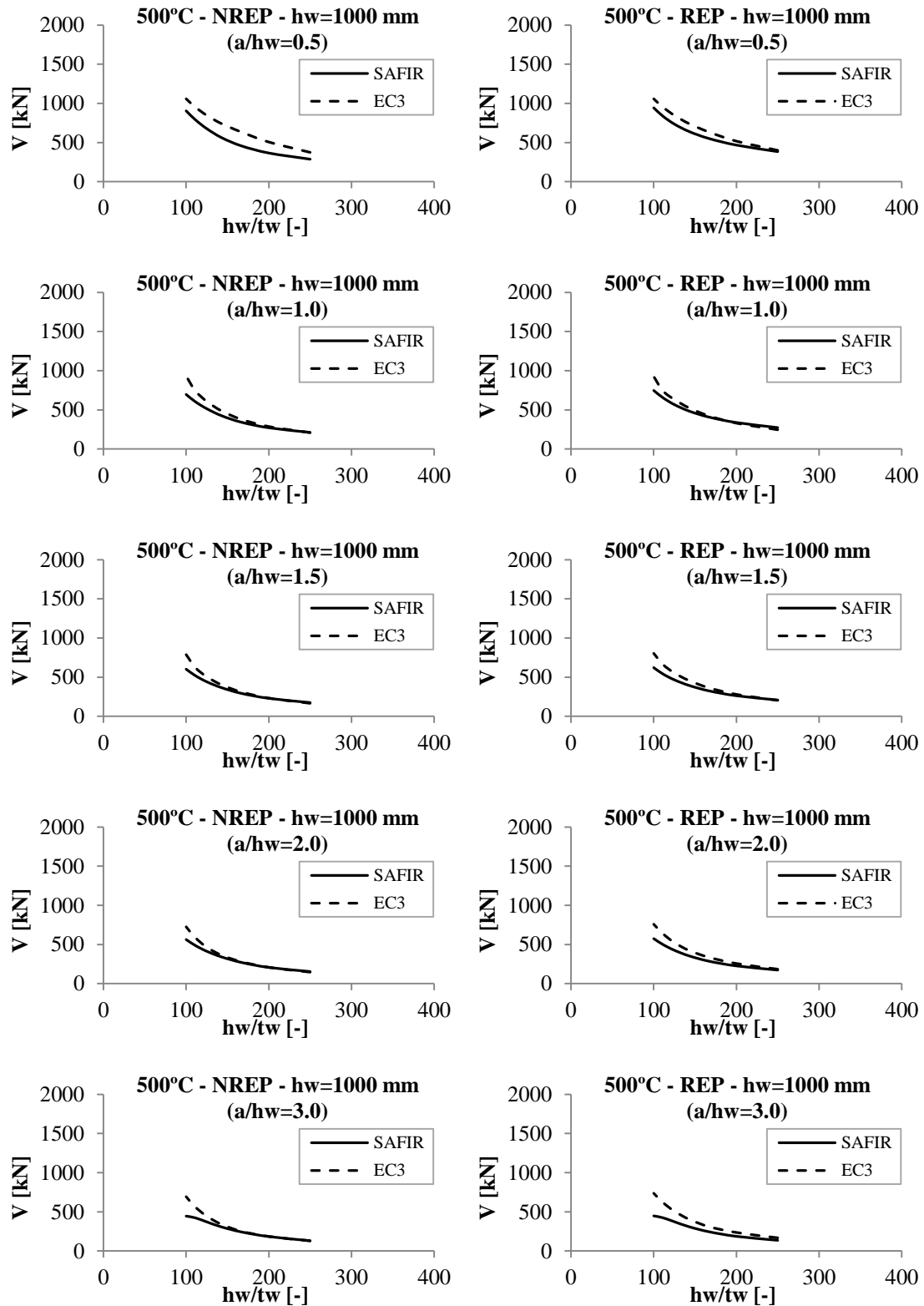


Figure 7.14 – Ultimate shear strength at 500°C in function of the web slenderness for the group II plate girders with $h_w=1000$ mm

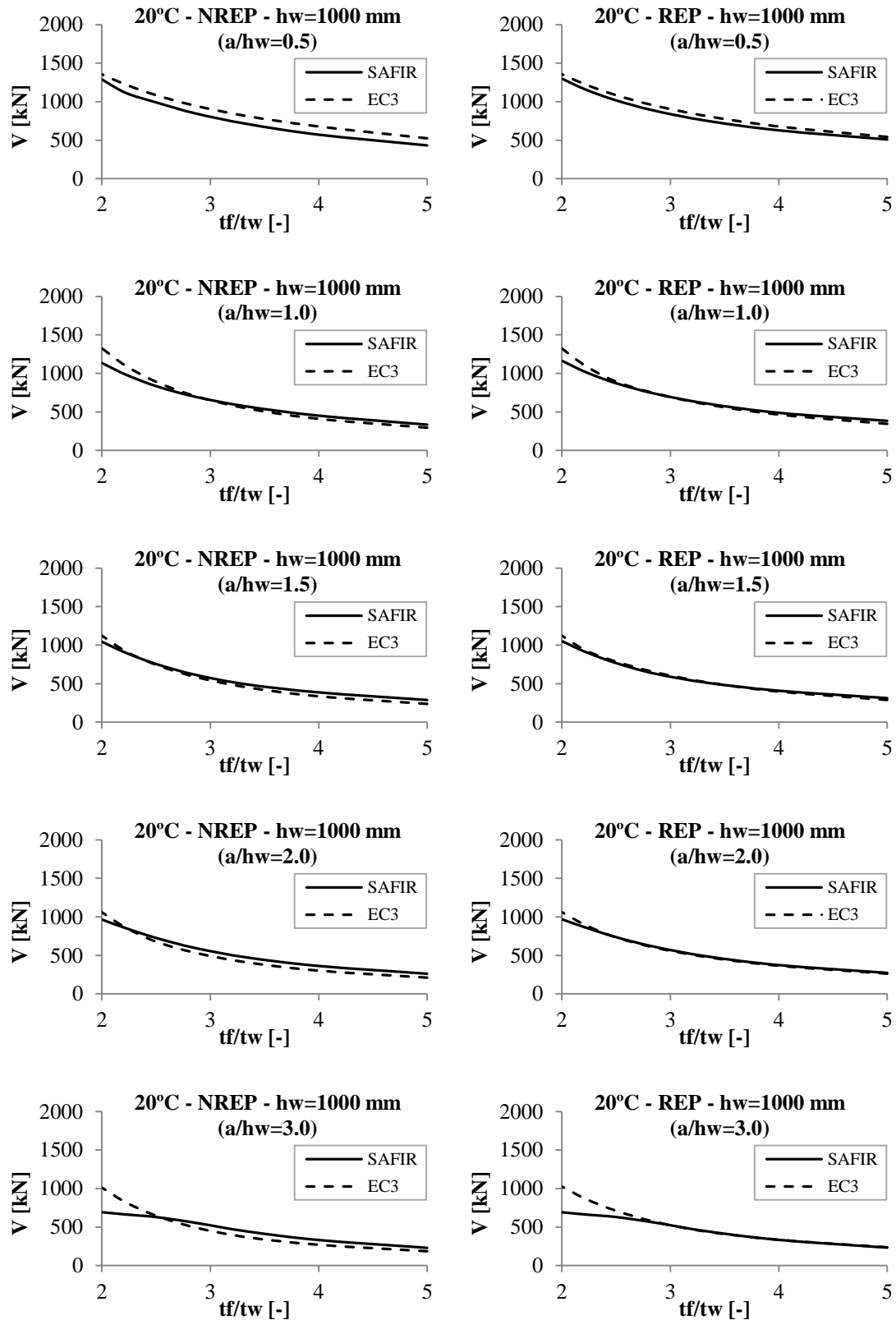


Figure 7.15 – Ultimate shear strength at 20°C in function of the ratio between the flanges and web thicknesses for the group II plate girders with $h_w = 1000$ mm

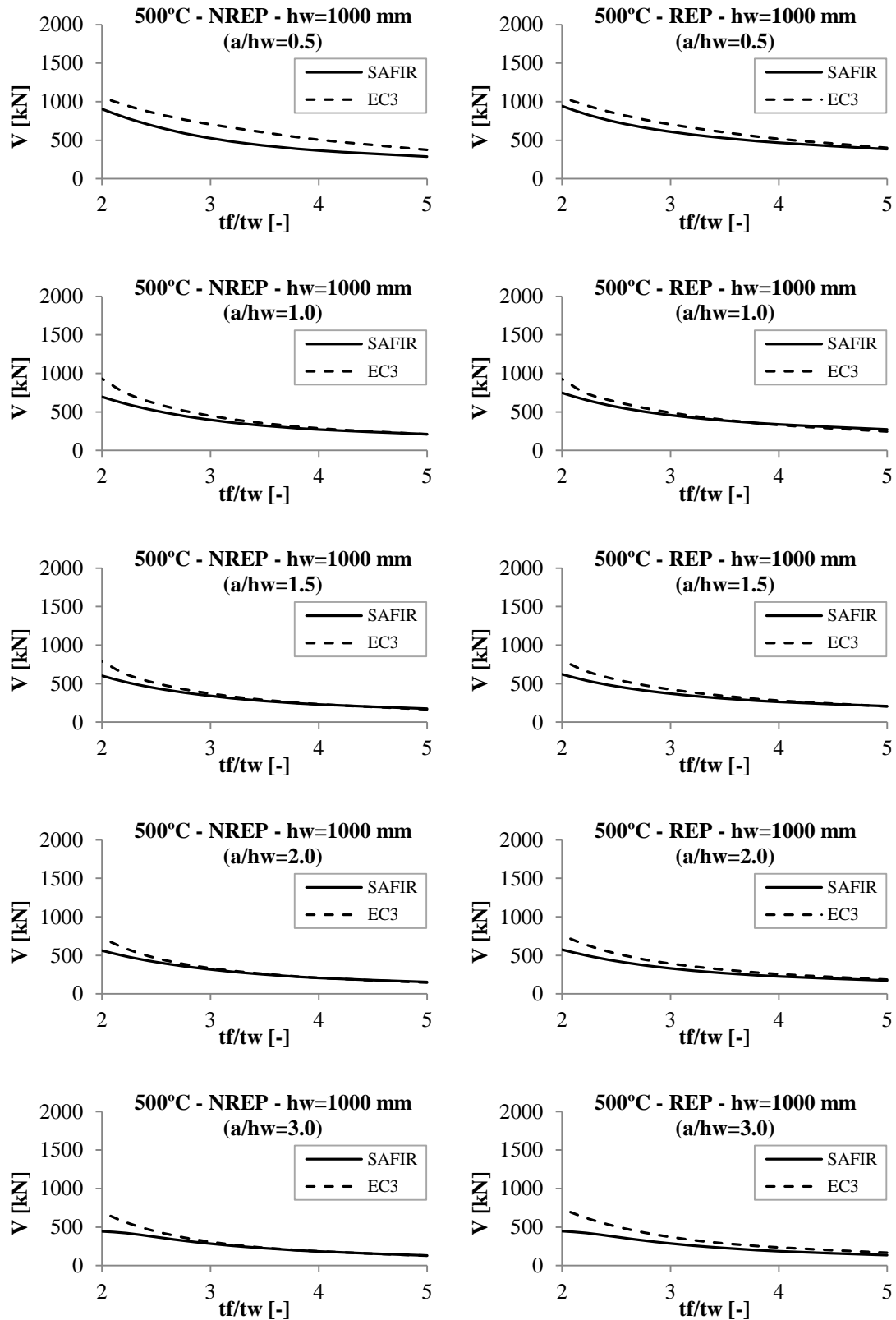


Figure 7.16 – Ultimate shear strength at 500°C in function of the ratio between the flanges and web thicknesses for the group II plate girders with $h_w=1000$ mm

The statistical analysis performed in section 7.4 will allow evaluating the influence of these parameters with more detail, but taking into account the modifications to the EC3 design procedure presented over in this thesis, which may lead to conclusions somewhat different of those presented here. For instance, with the current EC3 design expressions the most unsafe predictions correspond to the girders with the lowest aspect ratios. However, if the reduction factor for the web resistance to shear buckling proposed in next section is considered, these girders will have the most safe predictions.

7.3 Proposal of new design expressions

On the basis of the numerical investigation presented and discussed in Chapter 6 and Chapter 7 of this document, a proposal of new expressions to predict the ultimate shear strength of steel plated structural elements is presented. This proposal follows the EC3 principles, using all design rules presented in Chapter 3, only modifying two steps on the calculation of the shear resistance of a steel plate girder subjected to shear buckling.

One concerns to the application of the corrective coefficient, already presented in section 6.3, on the determination of the distance c needed for the calculation of the contribution from the flanges to shear buckling resistance. The other modification on the EC3 procedure consists in using a different reduction factor for the web contribution to shear buckling resistance. Instead of the reduction factor presented in Table 3.1, the reduction factor presented in Table 7.1 should be used for the design at 20°C, while the reduction factor given by Table 7.2 should be used for fire design. It is important to note that considering these proposals, the shear buckling resistance must be checked only when the following conditions are satisfied (instead of those presented in section 3.2):

- For unstiffened webs: $\frac{h_w}{t_w} > 43 \frac{\varepsilon}{\eta}$
- For stiffened webs: $\frac{h_w}{t_w} > 19 \frac{\varepsilon}{\eta} \sqrt{k_\tau}$

Table 7.1 – Proposal for the reduction factor for the web contribution to shear buckling resistance (χ_w) at normal temperature

	Rigid end post	Non rigid end post
$\bar{\lambda}_w < 0.50/\eta$	η	η
$0.50/\eta \leq \bar{\lambda}_w < 1.32$	$0.48 + 0.26/\bar{\lambda}_w$	$0.40 + 0.30/\bar{\lambda}_w$
$\bar{\lambda}_w \geq 1.32$	$1.37/(0.70 + \bar{\lambda}_w)$	$1.28/(0.72 + \bar{\lambda}_w)$

Table 7.2 – Proposal for the reduction factor for the web contribution to shear buckling resistance ($\chi_{w,\theta}$) at elevated temperatures

	Rigid end post	Non rigid end post
$\bar{\lambda}_{w,\theta} < 0.50/\eta$	η	η
$0.50/\eta \leq \bar{\lambda}_{w,\theta} < 1.50$	$0.24 + 0.38/\bar{\lambda}_{w,\theta}$	$0.20 + 0.40/\bar{\lambda}_{w,\theta}$
$\bar{\lambda}_{w,\theta} \geq 1.50$	$0.10 + 0.59/\bar{\lambda}_{w,\theta}$	$0.09 + 0.565/\bar{\lambda}_{w,\theta}$

These new design curves listed above are represented by the red lines in the charts below. The design curve at normal temperature for the girders with non-rigid end posts is presented in Figure 7.17a, while the design curve for girders with rigid end posts is presented in Figure 7.17b. It is visible that the proposed curves fit much better the numerical results. For the girders with non-rigid end posts, the design curve was readjusted for both the girders with $\bar{\lambda}_w < 1.32$ where the EC3 design curve was overestimating the web resistance and the girders with $\bar{\lambda}_w \geq 1.32$ where the EC3 design curve was underestimating the web resistance. Regarding the girders with rigid end posts, the new proposal only modifies the overestimated EC3 predictions ($\bar{\lambda}_w < 1.32$).

Concerning the proposed design curves for elevated temperatures, they are plotted in Figure 7.18. The range of unsafe results was quite large and the main goal of these new curves was to stop the overestimations given by the EC3, even though that there are some cases where the EC3 predictions will be very conservative, since the dispersion of results is larger at elevated temperatures when compared to normal temperature.

The improvements obtained by the proposed design curves for the determination of the ultimate shear strength of steel plate girders are presented in Figure 7.19 and Figure 7.20, for normal and elevated temperatures, respectively. These Figures may be compared with Figure 7.7 and Figure 7.8, where the proposals were not considered. As it can be seen, the EC3 procedure is providing safe predictions for almost all the analysed girders when these proposals are considered. The exceptions are the girders with very small web slenderness that are not very common in practice. Nevertheless, the unsafe differences are small and acceptable.

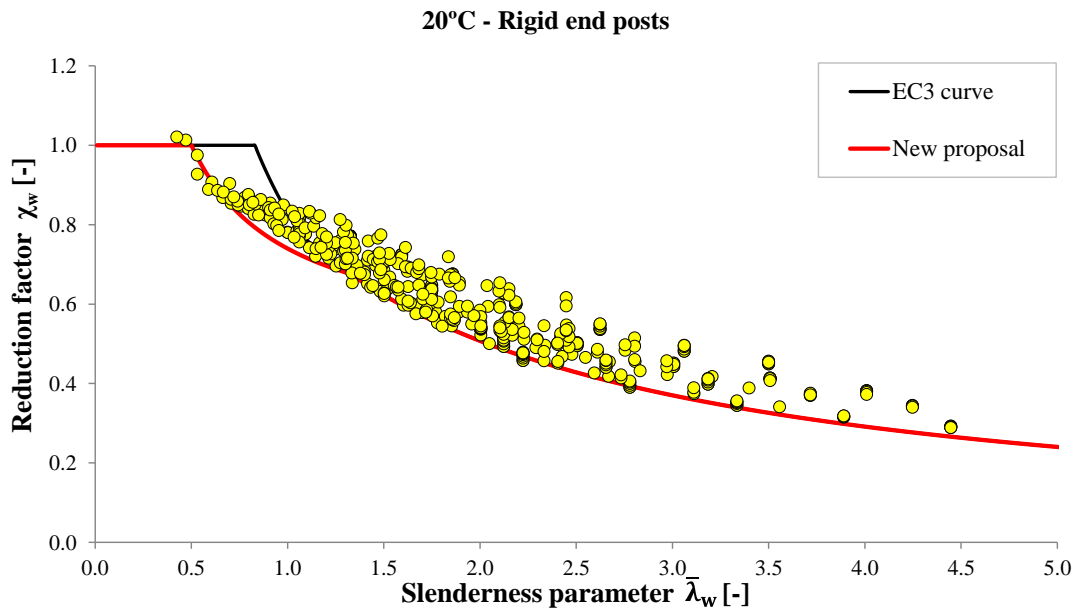
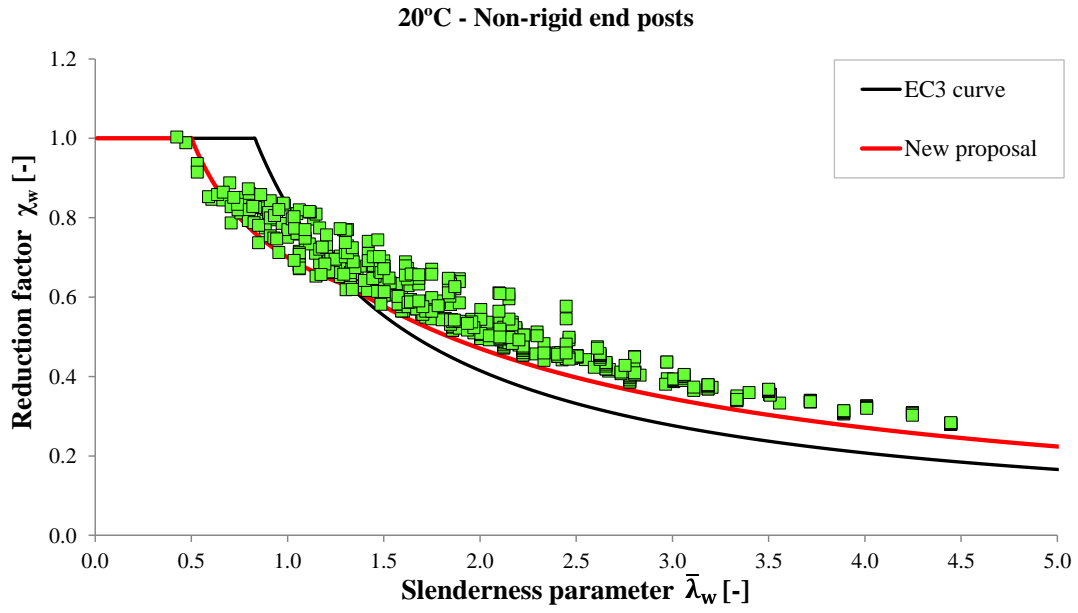


Figure 7.17 – New proposal for the web contribution to shear buckling at normal temperature

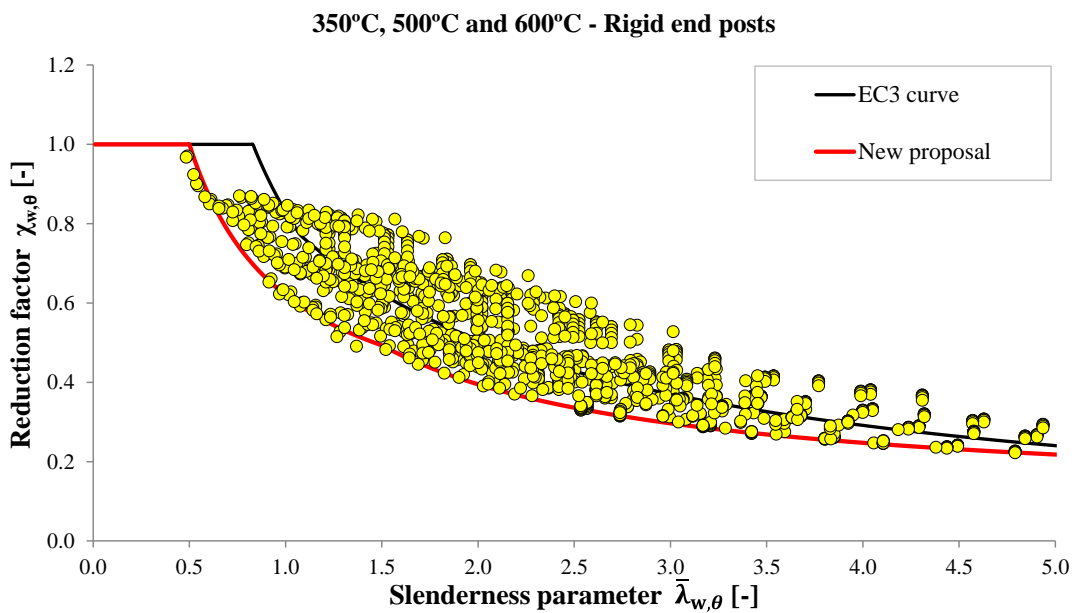
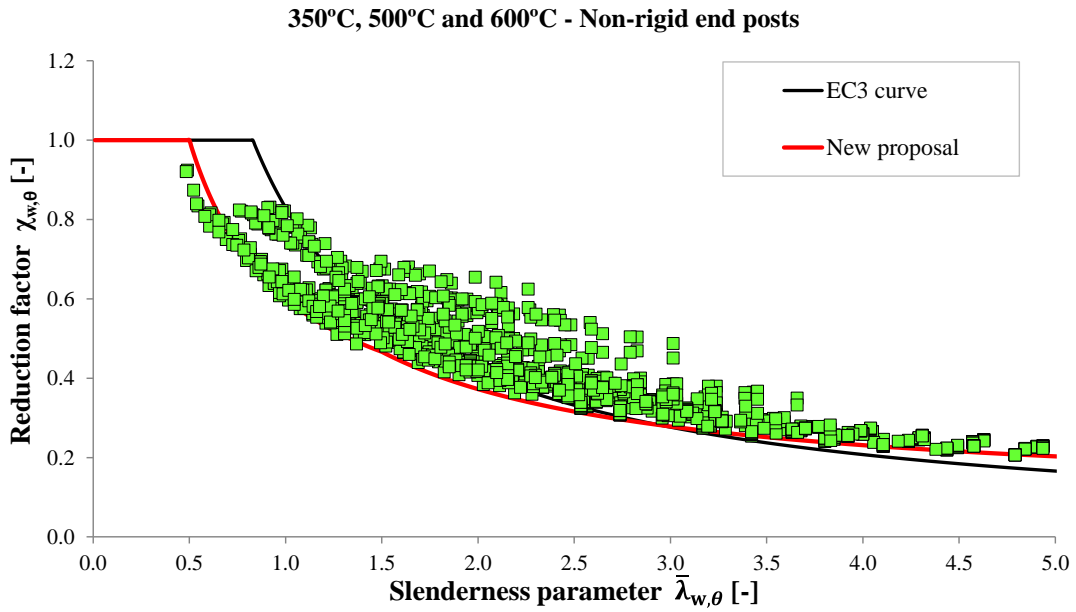


Figure 7.18 – New proposal for the web contribution to shear buckling at elevated temperatures

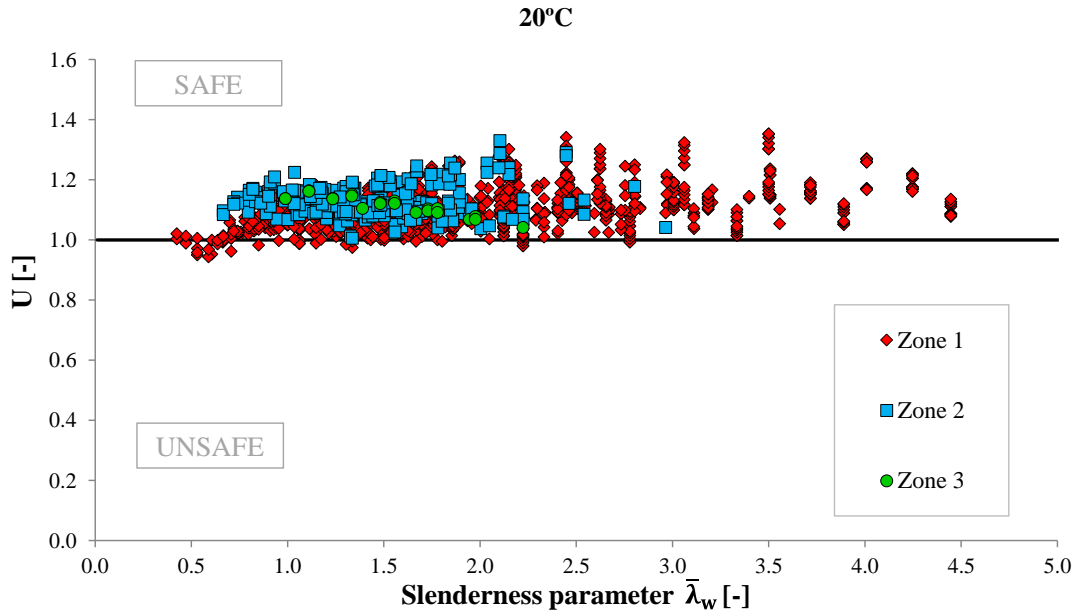


Figure 7.19 – Improvements on the EC3 predictions given by the application of the proposals for normal temperature

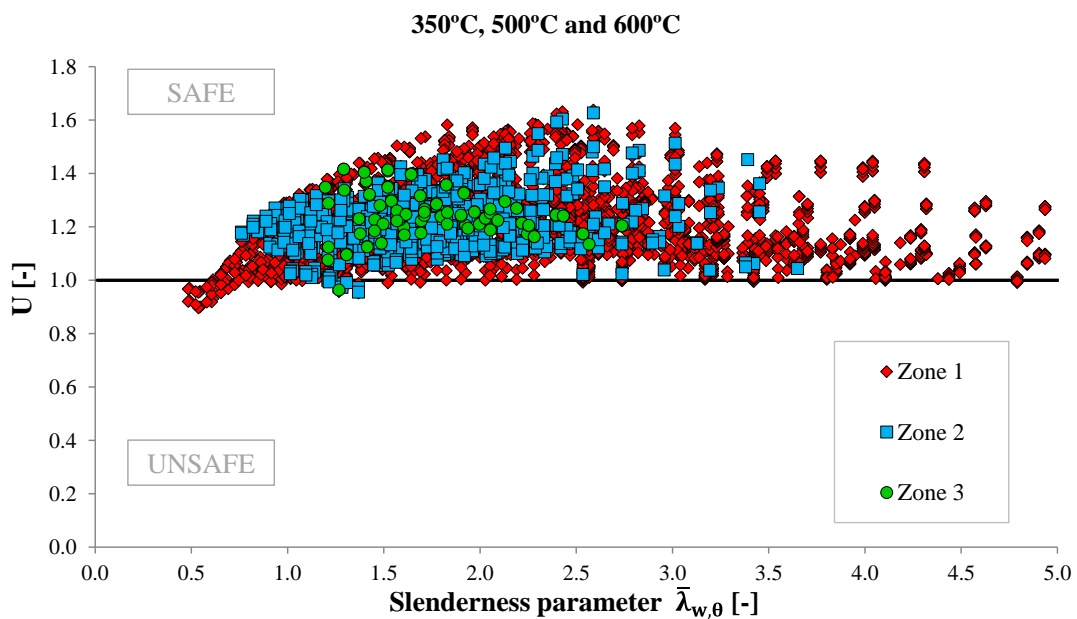


Figure 7.20 – Improvements on the EC3 predictions given by the application of the proposals for elevated temperatures

The improvements given by the proposals presented above are discussed in more detail in the next section, where a statistical analysis of results is performed for both normal and elevated temperatures.

7.4 Statistical analysis

The utilisation ratio (U) is used to compare the numerical results with the analytical results given by the EC3 expressions. A statistical analysis of the utilisation ratio values is presented here in order to understand the accuracy of the EC3 expressions and the improvements introduced by the application of the proposals presented before.

Table 7.3 presents such analysis for the results obtained at normal temperature. Results from different zones of the shear-bending interaction diagram (see Figure 5.4) are separately evaluated. Zone 1 comprises the results from the girders with a shear dominant failure, which are used to assess the expressions to predict the shear buckling resistance. Zone 2 contains the results from the girders with a combined shear plus bending failure, which are used to evaluate the expression for the interaction between shear and bending. Finally, the results from the girders with a bending dominant failure are included in zone 3. Furthermore, two design approaches were considered in the statistical analysis. One, called EC3 in the tables below, where the numerical results are compared with the analytical results provided by the unchanged EC3 expressions, and other (called EC3+P) where the results given by SAFIR are compared with the EC3 expressions modified by the proposals presented in this thesis. A similar analysis is presented in Table 7.4 for the results obtained at elevated temperatures.

Table 7.3 – Statistical analysis at normal temperature

Zone	D. A.	N Cases	Average	St. Dev.	Max	Min	% Unsafe	% U<0.95
1	EC3	931	1.11	0.15	1.51	0.79	24.6%	13.5%
	EC3+P	921	1.11	0.07	1.35	0.94	3.8%	0.2%
2	EC3	218	1.10	0.08	1.39	0.91	9.2%	0.9%
	EC3+P	233	1.13	0.05	1.33	1.01	0.0%	0.0%
3	EC3	27	1.10	0.05	1.16	0.97	7.4%	0.0%
	EC3+P	22	1.11	0.03	1.16	1.04	0.0%	0.0%

Table 7.4 – Statistical analysis at elevated temperatures

Zone	D. A.	N Cases	Average	St. Dev.	Max	Min	% Unsafe	% U<0.95
1	EC3	2377	1.02	0.14	1.46	0.69	45.8%	32.5%
	EC3+P	2701	1.20	0.14	1.64	0.90	2.7%	0.3%
2	EC3	738	1.06	0.12	1.57	0.72	30.9%	17.2%
	EC3+P	732	1.21	0.10	1.63	0.95	1.1%	0.0%
3	EC3	413	1.15	0.10	1.42	0.91	3.4%	1.2%
	EC3+P	95	1.25	0.09	1.42	0.96	1.1%	0.0%

A quick analysis allows concluding that the application of the proposals presented in this thesis induces significant improvements on the EC3 predictions at both normal and elevated temperatures. The application of β to the expression to determine the distance between plastic hinges that forms in the flanges improves the EC3 predictions for the flanges contribution to shear buckling ($V_{bf,Rd}$), which are reflected in the zone 1 results. On the other hand, the application of the new reduction factors for the web contribution to shear buckling (χ_w) improves the EC3 predictions for the web resistance ($V_{bw,Rd}$), which affects the results from the zones 1 and 2. Finally, the improvements in zone 3 results are due to a different zone classification of the utilisation ratios when the proposed $V_{bw,Rd}$ is used, since the boundaries of each zone are obtained using $V_{bw,Rd}$ (see Table 5.7). When analysing Table 7.4, a decrease on the number of girders with a bending dominant failure from 413 to 95 may be observed when the proposals are taken into account. It causes an increase on the percentage of safe results since some girders were classified as failing by bending and actually they fail before, due to the interaction between shear and bending, not reaching the resistance moment of the cross-section.

Hence, considering the zones classification where the proposals are taken into account, at normal temperature the failure was caused by shear in 78.3% of the analysed plate girders (zone 1), while a combined shear plus bending failure was observed in 19.8% (zone 2) and a bending dominant failure only happened in 1.9 % (zone 3). As regards the girders analysed at elevated temperatures, a shear dominant failure (zone 1) was observed in 2701 girders (76.6%), a combined shear plus bending failure (zone 2) was registered in 732 (20.7%) and, finally, the failure of 95 (2.7%) of the analysed girders was caused by bending (zone 3). In comparison with the results obtained at normal temperature, a slight decrease on the shear dominant failures was observed, while the number of failures caused by bending or by the interaction between shear and bending has grown.

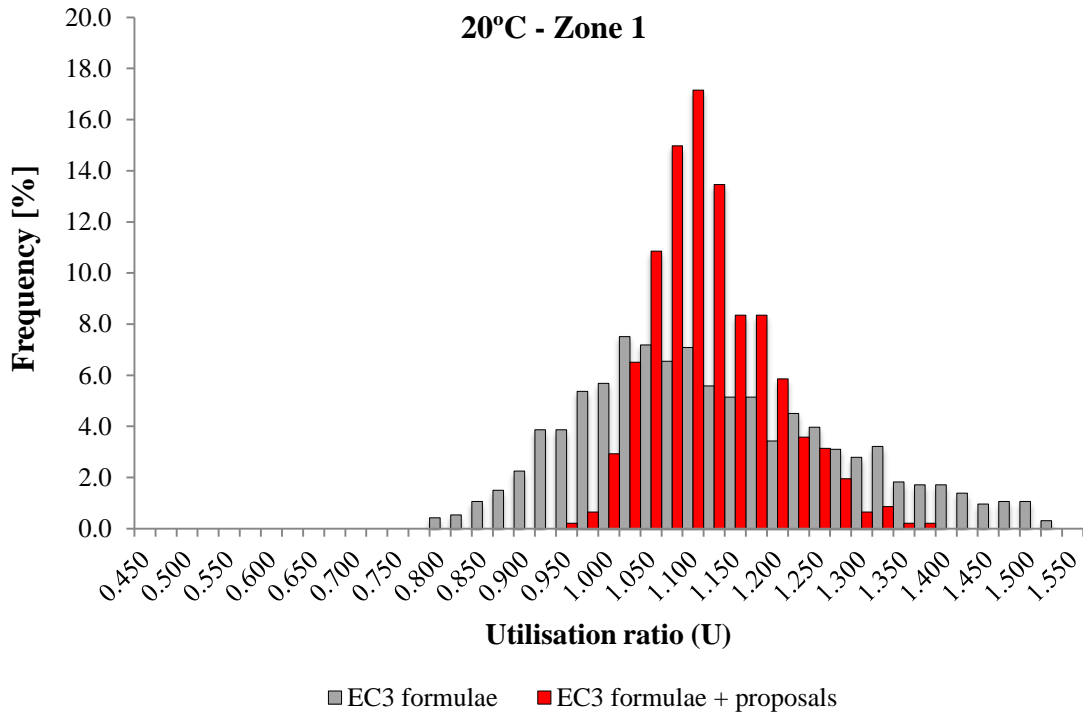
Concerning the results at normal temperature, Table 7.3 shows that both design approaches provide, on average, safe results since the average utilisation ratio is higher than 1.0. On the other hand, for the design approach considering the unchanged EC3 expressions, a larger deviation from the average is evident when compared to the design approach where the proposals presented in this document are taken into account. The results given by the unchanged EC3 procedure do not satisfy two of the three validation

criteria presented by CEN TC 250 (1999). Indeed, for the zone 1 plate girders, the ultimate shear strength predicted by EC3 is not on the safe side for almost 25% of the analysed girders, of which about 14% with an utilisation ratio lower than 0.95. This percentage of 25% of results on the unsafe side is larger than the maximum of 20 % recommended by CEN TC 250 (1999). Furthermore, CEN TC 250 (1999) also refers that the calculation result shall not be on the unsafe side by more than 15%. This is not satisfied by the EC3 procedure, since the maximum unsafe result is 0.79 (21%). When the proposals are considered, it is observed a substantial decrease on the standard deviation from 0.15 to 0.07, as well as a reduction on the percentage of unsafe results to 3.8%, of which only 0.2% with differences larger than 5%. Moreover, the maximum unsafe deviation decreased from 21% to 6%, while the maximum safe deviation also decreased from 51% to 35%.

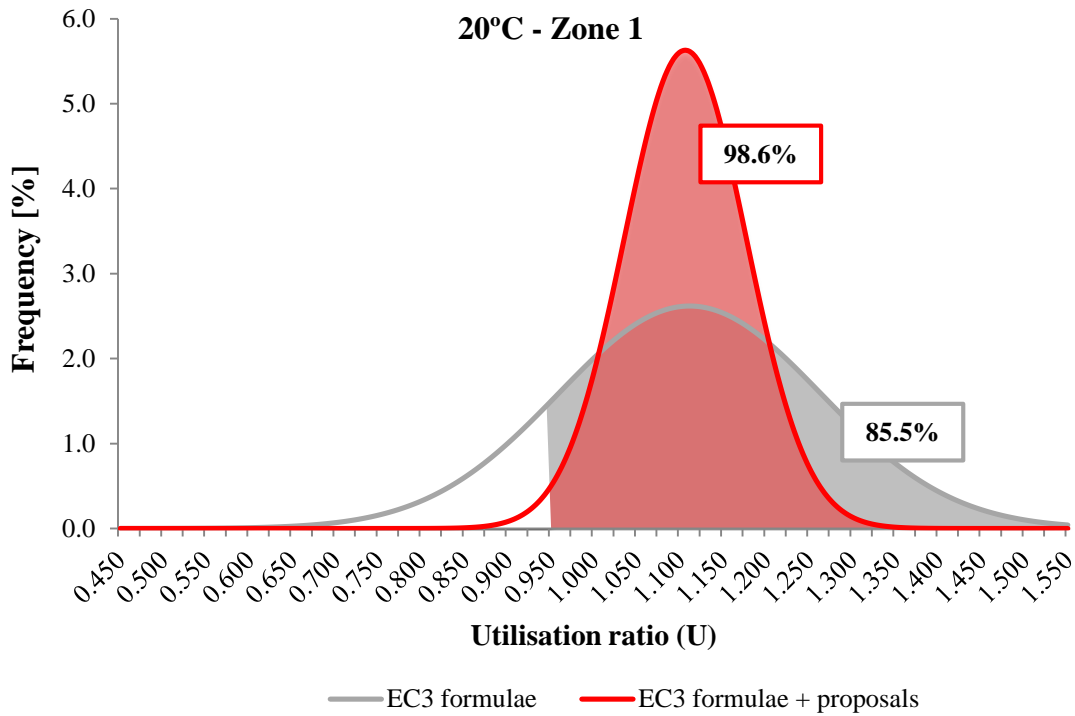
As it was observed for the plate girders with a shear dominant failure analysed at normal temperature, the EC3 design expressions are providing safe predictions for the plate girders affected by the interaction between shear and bending (zone 2). However, when the proposals are considered, a smaller deviation from the average is observed, no longer exist unsafe results and the maximum safe deviation is smaller.

Regarding fire design, despite the average utilisation ratio is on the safe side, the EC3 predictions are unsafe for almost 46% of the girders with a shear dominant failure and 31.0% of the girders with a combined failure. It is important to note that a large part of unsafe results are beyond the 5% margin. With the application of the proposals presented in this thesis, the percentage of unsafe results was reduced to 2.7% for the zone 1 girders. From those 2.7%, only 0.3% are differences larger than 5%. Furthermore, the maximum unsafe deviation fell significantly from 31% to 10%. Concerning the zone 2 plate girders, the percentage of unsafe results was substantially reduced to 1.1%, with no unsafe differences larger than 5%.

Histograms of relative frequency were made for the results of each zone of the shear-bending interaction diagram, considering the two design approaches above mentioned at normal and elevated temperatures. Moreover, working with data from Table 7.3 and Table 7.4, it is possible to fit the results onto the normal distributions. The histograms and the normal distributions are presented in Figure 7.21 to Figure 7.23 for normal temperature and in Figure 7.24 to Figure 7.26 for elevated temperatures.

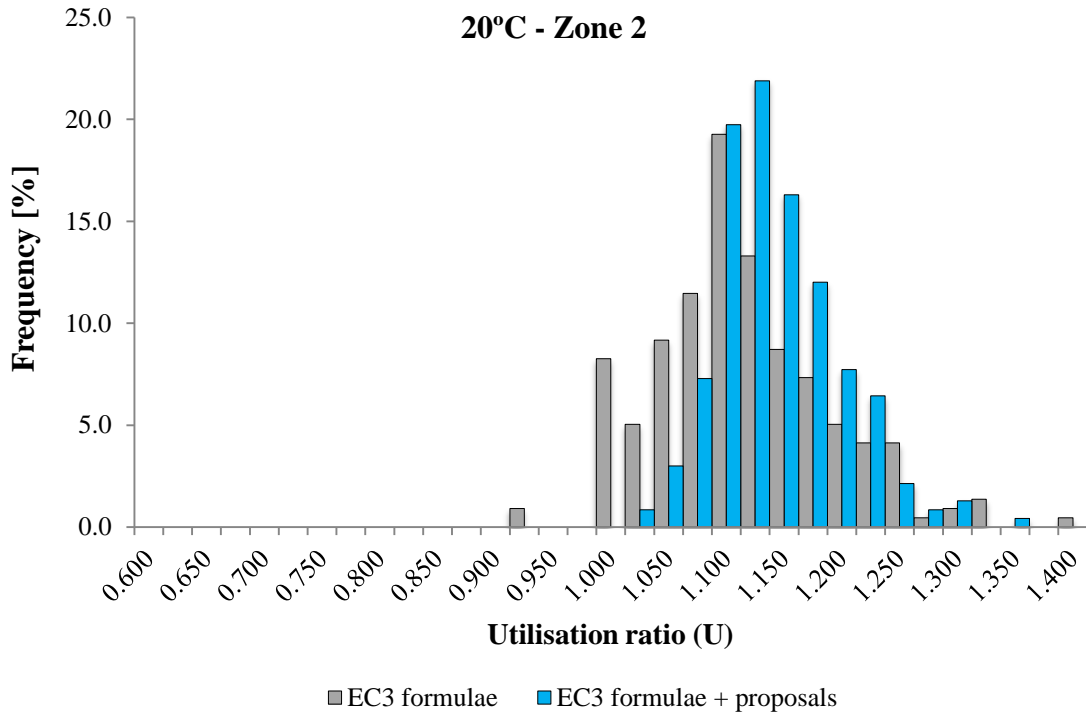


a) relative frequency

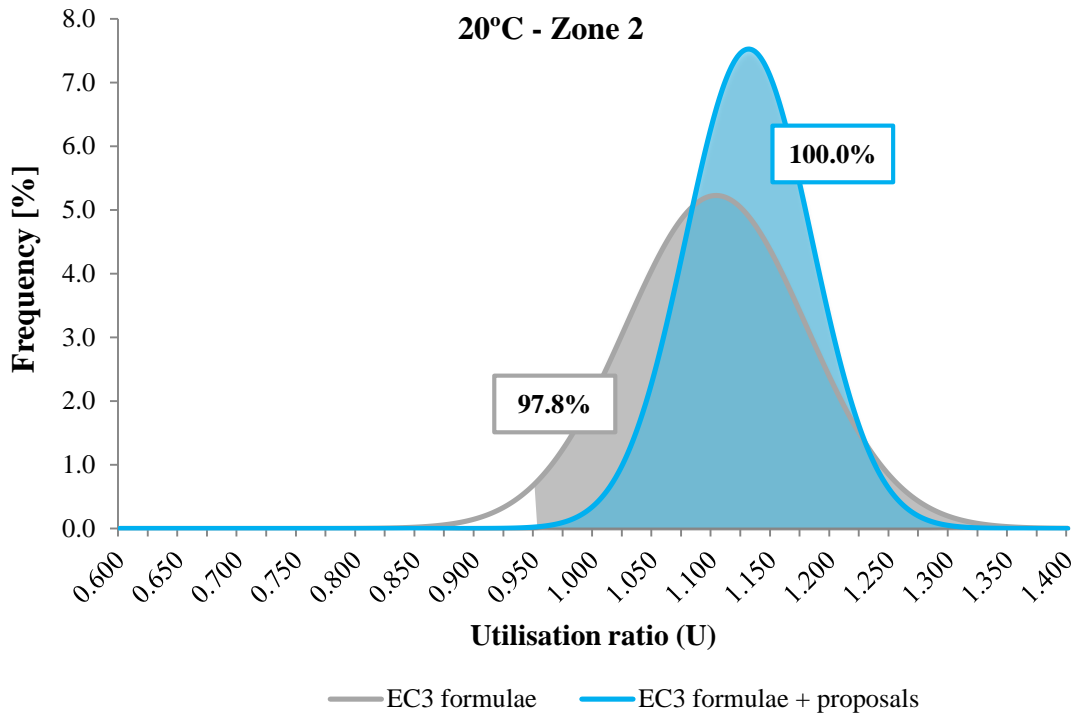


b) normal distribution

Figure 7.21 – Statistical analysis of the zone 1 results at normal temperature

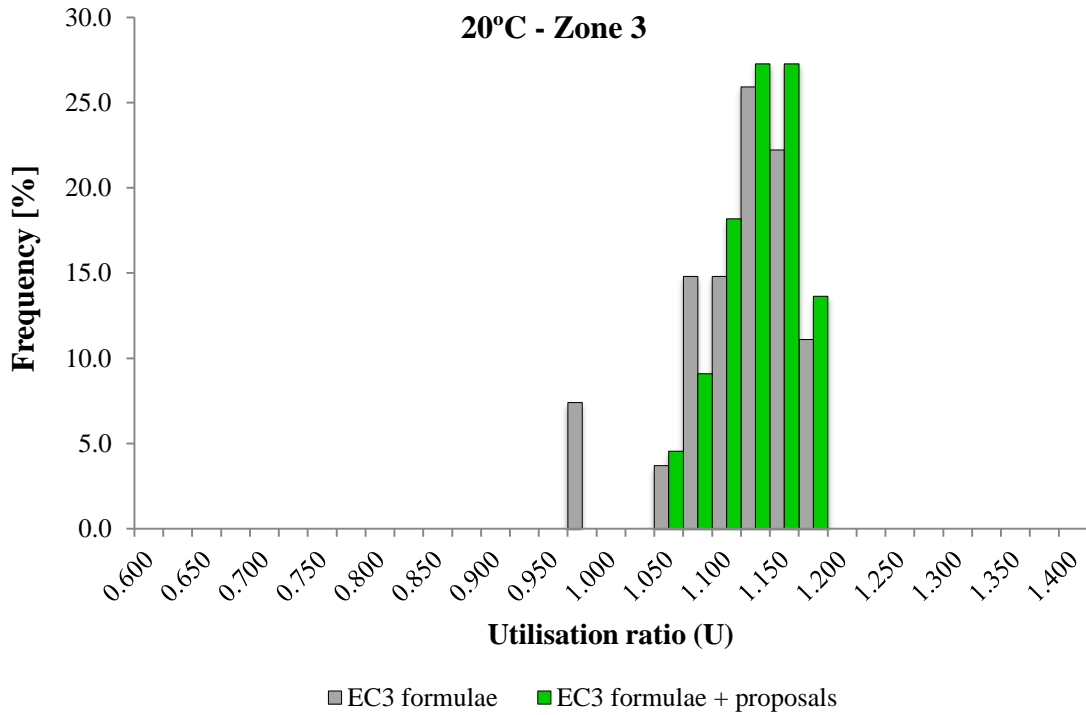


a) relative frequency

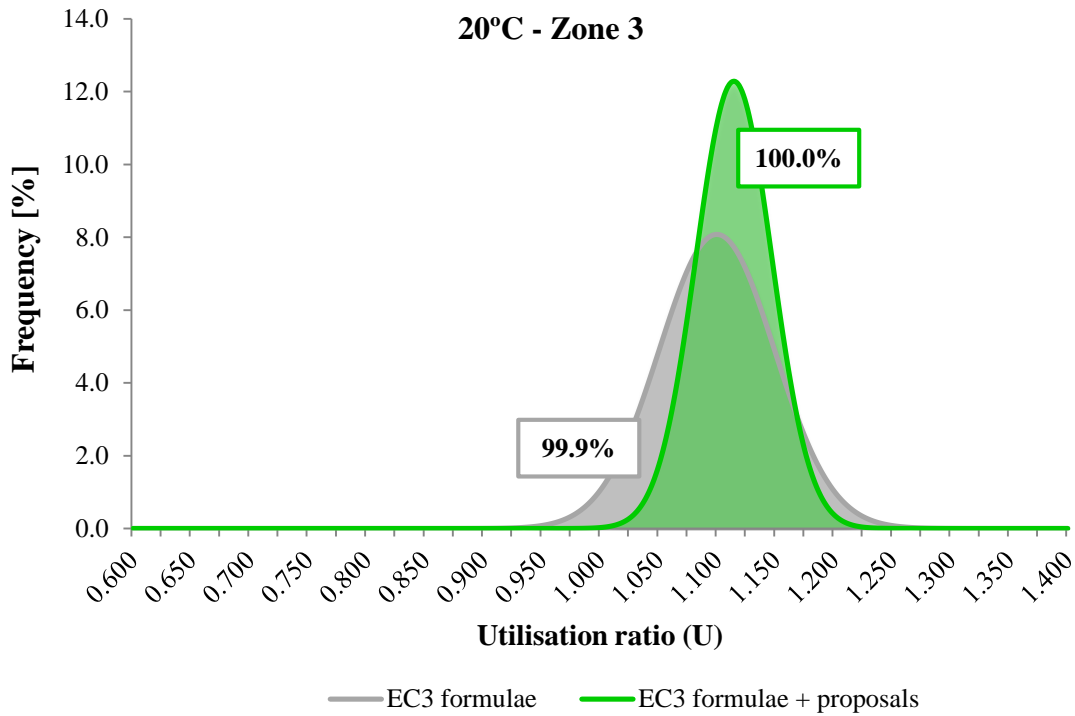


b) normal distribution

Figure 7.22 – Statistical analysis of the zone 2 results at normal temperature

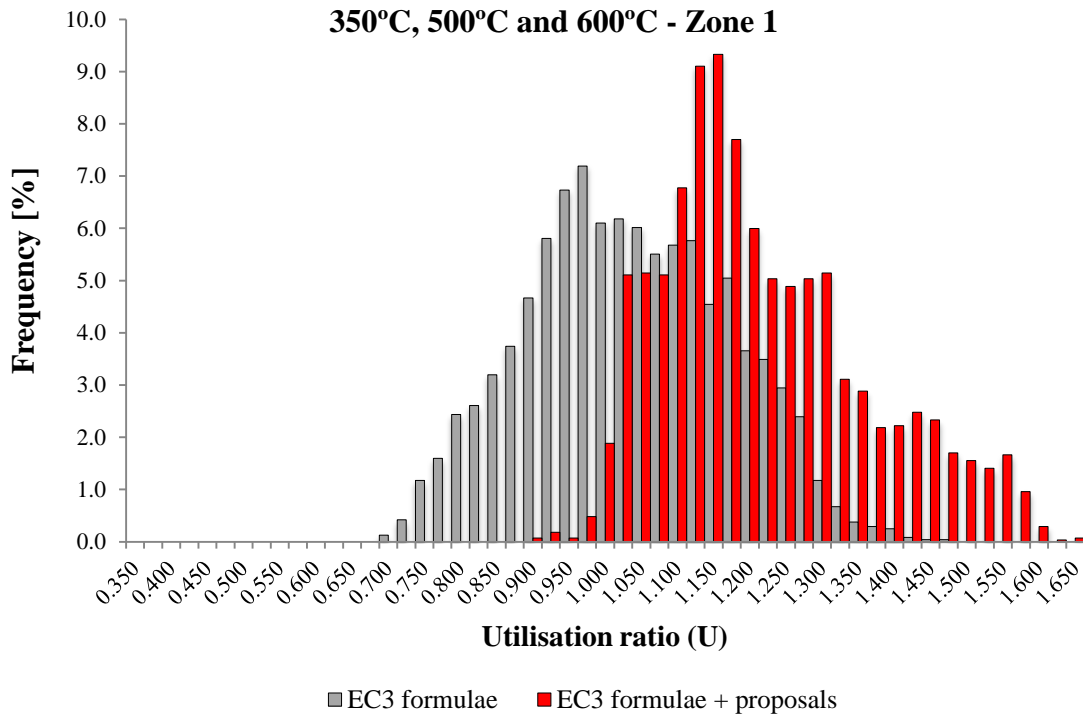


a) relative frequency

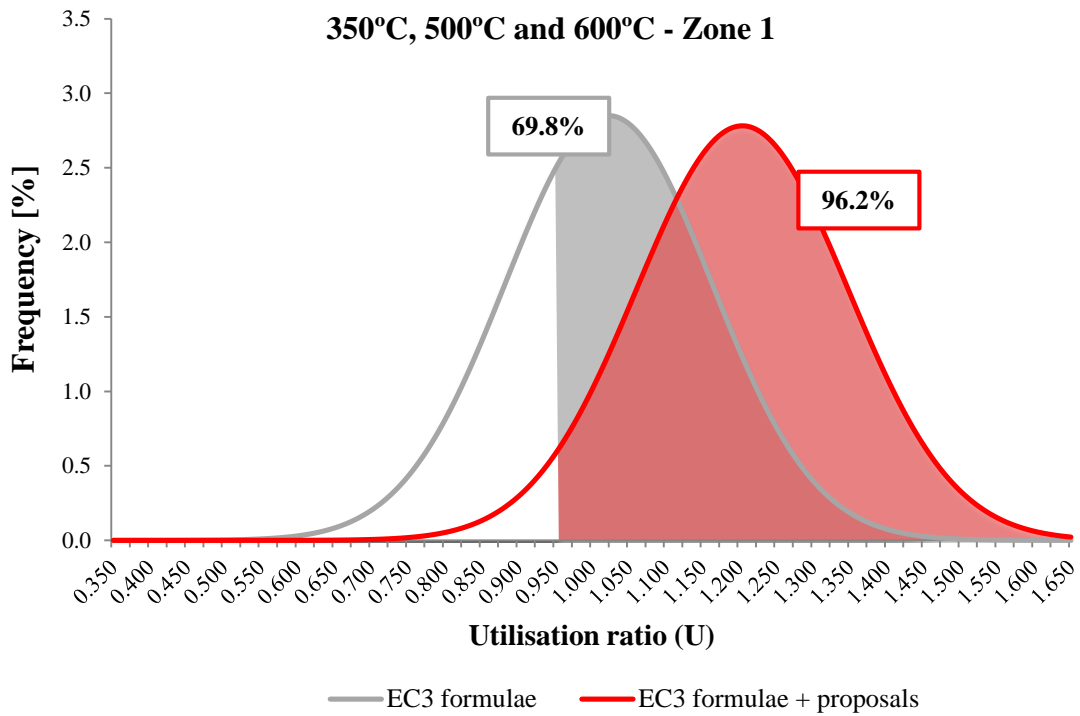


b) normal distribution

Figure 7.23 – Statistical analysis of the zone 3 results at normal temperature

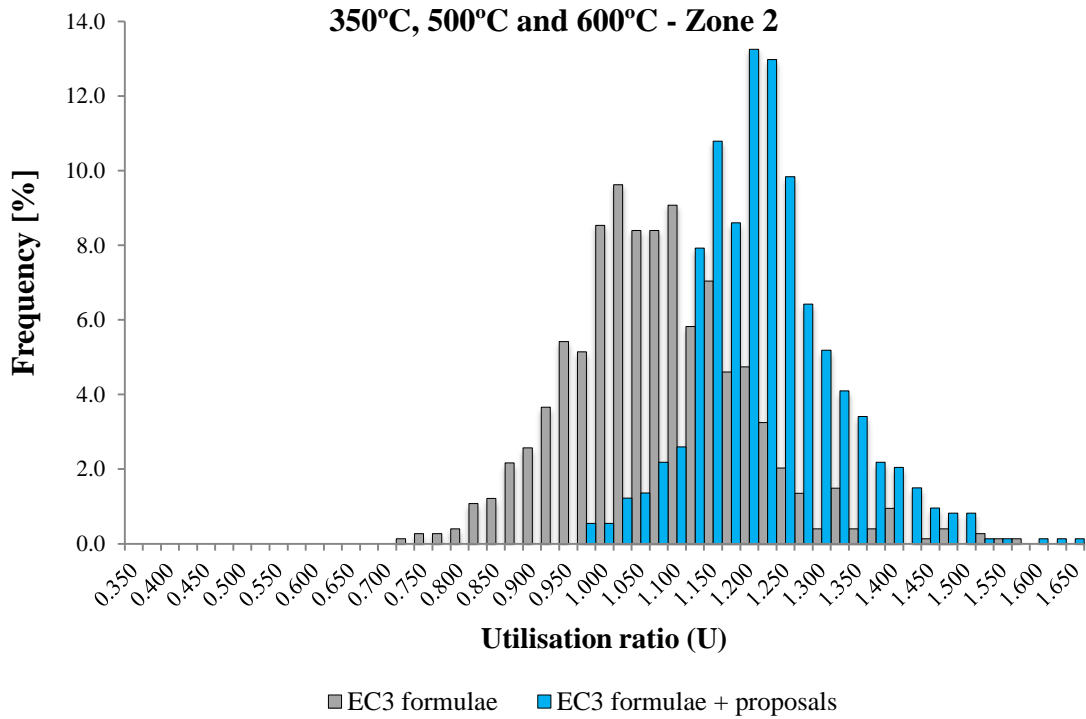


a) relative frequency

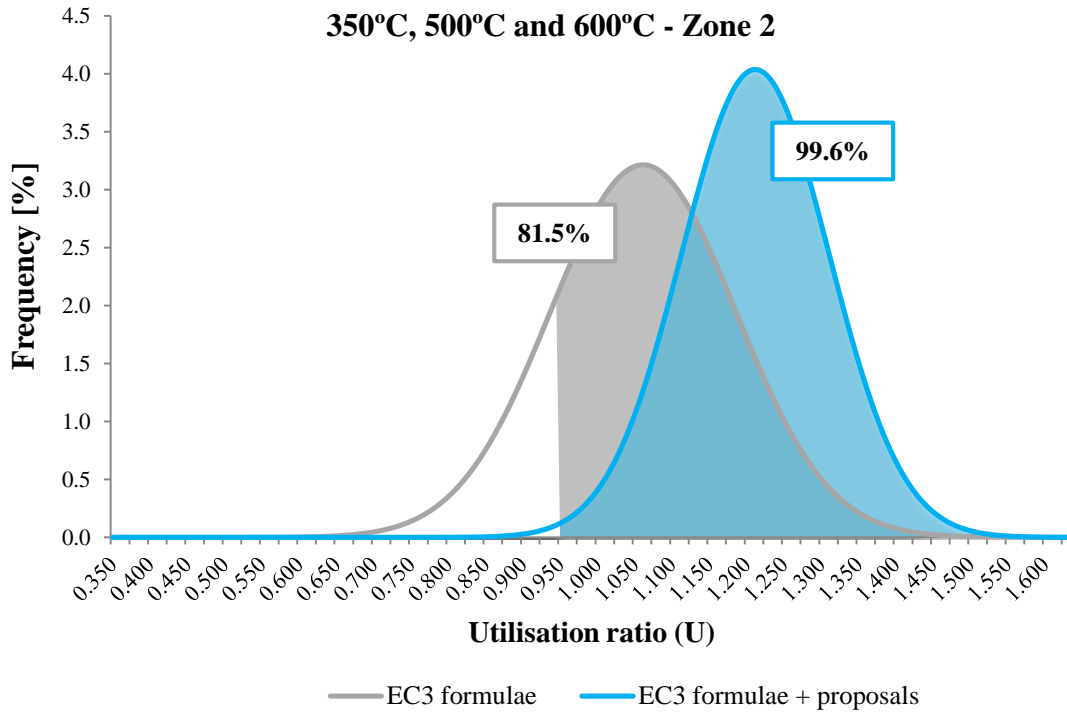


b) normal distribution

Figure 7.24 – Statistical analysis of the zone 1 results at elevated temperatures

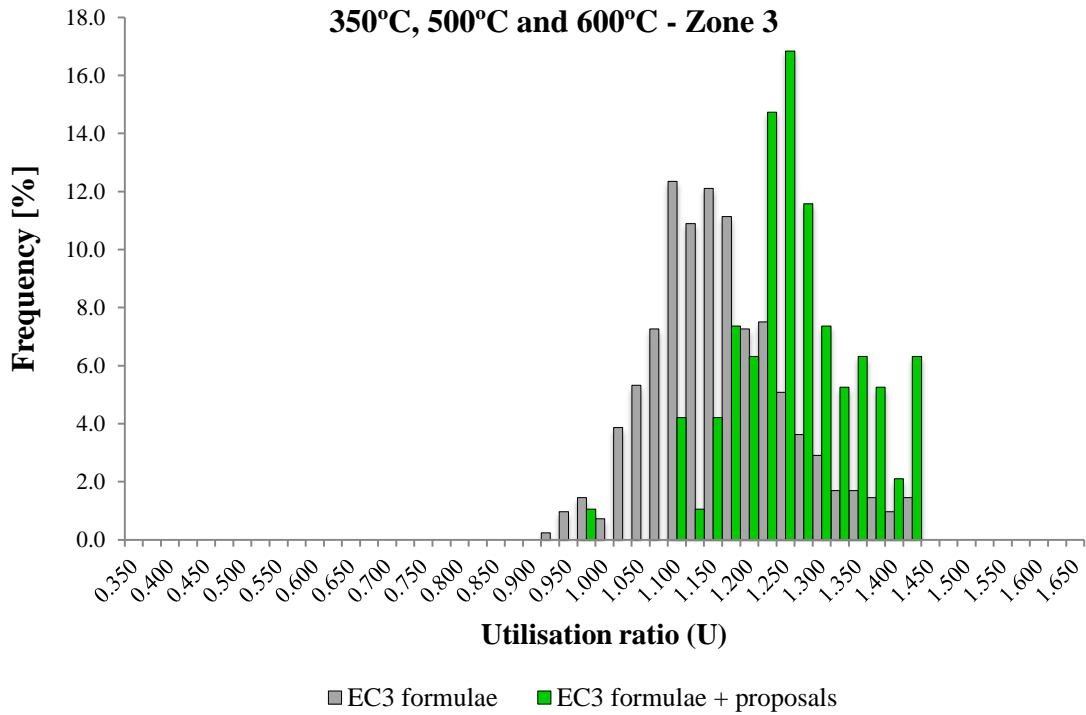


a) relative frequency

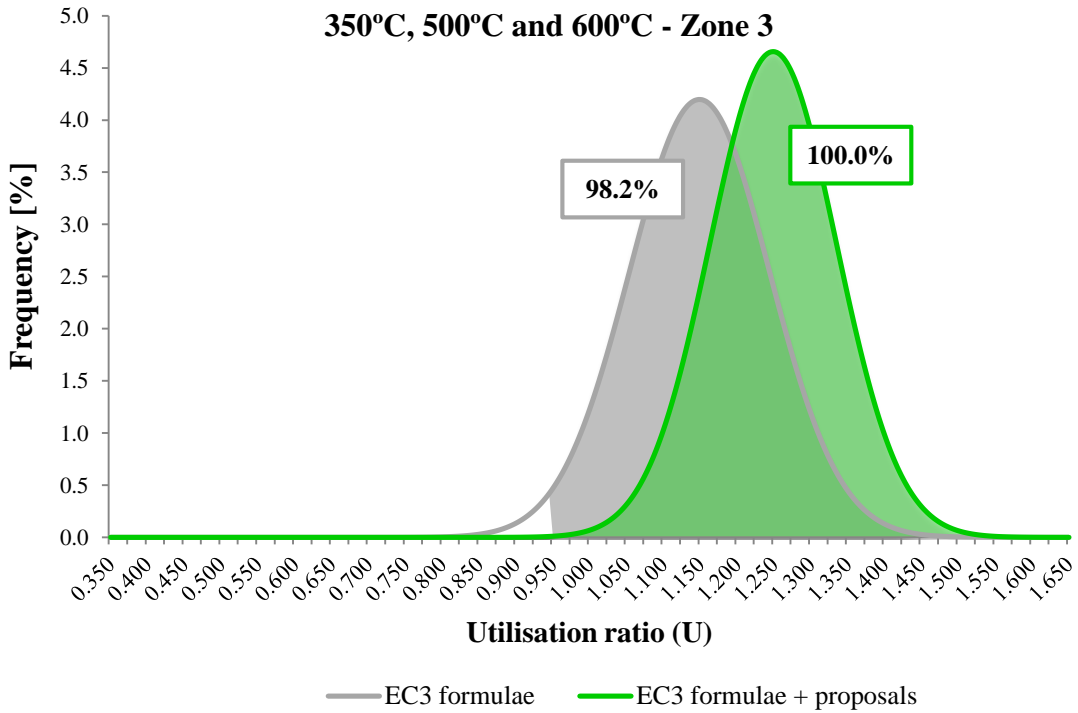


b) normal distribution

Figure 7.25 – Statistical analysis of the zone 2 results at elevated temperatures



a) relative frequency



b) normal distribution

Figure 7.26 – Statistical analysis of the zone 3 results at elevated temperatures

The results from Table 7.3 and Table 7.4 are clearly reflected on the histograms presented above. The larger standard deviation often observed when the proposals are not taken into account is coherent with the histograms presented in Figure 7.21 to Figure 7.26.

With respect to the normal distribution, also known as Gaussian distribution, it is the most important and most widely used distribution in statistics. Considering an arbitrary safety margin of 5%, the probability of safety predicted for the EC3 design procedures is always smaller when the proposals are not taken into account. As an example, looking for the results of the girders collapsing due to shear buckling, which are the focus of this thesis, a 85.5% probability of safety is forecast for the EC3 procedures at normal temperature against the 98.6% of its counterpart. Regarding fire design, a 69.8% probability of safety is predicted for the EC3 procedures adapted to elevated temperatures against the 96.2% of its counterpart. Not only is the modified procedure predicted to be safer overall, but the results are much closer to the average value (lower standard deviation), which certifies the proposals as a strong improvement over the EC3 design procedures.

A more detailed statistical analysis was also performed to understand the accuracy of the EC3 design procedure in function of different parameters, such as: normalized web slenderness parameter, aspect ratio, web slenderness, ratio between flanges and web thicknesses, steel grade and temperature. This detailed statistical analysis is presented in Table 7.5 for the zone 1 plate girders analysed at normal temperature. Table 7.6 shows the results for the zone 1 plate girders subjected to elevated temperatures. The data presented in these tables was obtained considering the proposals presented in this thesis. It is discussed below, together with some charts for an easier understanding of the achieved conclusions.

A similar procedure was accomplished for the zone 2 plate girders, i.e. the plate girders exhibiting a combined shear plus bending failure. The results are presented in Chapter 8, the chapter dedicated to the analysis of the interaction between shear and bending.

Table 7.5 – Detailed statistical analysis of the zone 1 plate girders tested at normal temperature

Parameter	Range	Non-rigid end posts							Rigid end posts						
		N Cases	Av.	St. Dev.	Max	Min	% Unsafe	% U<0.95	N Cases	Av.	St. Dev.	Max	Min	% Unsafe	% U<0.95
Normalized web slenderness	$\bar{\lambda}_w \leq 0.5$	2	1.00	0.01	1.00	0.99	50.0%	0.0%	2	1.02	0.01	1.02	1.01	0.0%	0.0%
	$0.5 < \bar{\lambda}_w \leq 1.0$	43	1.05	0.06	1.15	0.94	20.9%	4.7%	42	1.05	0.04	1.11	0.96	11.9%	0.0%
	$1.0 < \bar{\lambda}_w \leq 1.5$	103	1.08	0.06	1.20	0.98	9.7%	0.0%	94	1.08	0.04	1.19	0.97	2.1%	0.0%
	$1.5 < \bar{\lambda}_w \leq 2.0$	108	1.11	0.06	1.26	1.02	0.0%	0.0%	96	1.11	0.07	1.24	0.99	3.1%	0.0%
	$2.0 < \bar{\lambda}_w \leq 3.0$	147	1.11	0.06	1.34	1.04	0.0%	0.0%	140	1.12	0.09	1.31	0.98	3.6%	0.0%
	$\bar{\lambda}_w > 3.0$	72	1.13	0.03	1.19	1.06	0.0%	0.0%	72	1.17	0.09	1.35	1.01	0.0%	0.0%
Aspect ratio	$a/h_w \leq 1.0$	251	1.10	0.07	1.34	0.94	8.0%	0.8%	236	1.13	0.08	1.35	0.96	2.1%	0.0%
	$1.0 < a/h_w \leq 2.0$	164	1.11	0.04	1.22	1.02	0.0%	0.0%	153	1.10	0.07	1.27	0.97	2.0%	0.0%
	$2.0 < a/h_w \leq 3.0$	60	1.08	0.02	1.14	1.04	0.0%	0.0%	57	1.03	0.03	1.09	0.98	12.3%	0.0%
Web slenderness	$h_w/t_w \leq 100$	14	1.06	0.06	1.11	0.95	21.4%	7.1%	12	1.04	0.04	1.08	0.96	8.3%	0.0%
	$100 < h_w/t_w \leq 150$	96	1.09	0.05	1.25	0.94	5.2%	1.0%	85	1.06	0.05	1.23	0.97	10.6%	0.0%
	$150 < h_w/t_w \leq 225$	196	1.10	0.07	1.34	0.98	6.1%	0.0%	181	1.09	0.06	1.31	0.98	1.7%	0.0%
	$225 < h_w/t_w \leq 300$	104	1.10	0.05	1.28	1.00	0.0%	0.0%	103	1.13	0.07	1.30	0.99	1.9%	0.0%
	$300 < h_w/t_w \leq 400$	65	1.13	0.04	1.19	1.03	0.0%	0.0%	65	1.21	0.08	1.35	1.05	0.0%	0.0%
Ratio between flanges and web thicknesses	$1.5 \leq t_f/t_w \leq 2.0$	55	1.12	0.06	1.26	0.95	3.6%	1.8%	37	1.09	0.07	1.25	0.96	5.4%	0.0%
	$2.0 < t_f/t_w \leq 3.0$	149	1.09	0.06	1.28	0.94	5.4%	0.7%	139	1.09	0.07	1.35	0.97	3.6%	0.0%
	$3.0 < t_f/t_w \leq 4.0$	180	1.11	0.06	1.34	0.96	3.9%	0.0%	179	1.12	0.08	1.35	0.97	0.6%	0.0%
	$4.0 < t_f/t_w \leq 5.0$	91	1.09	0.05	1.18	0.99	3.3%	0.0%	91	1.13	0.09	1.32	0.98	7.7%	0.0%
Steel grade [MPa]	235	315	1.09	0.05	1.24	0.94	5.4%	0.6%	305	1.11	0.09	1.35	0.96	4.6%	0.0%
	275	51	1.12	0.06	1.26	0.99	2.0%	0.0%	45	1.08	0.05	1.19	1.00	2.2%	0.0%
	355	53	1.13	0.07	1.30	0.98	1.9%	0.0%	46	1.12	0.06	1.26	1.00	0.0%	0.0%
	460	56	1.14	0.07	1.34	1.00	1.8%	0.0%	50	1.15	0.07	1.31	1.01	0.0%	0.0%

Table 7.6 – Detailed statistical analysis of the zone 1 plate girders subjected to elevated temperatures

Parameter	Range	Non-rigid end posts							Rigid end posts						
		N Cases	Av.	St. Dev.	Max	Min	% Unsafe	% U<0.95	N Cases	Av.	St. Dev.	Max	Min	% Unsafe	% U<0.95
Normalized web slenderness	$\bar{\lambda}_w \leq 0.5$	2	0.92	0.00	0.92	0.92	100.0%	100.0%	2	0.97	0.00	0.97	0.97	100.0%	0.0%
	$0.5 < \bar{\lambda}_w \leq 1.0$	77	1.06	0.10	1.29	0.90	26.0%	9.1%	77	1.12	0.09	1.28	0.95	11.7%	0.0%
	$1.0 < \bar{\lambda}_w \leq 1.5$	208	1.13	0.09	1.37	0.99	1.0%	0.0%	199	1.24	0.12	1.46	0.95	2.5%	0.0%
	$1.5 < \bar{\lambda}_w \leq 2.0$	279	1.20	0.12	1.49	1.03	0.0%	0.0%	260	1.30	0.15	1.58	0.99	1.2%	0.0%
	$2.0 < \bar{\lambda}_w \leq 3.0$	485	1.20	0.12	1.56	1.03	0.0%	0.0%	451	1.29	0.16	1.64	0.99	1.3%	0.0%
	$\bar{\lambda}_w > 3.0$	333	1.11	0.08	1.54	0.97	5.1%	0.0%	328	1.20	0.14	1.57	0.98	2.1%	0.0%
Aspect ratio	$a/h_w \leq 1.0$	720	1.19	0.13	1.56	0.90	2.8%	1.3%	687	1.35	0.14	1.64	0.95	1.3%	0.0%
	$1.0 < a/h_w \leq 2.0$	486	1.15	0.08	1.37	0.99	0.4%	0.0%	461	1.19	0.08	1.39	0.99	0.9%	0.0%
	$2.0 < a/h_w \leq 3.0$	178	1.06	0.05	1.20	0.97	10.7%	0.0%	169	1.03	0.04	1.15	0.95	11.2%	0.0%
Web slenderness	$h_w/t_w \leq 100$	50	1.00	0.05	1.09	0.90	34.0%	18.0%	48	1.02	0.05	1.13	0.95	33.3%	0.0%
	$100 < h_w/t_w \leq 150$	269	1.19	0.13	1.55	0.97	2.6%	0.0%	245	1.20	0.12	1.52	0.99	1.2%	0.0%
	$150 < h_w/t_w \leq 225$	560	1.19	0.11	1.56	1.00	0.0%	0.0%	523	1.26	0.13	1.58	0.99	1.1%	0.0%
	$225 < h_w/t_w \leq 300$	310	1.13	0.09	1.54	1.00	0.6%	0.0%	306	1.29	0.16	1.64	1.00	0.7%	0.0%
	$300 < h_w/t_w \leq 400$	195	1.09	0.04	1.17	0.97	7.7%	0.0%	195	1.28	0.19	1.58	0.98	2.6%	0.0%
Ratio between flanges and web thicknesses	$1.5 \leq t_f/t_w \leq 2.0$	138	1.17	0.13	1.51	0.91	8.7%	2.9%	101	1.18	0.12	1.44	0.96	7.9%	0.0%
	$2.0 < t_f/t_w \leq 3.0$	436	1.16	0.11	1.55	0.90	3.2%	1.1%	413	1.23	0.14	1.64	0.95	2.7%	0.0%
	$3.0 < t_f/t_w \leq 4.0$	537	1.17	0.12	1.56	0.97	0.9%	0.0%	530	1.28	0.15	1.58	0.99	1.1%	0.0%
	$4.0 < t_f/t_w \leq 5.0$	273	1.13	0.10	1.48	0.98	3.7%	0.0%	273	1.27	0.17	1.58	0.99	2.6%	0.0%
Steel grade [MPa]	235	932	1.11	0.07	1.47	0.90	4.4%	1.0%	907	1.23	0.16	1.58	0.95	3.5%	0.0%
	275	143	1.22	0.10	1.52	1.07	0.0%	0.0%	135	1.26	0.11	1.50	1.02	0.0%	0.0%
	355	149	1.26	0.11	1.54	1.10	0.0%	0.0%	135	1.32	0.12	1.59	1.07	0.0%	0.0%
	460	160	1.30	0.11	1.56	1.12	0.0%	0.0%	140	1.36	0.14	1.64	1.09	0.0%	0.0%
T [°C]	350	475	1.17	0.11	1.56	0.90	1.3%	0.6%	456	1.25	0.15	1.63	0.96	0.9%	0.0%
	500	456	1.15	0.11	1.55	0.90	3.3%	0.9%	433	1.24	0.15	1.62	0.95	3.5%	0.0%
	600	453	1.15	0.12	1.55	0.91	4.4%	0.4%	428	1.26	0.16	1.64	0.95	3.0%	0.0%

✓ **Normalized web slenderness**

As mentioned before, the detailed statistical analysis allows evaluating the accuracy of the EC3 procedure, taken into account the proposals presented in this document, in function of different parameters.

Regarding the EC3 normalized web slenderness, it was observed in Table 7.5 that the highest the web slenderness parameter is, the more conservative the EC3 predictions are. The same trend was observed for girders with non-rigid and rigid end posts at both normal and elevated temperatures. As an example, Figure 7.27 shows the variation of the average utilisation ratio for six slenderness parameter ranges of the girders with non-rigid end posts analysed at normal temperature. The standard deviation is represented by the red bars and the maximum and minimum values are illustrated by the grey lines.

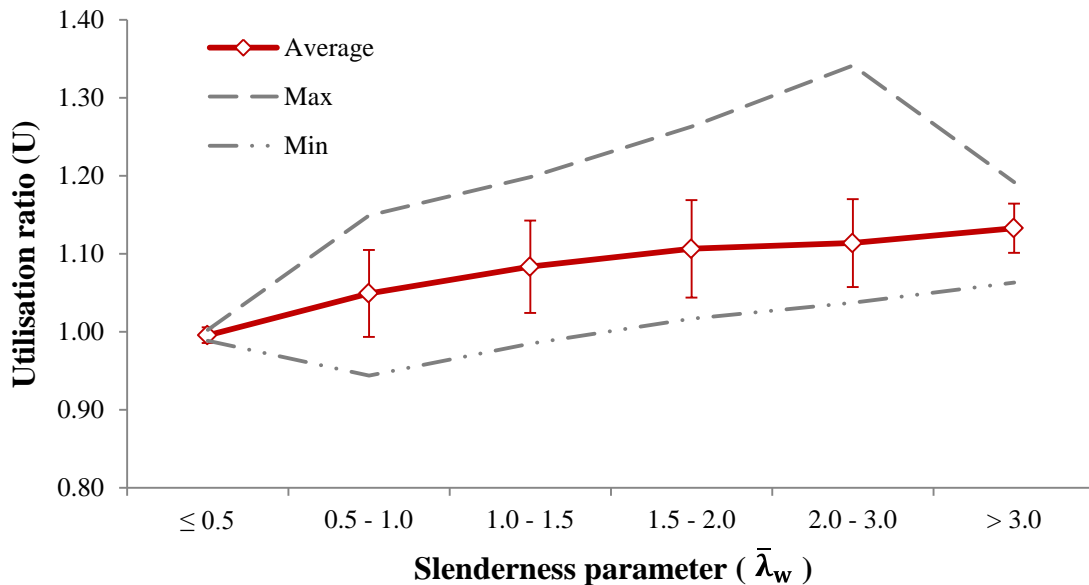


Figure 7.27 – Utilisation ratio in function of the web slenderness parameter for the plate girders with non-rigid end posts analysed at normal temperature

✓ **Aspect ratio**

The statistical analysis in terms of the aspect ratio showed that the lowest the aspect ratio is, the more conservative the EC3 procedure is. It may be clearly observed in Figure 7.28, where are plotted, for the group II of plate girders, the web contribution to shear buckling in terms of the girders aspect ratio. The charts on the left represent the girders analysed at normal temperature, while the charts on the right are related to the girders subjected to elevated temperatures. On the other hand, the results for the girders

with non-rigid end posts are presented in the top two charts, while the results of the girders with rigid end posts are placed below. The orange and yellow points represent the girders with larger aspect ratios, while the green and blue points correspond to the girders with lower aspect ratios. As one can see, the orange and yellow points are closer to the design curve, therefore the average nearest 1.0 and the lower standard deviation. On the other hand, the green and blue points are more distant from the design curve and so the higher value for the average utilisation ratio.

Figure 7.28 also indicates that there is a great dispersion of results on the girders with rigid end posts, when compared with the girders with non-rigid end posts. Furthermore, it is observed that such dispersion is larger at elevated temperatures. This observation is fully supported by the difference on the values of standard deviation presented in Table 7.5 and Table 7.6. As regards the girders with rigid end posts, the standard deviation at normal temperature is 0.08 for the girders with $a/h_w \leq 1$ and 0.07 for the girders with $1 < a/h_w \leq 2$. However, at elevated temperatures these values are 0.14 and 0.08, respectively. It represents a substantial increase on the girders with $a/h_w \leq 1$, while only a slight increase as observed for the girders with $1 < a/h_w \leq 2$.

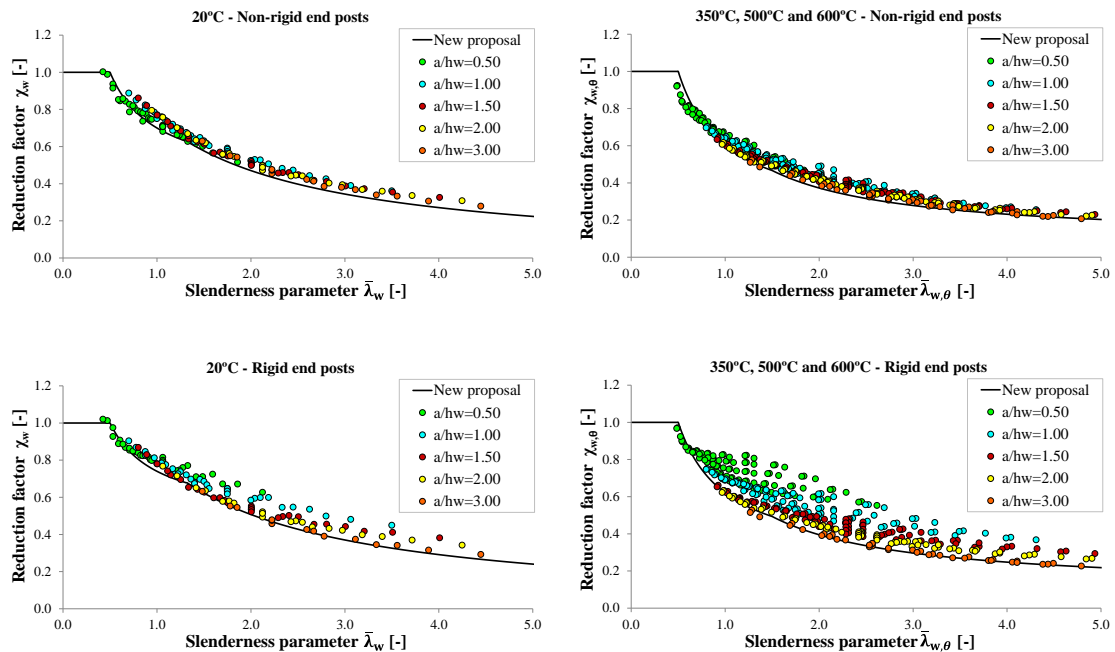


Figure 7.28 – Web contribution to shear buckling of the group II plate girders in function of the plate girders aspect ratio

✓ **Web slenderness**

The statistical results demonstrated that the highest the web slenderness is, the more conservative the EC3 predictions are, at both normal and elevated temperatures. The same trend was observed for rigid and non-rigid end posts. In order to exemplify, the results for the girders with rigid end posts are presented in Figure 7.29. In addition, a large deviation from the average is evident at elevated temperatures. Finally, it is perceptible that the majority of the unsafe results come from the girders with $h_w/t_w \leq 100$, mainly at elevated temperatures (see Table 7.6).

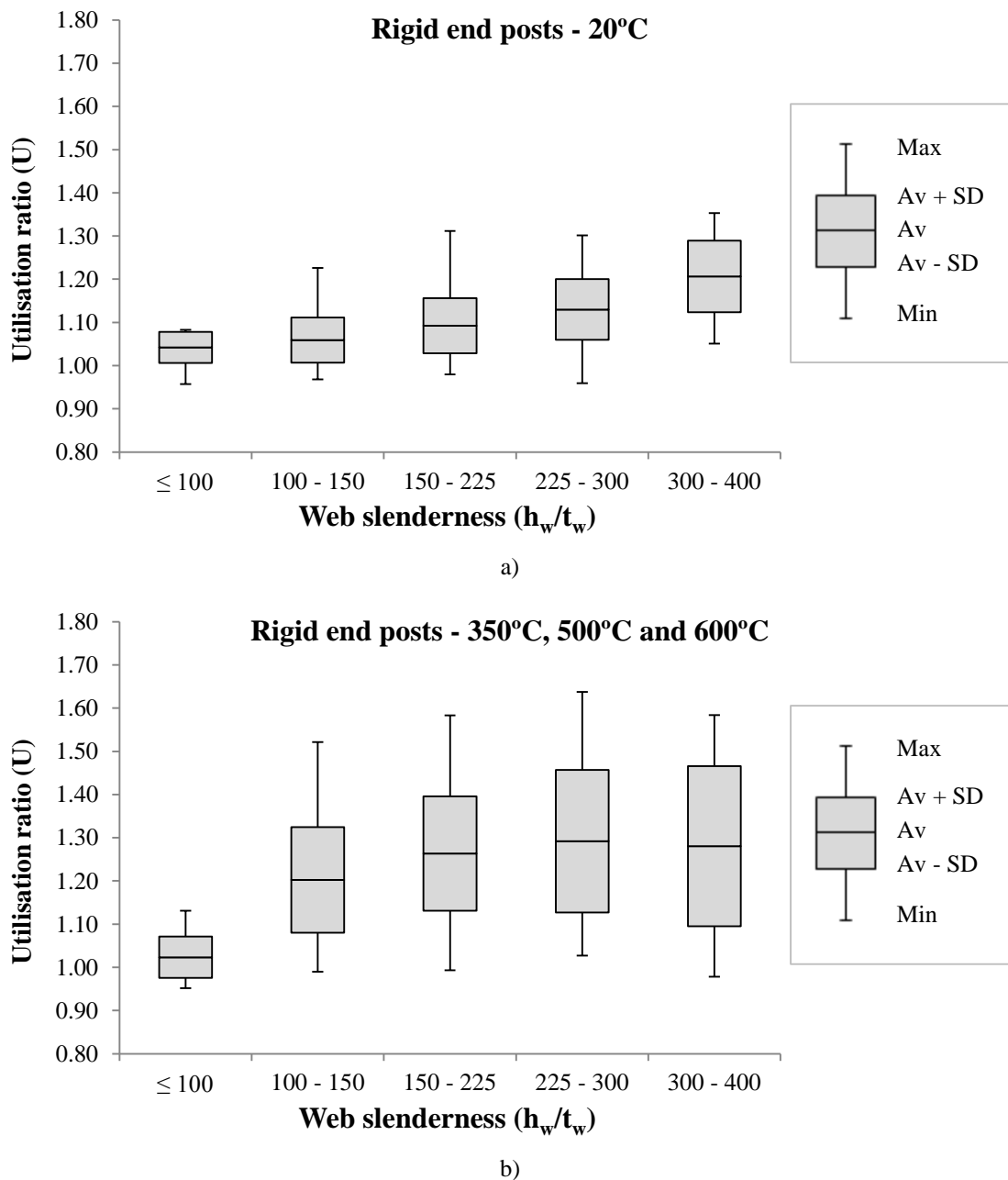


Figure 7.29 – Utilisation ratio in function of the web slenderness at elevated temperatures

✓ Ratio between flanges and web thicknesses

When analysing the data from Table 7.5 and Table 7.6, it was concluded that the ratio t_f/t_w is not a key factor on the accuracy of the EC3 predictions for the girders with non-rigid end posts at both normal and elevated temperatures. However, for the girders with rigid end posts that is not really true. In Figure 7.28 it was detected a bigger dispersion of results on the girders with rigid end posts, mainly at elevated temperatures. Now, it is possible to observe that there is a correlation between the ratio t_f/t_w and such dispersion, which occurs mainly for the girders with $t_f/t_w > 3$. Although there, this increase on the results dispersion is not so evident at normal temperature. But, at elevated temperatures, it can be easily seen in Figure 7.30.

In defence of the EC3 design procedure, it worth mentioning that the ratio $t_f/t_w > 3$ is not so common in practice. The ratio $t_f/t_w > 3$ results from the choice of testing girders with quite strong flanges in order to have in most of the cases a failure mode due to shear buckling. However, in practice, the flanges are designed to support the bending moments and the ratio t_f/t_w is not high often. Furthermore, it is important to have in mind that the EC3 design procedure is on the safe side, being more conservative for this kind of plate girders.

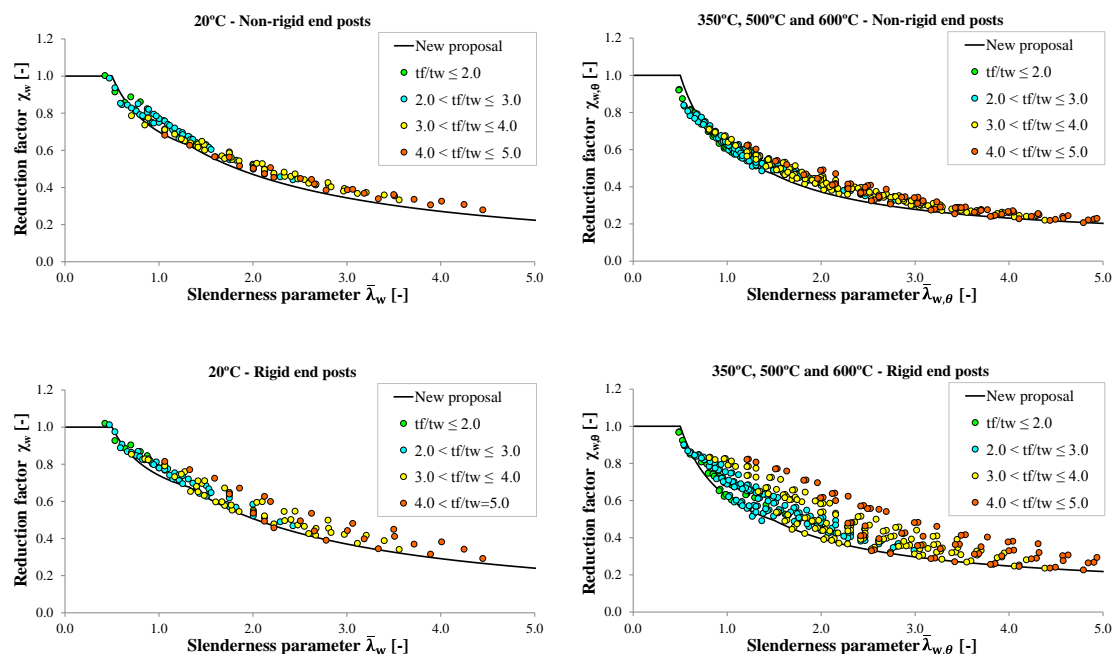


Figure 7.30 – Web contribution to shear buckling of the group II plate girders in function of the ratio between the flanges and web thicknesses

✓ **Steel grade**

The influence of the steel grade on the accuracy of the EC3 predictions is evaluated here. Four steel grades were analysed in this thesis. As it can be seen in Figure 7.31, the conservative nature of the EC3 predictions at normal temperature slightly increases with the increase of the steel grade. Regarding EC3 predictions at elevated temperatures, this behaviour is more evident. Furthermore, it is possible to note that the EC3 predictions are more conservative for the girders with rigid end posts, when compared with the girders with non-rigid end posts.

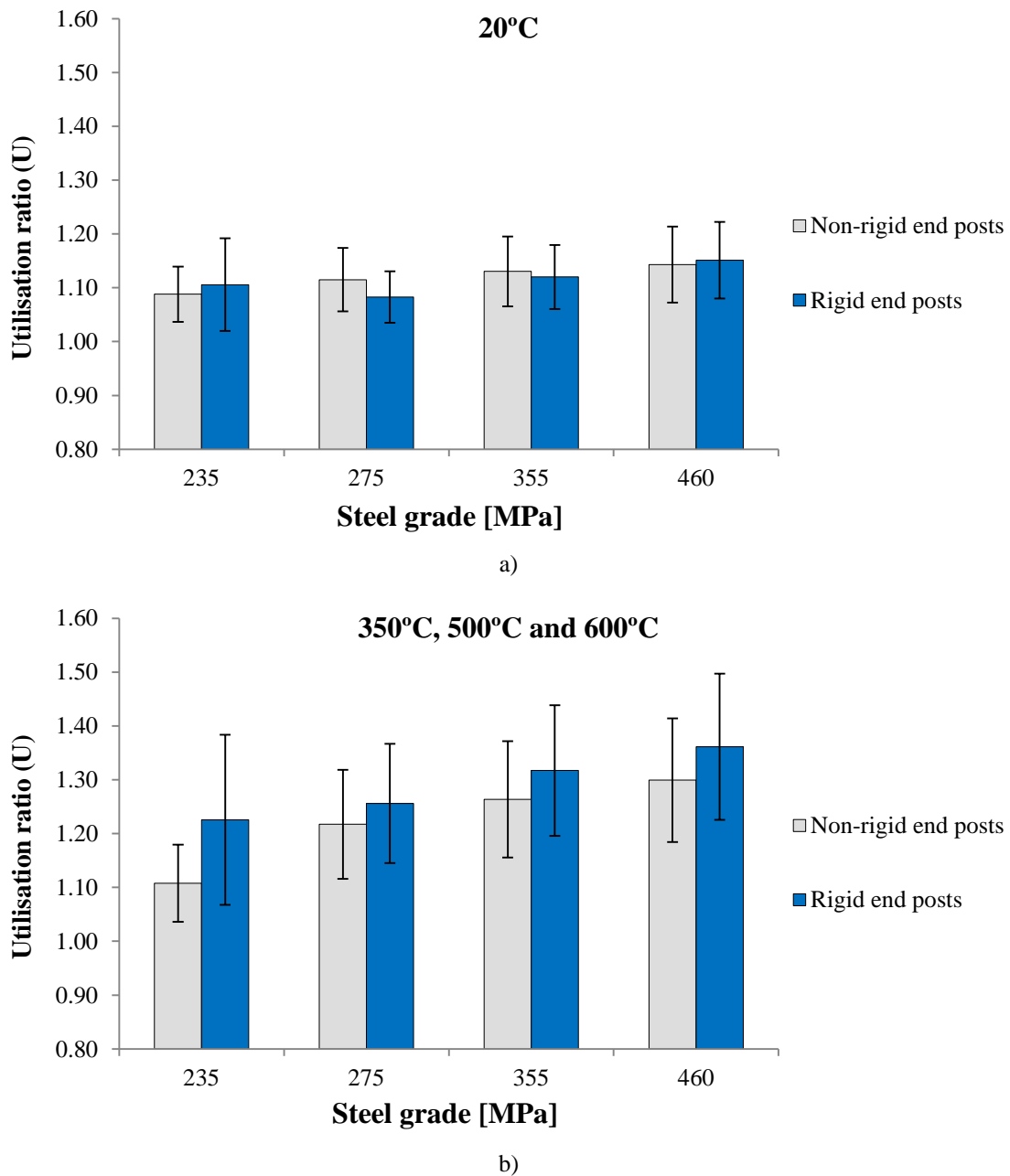


Figure 7.31 – Average utilisation ratio and standard deviation in function of the steel grade

✓ **Uniform elevated temperature**

Finally, the last parameter analysed on the detailed statistical analysis was the uniform elevated temperature that was imposed to the girders. The results presented in Table 7.6 are illustrated in Figure 7.32, which demonstrates that, for the analysed elevated temperatures, there is no correlation between the accuracy of the EC3 design procedure and the temperature range.

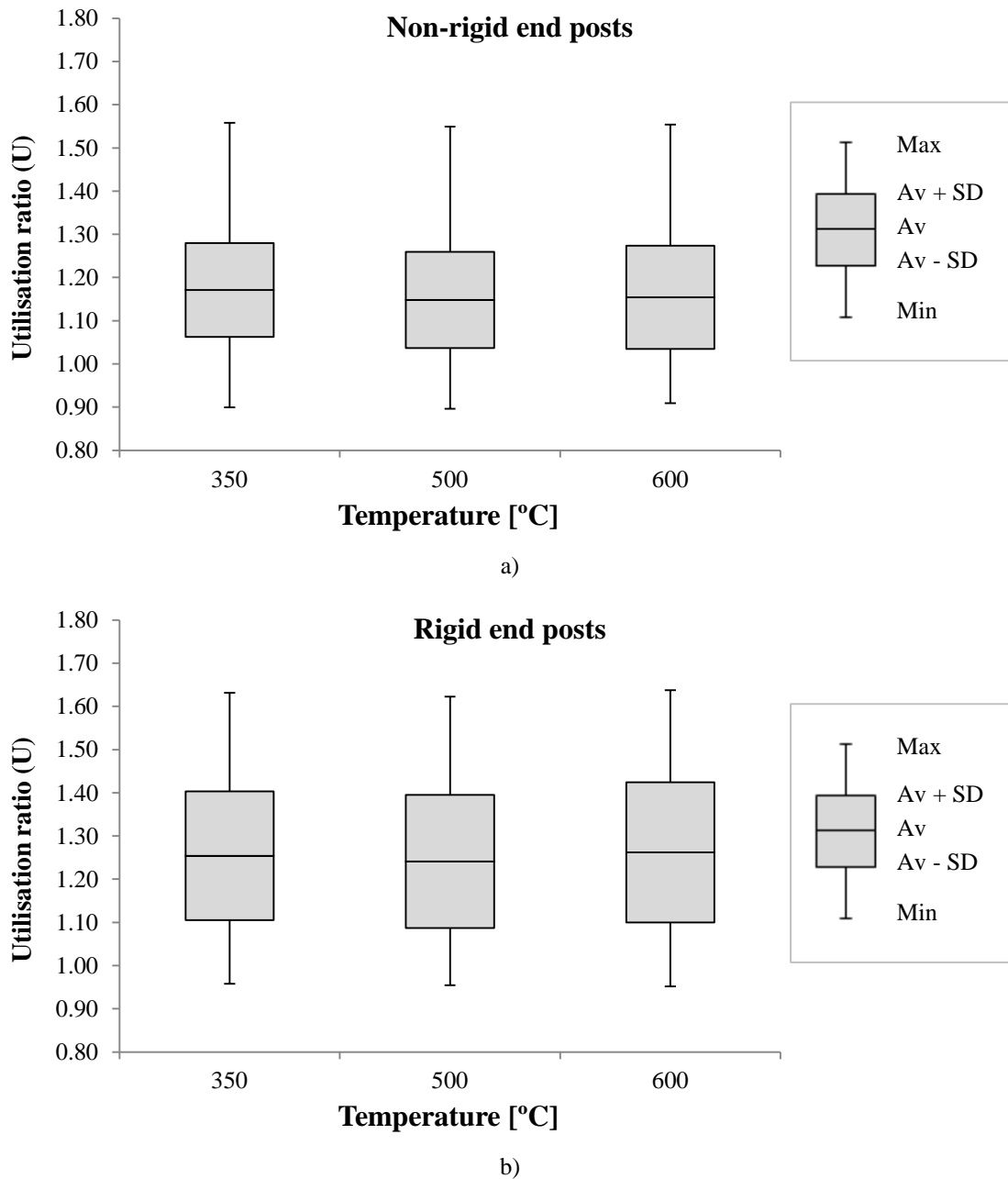


Figure 7.32 – Utilisation ratio in function of the temperature

7.5 Conclusions

Based on the work presented in Chapter 7, the following general conclusions are drawn:

- The EC3 design procedure to determine the web resistance to shear buckling at normal temperature is providing unsafe results for plate girders with normalized web slenderness lower than 1.3;
- Small modifications to the reduction factor for the web shear buckling resistance are proposed in order to improve the safety and precision of the EC3 predictions;
- For the fire design of steel plate girders affected by shear buckling, the application of the reduction factors for the stress-strain relationship of steel at elevated temperatures to the EC3 design procedure is not enough, since there are still too many unsafe predictions;
- Consequently, a new reduction factor for the web resistance to shear buckling in fire situation is proposed, providing safe results when incorporated in the EC3 design procedure.

Chapter 8

Shear-bending interaction

Chapter 8 Shear-bending interaction

8.1 Failure modes

8.2 Evaluation of the EC3 expression to check the interaction between shear and bending

8.3 Statistical analysis

8.4 Conclusions

Chapter 8 Shear-bending interaction

8.1 Failure modes

The interaction between shear and bending in steel plate girders subjected to shear buckling is analysed in this Chapter. Three different failure modes were observed in the parametric numerical study: a shear dominant failure characterized by the web shear buckling, a bending dominant failure recognized by the local buckling of the compression flange and, finally, a combined shear plus bending failure involving and interaction of the failure modes mentioned above.

Figure 8.1 shows three different failure modes observed for the same 2-panel plate girder in function of its aspect ratio. The plate girder presented in Figure 8.1 has rigid end posts and it was subjected to 500°C. The designation “PG 1000x10+300x20_S235” means: PG – plate girder; 1000 – web depth (mm); 10 – web thickness (mm); 300 – flanges width (mm); 20 – flanges thickness (mm); S235 – steel grade.

The typical deformed shape of the girders exhibiting a shear dominant failure may be observed in Figure 8.1a, where it is visible the web shear buckling and no buckling in the flanges. The shear dominant failure changes to a bending dominant failure when the girder length is increased from 2 m to 6 m (and consequently the aspect ratio from 1.0 to 3.0). The failure mechanism is presented in Figure 8.1c. Finally, a combined shear plus bending failure is obtained for an intermediate span (4 m), as shown in Figure 8.1b.

Different failure modes may also be observed for a plate girder with fixed length, as shown in Figure 8.2. This is obtained increasing the number of transverse stiffeners. The reduction of the distance between transverse stiffeners increases the ultimate shear strength of plate girders making them less susceptible to the occurrence of shear buckling.

As mentioned in Chapter 5, a single shear-bending interaction diagram must be drawn for each plate girder, since it depends on shear resistance ($V_{bw,Rd}$ and $V_{bf,Rd}$) and bending resistance ($M_{f,Rd}$ and $M_{pl,Rd}$). Figure 8.2 demonstrates that the plate girders classification into different zones of the shear-bending interaction diagram, performed as presented in Chapter 5, can be confirmed by the obtained deformed shape at failure.

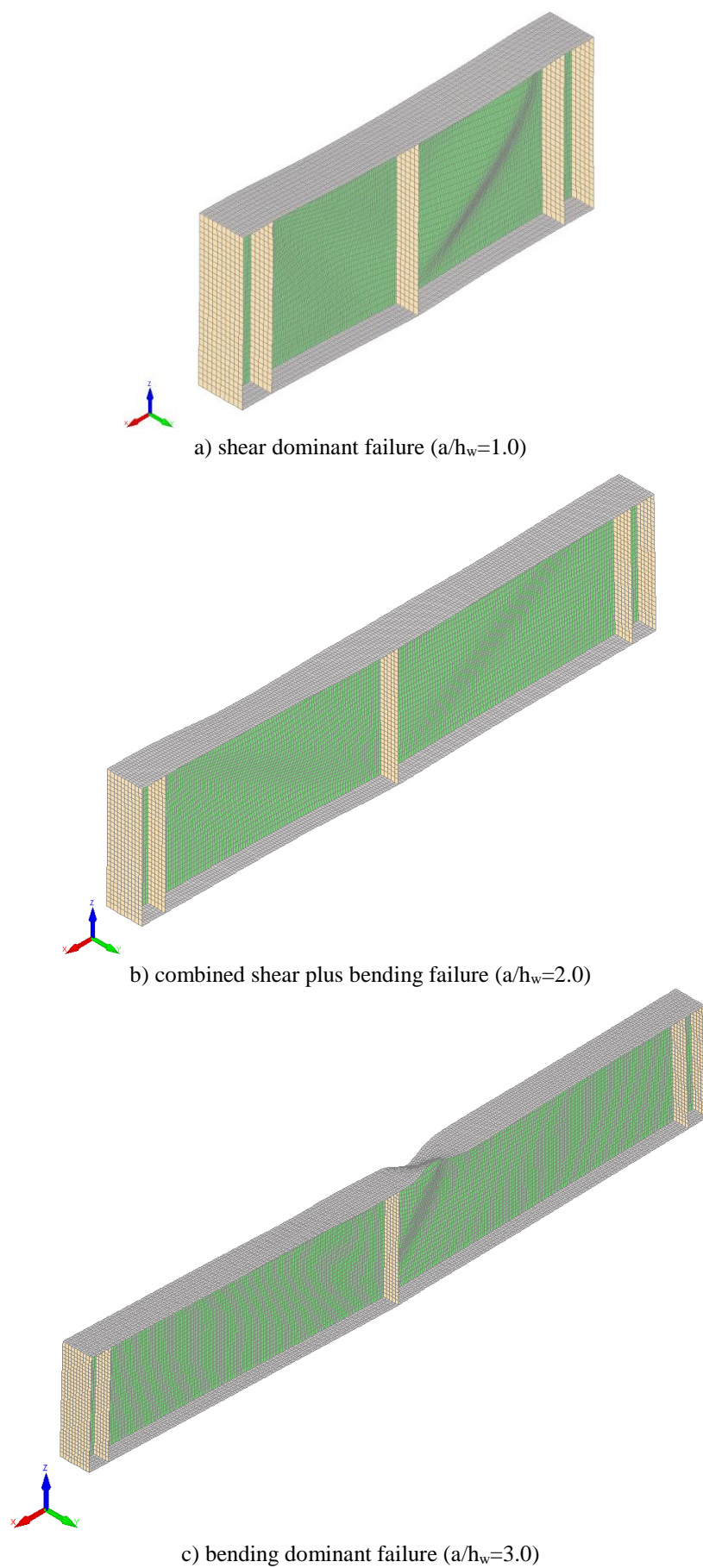


Figure 8.1 – Example of the failure modes observed for PG 1000x10+300x20_S235 at 500°C

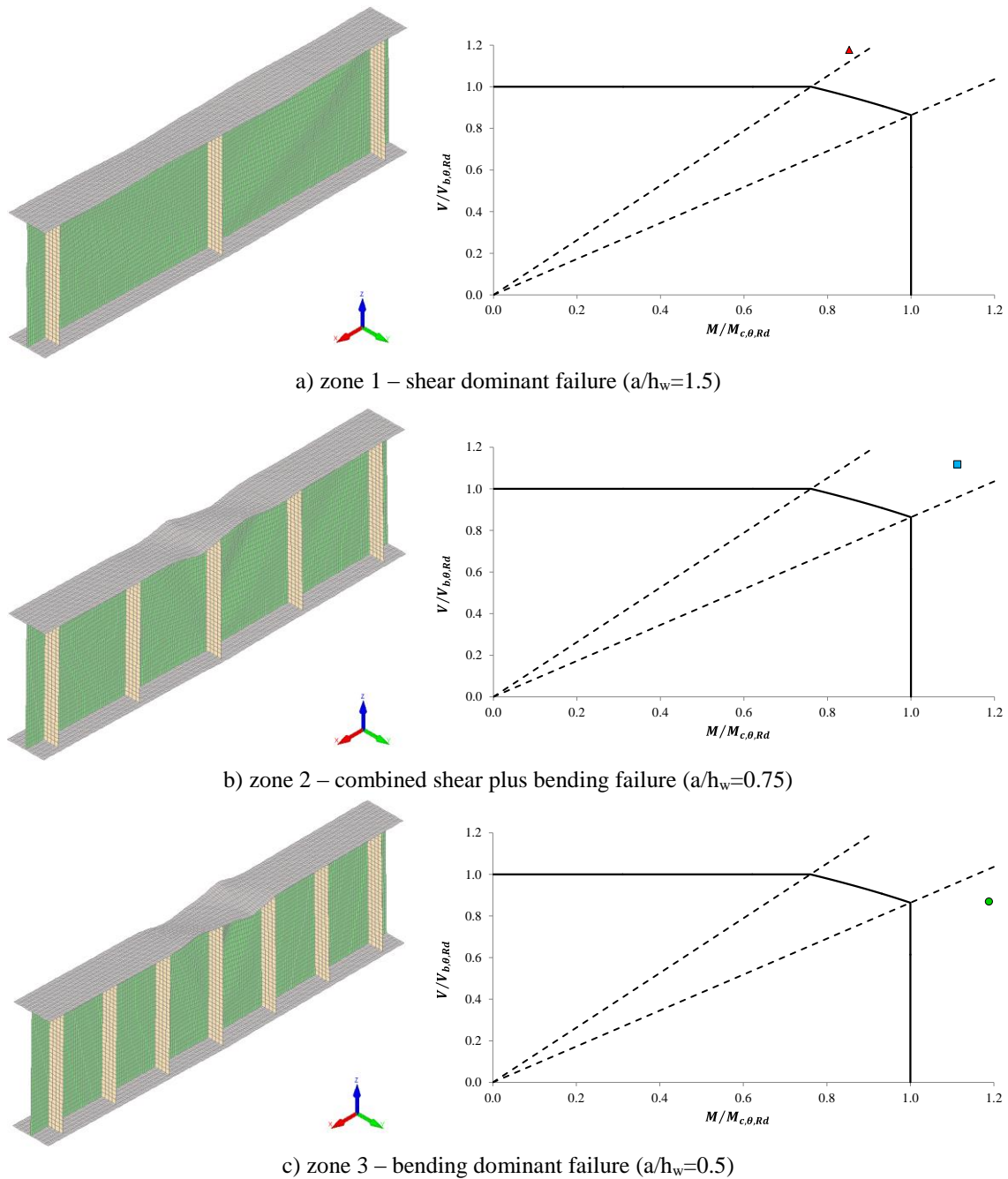


Figure 8.2 – Different failure modes observed for PG 600x4+200x7_S460 at 500°C

8.2 Evaluation of the EC3 expression to check the interaction between shear and bending

The design expression implemented in Part 1-5 of EC3 for the shear-bending interaction (Eq. (3.17)) is evaluated in this section. Only the girders with a combined shear plus bending failure (zone 2) are used to assess the accuracy of this expression. The improvements achieved by the application of the proposals presented in this thesis are presented in Figure 8.3.

As mentioned in section 7.4, it is important to note that the zones classification of the girders may change when the proposals are considered, since it depends on $V_{bw,Rd}$. For example, that is why in Figure 8.3b the “EC3” points with slenderness values higher than 4.0 do not have their equivalents in the “EC3 + proposals” points. Those girders were classified as zone 2 but with the application of the proposals are now classified as zone 1. It happens mainly for the points placed in the boundaries of each zone of the shear-bending interaction diagram.

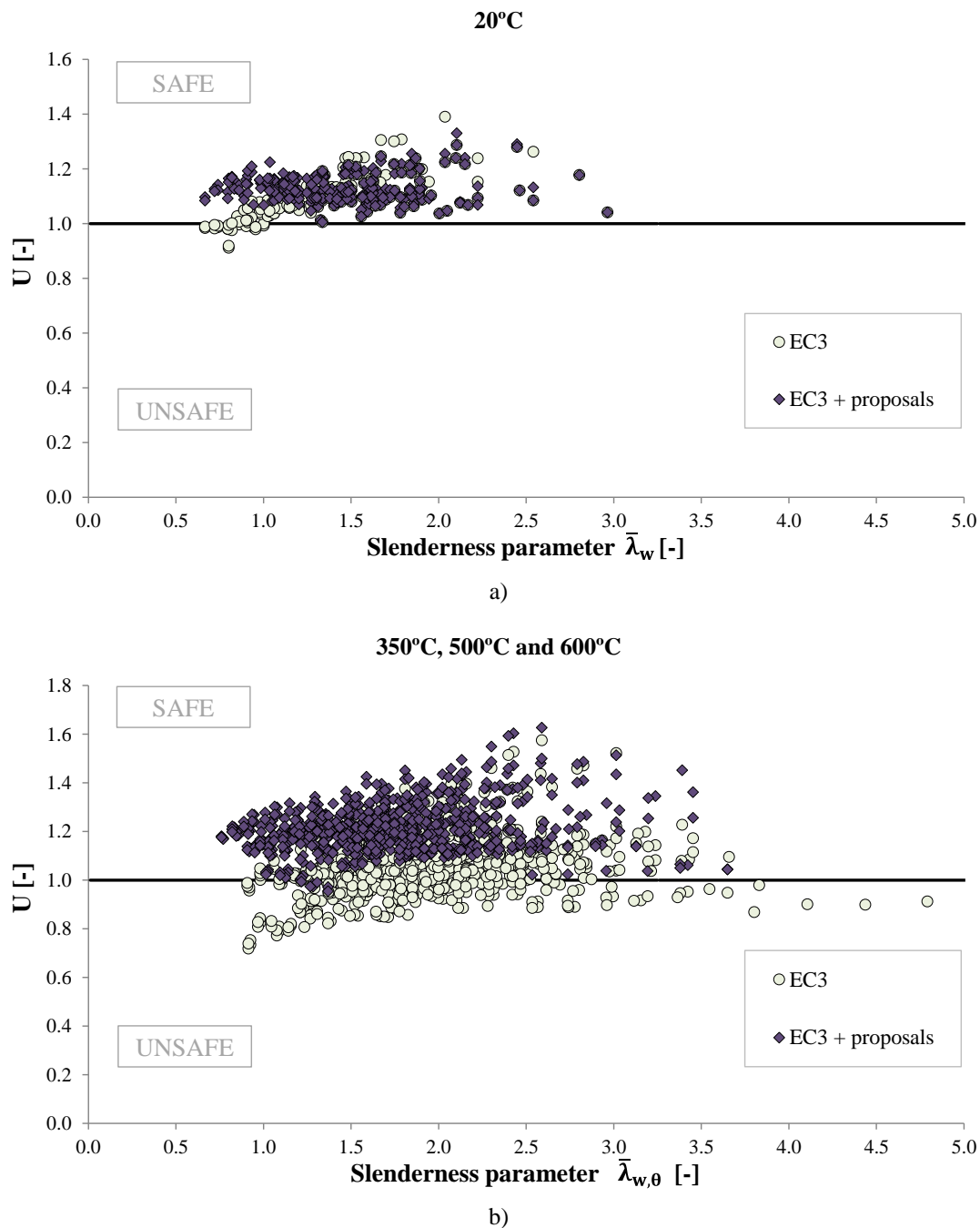


Figure 8.3 – Improvements for the zone 2 girders

At normal temperature, Figure 8.3a demonstrates that the obtained improvements are mainly related to the girders with $\bar{\lambda}_w \leq 1.0$. The statistical analysis presented in Table 7.3 indicates that EC3 design expression is providing good results, with only 9.2% of unsafe results. A 97.8% probability of safety is predicted for the EC3 design expression, if an arbitrary safety margin of 5% is considered, as it can be seen in Figure 7.22. However, the proposals presented in this thesis to improve the EC3 predictions for the web resistance to shear buckling ($V_{bw,Rd}$) also improved the results of the shear-bending interaction expression, since $V_{bw,Rd}$ is incorporated in this expression. The dispersion of results was reduced (lower standard deviation, lower maximum safe deviation) and the probability of safety predicted for the EC3 design procedure is now 100%.

As concerns elevated temperatures, the improvements given by the proposals were more significant, as shown in Figure 8.3b. The percentage of unsafe results decreased from 30.9% to 1.1% and the standard deviation was also reduced (see Table 7.4). The probability of safety predicted for the EC3 interaction expression applied to fire design rose from 81.5% to 99.6%, as it can be seen in Figure 7.25.

Furthermore, it is perceptible that the highest the web slenderness parameter is, the lowest is the tendency for the girders have a combined shear plus bending failure mechanism. At normal temperature, it is visible that the majority of the girders with a combined shear plus bending failure has $\bar{\lambda}_w$ comprised between 0.7 and 2.2. Regarding the girders subjected to elevated temperatures, a failure caused by the interaction between shear and bending is registered mainly for girders with $0.8 \leq \bar{\lambda}_{w,\theta} \leq 2.7$.

8.3 Statistical analysis

A detailed statistical analysis, similar to the one performed for the plate girders with a shear dominant failure (zone 1), was performed for the zone 2 plate girders (combined shear plus bending failure). Table 8.1 shows the results for the girders tested at normal temperature, while the results for the girders subjected to elevated temperatures are listed in Table 8.2. The data from both tables is discussed below. As mentioned for the zone 1 girders, the results for the zone 2 girders were also obtained considering the EC3 design procedures modified by the proposals previously presented.

Table 8.1 – Detailed statistical analysis of the zone 2 plate girders tested at normal temperature

Parameter	Range	Non-rigid end posts							Rigid end posts						
		N Cases	Av.	St. Dev.	Max	Min	% Unsafe	% U<0.95	N Cases	Av.	St. Dev.	Max	Min	% Unsafe	% U<0.95
Normalized web slenderness	$\bar{\lambda}_w \leq 0.5$	0	-	-	-	-	-	-	0	-	-	-	-	-	-
	$0.5 < \bar{\lambda}_w \leq 1.0$	16	1.15	0.03	1.19	1.10	0.0%	0.0%	17	1.13	0.04	1.21	1.07	0.0%	0.0%
	$1.0 < \bar{\lambda}_w \leq 1.5$	47	1.14	0.03	1.21	1.08	0.0%	0.0%	55	1.11	0.04	1.22	1.01	0.0%	0.0%
	$1.5 < \bar{\lambda}_w \leq 2.0$	33	1.14	0.05	1.26	1.05	0.0%	0.0%	43	1.12	0.06	1.25	1.03	0.0%	0.0%
	$2.0 < \bar{\lambda}_w \leq 3.0$	8	1.19	0.10	1.33	1.07	0.0%	0.0%	14	1.14	0.09	1.29	1.04	0.0%	0.0%
	$\bar{\lambda}_w > 3.0$	0	-	-	-	-	-	-	0	-	-	-	-	-	-
Aspect ratio	$a/h_w \leq 1.0$	61	1.17	0.05	1.33	1.09	0.0%	0.0%	76	1.15	0.05	1.29	1.06	0.0%	0.0%
	$1.0 < a/h_w \leq 2.0$	28	1.11	0.03	1.16	1.05	0.0%	0.0%	39	1.08	0.03	1.18	1.01	0.0%	0.0%
	$2.0 < a/h_w \leq 3.0$	15	1.11	0.02	1.15	1.07	0.0%	0.0%	14	1.07	0.02	1.13	1.04	0.0%	0.0%
Web slenderness	$h_w/t_w \leq 100$	4	1.14	0.03	1.16	1.10	0.0%	0.0%	6	1.10	0.03	1.13	1.07	0.0%	0.0%
	$100 < h_w/t_w \leq 150$	41	1.12	0.02	1.20	1.07	0.0%	0.0%	50	1.09	0.04	1.21	1.01	0.0%	0.0%
	$150 < h_w/t_w \leq 225$	46	1.15	0.05	1.29	1.05	0.0%	0.0%	59	1.14	0.06	1.28	1.03	0.0%	0.0%
	$225 < h_w/t_w \leq 300$	13	1.19	0.06	1.33	1.13	0.0%	0.0%	14	1.16	0.06	1.29	1.04	0.0%	0.0%
	$300 < h_w/t_w \leq 400$	0	-	-	-	-	-	-	0	-	-	-	-	-	-
Ratio between flanges and web thicknesses	$1.5 \leq t_f/t_w \leq 2.0$	62	1.17	0.05	1.33	1.09	0.0%	0.0%	80	1.15	0.05	1.29	1.04	0.0%	0.0%
	$2.0 < t_f/t_w \leq 3.0$	42	1.11	0.02	1.15	1.05	0.0%	0.0%	48	1.08	0.03	1.13	1.01	0.0%	0.0%
	$3.0 < t_f/t_w \leq 4.0$	0	-	-	-	-	-	-	1	1.04	0.00	1.04	1.04	0.0%	0.0%
	$4.0 < t_f/t_w \leq 5.0$	0	-	-	-	-	-	-	0	-	-	-	-	-	-
Steel grade [MPa]	235	48	1.12	0.03	1.18	1.05	0.0%	0.0%	54	1.09	0.03	1.13	1.01	0.0%	0.0%
	275	21	1.14	0.03	1.20	1.09	0.0%	0.0%	27	1.11	0.03	1.16	1.06	0.0%	0.0%
	355	19	1.16	0.05	1.26	1.09	0.0%	0.0%	26	1.14	0.05	1.22	1.05	0.0%	0.0%
	460	16	1.19	0.06	1.33	1.10	0.0%	0.0%	22	1.19	0.06	1.29	1.10	0.0%	0.0%

Table 8.2 – Detailed statistical analysis of the zone 2 plate girders subjected to elevated temperatures

Parameter	Range	Non-rigid end posts							Rigid end posts						
		N Cases	Av.	St. Dev.	Max	Min	% Unsafe	% U<0.95	N Cases	Av.	St. Dev.	Max	Min	% Unsafe	% U<0.95
Normalized web slenderness	$\bar{\lambda}_w \leq 0.5$	0	-	-	-	-	-	-	0	-	-	-	-	-	-
	$0.5 < \bar{\lambda}_w \leq 1.0$	21	1.20	0.04	1.27	1.13	0.0%	0.0%	21	1.18	0.04	1.24	1.11	0.0%	0.0%
	$1.0 < \bar{\lambda}_w \leq 1.5$	106	1.19	0.08	1.36	0.97	2.8%	0.0%	102	1.17	0.08	1.34	0.95	4.9%	0.0%
	$1.5 < \bar{\lambda}_w \leq 2.0$	136	1.22	0.08	1.45	1.06	0.0%	0.0%	144	1.20	0.08	1.42	1.07	0.0%	0.0%
	$2.0 < \bar{\lambda}_w \leq 3.0$	76	1.27	0.14	1.63	1.09	0.0%	0.0%	107	1.23	0.11	1.50	1.02	0.0%	0.0%
	$\bar{\lambda}_w > 3.0$	7	1.21	0.16	1.51	1.04	0.0%	0.0%	12	1.23	0.16	1.45	1.04	0.0%	0.0%
Aspect ratio	$a/h_w \leq 1.0$	211	1.26	0.09	1.63	1.08	0.0%	0.0%	230	1.24	0.09	1.50	1.07	0.0%	0.0%
	$1.0 < a/h_w \leq 2.0$	90	1.18	0.07	1.36	1.00	0.0%	0.0%	107	1.18	0.07	1.36	0.99	1.9%	0.0%
	$2.0 < a/h_w \leq 3.0$	45	1.11	0.06	1.23	0.97	6.7%	0.0%	49	1.08	0.05	1.14	0.95	6.1%	0.0%
Web slenderness	$h_w/t_w \leq 100$	10	1.01	0.03	1.05	0.97	30.0%	0.0%	11	1.00	0.02	1.03	0.95	45.5%	0.0%
	$100 < h_w/t_w \leq 150$	135	1.21	0.08	1.45	1.06	0.0%	0.0%	147	1.18	0.07	1.41	1.05	0.0%	0.0%
	$150 < h_w/t_w \leq 225$	160	1.24	0.09	1.55	1.08	0.0%	0.0%	183	1.22	0.09	1.49	1.02	0.0%	0.0%
	$225 < h_w/t_w \leq 300$	41	1.27	0.13	1.63	1.04	0.0%	0.0%	45	1.23	0.13	1.50	1.04	0.0%	0.0%
	$300 < h_w/t_w \leq 400$	0	-	-	-	-	-	-	0	-	-	-	-	-	-
Ratio between flanges and web thicknesses	$1.5 \leq t_f/t_w \leq 2.0$	214	1.24	0.11	1.63	0.97	1.4%	0.0%	234	1.23	0.10	1.50	0.95	1.7%	0.0%
	$2.0 < t_f/t_w \leq 3.0$	129	1.19	0.08	1.45	1.01	0.0%	0.0%	142	1.17	0.07	1.41	0.99	0.7%	0.0%
	$3.0 < t_f/t_w \leq 4.0$	3	1.14	0.15	1.32	1.04	0.0%	0.0%	10	1.11	0.12	1.31	1.02	0.0%	0.0%
	$4.0 < t_f/t_w \leq 5.0$	0	-	-	-	-	-	-	0	-	-	-	-	-	-
Steel grade [MPa]	235	152	1.15	0.06	1.32	0.97	2.0%	0.0%	160	1.13	0.06	1.30	0.95	3.1%	0.0%
	275	71	1.22	0.06	1.36	1.11	0.0%	0.0%	76	1.19	0.05	1.31	1.08	0.0%	0.0%
	355	67	1.27	0.08	1.46	1.14	0.0%	0.0%	78	1.25	0.07	1.40	1.11	0.0%	0.0%
	460	56	1.35	0.10	1.63	1.22	0.0%	0.0%	72	1.32	0.09	1.50	1.12	0.0%	0.0%
T [°C]	350	106	1.22	0.09	1.60	0.99	0.9%	0.0%	120	1.19	0.09	1.47	0.97	0.8%	0.0%
	500	120	1.21	0.10	1.59	0.97	0.8%	0.0%	131	1.19	0.09	1.46	1.00	0.8%	0.0%
	600	120	1.24	0.11	1.63	0.97	0.8%	0.0%	135	1.22	0.10	1.50	0.95	2.2%	0.0%

From the data presented above, it is noticeable that the probability of occurrence of a combined shear plus bending failure is quite small for the plate girders with the following characteristics: $\bar{\lambda}_w > 3$, $h_w/t_w > 300$ or $t_f/t_w > 3$. The girders with high web slenderness ($\bar{\lambda}_w > 3$, $h_w/t_w > 300$) are extremely susceptible to the occurrence of shear buckling, while the girders with high stiffness flanges ($t_f/t_w > 3$) have a considerable bending resistance being likely to collapse due to shear.

Concerning the web slenderness, the higher it is, the more conservative the EC3 predictions are at both normal and elevated temperatures. Furthermore, the dispersion of results increases with the increase of the web slenderness, as can be verified in the values of standard deviation listed in the tables presented above.

Regarding the aspect ratio, it is observed the opposite. The lowest the aspect ratio is, the more conservative the EC3 design procedure is and the highest the dispersion of results is, for both normal and elevated temperatures. With respect to the influence of the ratio between the flanges and web thicknesses, Table 8.1 and Table 8.2 demonstrate that the expression for the interaction between shear and bending suits better the girders with t_f/t_w between 2 and 3.

As regards the steel grade, it is perceptible at both normal and elevated temperatures that the increase of the steel yield strength is reflected by an increase on the conservative degree of the EC3 predictions. Moreover, an higher standard deviation is also observed for the girders with higher steel grade.

Finally, when evaluating the influence of the elevated temperature range it was concluded that, as it happened for the zone 1 plate girders, there is no correlation between the accuracy of the EC3 design expression and the temperature range.

8.4 Conclusions

Based on the work presented in Chapter 8, the following general conclusions are drawn:

- The EC3 expression for the V-M interaction provides reasonable results at normal temperature. Nevertheless, a small improvement can be observed when the proposals from previous chapters are taken into account;
- In fire situation the results given by this EC3 expression are not satisfactory, being recommended to always have the proposals into account.

Chapter 9

*Influence of different parameters on the
ultimate shear strength of steel plate
girders*

Chapter 9 Influence of different parameters on the ultimate shear strength of steel plate girders

9.1 Shear strength in function of cross-section properties

9.1.1 Normal temperature

9.1.2 Elevated temperatures

9.2 Reduction of strength caused by the elevated temperatures

9.3 End posts

9.3.1 Increase of strength given by the rigid end posts

9.3.2 Influence of the configuration of the rigid end post

9.4 Conclusions

Chapter 9 Influence of different parameters on the ultimate shear strength of steel plate girders

9.1 Shear strength in function of cross-section properties

In today's world, civil engineers face the big challenge of providing safe, cost-effective and environmentally healthy structures. With this thesis it is intended to help engineers on the development of rules which will help designing safe and cost-effective steel plate girders subjected to shear buckling. The safety of the expressions adopted in current European Standards for the design of steel plate girders subjected to shear buckling was evaluated throughout Chapters 6 to 8.

In this section, the strength enhancement caused by the increase of cross-section properties of steel plate girders was evaluated, such as: web thickness, web depth, flange thickness and steel yield strength, using the numerical results presented before. The main goal of this analysis is to help designers providing cost-effective steel plate girders. Lately, the influence of the end supports (rigid or non-rigid end posts) on the ultimate shear strength of steel plate girders affected by shear buckling is also evaluated. These evaluations are based on the results given by the numerical model.

9.1.1. Normal temperature

The increase of strength provided by the increase of the web thickness was evaluated using the plate girders belonging to group II whose dimensions and geometric configuration are presented in Table 5.2 and Figure 5.1, respectively. The strength enhancement provided by the increase of the web depth was assessed considering the same group of girders. The increase of strength given by the increase of the flange thickness was evaluated using the group I of plate girders, whose geometric properties are listed in Table 5.1. Finally, it was calculated the increase of strength provided by the increase of the steel yield strength taking into account the plate girders with distance between transverse stiffeners equal to 900 mm belonging to group III, whose dimensions and geometric configuration are presented in Figure 5.3 and Table 5.3, respectively.

The strength enhancement given by the increase of 1 mm on the web thickness is presented in Figure 9.1 for plate girders with non-rigid end posts and different aspect

ratios. Figure 9.2 illustrates the results for the plate girders with rigid end posts. As one can see, the highest the aspect ratio is, the highest the strength enhancement is, for both plate girders with non-rigid and rigid end posts. For example, the increase of the web thickness from 4 to 5 mm in a plate girder with non-rigid end posts, $h_w=1200$ mm and $a/h_w=0.5$ provides a strength enhancement of 34%. On the other hand, the same girder with $a/h_w=3.0$ provides a strength enhancement of 44%.

It is important to note that some percentages are lower than expected because the failure mode of the girders changes. In some cases, increasing 1 mm on the web thickness causes the change of the girder failure mode. It happens for the girders with $a/h_w=1.5$ and $t_w=10$ mm, $a/h_w=2.0$ and $t_w=9$ and 10 mm, and $a/h_w=3.0$ and $t_w=7, 8, 9$ and 10 mm.

Furthermore, the percentage of the increase on the ultimate resistance is generally higher than the increased percentage of steel area. The girders where the failure mode changes with the increase of the web thickness are the exception. For instance, increasing the web thickness from 4 to 5 mm means to increase the area of steel in 25%. But this increase of steel area equal to 25% caused an increase on the ultimate bearing capacity from 31% ($a/h_w=0.5$) up to 44% ($a/h_w=3.0$). Other example is when the web thickness is increased from 7 to 8 mm, which means increasing the steel area in approximately 14%. In this case, the increase on the ultimate resistance ranged between 16% and 22%, always higher than 14%.

It is also possible to observe that, for the analysed plate girders, the strength enhancement caused by the increase of the web thickness does not vary much with the dimension of the web depth, since the increase of steel area is the same irrespective of the web depth. In some cases, it slightly increases with the increase of the web depth. For example, the increase of the web thickness from 7 to 8 mm, in a plate girder with non-rigid end posts and $a/h_w=1.0$, provides a strength enhancement of 20% for the girder with $h_w=800$ mm and 21% for the girder with $h_w=1600$ mm.

Finally, comparing Figure 9.1 with Figure 9.2, it is noticeable that the increase on the web thickness is more effective on the plate girders with non-rigid end posts, i.e. for the same increase on the web thickness, the percentage of the strength enhancement is larger on the girders with non-rigid end posts, when compared with the girders with rigid end posts. Those differences vary from 1% for the girders with high aspect ratios ($a/h_w=3.0$) to 9% for the girders with low aspect ratios ($a/h_w=0.5$).

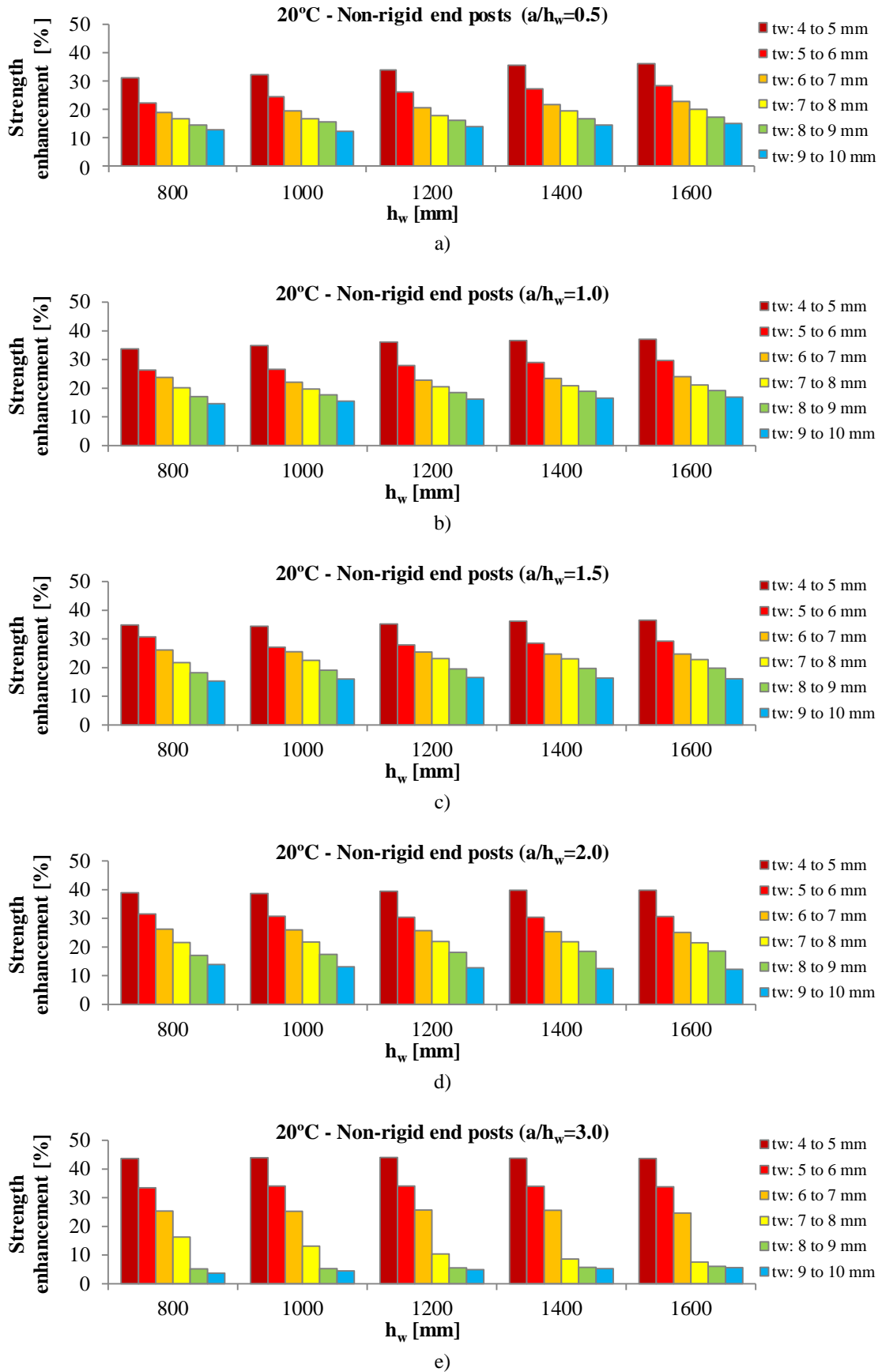


Figure 9.1 – Increase of strength at 20°C given by the increase of the web thickness for the girders with non-rigid end posts

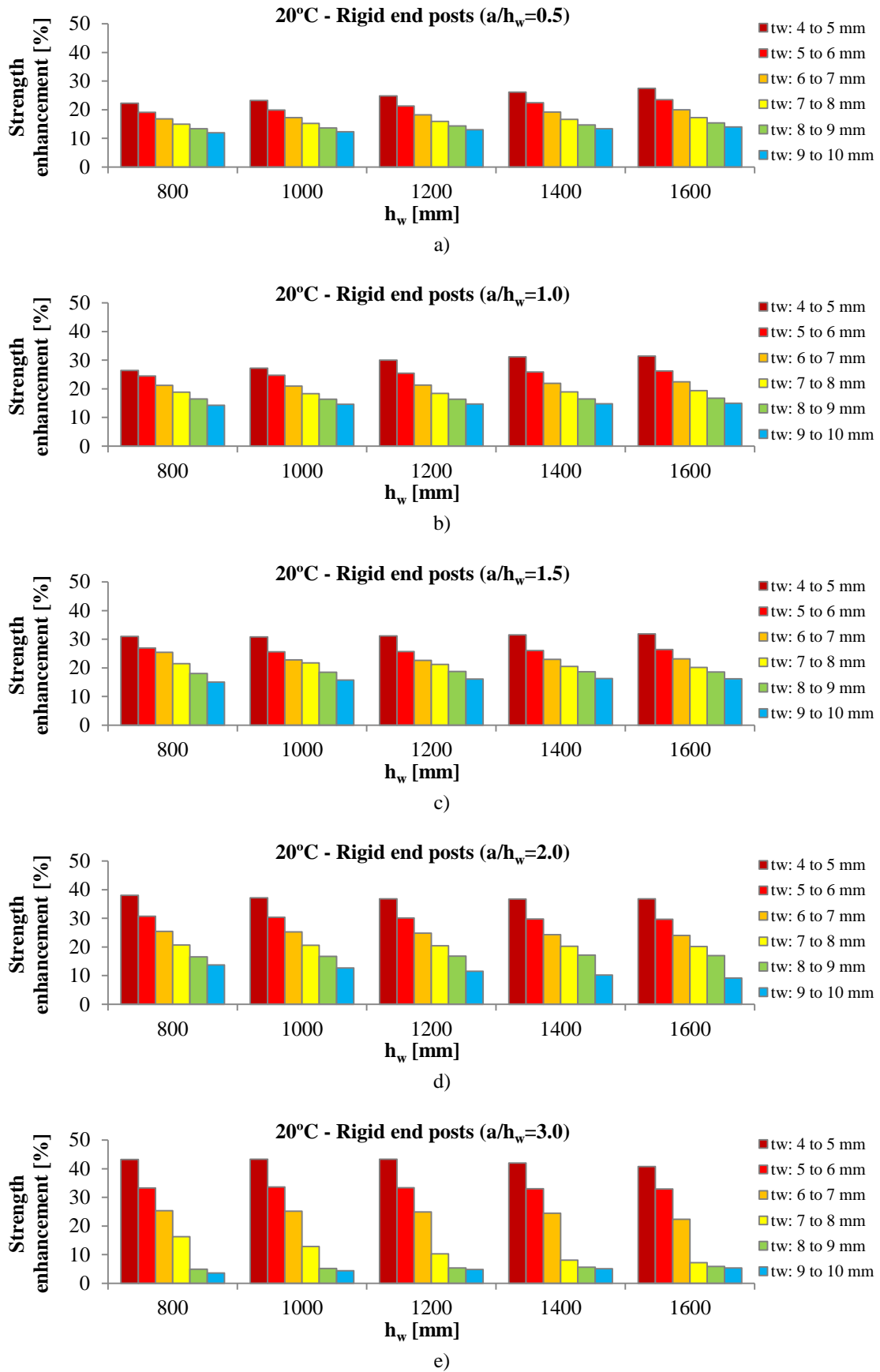


Figure 9.2 – Increase of strength at 20°C given by the increase of the web thickness for the girders with rigid end posts

Figure 9.3 shows the strength enhancement caused by the increase of the web depth. The plate girders with $t_w=5$ mm are used as an example since the observed behaviour is the same irrespective of the web thickness. Unlike what happened with the increase of the web thickness, the highest the aspect ratio is, the lowest the strength enhancement is. Again in contrast to previously noted when analysing the strength enhancement caused by the increase of the web thickness, the increase of the web depth is more effective on the girders with rigid end posts, when compared with girders with non-rigid end posts. In the girders with non-rigid end posts the strength enhancement ranges from 3% up to 11%. On the other hand, the increase of strength varies between 4% and 14% in the girders with rigid end posts.

Moreover, the percentage of increased steel is always higher than the percentage of strength enhancement. For instance, the increase of steel area caused by the increase of the web depth from 800 to 1000 mm is 25% but the maximum strength enhancement was 14%. When the web depth is increased from 1400 to 1600 mm (steel area increases 14%), the maximum strength enhancement is only 7%. It makes clear that increasing the web depth is not the best solution when it is needed to increase the ultimate shear strength of steel plate girders. Assuming the cost as directly proportional to the quantity of steel, increasing the web depth should be only considered when there is a need to increase the resistance bending moment.

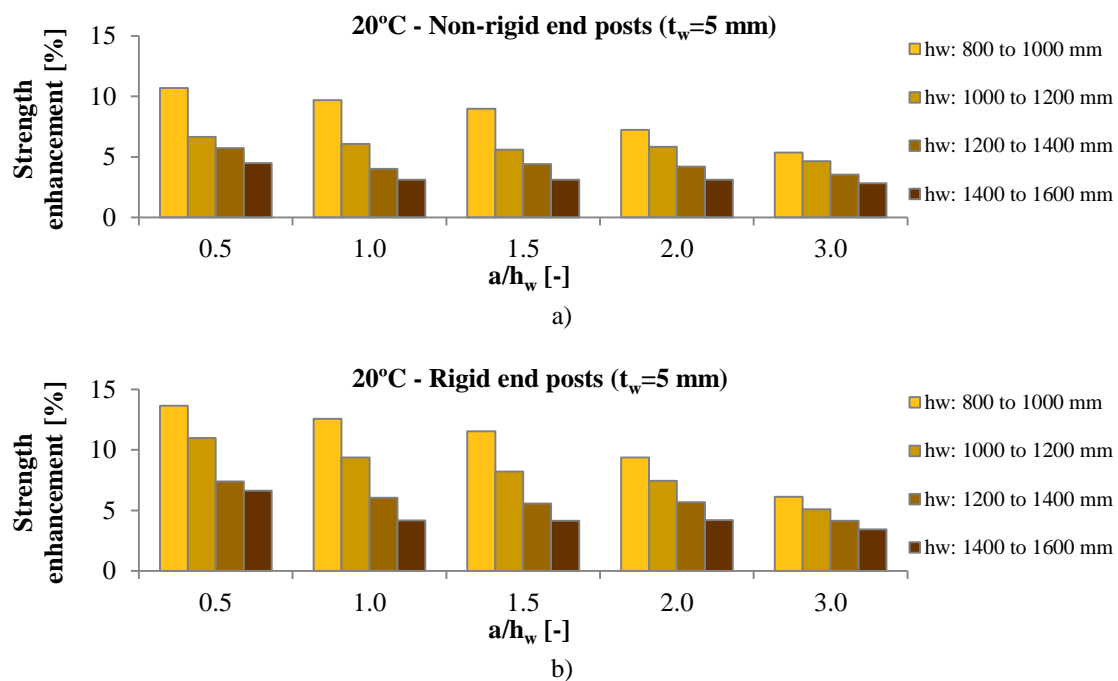


Figure 9.3 – Increase of strength at 20°C given by the increase of the web depth for the girders with $t_w=5$ mm

The influence of increasing the flanges thickness on the ultimate resistance of steel plate girders subjected to shear buckling was also evaluated. With that purpose the girders belonging to group I were analysed, as mentioned before. As an example, Figure 9.4 shows the increase of strength caused by increments of 2 mm on the flanges thickness for the plate girders with $h_w=1000$ mm, since the results are identical irrespective of the web depth. As one can see, the increase of the flanges thickness does not cause a significant strength enhancement, ranging from 0.7 up to 3.1 %. It is visible a tendency showing that the highest the aspect ratio is, the lower the strength enhancement is.

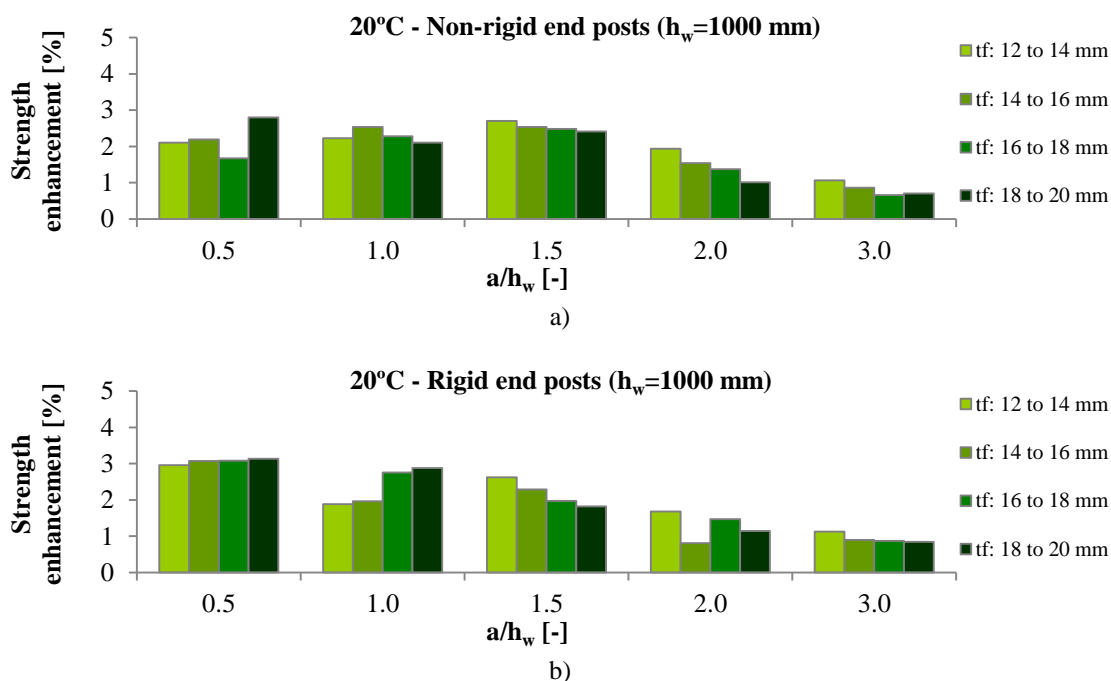


Figure 9.4 – Increase of strength at 20°C given by the increase of the flanges thickness for the girders with $h_w=1000$ mm

The increase of strength caused by the increase of the steel yield strength was also evaluated using the 2-panel plate girders from group III ($a=900$ mm) in order to analyse only girders with a shear dominant failure. Four different steel grades were considered, as presented in Table 5.5. The results of this analysis are presented in Figure 9.5 and Figure 9.6 for girders with non-rigid and rigid end posts, respectively.

It is possible to observe that the influence of the web slenderness (h_w/t_w) on the strength enhancement is not significant. Furthermore, it is perceptible that the strength enhancement slightly decreases for $a/h_w=3.0$. Finally, comparing Figure 9.5 with Figure 9.6 it is visible that the strength enhancement is slightly higher for the girders with rigid end posts.

Increasing the steel grade from S235 to S275 corresponds to an increase of 17% on the steel yield strength, while increasing the steel grade from S275 to S355 and S355 to S460 corresponds to an increase of the steel yield strength around 29%. As expected, due the buckling phenomena, these values are not reflected on the increase of the ultimate resistance, which is somewhat lower. According to the obtained results, generally the increase on the ultimate resistance is about 71% of the percentage increase in steel yield strength for girders with non-rigid end posts and 75% for girders with rigid end posts. For instance, for the girders with non-rigid end posts, the average increase on the ultimate resistance is 12% when the steel yield strength increases from S235 to S275 and 21% for the other consecutive steel grades. Regarding the girders with rigid end posts, the increase on the ultimate resistance is slightly higher: 13% and 23%.

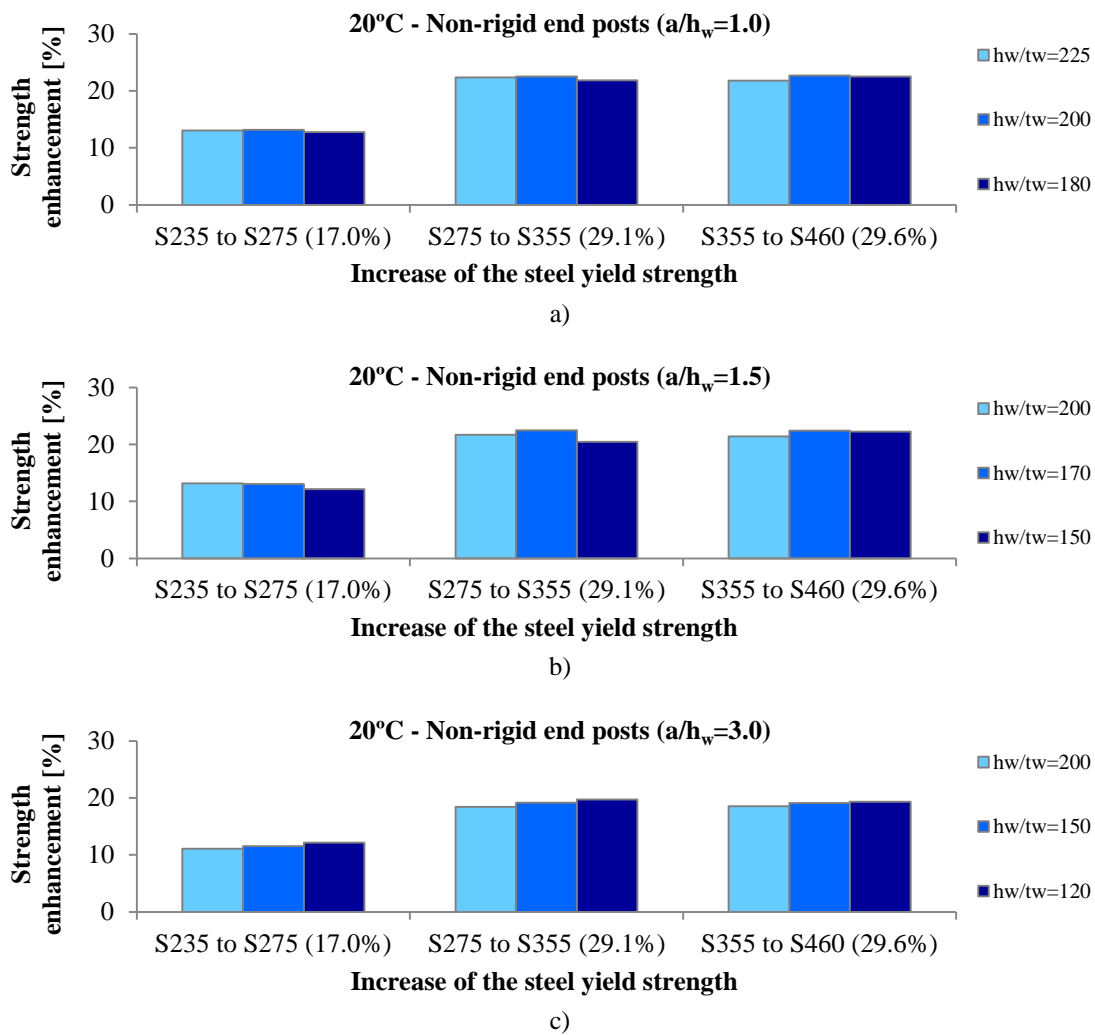


Figure 9.5 – Increase of strength at 20°C given by the increase of the steel yield strength for the girders with non-rigid end posts

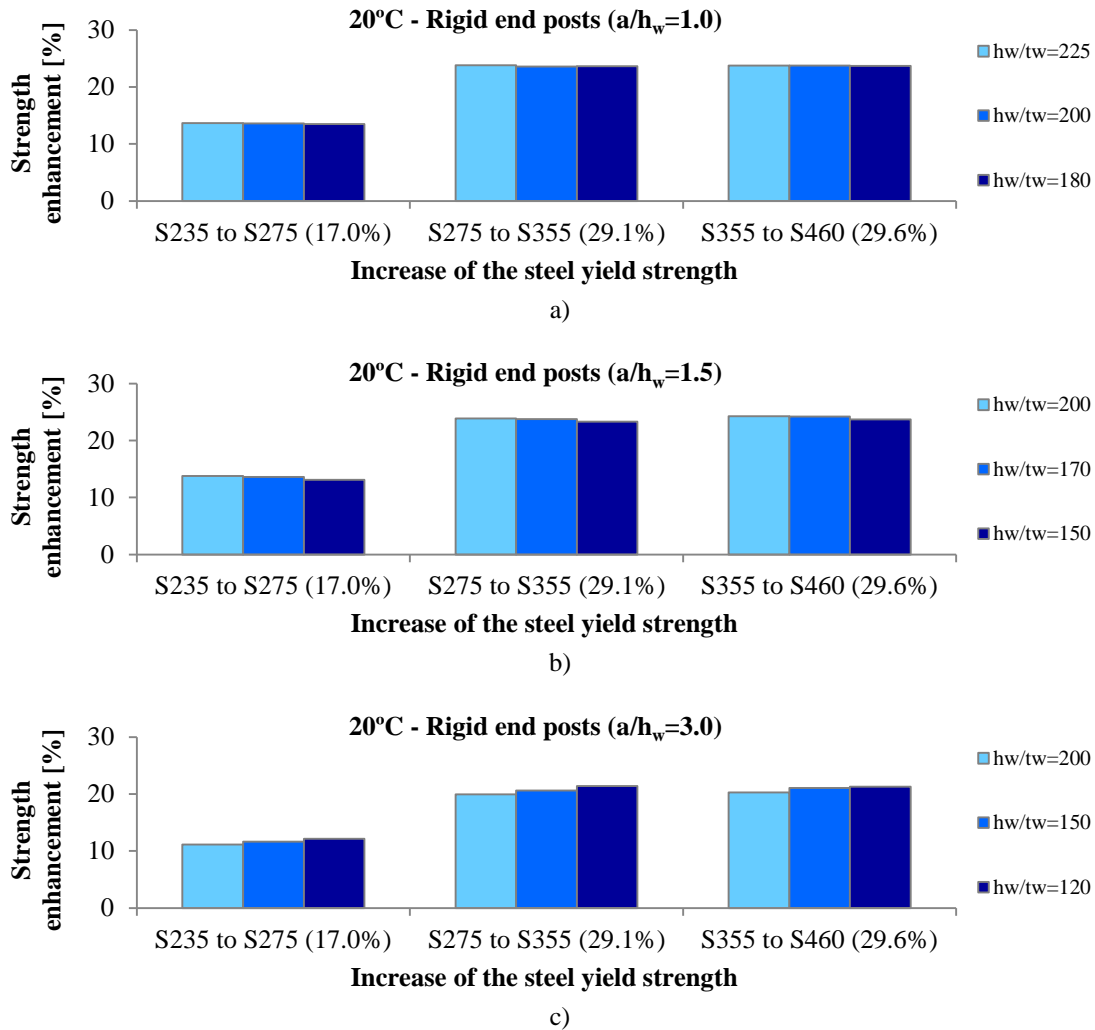


Figure 9.6 – Increase of strength at 20°C given by the increase of the steel yield strength for the girders with rigid end posts

After the analysis of the influence of different cross-section properties (web thickness, web depth, flanges thickness and steel yield strength) on the ultimate shear strength of steel plate girders subjected to shear buckling at normal temperature, it seems clear that the most cost-effective solution to improve the ultimate shear strength of a steel plate girder with a shear dominant failure is to increase the web thickness.

9.1.2. Elevated temperatures

An analogous analysis to the one conducted at 20°C was performed for 350°C, 500°C and 600°C. The results are quite similar, so only the results of the plate girders tested at 500°C are presented here. Moreover, the fundamental conclusions obtained for elevated temperatures are equal to those obtained for normal temperature. For that reason, they are more briefly described.

The impact of the web thickness increase is illustrated in Figure 9.7 for the girders with $h_w=1200$ mm, since as it was at normal temperature the results are not significantly influenced by the size of the web depth. Figure 9.7 demonstrates that the highest the aspect ratio is, the highest the strength enhancement is, for both plate girders with non-rigid and rigid end posts. Comparing with 20°C, the strength enhancement is usually 2% lower at elevated temperatures.

Furthermore, it is visible that the web thickness increase is more effective on the plate girders with non-rigid end posts. It is also important to note that the percentage of strength enhancement is higher than the increased percentage of steel area, with exception of the girders not exhibiting a shear dominant failure. It makes clear that increasing the web thickness is the best solution in order to increase the resistance of steel plate girders affected by shear buckling.

The strength enhancement caused by the increase of the web depth is presented in Figure 9.8. Analysing the girders with non-rigid end posts, it is observed that the lowest the aspect ratio is, the highest the strength enhancement is, in contrast to what occurred at normal temperature. For the girders with low aspect ratio, the strength enhancement was in some cases 5% lower than recorded at 20°C.

Regarding the girders with rigid end posts, it was observed the same pattern obtained at normal temperature: the lowest the aspect ratio is, the highest the strength enhancement is. The strength enhancement was generally 1% lower. Moreover, as it happened for normal temperature, the percentage of strength enhancement is always lower than the percentage of increased steel area.

Figure 9.9 shows the strength enhancement provided by the increase of the flanges thickness. It was observed an increase on the ultimate resistance up to 2%, when compared to the results obtained at normal temperature. At elevated temperatures, the strength enhancement caused by the increase of the flanges thickness ranges between 1 and 5%, which is still considered a non-significant strength enhancement. Furthermore, it is perceptible that the highest the aspect ratio is, the lower the strength enhancement is.

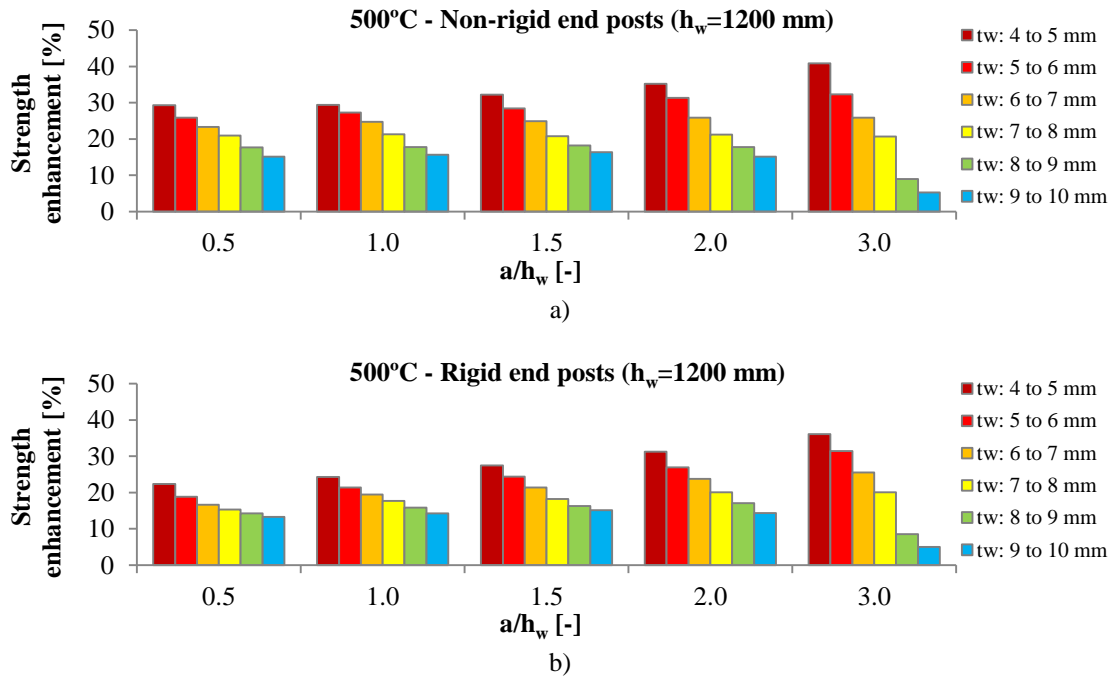


Figure 9.7 – Increase of strength at 500°C given by the increase of the web thickness for the girders with $h_w=1200$ mm

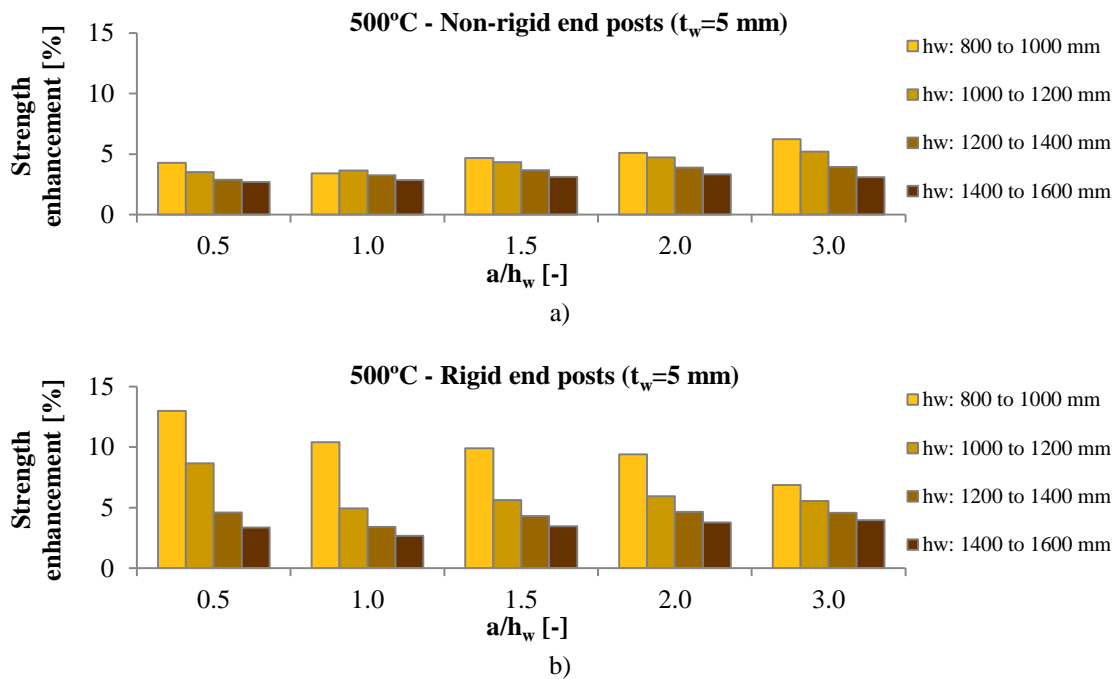


Figure 9.8 – Increase of strength at 500°C given by the increase of the web depth for the girders with $t_w=5$ mm

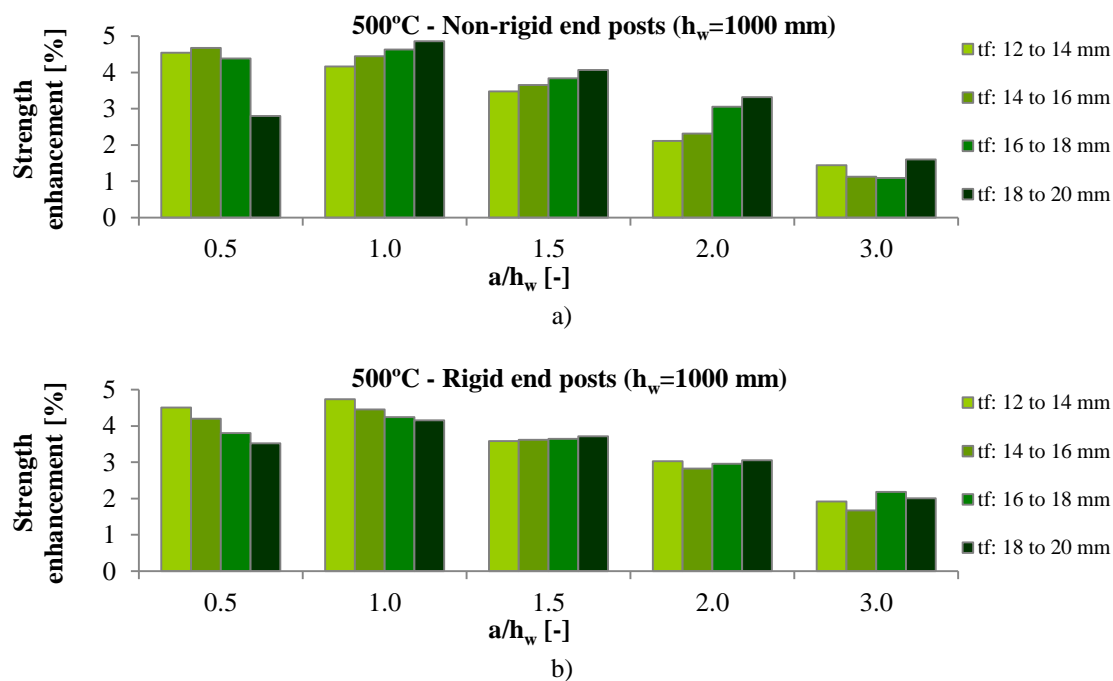


Figure 9.9 – Increase of strength at 500°C given by the increase of the flanges thickness for the girders with $h_w=1000$ mm

The strength enhancement obtained with the increase of the steel yield strength was also evaluated at elevated temperatures. The results for the girders with non-rigid end posts are presented in Figure 9.10, while Figure 9.11 shows the results for the girders with rigid end posts.

As it was observed at normal temperature, the web slenderness (h_w/t_w) has no significant influence on the strength enhancement. Additionally, it is noticeable that the strength enhancement decreases about 1% for the girders with aspect ratio equal to 3.0. Finally, it is perceptible when comparing Figure 9.10 with Figure 9.11 that the strength enhancement is slightly higher for the girders with rigid end posts.

Furthermore, it was observed that increasing the steel yield strength causes greater resistance benefits at elevated temperatures. At normal temperature, the increase on the ultimate resistance in the girders with non-rigid end posts was about 71% of the percentage increase in steel yield strength. But, in fire situation it is around 85%. This value increases to 88% for the girders with rigid end posts.

After the analysis of the results at elevated temperatures, it can be said that the most cost-effective solution to improve the ultimate resistance of a steel plate girder affected by shear buckling is to increase the web thickness, as it was at normal temperature.

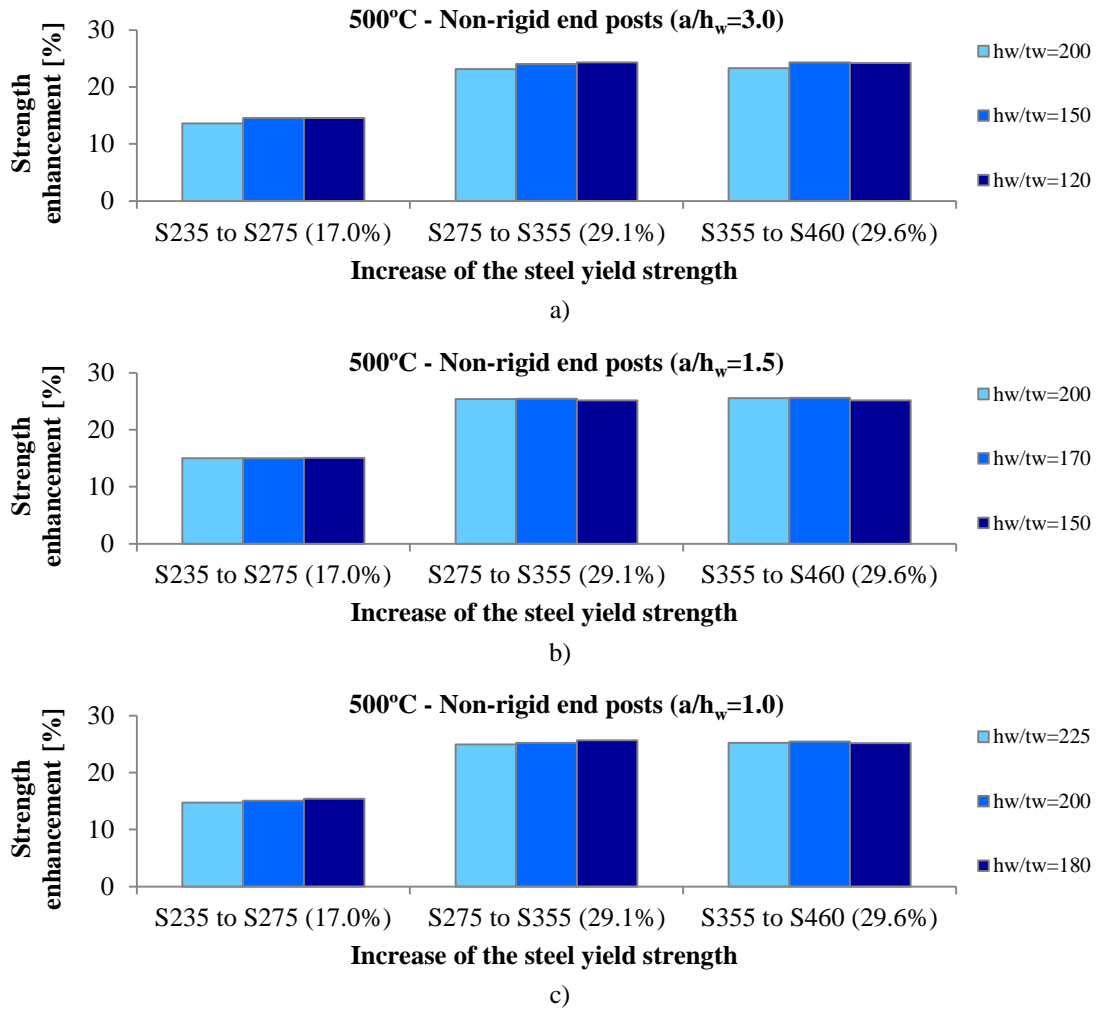
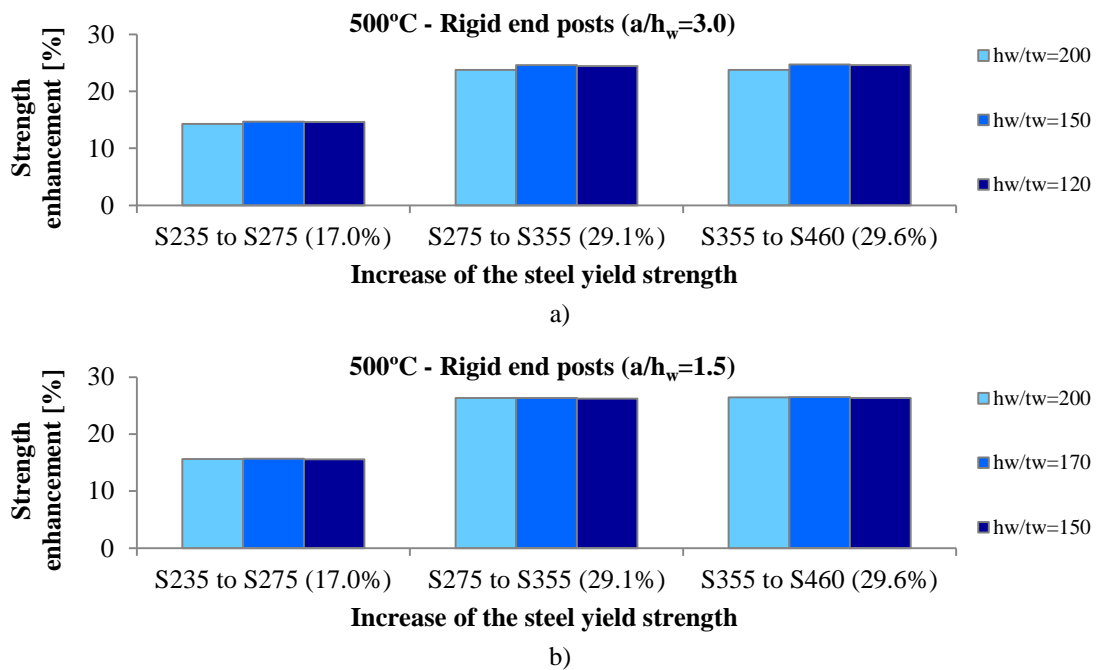


Figure 9.10 – Increase of strength at 500°C given by the increase of the steel yield strength for the girders with non-rigid end posts



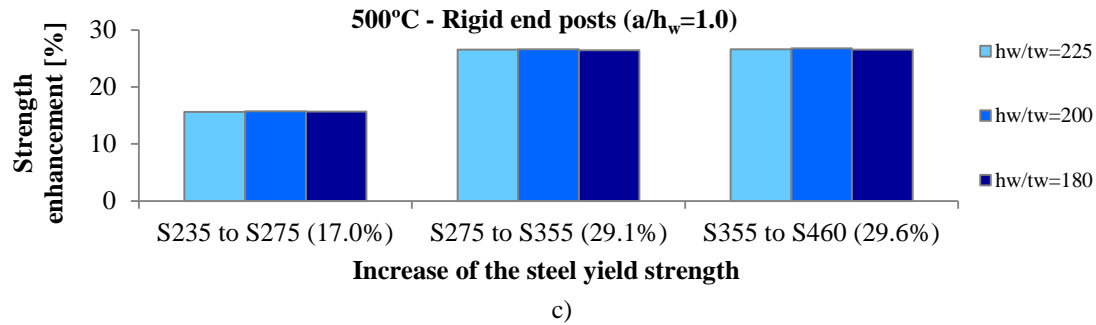


Figure 9.11 – Increase of strength at 500°C given by the increase of the steel yield strength for the girders with rigid end posts

9.2 Reduction of strength caused by the elevated temperatures

The reduction of strength caused by the elevated temperatures is analysed in this section. With that purpose, the numerical results of the plate girders belonging to group II were considered. In order to analyse only girders with a failure caused by shear buckling, only the girders with web thickness equal to 4 mm were taken into account.

It was observed that the reduction of resistance, caused by the elevated temperatures, increases with the increase of the web depth dimension, for the girders with $a/h_w=0.5$, ranging between 11% and 20%. For the remaining girders, with higher aspect ratios, the variation of the percentage of strength reduction with the increase of the web depth is quite small. In order to analyse the influence of the aspect ratio on the reduction of resistance caused by the elevated temperatures, it was decided to present here (see Figure 9.12) only the girders with $h_w=1000$ mm, since the conclusions are the same irrespective of the web depth. Figure 9.12 demonstrates that the highest the aspect ratio is, the highest the strength reduction caused by the elevated temperatures is.

Furthermore, the strength reduction on the girders with non-rigid end posts is higher when compared with the girders with rigid end posts. The lower the aspect ratio is, the higher this difference is. It means that the girders with rigid end post are more capable to anchor the different stresses distribution imposed by the elevated temperatures that occur during a fire. For the girders with non-rigid end posts, the average values of the strength reduction according to the applied uniform elevated temperatures of 350°C, 500°C and 600°C are 21%, 39% and 64%, respectively. Regarding the girders with rigid end posts, these values decrease to 14%, 33% and 60%.

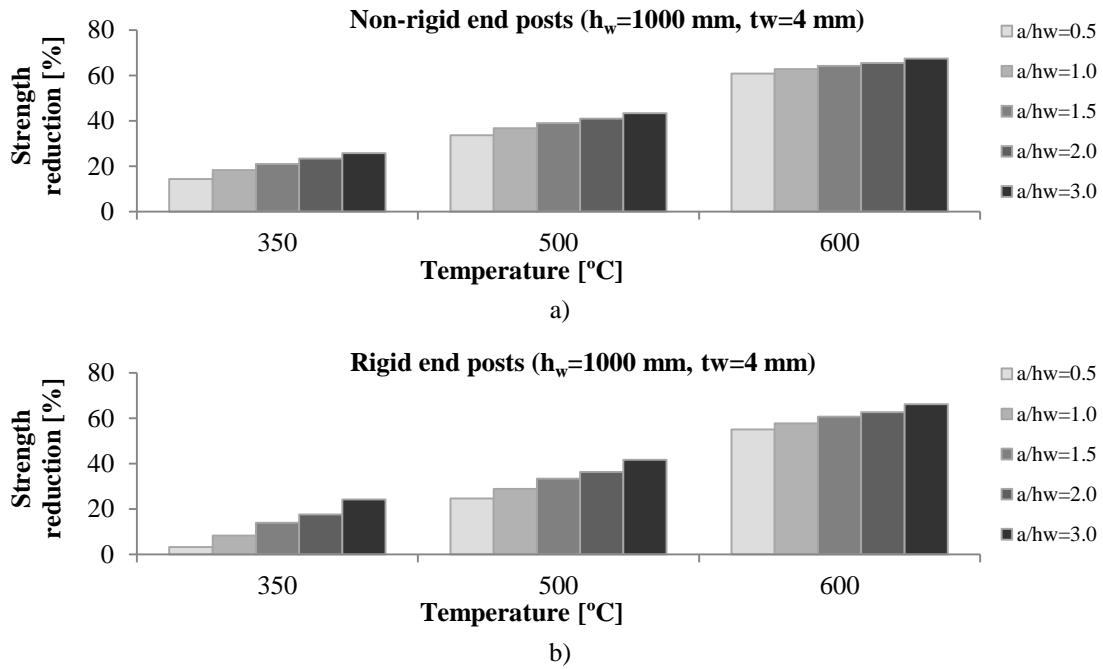


Figure 9.12 – Strength reduction caused by the temperature increase

9.3 End posts

Normally, steel plate girders are provided with end posts. Girders with rigid end posts involve higher costs resulting from the additional plates, but also from the welding. Hence, when designing, it is very important to know when the rigid end posts are more effective and the extra costs are reflected in a considerable additional resistance. With that purpose, an analysis about their influence was performed. The increase of strength given by the rigid end posts is evaluated, as well as the influence of its configuration, i.e. the distance between the transverse stiffeners which form the rigid end post and the thickness of the transverse stiffener which is not supporting the reaction force.

9.3.1 Increase of strength given by the rigid end posts

Firstly, the increase of strength given by the condition of rigid end post is evaluated. The numerical results from the group II of plate girders, where five different aspect ratios (a/h_w) were considered, are used to perform this analysis. Figure 9.13 illustrates the differences on the resistance from the web to shear buckling given by the application of a rigid end post instead of a non-rigid end post. On the left are placed the results at normal temperature and on the right it is possible to find the results obtained for the girders subjected to 500°C. Only one elevated temperature is presented here, since the results are quite similar for the three analysed temperatures.

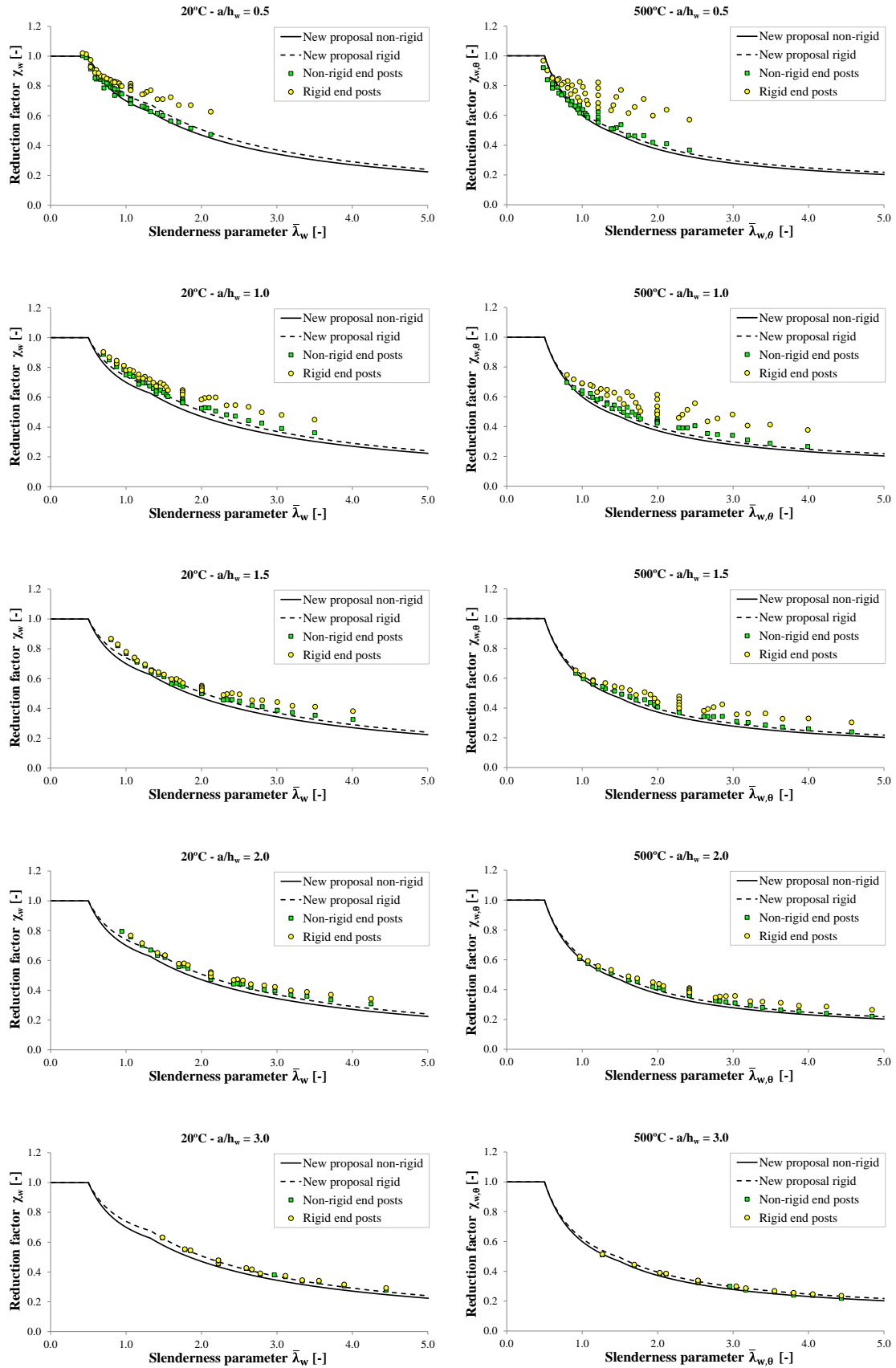


Figure 9.13 – Difference between rigid and non-rigid end posts on the web contribution to shear buckling of the group II plate girders in function of the aspect ratio at 20°C and 500°C

Figure 9.13 demonstrates that the condition of rigid end post is as effective as the lower aspect ratio is, at both 20°C and 500°C. It can be clearly observed in the charts from Figure 9.13, where the increase in the web resistance is significant for low aspect ratios (0.5 and 1.0), decreasing to girders with intermediate aspect ratios (1.5 and 2.0), to finally be almost null for girders with $a/h_w = 3.0$. It is directly related to the fact that the lower the aspect ratio is, the more the condition of rigid end post influences the whole behaviour of the web panel, since the percentage of the perimeter constrained gets higher. Furthermore, it is perceptible that the highest the web slenderness parameter is, the highest the increase of strength given by the rigid end post is.

Figure 9.14 shows the average strength enhancement, between the plate girders with rigid and non-rigid end posts, in function of the plate girders aspect ratio (a/h_w). As one can see, it is clear that the lower the aspect ratio is, the more effective the rigid end post is. At normal temperature, the average strength enhancement of the group II of plate girders was 9.2% for the girders with $a/h_w=0.5$, decreasing for girders with intermediate aspect ratios, being almost negligible (0.6%) for girders with $a/h_w=3.0$.

Moreover, Figure 9.14 also reveals that the rigid end post is more effective at elevated temperatures than at normal temperature. At elevated temperatures, the strength enhancement is higher but the tendency observed at normal temperature remains the same, with the average values ranging from 1.7% ($a/h_w=3.0$) up to 20.3% ($a/h_w=0.5$).

The influence of other geometrical ratios was also analysed, as illustrated in Figure 9.15. The strength enhancement provided by the rigid end post is represented in Figure 9.15a in function of the web slenderness and in Figure 9.15b in terms of the ratio between the flanges and web thicknesses. It is visible that the higher these ratios are, the higher the increase of strength is, at both normal and elevated temperatures. On the other hand, it is also possible to notice that the maximum strength enhancement is 26.5% at normal temperature and 46.5% in fire situation, which is a significant difference.

Thus, it was concluded that the steel plate girders where the application of rigid end posts, instead of non-rigid end posts, is more profitable are those with the following characteristics: low a/h_w , high h_w/t_w and high t_f/t_w .

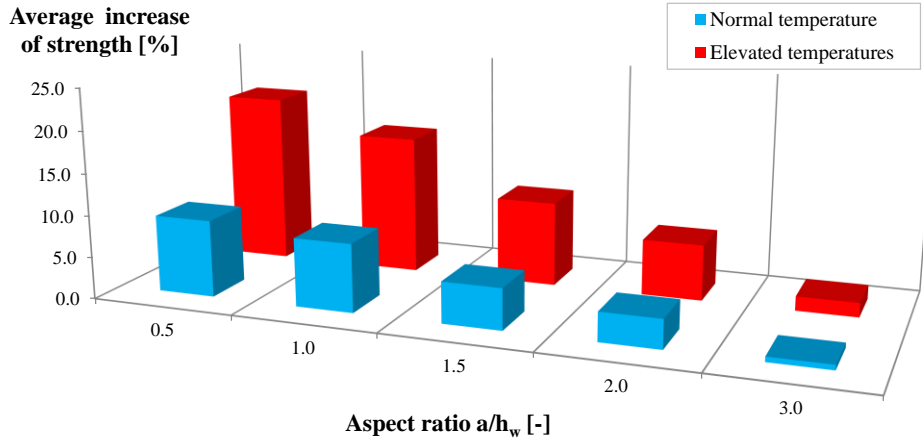
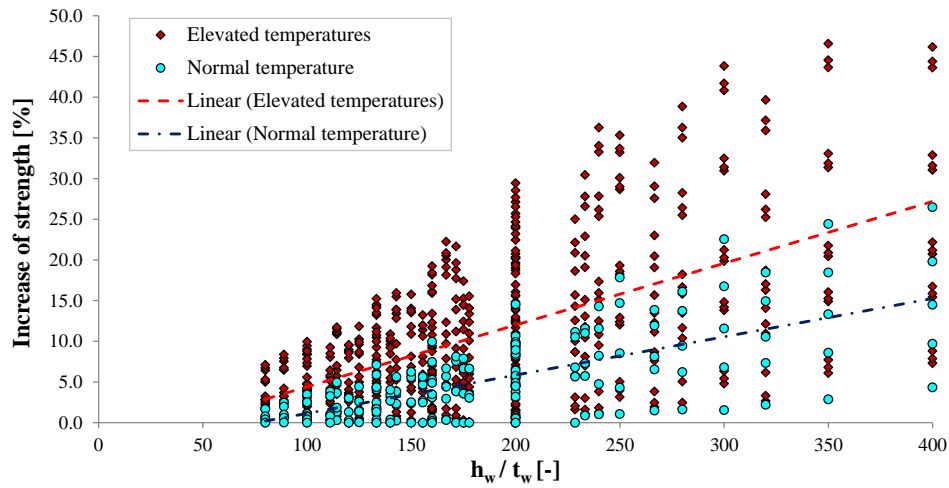
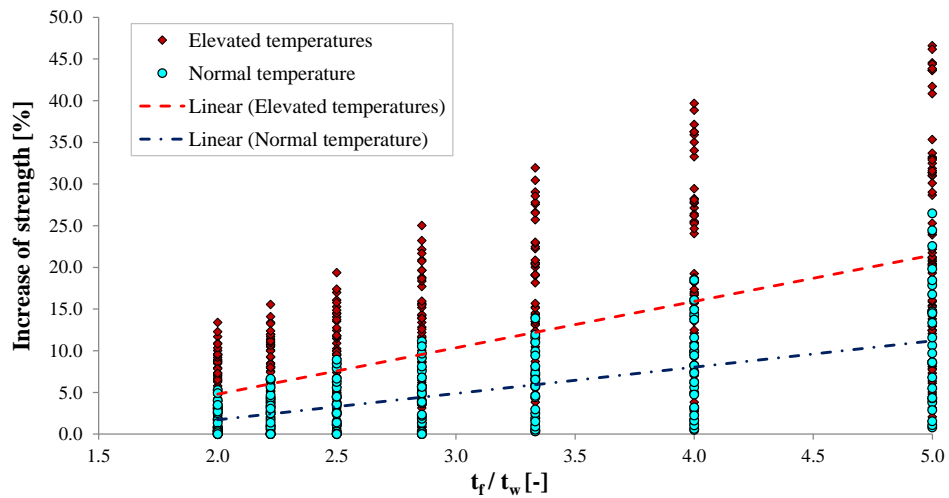


Figure 9.14 – Average increase of strength given by the rigid end posts



a)



b)

Figure 9.15 – Influence of different geometrical ratios on the increase of strength given by the rigid end posts

9.3.2 Influence of the configuration of the rigid end post

An end post is considered as rigid if it satisfies the requirements presented in section 3.4.1.1 of this document. The condition of rigid end post depends on the distance between the transverse stiffeners which forms the end post and on the area of the transverse stiffeners. Thus, a rigid end post may have different configurations. In this section it is intended to evaluate the influence of the rigid end post configuration on the ultimate shear strength of the plate girder.

With that purpose, the numerical model presented in Chapter 4 was used, considering a 2-panel plate girder with $h_w = 1000$ mm, $b_f = 300$ mm and $t_f = 20$ mm. Three different web thicknesses were considered (4, 5 and 6 mm). The intermediate transverse stiffener (placed at mid-span on the position of application of forces) has 20 mm thickness, as well as the internal transverse stiffeners of the rigid end posts which carry the reaction forces of the supports (stiffener “A_u” in Figure 3.14).

The influence on the ultimate shear strength of the rigid end post configuration was evaluated in two ways. Firstly, influence of the distance between the transverse stiffeners which form the rigid end post (distance “e” in Figure 3.14) was evaluated, considering three different values: 100 mm, 200 mm (the value considered in the numerical analyses presented before) and 300 mm, as shown in Figure 9.16. Afterwards, the thickness of the external transverse stiffeners of the rigid end posts (stiffener “A_e” in Figure 3.14 and the blue stiffener in Figure 9.16) was ranged from 5 up to 20 mm, by increments of 5 mm, in order to assess its influence on the ultimate shear capacity of steel plate girders subjected to shear buckling.

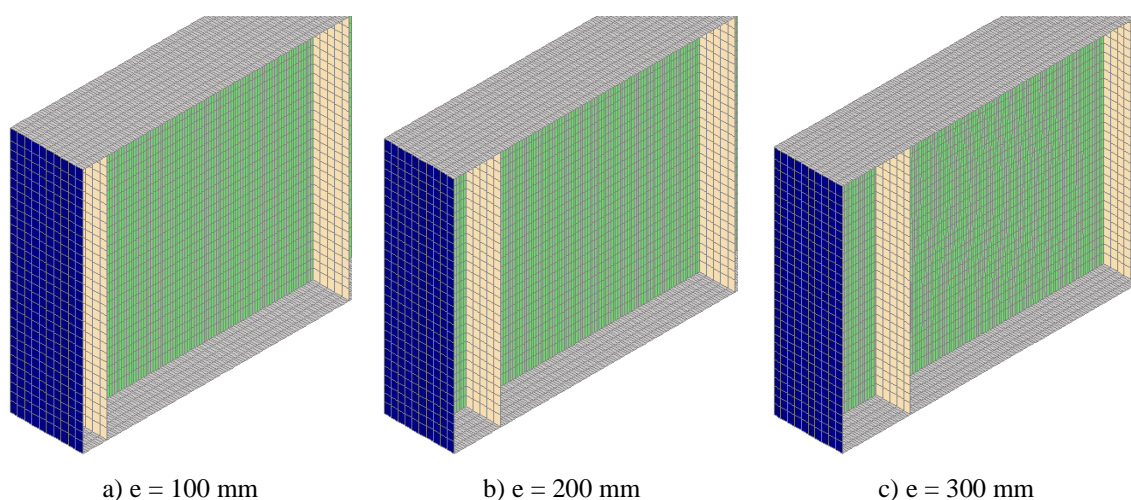


Figure 9.16 – Rigid end post configurations analysed in this section (example for $a/h_w = 1.0$)

The girders were tested at normal temperature and subjected to a uniform elevated temperature of 500°C, which results in a total of 234 additional numerical tests. The geometric imperfections and the residual stresses were taken into account. The results obtained for the girders analysed at normal temperature are listed in Table 9.1, while the results of the girders subjected to 500°C are presented in Table 9.2. The ultimate shear capacity numerically obtained is called “ V_{nr} ” and “ V_r ” for the girders with non-rigid and rigid end posts, respectively. The columns “Dif.” correspond to the increase of strength provided by the different configurations of the rigid end post when compared to the resistance of the girders with non-rigid end posts.

Regarding the influence at 20°C of the distance “ e ” between the transverse stiffeners which form the rigid end post, usually the highest it is, the lowest the increase of strength is, as illustrated in Figure 9.17a. However, at 500°C the opposite may be observed for the girders with $a/h_w=1.0$ and 2.0 (see Figure 9.17b). Figure 9.17 also shows that the condition of rigid end post is more effective in fire situation. Moreover, the increase of strength at elevated temperature comparatively to normal temperature is so much higher as the greater the distance “ e ” is. For example, the increase of strength of the girder with $a/h_w=1.0$, $h_w/t_w=200$ and $e=100$ mm is 9.4% at 20°C and 17.0% at 500°C (7.6% higher), and for the girder with $a/h_w=1.0$, $h_w/t_w=200$ and $e=200$ mm the correspondent values are 8.2% at 20°C and 24.5% at 500°C (16.3% higher). On the other hand, it is also perceptible that the higher the web slenderness (h_w/t_w) is, the more evident the increase in the ultimate shear strength given by the rigid end post is, at both normal and elevated temperatures. It is also observed that, as mentioned before, the lowest the aspect ratio is, the highest the strength enhancement is, due to the increase of the percentage of the perimeter constrained.

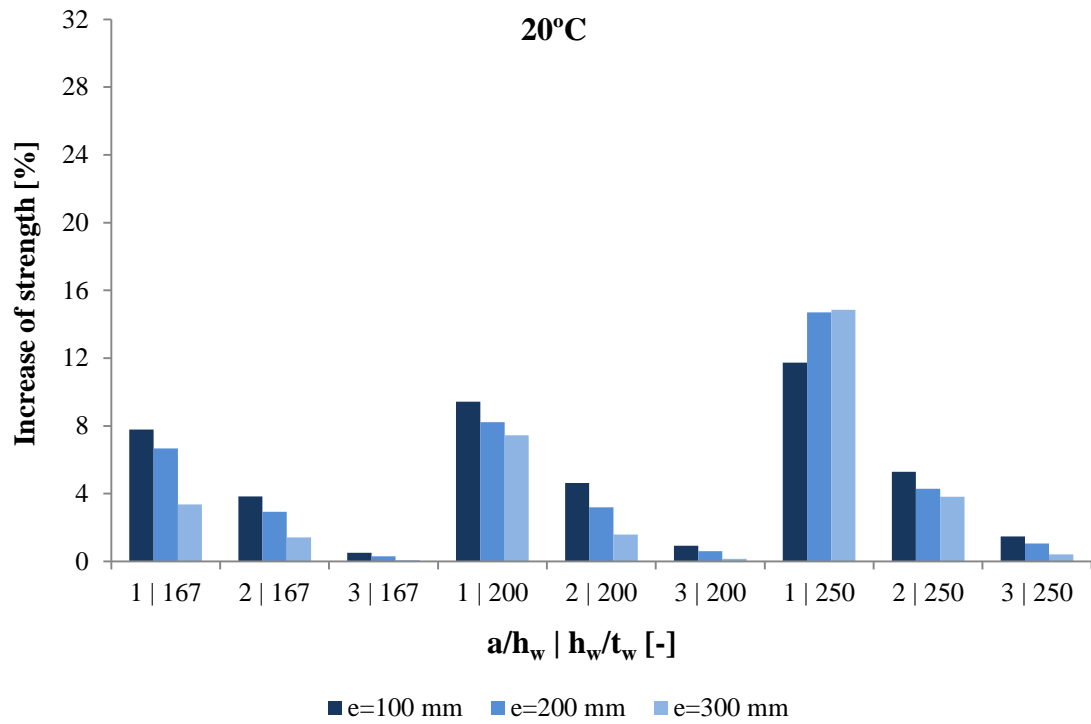
Concerning the thickness of the external transverse stiffener of the rigid end post, Figure 9.18 demonstrates its influence on the increase of strength given by the rigid end post is not quite significant. By another words, providing a girder with non-rigid end posts with two additional transverse stiffeners changing the end configuration to rigid end posts may cause a substantial impact on the ultimate shear strength (the maximum increase observed was almost 15% and 30% at 20°C and 500°C, respectively). However, increasing the thickness of these transverse stiffeners does not cause a considerable impact on the ultimate shear strength. The maximum observed was 4% at normal temperature and 8% at elevated temperature.

Table 9.1 – Influence of the rigid end post configuration on the ultimate shear strength of steel plate girders at normal temperature

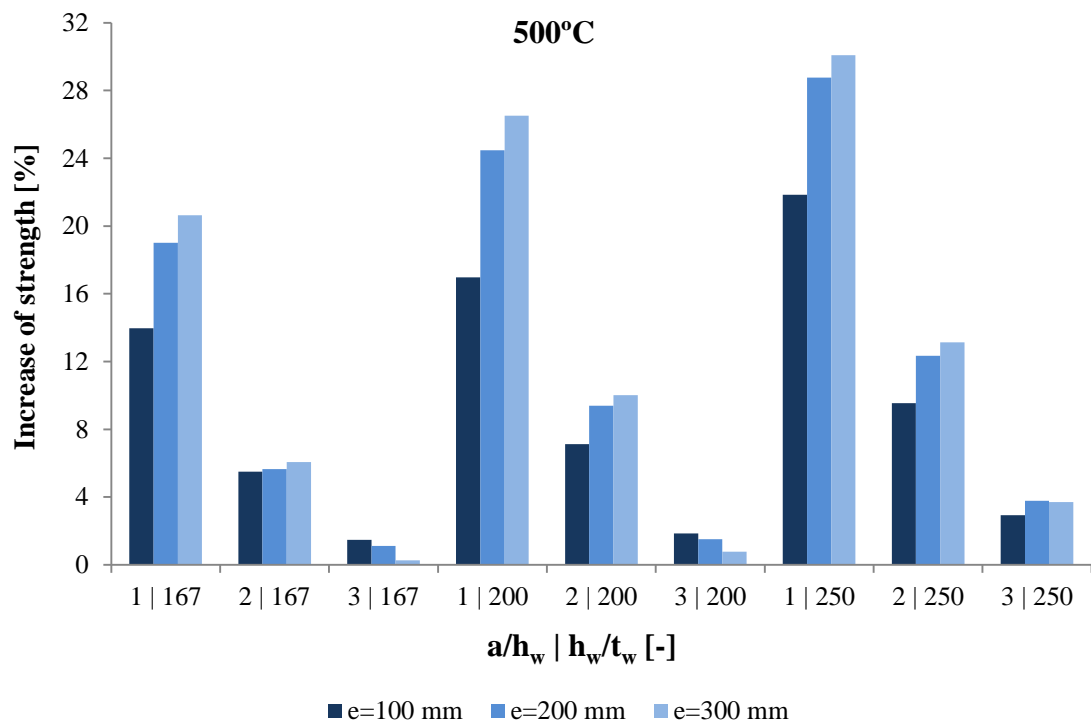
a/h _w [-]	e [mm]	t _s [mm]	t _w = 4 mm			t _w = 5 mm			t _w = 6 mm		
			V _{nr} [kN]	V _r [kN]	Dif. [%]	V _{nr} [kN]	V _r [kN]	Dif. [%]	V _{nr} [kN]	V _r [kN]	Dif. [%]
1.0	100	5	323.4	348.8	7.8	425.5	454.5	6.8	542.3	569.1	5.0
		10		352.0	8.9		459.6	8.0		577.3	6.4
		15		356.1	10.1		462.7	8.7		581.6	7.2
		20		361.4	11.7		465.7	9.4		584.5	7.8
	200	5	335.0	377.9	12.8	451.6	483.3	7.0	571.7	601.0	5.1
		10		380.1	13.5		486.3	7.7		606.0	6.0
		15		382.2	14.1		487.8	8.0		608.3	6.4
		20		384.2	14.7		488.7	8.2		609.7	6.7
	300	5	343.4	392.8	14.4	465.2	497.2	6.9	597.3	612.9	2.6
		10		393.7	14.7		498.7	7.2		615.4	3.0
		15		394.2	14.8		499.4	7.3		616.6	3.2
		20		394.5	14.9		499.8	7.4		617.4	3.4
2.0	100	5	253.1	262.6	3.7	351.0	361.5	3.0	462.0	472.0	2.2
		10		264.6	4.5		364.5	3.8		475.9	3.0
		15		265.7	4.9		366.2	4.3		478.2	3.5
		20		266.5	5.3		367.3	4.6		479.7	3.8
	200	5	261.4	270.7	3.5	362.5	371.1	2.4	473.8	483.5	2.1
		10		271.7	3.9		372.7	2.8		485.8	2.5
		15		272.3	4.2		373.5	3.0		487.0	2.8
		20		272.7	4.3		374.0	3.2		487.7	2.9
	300	5	264.8	274.0	3.4	370.5	374.8	1.2	483.6	488.3	1.0
		10		274.5	3.7		375.6	1.4		489.4	1.2
		15		274.8	3.8		376.1	1.5		490.1	1.3
		20		274.9	3.8		376.4	1.6		490.4	1.4
3.0	100	5	229.0	231.2	1.0	330.8	332.8	0.6	444.3	445.6	0.3
		10		231.8	1.2		333.3	0.8		446.0	0.4
		15		232.2	1.4		333.6	0.8		446.3	0.5
		20		232.4	1.5		333.8	0.9		446.5	0.5
	200	5	230.7	232.5	0.8	332.0	333.5	0.4	445.0	445.9	0.2
		10		232.8	0.9		333.7	0.5		446.1	0.3
		15		233.0	1.0		333.9	0.6		446.3	0.3
		20		233.1	1.1		334.0	0.6		446.3	0.3
	300	5	232.4	232.9	0.2	333.4	333.6	0.1	445.7	445.7	0.0
		10		233.1	0.3		333.7	0.1		445.8	0.0
		15		233.2	0.4		333.8	0.1		445.9	0.0
		20		233.3	0.4		333.9	0.2		446.0	0.1

Table 9.2 – Influence of the rigid end post configuration on the ultimate shear strength of steel plate girders at 500°C

a/h _w [-]	e [mm]	t _s [mm]	t _w = 4 mm			t _w = 5 mm			t _w = 6 mm		
			V _{nr} [kN]	V _r [kN]	Dif. [%]	V _{nr} [kN]	V _r [kN]	Dif. [%]	V _{nr} [kN]	V _r [kN]	Dif. [%]
1.0	100	5	209.7	238.2	13.6	268.2	294.9	10.0	332.2	359.5	8.2
		10		242.7	15.8		300.8	12.1		366.7	10.4
		15		248.9	18.7		306.9	14.4		372.3	12.1
		20		255.4	21.8		313.7	17.0		378.6	14.0
	200	5	212.2	264.4	24.6	271.6	327.1	20.4	342.7	395.6	15.4
		10		267.1	25.8		331.0	21.9		400.9	17.0
		15		270.4	27.4		334.7	23.2		404.4	18.0
		20		273.2	28.8		338.1	24.5		407.8	19.0
	300	5	215.6	278.1	29.0	276.5	346.2	25.2	350.4	418.6	19.5
		10		278.9	29.3		347.5	25.7		420.3	19.9
		15		279.8	29.7		348.6	26.1		421.5	20.3
		20		280.5	30.1		349.8	26.5		422.7	20.6
2.0	100	5	153.2	162.5	6.1	204.0	213.5	4.6	263.6	273.5	3.8
		10		163.9	7.0		215.0	5.3		275.1	4.4
		15		165.8	8.3		216.7	6.2		276.6	4.9
		20		167.8	9.5		218.6	7.1		278.1	5.5
	200	5	154.4	171.1	10.9	207.2	224.1	8.1	271.5	284.7	4.9
		10		171.9	11.3		225.0	8.6		285.5	5.2
		15		172.7	11.9		225.9	9.0		286.2	5.4
		20		173.4	12.3		226.7	9.4		286.8	5.7
	300	5	156.0	175.6	12.5	210.1	230.0	9.5	275.2	290.8	5.7
		10		175.9	12.8		230.4	9.7		291.3	5.9
		15		176.2	13.0		230.8	9.9		291.6	6.0
		20		176.5	13.1		231.1	10.0		291.9	6.1
3.0	100	5	130.4	132.8	1.9	181.6	184.1	1.4	240.9	243.3	1.0
		10		133.2	2.2		184.6	1.6		243.9	1.3
		15		133.6	2.5		184.9	1.8		244.3	1.4
		20		134.2	2.9		185.0	1.9		244.4	1.5
	200	5	131.0	135.5	3.4	183.7	186.0	1.2	242.8	244.9	0.9
		10		135.7	3.6		186.3	1.4		245.2	1.0
		15		135.8	3.7		186.4	1.5		245.4	1.1
		20		136.0	3.8		186.5	1.5		245.5	1.1
	300	5	131.8	136.6	3.6	185.5	186.7	0.6	245.1	245.4	0.1
		10		136.6	3.6		186.8	0.7		245.5	0.2
		15		136.6	3.6		186.9	0.7		245.6	0.2
		20		136.7	3.7		187.0	0.8		245.7	0.3



a)



b)

Figure 9.17 – Influence of the distance between the transverse stiffeners which form the rigid end post for the girders with $t_s = 20$ mm

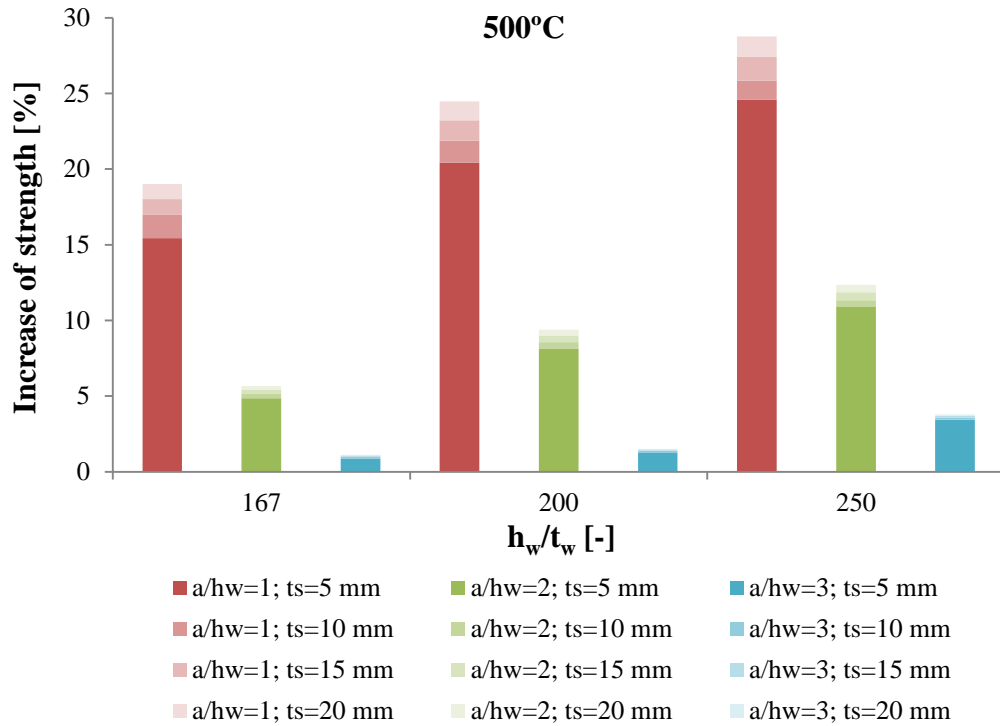
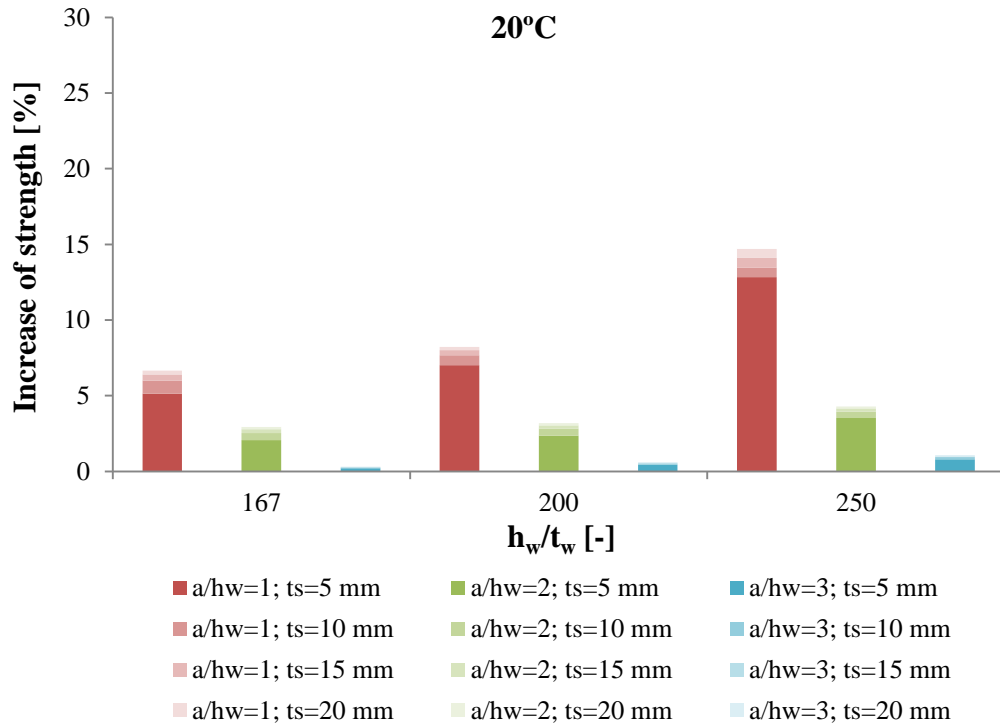


Figure 9.18 – Influence of the thickness of the external transverse stiffener of the rigid end post for the girders with $e = 200$ mm

The EC3 design procedure for girders with rigid end posts does not depend on the configuration of the rigid end posts. It only refers that the requirements presented in section 3.4.1.1 of this document should be satisfied. However, it is important to note that the variation of the configuration of the rigid end posts (distance “e” between transverse stiffeners and thickness of the external transverse stiffener) may change the safety nature of the EC3 predictions, as shown in Table 9.3. Although its influence is not so significant for girders with high aspect ratios, the configuration of the rigid end post may be relevant for the safety nature of the EC3 predictions of the girders with low aspect ratios. Thus, the implementation of some design rules in EC3 which had into account the stiffness of the rigid end posts should be considered, mainly for girders with low aspect ratios, where the influence of the rigid end posts is more significant.

Table 9.3 – Influence of the rigid end post configuration on the safety nature of the EC3 predictions at normal temperature

h_w/t_w [-]	a/h_w [-]	V_{EC3} (1) [kN]	V_{SAFIR} (2) [kN]	(2)/(1) [-]
167	1	598.8	569.1 – 617.4	0.95 – 1.03
	2	478.6	472.0 – 490.4	0.99 – 1.02
	3	441.3	445.6 – 446.0	1.01 – 1.01
200	1	465.9	454.5 – 499.8	0.98 – 1.07
	2	364.8	361.5 – 376.4	0.99 – 1.03
	3	334.7	332.8 – 333.9	0.99 – 1.00
250	1	345.4	348.8 – 394.5	1.01 – 1.14
	2	262.1	262.6 – 274.9	1.00 – 1.05
	3	237.8	231.2 – 233.3	0.97 – 0.98

9.4 Conclusions

The main objective of this section was to provide information to better understand the behaviour of plate girders subjected to shear, which can for instance help designers executing an optimum design. Based on the work presented in Chapter 9, the following general conclusions are drawn:

- The most cost-effective solution to improve the ultimate bearing capacity of steel plate girders under shear loading is to increase the web thickness;
- The reduction of resistance in case of fire is higher in the girders with non-rigid end posts, when compared to the girders with rigid end posts;
- The highest the aspect ratio is, the highest the strength loss caused by the elevated temperatures is;

- The application of rigid end posts is more profitable in girders with the following characteristics: low a/h_w , high h_w/t_w and high t_f/t_w ;
- The influence of the configuration of the rigid end posts is not significant in plate girders with high aspect ratios. However, it may be important for the safety nature of the EC3 predictions of the girders with low aspect ratios.

Chapter 10

Final considerations

Chapter 10 Final considerations

10.1 Conclusions

10.2 Future developments

Chapter 10 Final considerations

10.1 Conclusions

The lack of guidance for the fire design of steel plate girders subjected to shear buckling has been the main motivation for this research work. In this section, the main findings and conclusions achieved during the research are presented.

The first stage of this research has been a literature review in order to better understand the behaviour of steel plate girders affected by shear buckling. Having finalised this stage, it has been important to analyse the design recommendations implemented in the European Standards in order to know where they would be improved. Then, bearing in mind that the absence of fire design guidelines needed to be corrected, a plan comprising different tasks has been established.

The first was to develop a solid numerical model able to accurately reproduce the behaviour of steel plate girders affected by shear buckling at both normal and elevated temperatures, which would be the basis of the parametric study involving around 5000 numerical simulations conducted for evaluating the accuracy of the design procedure implemented in EC3 to predict the ultimate shear strength of steel plate girders affected by shear buckling. Then, this numerical model was duly validated against experimental tests at both normal and elevated temperatures. It was shown that the numerical model developed in the FEM software SAFIR provides a good approximation to the actual behaviour of steel plate girders and it is able to accurately predict the ultimate shear strength of steel plate girders under shear, as well as their failure modes.

A numerical study about the influence of the geometric imperfections and residual stresses on the ultimate resistance of steel plate girders at normal temperature and in case of fire was also performed. It was observed that do not have into account the geometric imperfections conducts to unrealistic shear buckling resistances. At 20°C, the higher the maximum amplitude of the geometric imperfections is, the more conservative the results are. However, at elevated temperatures the maximum amplitude of the geometric imperfections has no significant influence on the ultimate capacity of the analysed plate girders. Furthermore, the consideration of the maximum amplitude recommended in EC3 is too severe for the numerical modelling of experimental tests, being $t_w/10$ an appropriate value to use for that purpose. Regarding the residual stresses,

their influence on the ultimate shear strength of steel plate girders is high at normal temperature. However, they have no significant influence in fire situation.

Afterwards, based on the results of the parametric numerical study, the EC3 design procedure at normal temperature and its use for fire design by the application of the reduction factors from Part 1-2 of EC3 (CEN, 2010b) were evaluated. It has been demonstrated that the EC3 expression for the prediction of the flanges contribution to shear buckling resistance was not providing accurate results at both normal and elevated temperatures. A corrective coefficient to improve the accuracy of the expression to determine the position of the plastic hinges in the flanges, and consequently improve the precision of the EC3 predictions for the contribution from the flanges to shear buckling resistance, has been proposed.

The next task of the plan initially created was to evaluate the EC3 design procedure to determine the resistance from the web to shear buckling. For that purpose, the contribution from the flanges previously improved was subtracted from the full resistance of the girder given by the numerical model, since it could not give the web resistance alone. Small modifications to the EC3 design procedure at normal temperature have been proposed in order to provide safer and more accurate predictions. Furthermore, new expressions for the calculation of the web resistance to shear buckling in fire situation have also been proposed.

To finish the assessment of the accuracy of the EC3 design expressions, the expression for the interaction between shear and bending was also evaluated. It has been observed that the EC3 expression provides satisfactory results at normal temperature. Nevertheless, a slight improvement may be observed when the proposals are taken into account. Regarding fire design, the results given by this EC3 expression are not satisfactory (around 1/3 of unsafe results), being recommended to always have the proposals into account.

In the last stage, a study about the influence of different parameters on the ultimate shear strength of steel plate girders has been performed in order to help the designer to provide cost-effective plate girders. The strength enhancement caused by the increase of the cross-section properties (web thickness, web depth, flange thickness and steel yield strength) of a steel girder was evaluated. It was observed that the most cost-effective

solution to improve the ultimate resistance of a steel plate girder affected by shear buckling is to increase the web thickness.

The reduction of strength caused by the elevated temperatures was also evaluated. It has been demonstrated that the highest the aspect ratio is, the highest the strength reduction caused by the elevated temperatures is. Furthermore, it has been observed that this strength reduction is more significant on the girders with non-rigid end posts, when compared to the girders with rigid end posts.

Afterwards, an analysis about the influence of the end posts has been carried out. Firstly, the increase of strength given by the condition of rigid end post has been evaluated, being concluded that the steel plate girders where the application of rigid end posts is more profitable are those with the following characteristics: low a/h_w , high h_w/t_w and high t_f/t_w .

Finally, the influence of the configuration of the rigid end post has been analysed. It was concluded that its influence is not substantial for plate girders with high aspect ratios. However, the configuration of the rigid end post may be relevant for the safety nature of the EC3 predictions of the girders with low aspect ratios.

10.2 Future developments

During the development of this research work, different important issues related to the occurrence of shear buckling in steel plate girders exposed to fire are discussed and some new design expressions are proposed. The main effort was done in order to fulfill the lack of guidance on the European Standards about this topic. However, further investigation is still needed. This final section describes possible future research areas.

✓ Fire resistance experimental tests

The results of this thesis were based in numerical simulations, through the use of the finite element methods. Although the numerical model was duly validated against some of the few experimental tests found in the literature, numerical simulations do not always reproduce perfectly the real behaviour of the structures.

Due to the limited size of furnaces and the high cost of the fire resistance experimental tests, there are in the literature only few experimental tests of steel plate girders under shear loading at elevated temperatures. It would be important performing more fire

resistance experimental tests, since they could reduce the distance between the real behaviour of the structures and test conditions, when compared with numerical simulations.

✓ **Fire resistance experimental tests on stainless steel plate girders**

The absence of fire resistance experimental tests is even more serious in stainless steel plate girders. During the development of this thesis it was possible to develop a numerical model for stainless steel plate girders subjected to shear buckling (Reis, et al., 2016b). This numerical model was satisfactorily validated with experimental tests at normal temperature. However, no fire resistance experimental tests in stainless steel plate girders under shear loading were found on the literature. As there is no guidance on the European Standards for the design of stainless steel plate girders affected by shear buckling, it would be of significant importance performing fire resistance experimental tests in order to validate the numerical model, that posteriorly would be the basis of a parametric numerical study whose results are necessary for the evaluation of the application of the design expressions at normal temperature from Part 1-4 of EC3 (CEN, 2006a) to fire design.

✓ **Stainless steel**

Although more expensive than the carbon steel, stainless steel plate girders may be competitive due to their smaller need of thermal protection against fire, adding this advantage to others such as the durability, low maintenance, aesthetic appearance and corrosion resistance.

However, as mentioned in previous point, there is no guidance in EC3 for the fire design of stainless steel plate girders subjected to shear buckling at elevated temperatures. Thus, a research work similar to the one performed in this thesis should be performed for stainless steel plate girders, in order to cover the lack of fire design rules in EC3.

✓ **Plate girders with longitudinal stiffeners**

The design expressions proposed in this thesis for the safety evaluation of shear buckling in steel plate girders exposed to fire were based on transversally stiffened plate girders. Despite the application of longitudinal stiffeners is not so common as the use of

transverse stiffeners, further analysis is required in this specific topic in order to extend the conclusions achieved for the evaluated case to a general case of longitudinal stiffening.

✓ **Different loading types and steel grades**

The numerical model developed in this thesis considers the loading by the application of a concentrated force at mid-span. Other loading types should be considered, as for example the application of uniformly distributed loading over all span of the girder. Furthermore, only steel grades until 460 MPa were taken into account in this thesis. High strength steel grades should also be considered in the future.

✓ **Non-uniform temperatures**

Non-uniform temperatures may impose additional forces on the thin webs of steel plate girders and even change the failure mode. Thus, it would be important to study their influence on the ultimate shear strength of steel plate girders.

However, it is important do not forget the difficulty of implementing in the European Standards a simple calculation method that includes non-uniform temperatures.

Bibliographic references

Bibliographic references

- AISC. (1963). Specification for the design, fabrication and erection of structural steel for building. American Institute of Steel Construction.
- Basler, K. (1961a). *Strength of plate girders in shear* (Report). Proc. ASCE, 87 (ST7), Fritz Laboratory Reports. Paper 70.
- Basler, K. (1961b). Strength of plate girders under combined bending and shear. *Journal of the Structural Division, ASCE*, 87.
- Basler, K., & Thürlimann, B. (1959a). *Plate girder research* (Report). AISC National Engineering Conference Proceedings.
- Basler, K., & Thürlimann, B. (1959b). Strength of plate girders in bending. In *Proc. ASCE, 87 (ST6)* (Vol. Paper n. 2, pp. 153–181). Conference Proceedings.
- Basler, K., Yen, B. T., Mueller, J. A., & Thürlimann, B. (1960). *Web Buckling Tests on Welded Plate Girders*. Book, Welding Research Council.
- Bazant, Z. P. (2000). Structural stability, 37, 55–67.
- Beg, D., Kuhlmann, U., Davaine, L., & Braun, B. (2010). *Design of Plated Structures - Eurocode 3: Design of Steel Structures, Part 1-5: Design of Plated Structures*. Book, ECCS - Eurocode Design Manuals, Ernst & Sohn.
- CEA. (2012). CAST3M is a research FEM environment; its development is sponsored by the French Atomic Energy Commission. <<http://www-cast3m.cea.fr/>>.
- CEN. (2006a). *Eurocode 3 – Design of Steel Structures. Part 1-4: General rules - Supplementary rules for stainless steels*, Brussels, Brussels.
- CEN. (2006b). Eurocode 3 – Design of steel structures. Part 1-5: Plated structural elements. *EN 1993-1-5*. Legal Rule or Regulation.
- CEN. (2010a). Eurocódigo 3 – Projecto de estruturas de aço. Parte 1-1: Regras gerais e regras para edifícios. NP EN 1993-1-1.
- CEN. (2010b). Eurocódigo 3 – Projecto de estruturas de aço. Parte 1-2: Regras gerais de verificação da resistência ao fogo. NP EN 1993-1-2.
- CEN. (2011). EN 1090-2:2008+A1, Execution of steel structures and aluminium structures - Part 2: Technical requirements for steel structures.
- CEN TC 250. (1999). HORIZONTAL GROUP FIRE. Document n° 99/130. Proposal for a methodology to check the accuracy of assessment methods.
- Chern, C., & Ostapenko, A. (1969). *Ultimate strength of plate girders under shear* (Report). Fritz Engineering Laboratory, Report N. 328.7: Lehigh University.
- Cooper, P. B. (1965). *Bending and shear strength of longitudinally stiffened plate girders*.
- Couto, C., Vila Real, P., & Lopes, N. (2013). RUBY “an interface software for running a buckling analysis of SAFIR models using Cast3M”, University of Aveiro.
- ECCS. (1976). Manual on stability of steel structures. Publication no. 22. ECCS - Technical Committee 8 - Structural Stability.
- ECCS. (1984). Ultimate limit state calculation of sway frames with rigid joints. Publication no. 33. ECCS - Technical Committee 8 - Structural Stability, Technical Working Group 8.2 - System.

- Estrada, I., Real, E., & Mirambell, E. (2007a). General behaviour and effect of rigid and non-rigid end post in stainless steel plate girders loaded in shear. Part I: Experimental study. *Journal of Constructional Steel Research*, 63(7), 970–984. Journal Article.
- Estrada, I., Real, E., & Mirambell, E. (2007b). General behaviour and effect of rigid and non-rigid end post in stainless steel plate girders loaded in shear. Part II: Extended numerical study and design proposal. *Journal of Constructional Steel Research*, 63(7), 985–996.
- Foppl, A. (1907). *Vorlesungen über technische mechanik* (in German). In six volumes, vol. 5. Druck und Verlag von B.G. Teubner, Leipzig.
- Franssen, J. M. (1993). Residual stresses in steel profiles submitted to the fire: an analogy. In *Proceedings of 3rd CIB/W14 Workshop "Modelling"*. TNO Building and Construction Research.
- Franssen, J. M. (2005). SAFIR. A thermal/structural program for modelling structures under fire. *Engineering Journal*, 43(3), 143–158.
- Franssen, J. M. (2011). User's manual for SAFIR - a computer program for analysis of structures subjected to fire": Department ArGENCO. University of Liège.
- Franssen, J. M., & Vila Real, P. (2010). *Fire design of steel structures* (1st Editio). ECCS - European Convention for Constructional Steelwork.
- Fujii, T. (1971). A comparison between theoretical values and experimental results for the ultimate shear strength of plate girders. In *IABSE, Proc. Colloq. Design of Plate and Box Girders for Ultimate Strength*. Conference Proceedings.
- Galambos, T. V. (1988). *Guide to Stability Design Criteria for Metal Structures*, 4th ed. Book, John Wiley & Sons.
- Garlock, M., & Glassman, J. (2014). Elevated temperature evaluation of an existing steel web shear buckling analytical model. *Journal of Constructional Steel Research*, 101, 395–406.
- Garlock, M., Payá-Zaforteza, I., Kodur, V., & Gu, L. (2011). Fire hazard in bridges: review, assessment and repair strategies. *Engineering Structures*, (35), 89–98.
- Gervásio, H. (1998). *Estudo comparativo da capacidade resistente de vigas de alma cheia sujeitas a esforço transversal* (Thesis in portuguese). Departamento de Engenharia Civil. Universidade de Coimbra - Faculdade de Ciências e Tecnologia.
- Gomes, C., Cruz, P., & Silva, L. (2000). Experimental evaluation of shear behaviour of slender steel beams (in Portuguese). *Engineering Civil Magazine of University of Minho*, no. 7.
- Graciano, C., & Ayestarán, A. (2013). Steel plate girders under combined patch loading, bending and shear. *Journal of Construction Steel Research*, 80, 202–212.
- Hancock, G. J. (1981). Nonlinear analysis of thin sections in compression. *Journal of the Structural Division, ASCE*, 107(3), 455–471.
- Herzog, M. (1974). Ultimate strength of plate girders from tests. *ASCE J. Struc. Div.*, 100(ST5), 849–864. Journal Article.
- Höglund, T. (1971a). *Behavior and load carrying capacity of thin-plate I-girders* (Report). Royal Institute of Technology, N. 93.
- Höglund, T. (1971b). Simply supported thin-plate I-girders without web stiffeners

- subjected to distributed transverse load. *IABSE, Proc. Colloq. Design of Plate and Box Girders for Ultimate Strength*. Conference Paper.
- Höglund, T. (1972). *Design of thin plate I girders in shear and bending, with special reference to web buckling*. Book, Royal Institute of Technology, Department of Building Statics & Structural Engineering: Petterson.
- Höglund, T. (1997). Shear buckling resistance of steel and aluminium plate girders. *Thin-Walled Structures*, 29(1–4), 13–30. Journal Article.
- IPQ. (1998). Eurocode 3 - Design of Steel Structures. Part 1-1: General rules and rules for buildings (NP ENV 1993-1-1).
- Johansson, B., Maquoi, R., Sedlacek, G., Muller, C., & Beg, D. (2007). Commentary and worked examples to EN 1993-1-5 “plated structural elements”. JRC scientific and technical reports.
- Kodur, V. K. R., Esam, M. A., & Dwaikat, M. M. S. (2013). Evaluating fire resistance of steel girders in bridges. *Journal of Bridge Engineering*, 18(7), 633–643.
- Kodur, V. K. R., & Naser, M. Z. (2014). Effect of shear on fire response of steel beams. *Journal of Constructional Steel Research*, 97, 48–58.
- Komatsu, S. (1971). Ultimate strength of stiffened plate girders subjected to shear. In *IABSE, Proc. Colloq. Design of Plate and Box Girders for Ultimate Strength*. Conference Proceedings.
- Kövesdi, B., Alcaine, J., Dunai, L., Mirambell, E., Braun, B., & Kuhlmann, U. (2014a). Interaction behaviour of steel I-girders Part I: Longitudinally unstiffened girders. *Journal of Constructional Steel Research*, 103, 327–343.
- Kövesdi, B., Alcaine, J., Dunai, L., Mirambell, E., Braun, B., & Kuhlmann, U. (2014b). Interaction behaviour of steel I-girders Part II: Longitudinally stiffened girders. *Journal of Constructional Steel Research*, 103, 344–353.
- Kuhlmann, U., Braun, B., Feldmann, M., Naumes, J., Martin, P.O., Galéa, Y., Johansson, B., Collin, P., Eriksen, J., Degée, H., Hausoul, N., Chica, J., Meno, S., Raoul, J., Davaine, L., & Petel, A. (2007). *Competitive steel and composite bridges by improved steel plated structures (COMBRI). Final report, RFS-CR-03018* (Report). European Commission - Research Fund for Coal and Steel.
- Kuhn, P. (1956). Stresses in aircraft and shell structures. *McGraw-Hill*. Journal Article.
- Lahde, R., & Wagner, H. (1936). *Test for determination of stress concentration in tension fields* (Report). *NATA Tech. Memo. 809*.
- Lee, S., Davidson, J., & Yoo, C. (1996). Shear buckling coefficients of plate girder web panels. *Computers and Structures*, 59(5), 789–795.
- Lee, S., Lee, D., & Yoo, C. (2008). Ultimate shear strength of long web panels. *Journal of Constructional Steel Research*, 64(12), 1357–1365.
- Lee, S., & Yoo, C. (1998). Strength of plate girder web panels under pure shear. *Journal of Structural Engineering*, 124(2), 184–194.
- Lee, S., & Yoo, C. (1999). Experimental study on ultimate shear strength of web panels. *Journal of Structural Engineering*, 125, 838–846.
- Levy, S. K., Fienup, K. L., & Wooley, R. M. (1945). *Analysis of square shear web above buckling load* (Report). *NATA Tech. Note 962*.
- Levy, S. K., Fienup, K. L., & Wooley, R. M. (1946). *Analysis of deep shear web above*

- buckling load (Report). NATA Tech. Note 1009.
- Lopes, N., Vila Real, P., Simões da Silva, L., & Franssen, J. M. (2010). Numerical modelling of thin-walled stainless steel structural elements in case of fire. *Fire Technology*, 46(1), 91–108.
- MDT. (2011). New Mississippi River Bridge - Steel girders on the Illinois approach. Missouri Department of Transportation. Retrieved from <http://www.newriverbridge.org/Illinoisconstruction-November2011.htm>
- MSC. (2001). MARC user's guide. MSC Software Corporation.
- Olsson, A. (2001). *Stainless steel plasticity-material modelling and structural applications*. Doctoral thesis. Lulea University of Technology, Sweden.
- Pavlovčić, L., Beg, D., & Kuhlmann, U. (2007). Shear resistance of longitudinally stiffened panels — Part 2: Numerical parametric study. *Journal of Constructional Steel Research*, 63(3), 351–364. Journal Article.
- Payá-Zaforteza, I., & Garlock, M. (2012). A numerical investigation on the fire response of a steel girder bridge. *Journal of Constructional Steel Research*, 75, 93–103.
- Porter, D. M., Rockey, K. C., & Evans, H. R. (1975). The collapse behaviour of plate girders loaded in shear. *The Structural Engineer*, 53(8), 313–325.
- Quiel, S., & Garlock, M. (2010). Calculating the buckling strength of steel plates exposed to fire. *Thin-Walled Structures*, 48, 684–695.
- Real, E., Mirambell, E., & Estrada, I. (2007). Shear response of stainless steel plate girders. *Engineering Structures*, 29, 1626–1640.
- Reis, A., Lopes, N., Real, E., & Vila Real, P. (2016a). Numerical modelling of steel plate girders at normal and elevated temperatures. *Fire Safety Journal*, 86, 1–15.
- Reis, A., Lopes, N., Real, E., & Vila Real, P. (2016b). Stainless steel plate girders subjected to shear buckling at normal and elevated temperatures. *Fire Technology*, 1–29.
- Reis, A., Lopes, N., & Vila Real, P. (2016c). Numerical study of steel plate girders under shear loading at elevated temperatures. *Journal of Constructional Steel Research*, 117, 1–12.
- Reis, A., Lopes, N., & Vila Real, P. (2016d). Shear-bending interaction in steel plate girders subjected to elevated temperatures. *Thin-Walled Structures*, 104, 34–43.
- Rockey, K. C., Evans, H. R., & Porter, D. M. (1974). The ultimate strength behavior of longitudinally stiffened reinforced plate girders. In *Proc. Symp. Structural Analysis, Nonlinear Behavior and Technique, Transport and Road Research Laboratory* (pp. 163–174). Conference Proceedings.
- Rockey, K. C., Evans, H. R., & Porter, D. M. (1978). A design method for predicting the collapse behavior of plate girders. In *Proc. Inst. Civ. Engrs., Part 2* (pp. 85–112). Conference Proceedings.
- Rockey, K. C., & Skaloud, M. (1968). Influence of flange stiffness upon the load carrying capacity of webs in shear. In *IABSE 8th Cong., Final Report*. Conference Proceedings.
- Rockey, K. C., & Skaloud, M. (1969). Influence of the flexural rigidity of flanges upon the load-carrying capacity and failure mechanism in shear. In *Acta Technica CSAV*.

- Rockey, K. C., & Skaloud, M. (1972). The ultimate load behavior of plate girders loaded in shear. *Structural Engineer*, 50(11), 29–48. Journal Article.
- Rode, H. H. (1916). *Beitrage zur theorie der knickerscheinungen mit anwendungen im eisenbau (in German)* (Vol. 7). Book, Wilhelm Engelmann.
- Rubert, A., & Schaumann, P. (1985). Tragverhalten stahler rahmensysteme bei brandbeanspruchung (in German). *Stahlbau*, 9, 280–287.
- Saliba, N., Real, E., & Gardner, L. (2014). Shear design recommendations for stainless steel plate girders. *Engineering Structures*, 59, 220–228.
- Salminen, M., & Heinisuo, M. (2014). Numerical analysis of thin steel plates loaded in shear at non-uniform elevated temperatures. *Journal of Constructional Steel Research*, 97, 105–113.
- SC. (2012). Steel plate girders. Steel Construction. Retrieved from http://www.steelconstruction.info/images/f/ff/Plate_Girder_3.jpg
- Scandella, C., Knobloch, M., & Fontana, M. (2014). Numerical analysis on the fire behaviour of steel plate girders. In *Proc. of the 8th International Conference on Structures in Fire* (pp. 105–112).
- Sharp, M. L., & Clark, J. W. (1971). Thin aluminum shear webs. *Journal of the Structural Division-Asce*, 97(4), 1021–1038. Journal Article.
- Simões da Silva, L., Simões, R., & Gervásio, H. (2010). *Design of steel structures: Eurocode 3: Design of steel structures, Part 1-1 - General rules and rules for buildings*. ECCS - Eurocode Design Manuals, Ernst & Sohn.
- Sinur, F., & Beg, D. (2013a). Moment-shear interaction of stiffened plate girders – Numerical study and reliability analysis. *Journal of Construction Steel Research*, 88, 231–243.
- Sinur, F., & Beg, D. (2013b). Moment-shear interaction of stiffened plate girders – Tests and numerical model verification. *Journal of Construction Steel Research*, 85, 116–129.
- Skaloud, M. (1971). Ultimate load and failure mechanism of webs in shear. In *IABSE, Proceedings of Colloquium Design of plate and box girders for ultimate strength* (p. 115–130, Vol. II).
- Steinhardt, O., & Schroter, W. (1971). Postcritical behavior of aluminum plate girders with transverse stiffeners. In *IABSE, Proc. Colloq. Design of Plate and Box Girders for Ultimate Strength*. Conference Proceedings.
- Takeuchi, T. (1964). *Investigation of the load-carrying capacity of plate girders* (Thesis). University of Kyoto.
- Talamona, D., & Franssen, J. M. (2005). A quadrangular shell finite element for concrete and steel structures subjected to fire. *Journal of Fire Protection Engineering*, 15(4), 237–264.
- Tan, K.-H., & Qian, Z.-H. (2008). Experimental behaviour of a thermally restrained plate girder loaded in shear at elevated temperature. *Journal of Constructional Steel Research*, 64(5), 596–606.
- Tide, R. (1998). Integrity of structural steel after exposure to fire. *AISC Engineering Journal*, 35, 26–38.
- Vila Real, P. (2010). Encurvadura de placas e esforço transversal. Univ. de Aveiro.

- Vimonsatit, V., Tan, K. H., & Ting, S. K. (2007a). Shear strength of plate girder web panel at elevated temperature. *Journal of Constructional Steel Research*, 63(11), 1442–1451.
- Vimonsatit, V., Tan, K., & Qian, Z. (2007b). Testing of plate girder web panel loaded in shear at elevated temperature. 2007; 133(6): 815-24. *Journal of Structural Engineering*, 133(6), 815–824.
- von Karman, T. (1910). Untersuchungen uber knickfestigkeit (in German). Mitteilungen uber Forschungsarbeiten auf dem Gebiete des Ingenieurwesens, No. 81 Berlin.
- Wagner, H. (1931). Flat sheet metal girder with very thin metal web. *NACA Tech. Memo*, N. 604, 605 and 606. Journal Article.
- Wilson, J. M. (1886). On specifications for strength of iron bridges. *American Society of Civil Engineers (ASCE)*, XV(335), 401-403-490. Journal Article.
- Yoo, C., & Lee, S. (2006). Mechanics of web panel postbuckling behaviour in shear. *Journal of Structural Engineering, ASCE*, 132(10), 1580–1589.